Vol. 189 No. 2, November 28, 1986
Completing Vol. 189

ISSN 0003-2670

ANALYTICA CHIMICA ACTA

International journal devoted to all branches of analytical chemistry

ELSEVIER

ANALYTICA CHIMICA ACTA

International journal devoted to all branches of analytical chemistry
Revue internationale consacrée à tous les domaines de la chimie analytique
Internationale Zeitschrift für alle Gebiete der analytischen Chemie

PUBLICATION SCHEDULE FOR 1986

	J	F	M	A	M	J	J	A	S	O	N	D
Analytica Chimica Acta	179	180	181	182	183	184	185	186	187	188	189/1 189/2	190/1 190/2 191

Scope. *Analytica Chimica Acta* publishes original papers, short communications, and reviews dealing with ever aspect of modern chemical analysis both fundamental and applied.

Submission of Papers. Manuscripts (three copies) should be submitted as designated below for rapid and efficier handling:

Papers from the Americas to: Professor Harry L. Pardue, Department of Chemistry, Purdue University, West Lafayett IN 47907, U.S.A.

Papers from all other countries to: Dr. A. M. G. Macdonald, Department of Chemistry, The University, P.O. Box 36 Birmingham B15 2TT, England. Papers dealing particularly with computer techniques to: Professor J. T. Cler Universität Bern, Pharmazeutisches Institut, Baltzerstrasse 5, CH-3012 Bern, Switzerland.

Submission of an article is understood to imply that the article is original and unpublished and is not being considere for publication elsewhere. Upon acceptance of an article by the journal, authors will be asked to transfer the copyrigl of the article to the publisher. This transfer will ensure the widest possible dissemination of information.

Information for Authors. Papers in English, French and German are published. There are no page charge Manuscripts should conform in layout and style to the papers published in this Volume. Authors should consu Vol. 170 for detailed information. Reprints of this information are available from the Editors or from: Elsevier Editori Services Ltd., Mayfield House, 256 Banbury Road, Oxford OX2 7DH (Great Britain).

Reprints. Fifty reprints will be supplied free of charge. Additional reprints (minimum 100) can be ordered. An ord form containing price quotations will be sent to the authors together with the proofs of their article.

Advertisements. Advertisement rates are available from the publisher.

Subscriptions. Subscriptions should be sent to: Elsevier Science Publishers B.V., Journals Department, P.O. Bc 211, 1000 AE Amsterdam, The Netherlands. Tel: 5803 911, Telex: 18582.

Publication. *Analytica Chimica Acta* appears in 13 volumes in 1986. The subscription for 1986 (Vols. 179–191) Dfl. 2730.00 plus Dfl. 312.00 (p.p.h.) (total approx. US $1192.94). All earlier volumes (Vols. 1–178) except Vols. 2 and 28 are available at Dfl. 231.00 (US $90.59), plus Dfl. 17.00 (US $6.67) p.p.h., per volume.

Our p.p.h. (postage, packing and handling) charge includes surface delivery of all issues, except to subscribers in th U.S.A., Canada, Japan, Australia, New Zealand, P.R. China, India, Israel, South Africa, Malaysia, Thailand, Singapor South Korea, Taiwan, Pakistan, Hong Kong, Brazil, Argentina and Mexico, who receive all issues by air delive (S.A.L. — Surface Air Lifted) at no extra cost. For the rest of the world, airmail and S.A.L. charges are available upc request.

Claims for issues not received should be made within three months of publication of the issues. If not they cannot b honoured free of charge.

For further information, or a free sample copy of this or any other Elsevier Science Publishers journal, readers in th U.S.A. and Canada can contact the following address: Elsevier Science Publishing Co. Inc., Journal Informatic Center, 52 Vanderbilt Avenue, New York, NY 10017, U.S.A., Tel: (212) 916-1250.

0003-2670/86/$03.

Printed in The Netherlands

Analytica Chimica Acta, 189 (1986) 217—228
Elsevier Science Publishers B.V., Amsterdam – Printed in The Netherlands

IMPEDANCE MEASUREMENTS FOR PRESSED-PELLET ELECTRODE MEMBRANES BASED ON SILVER IODIDE AND SILVER IODIDE/ SILVER SULFIDE WITH SOLUTION CONTACTS

MIKLÓS GRATZL and ERNŐ PUNGOR*

Institute for General and Analytical Chemistry, The Technical University of Budapest, 1111-Budapest (Hungary)

RICHARD P. BUCK

Department of Chemistry, University of North Carolina, Chapel Hill, NC 27514 (U.S.A.)

(Received 11th June 1986)

SUMMARY

Impedance characteristics of pressed pellet membranes based on silver iodide, mixed AgI/Ag_2S with molar ratios of 10:1, 1:1 and 1:10, and silver sulfide are investigated by using solution contacts and a computer-controlled automatic measuring system. As membrane bulk impedances were commensurable with those of contacting solutions, special regression methods were necessary for evaluation. Typical resistivities were, in the order indicated above, as follows: 14, 2, 0.3, 0.1 and 0.1 kΩ cm, respectively. Thus, mixing of silver sulfide into the silver iodide matrix decreases dramatically the membrane resistance. These measured bulk membrane resistances are not affected by changes in composition and concentration of bathing solutions, and even the low-frequency parts of impedance plots were not influenced by different stirring conditions, even in presence of corroding solutions such as thiosulfate or cyanide. Sorption also had no manifest effect on the impedance characteristics, but increasing pressure during membrane preparation or heat treatment significantly increased membrane resistances.

Silver halide-based ion-selective membrane electrodes are suitable for measuring activities of ligands which form species of higher stability than that of the constituent halide salt [1]. The chemical reaction taking place between ligand and membrane material, however, causes a continuous dissolution of the sensing surface layers. To minimize this disadvantage, pressed pellet membranes of mixed composition, such as AgI/Ag_2S of molar ratios of 1:1 [2] or 7:3 [3] have been introduced with the hope that the practically insoluble silver sulfide component would deter membrane material loss. According to recent studies, these mixed salt membrane-based electrodes are practically equivalent to the pure silver halide-based versions with respect to calibration characteristics and response times [4, 5]. When used as reactive electrodes in corroding solutions, such as cyanide, thiosulfate or ammonia, typical lifetimes of the mixed and pure membranes have been found also to be nearly identical [4, 6], because their respective dissolution mechanisms are characterized by similar dissolution rates [7].

0003-2670/86/$03.50

The impedance characteristics of pure and mixed membrane-based ion-selective electrodes, however, have not yet been investigated and compared in detailed studies. Hence, pure silver iodide, and mixed AgI/Ag_2S membranes with molar ratios of 10:1, 1:1 and 1:10, as well as pure silver sulfide membranes were prepared and investigated in this work from the point of view of their impedances. These studies were done on membranes built into electrode bodies, and provided with different solution contacts, in order to furnish information relevant to the circumstances of real analytical applications.

Papers dealing with impedance measurements on precipitate-based ion-selective electrodes are not numerous [8—10]. First of all, single-crystal membranes were investigated (AgCl, AgBr [8, 9]), with both solid and solution contacts. As the impedances of polycrystalline pressed pellets are smaller by orders of magnitudes than those of single-crystal membranes, the impedance measuring techniques used in the latter cases could not be used similarly in this work. The reason for special measurement requirements is that the impedances arising from solution contacts, are generally comparable in magnitude with those of the pressed membrane pellets themselves, and hence, special care is needed for separation of membrane impedance from other impedance components. To improve reliability and accuracy, all measurements and evaluations were done with a completely automatic computer-controlled system.

EXPERIMENTAL

Materials

Chemicals of analytical grade produced by Fischer, Mallinkrodt, Merck and Reanal were used throughout the work.

Membrane materials were prepared by precipitation and, in cases of mixed membranes, by coprecipitation in corresponding molar ratios, as described earlier [11]. After filtering, washing, and drying of the precipitates, pellets of 13-mm diameter and of selected thickness between 0.5 and 3.7 mm were pressed under a pressure of 13 MPa for 1 min. A series of silver sulfide membranes of 1-mm thickness were pressed under different pressures between 10 and 12 MPa.

Glass tubes were used as electrode bodies, and glass membranes were used as blank "electrodes". The glass selected was Corning borosilicate Pyrex no. 7740 (ϵ = 4.7 at 10 kHz and 20° C). Electrode membranes were attached to glass bodies in most cases with a white plastic porcelain repair material (Loctite Co.), which exhibited ideal viscosity and fast adhesive properties, the bright white material permitting easy recognition of fabrication flaws (e.g., parts of membrane surfaces covered by adhesive) and stable high resistance during etching in silver nitrate and other solutions. It was found to be appropriate also for heat treatments up to 100°C.

In most cases, silicone rubber adhesive (RTV 108; General Electric) could

also be used for the same purpose. Although its bonding takes much longer and it is much less visible than the former glue, its inertness was found to be even better. Many other glues were also tested in blank "electrodes" containing glass membranes, but all of them showed drawbacks; epoxy-based adhesives often became good conductors when etched in silver nitrate.

Apparatus

Because the impedances of the contacting solutions were often comparable with those of the membranes, all measurements had to be done under strictly fixed geometrical conditions. To ensure this condition, membranes were attached to glass tubes (i.d. 14 mm, o.d. 16 mm, length 40 mm) as shown in Fig. 1. Special care was taken not only to avoid covering parts of flat membrane surfaces by the adhesive but also to fill completely the space between the glass body and the cylindrical membrane surface. During measurements, the glass body was filled with an inner contacting solution to a height of 30 mm from above the membrane, and covered by a special plexiglas lid

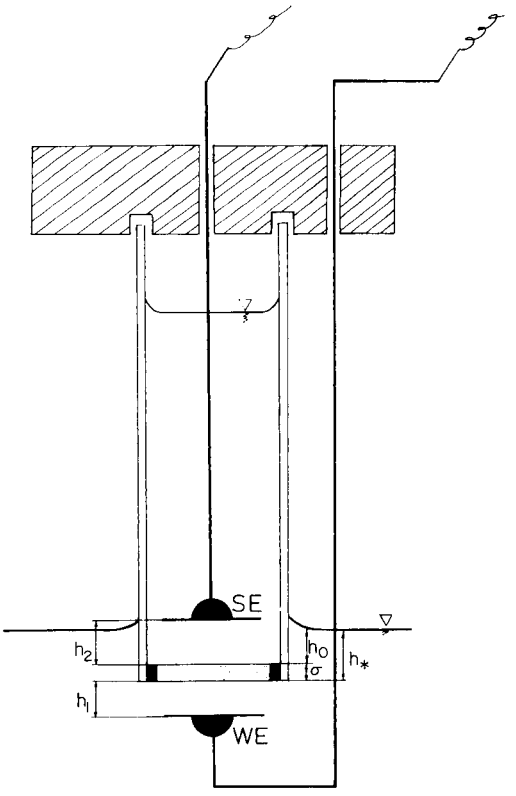

Fig. 1. Geometry of the impedance measuring cells. WE, SE are working and secondary electrodes, respectively; h_0, h_1 and h_2 are adjustable distances and δ is membrane thickness.

holding the working and secondary electrodes in adjustable geometrical positions (Fig. 1). The values of h_0, h_1 and h_2 were varied according to the demands of the measurements. Working and secondary electrodes were made of 0.25-mm thick silver plates (Alfa), both having a surface area of 1 cm^2 (diameter 11.3 mm). Their outer surfaces and the connecting wires were sealed by the adhesive, mentioned above, and by plastic sealant.

When measurements were made in corroding media (cyanide, thiosulfate or ammonia containing solutions), two of the membrane electrodes described above were used. In this case, the configuration

SE|0.1 M $AgNO_3$|membrane|corroding soln.|membrane|0.1 M $AgNO_3$|WE

replaced the configuration in Fig. 1, which is

SE|0.1 M $AgNO_3$|membrane|0.1 M $AgNO_3$|WE

Thus, any direct contact between possibly corroding solutions and silver electrodes (SE, WE) could be avoided. In these cases, silver flags of surface area of 1.5 cm^2 were used. These two-membrane arrangements were used also when temperature dependences were studied, to increase the total membrane impedance and improve statistical reliability. For minimizing solution impedances, the two glass bodies were positioned closely together. The same two-electrode arrangement was applied during experiments with stirred solutions.

Stirring, when used, was done with a glass stirring rod driven by a remote electric motor (situated 60 cm above the cell), and in other cases by an ordinary magnetic stirrer. The first experiments were done with the remote motor to eliminate any effects of rotating electromagnetic fields. As no deteriorating effects could be observed, later the magnetic stirrer was used. The sole bad effect was somewhat greater noise at impedance points close to 60 Hz.

For impedance measurements, a microprocessor-controlled Solartron 1250 frequency response analyzer was used. It was connected with the impedance cell through a Solartron 1186 electrochemical interface, and with an HP85B personal computer through an HP-IB bus. The frequency response analyzer operates on the basis of correlating the sinusoidal voltage input to current output signal [12]. The computer controlled the entire measurement, and provided fully automatic data acquisition and evaluation.

Procedures

The current gain resistor of the electrochemical interface was always carefully adjusted to the measured impedance and to the investigated frequency range. Thus, systematic distortion of impedance plots as well as random noise could be minimized. To check systematic errors, measurements with standard cells containing known resistors and capacitors were done regularly.

The frequency response analyzer was used in potentiostatic mode. It was controlled through the keyboard of the HP85B computer. In addition to control functions, the computer provided a completely automatic evaluation of the data. Thus, it furnished graphical information such as the complex

impedance plot (Figs. 2—4), and the corresponding real and imaginary resistances as functions of log ω. An automatic calculation of the parameters of the impedance semicircles was also possible, on the basis of a least-squares curve-fitting algorithm. Thus, radius and center coordinates as well as the value of corresponding real resistance, and the parameter α could be automatically obtained (the α parameter characterizes the non-ideality of "sunken" semicircles [10]). Residual error of fitting was also monitored.

When a sufficiently large part of the impedance semicircle could be obtained by the measuring system, an automatic calculation of ω_{max} and hence that of the corresponding capacitance became possible. Quadratic interpolation, convolutional smoothing with respect to log ω, and a curve-fitting procedure using the theoretical formula of real impedance component as a function of log ω, were developed and applied. With this latter method, a useful extrapolation to high frequencies became possible, for cases in which ω_{max} was higher than the maximum frequency of the apparatus, 65 500 Hz. This situation occurred often in this work, as relatively small membrane impedances had to be measured. The principles of this automatic evaluation system will be described elsewhere.

EVALUATION, RESULTS AND DISCUSSION

Evaluation

It is well known that very large impedances are difficult to measure, because of accompanying large noise. It can, however, be surprisingly difficult to measure relatively small impedances, as in this case the connecting elements (e.g. contacting solutions) contribute, sometimes significantly, to the observed responses and measured data. Thus, in these extreme cases, large systematic errors may distort the results.

Another difficulty is caused by the fact that membranes of small resistivity and of ordinary permittivity are characterized by extremely small time constants, which can be defined by

$$\tau = RC = \epsilon_0 \epsilon_r / \sigma \tag{1}$$

where R and C are resistance and geometric capacitance, while ϵ_r and σ represent relative permittivity and specific conductivity, respectively; ϵ_0 is the permittivity of free space. The right-hand side of Eqn. 1, which can be derived directly for plane parallel membranes, reflects the fact that it is impossible to modify (e.g., increase) the so-called "electrical relaxation" time constant by any geometrical modification. When, for example, thicker membranes are used, R increases, but simultaneously C decreases in the same proportion. Thus, at given membrane materials, ω_{max} can definitely and unchangeably exceed the range of the apparatus. The origin of this equation is rarely described in the electrochemical literature, because it combines application of both transport equations and Poisson's equation. A simple derivation, applicable to ionic and mixed conductor systems, is given in Appendix 1.

Most of the mixed electrode membranes examined here, because of their polycrystalline structure, exhibited such small resistances that both of the above-mentioned problems caused difficulties. As one of the purposes of this study was to conduct measurements under characteristic circumstances of ordinary practice, solution contacts could not be replaced by metallic ones. Consequently, special techniques had to be applied for separating membrane bulk resistance from contacting solution contributions, as both often have similar values. A further consequence was that the ω_{max} values, corresponding to the small time constants, were beyond the frequency range of the apparatus. Hence, in most cases only data belonging to a very small low-frequency part of the impedance semicircle could be obtained, which sometimes rendered impossible the evaluation of ω_{max}, R, and C, even by the extrapolation procedure. In exceptional cases, mostly in those of silver iodide membranes, the high-frequency impedance semicircle could, however, be partially measured and the data fitted by least squares (see Appendix 2), which provided directly the value of membrane bulk resistance (Fig. 2).

The problem of separating membrane bulk and solution resistances was examined in two ways. In the first procedure, when a given membrane was measured, the distances of the working and secondary electrodes from the membrane surfaces (h_1 and h_2 on Fig. 1) were varied, and linear regression was calculated by correlating observed resistance and distance ($h_1 = h_2$ during these studies). By extrapolating to a zero solution thickness, the membrane bulk impedance could be obtained. In the second procedure, fixed

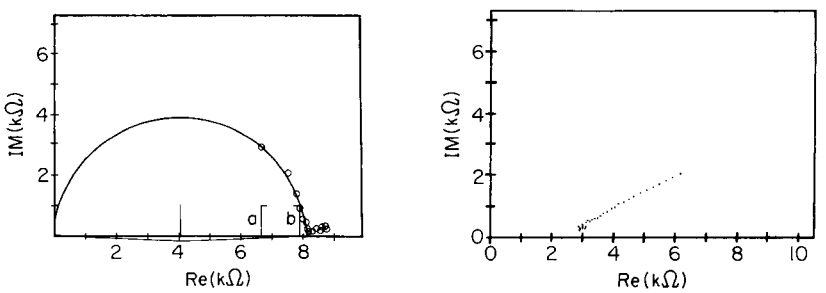

Fig. 2. Complex impedance plot measured with an AgI membrane. Measurements were made with 0.05 M KNO_3/0.005 M $AgNO_3$ both inside and outside the electrode body. Frequency range was 0.01—65 500 Hz, with 3 points/decade and 3 integration cycles/point. Exciting voltage was 200 mV (effective amplitude) and a 1-kΩ standard gain resistor was used in the electrochemical interface. Least-squares semicircle fitting was done in the interval marked by a and b on the figure.

Fig. 3. Typical impedance plot when low resistance membranes were measured with the cell shown on Fig. 1. Data for the plot are as follows: AgI membrane with δ = 2.1 mm in 0.2 M $AgNO_3$ solution at both sides, with $h_0 = h_1 = h_2 = 4$ mm, from 50 to 65 500 Hz. Other parameters: 10 points/decade, 100 cycles/point, 50-mV exciting effective voltage, 0.1-kΩ standard gain resistor. Practically, only the diffusional part of the impedance plot can be obtained because of the low membrane bulk time constant.

electrode distances were used ($h_1 = h_2 = 4$ mm), with membranes of the same composition but of different thicknesses, δ. Specific membrane resistance could be obtained in these cases after linear regression between total measured resistances and membrane thicknesses: the slope of the resulting straight line provided the necessary information.

When ω_{max} values were too large, even the determination of total resistance (e.g., resistance of membrane bulk plus that of contacting solutions) was problematic, because no well-established semicircles could be obtained. In such poorly represented impedance plots, most points belonged to diffusional impedances (Figs. 3 and 4). In these cases, total resistance was defined by the value of real impedance component corresponding to the minimum point of the impedance plane plot (Fig. 4). To increase accuracy, many points were measured in a narrow range and with high integration times (often with 10^6 repetitions). Typical logarithmic Bode plots (Fig. 5) were found not to be useful. When no clear minimum could be obtained, simply the real impedance measured at the highest possible frequency was used in subsequent evaluation. Values thus found were used for final evaluation of membrane resistances by the regression techniques described above.

Results

A readily analyzed impedance plane plot for a silver iodide membrane is shown in Fig. 2. Results of the least-squares semicircle fitting were as follows: the radius calculated was 4.075 kΩ, and the coordinates of the center were 4.047 and −0.146 kΩ with a residual error/point of 0.087 kΩ. The membrane bulk resistance (ca. 8.1 kΩ) was increased by heat treatment before measurement. Such relatively well established semicircles could be obtained only in the course of preliminary measurements, when curved electrode bodies with large surfaces were used. The increased value of the parallel

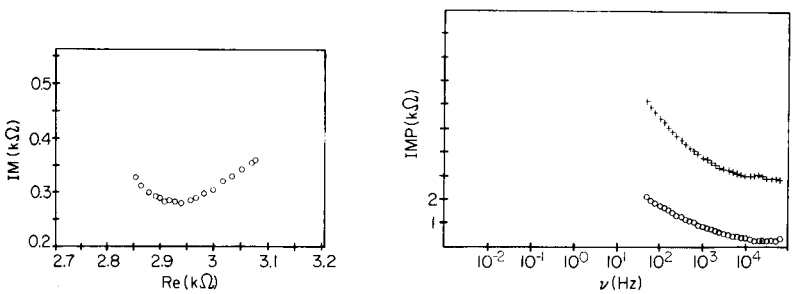

Fig. 4. Enlarged and refined high-frequency part of the same membrane as in Fig. 3 (10—65.5 kHz, 20 points/decade, 10 000 cycles/point, 50-mV exciting voltage). The x coordinate of the minimum point can be accepted as total (membrane bulk + solution bulk) resistance.

Fig. 5. The Bode plot of the same measurement as shown in Fig. 3: (+) real; (○) imaginary.

coupled capacitance (through the electrode body), thus decreased ω_{max}. Typical results are illustrated in Figs. 3 and 4.

When the various computational methods are applied to Ag_2S, AgI and AgI/Ag_2S mixed membranes, bulk resistance vs. membrane thickness plots were obtained. The corresponding resistivity values and statistics are compiled in Table 1. A typical plot, for the (1:1) membrane is given in Fig. 6.

The data in Table 1 were obtained for 0.1 M silver nitrate as inner and

TABLE 1

Resistivities, ρ, determined by linear regression as a function of membrane thickness, δ (see Experimental)

Membrane type	No. of points in one regression	Regression coefficient (r^2)	ρ (Ω cm)
AgI	5	0.9776	14140
	6	0.9814	14485
	9	0.9868	13589
AgI/Ag_2S (mixed)			
10:1	4	0.9990	1769
	4	0.9992	1674
1:1	5	0.9960	226
	11	0.9729	330
1:10	11	0.8861	60
	5	0.8900	121
Ag_2S	7	0.9354	97
	10	0.9586	166

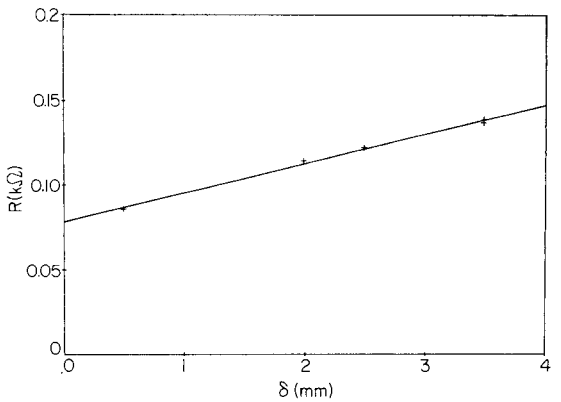

Fig. 6. Derived total resistance/thickness plot for AgI/Ag_2S (1:1) membranes (total resistance = membrane bulk + solution bulk resistance). Bathing solutions: 0.02 M $AgNO_3$/ 0.1 M KNO_3. $R(k\Omega) = M\delta$ (mm) + B with M = 0.0170, B = 0.0776 and r^2 = 0.9960.

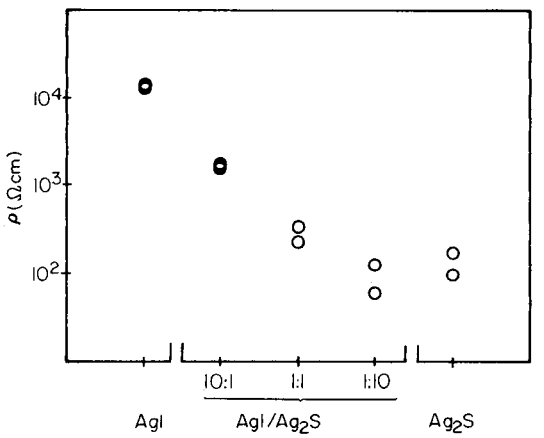

Fig. 7. Specific bulk resistance as a function of composition for AgI/Ag_2S membranes.

outer contacting solutions. However, data were also obtained when the composition and concentration of the outer solution were varied, using the double membrane arrangement (see Experimental). The changes could not affect the operation of the silver working and secondary electrodes. No significant variations were observed, in either the high- or low-frequency parts of the impedance plots of any membrane types when, instead of 0.1 M KNO_3/0.02—0.2 M $AgNO_3$, only KNO_3, or potassium iodide, sodium thiosulfate or even potassium cyanide solutions were used as outer solution. In diluted solutions (e.g., 5×10^{-5} M iodide), however, solution resistance greatly increased, causing a shift of the impedance plot in the direction of higher real resistances. It is important to note that even the low-frequency part (from 0.01 Hz), corresponding to diffusional current, did not show any systematic change when corroding media (thiosulfate, cyanide) were used with silver-iodide-containing membranes. The stability of the impedance plots was also maintained when results in unstirred, stirred and strongly stirred solutions were compared. This indifference to stirring was also observed in non-corroding solutions ($AgNO_3$, KNO_3, KI).

Adsorption/desorption effects did not appear in the plots, when silver iodide membranes were studied first in highly dilute (5×10^{-5} M) potassium iodide solution and then in the same solution but with a suddenly increased sodium bromide content (0.1 M). In such cases, desorption of iodide ions from the membrane surface takes place [13, 14], which was not indicated by the impedance technique. When the pressure during membrane preparation was increased, bulk resistances seemingly increased too; e.g., for pressure changes from 10 to 12 MPa, resistances of the silver sulfide membrane increased by 30—40%. More quantitative conclusions, however, cannot be drawn from this work because of the relatively narrow pressure range investigated. Heat treatment caused a significant increase in membrane bulk resistance; the membrane dealt with in Fig. 2 exhibited a resistance increase from

ca. 3 kΩ to 8 kΩ, after being heated briefly (2–3 min) at ca. 150°C. After being heated at 100°C during 12 h, most membrane types investigated showed a clear resistance increase of ca. 100%, except membranes of 10:1 AgI/Ag_2S composition. The latter resistances increased about by one order of magnitude. These changes can be explained by the fact that at higher temperatures spontaneous phenomena of microcrystal growth take place faster, by orders of magnitude, than at room temperature, thus accelerating formation of macrocrystalline structure, characterized by much higher resistances.

Finally, a plot of membrane resistance vs. composition is given in Fig. 7. Clearly, mixing of silver sulfide into the silver iodide membrane matrix decreases the membrane resistances by orders of magnitude. However, even the electrodes with highest resistances (pure silver iodide membranes) do not cause any practical problem in analytical practice, as their resistances can also be considered as relatively low compared to those of most potentiometric sensors.

Support from NSF (under Grants CHE8406976 and INST8403331) and the Hungarian Academy of Sciences, and the advice of K. Tóth are gratefully acknowledged.

APPENDIX 1. ORIGIN AND MEANING OF THE HIGH-FREQUENCY, "GEOMETRIC" IMPEDANCE OF CONDUCTING FILMS/MEMBRANES

Ionic and mixed-conductor films and membranes with internal charge transport in one dimension usually have large resistances compared with contacting phases such as metals or ionic, aqueous electrolytes. At high frequencies, externally applied fields generate space charge in the external phases, of opposite sign at each interface. The internal charge transport causes charge carriers merely to oscillate in place according to the so-called high-frequency resistance. The capacitance is thus "geometric" and no appreciable space charge is generated in the membrane phase at the high-frequency limit.

Within the homogeneous internal phase, charge carriers attempt to move according to diffusion and migration. Field-induced "migration" is called "drift" by solid-state physicists. Internal current density, I(int.), is related to charge carrier fluxes, J_i, in the normal fashion: $I(\text{int.}) = F \sum_i z_i J_i$. However, external circuit current, I, also includes the external charge accumulation:

$$I/A = F \sum_i z_i J_i + \rho \, dx/dt = F \sum_i z_i J_i - \epsilon \partial^2 \phi / \partial x \partial t$$

where $\epsilon = \epsilon_r \epsilon_0$, A = area and ϕ is potential

The combination of Poisson's equation with Nernst–Planck equations into this form has been derived in some detail recently [15]. At high frequencies, only the migration term in the Nernst–Planck flux expressions for each charge carrier is retained:

$$J_i = -\sum_i (D_i z_i F/RT)\, c_i\, (\partial\phi/\partial x)$$

$$= -\sum_i u_i z_i F c_i\, (\partial\phi/\partial x)$$

$$= -\sum_i u_i^* c_i\, (\partial\phi/\partial x)$$

using diffusion coefficients, D_i, chemical mobilities, u_i, or physical mobilities, u_i^*, respectively. The transform of current is

$$\bar{I}/A = -\sum_i [D_i (z_i F)^2/RT]\, c_i\, (\partial\bar{\phi}/\partial x) - j\omega\epsilon\, (\partial\bar{\phi}/\partial x)$$

using diffusion coefficients and constant concentrations, c_i. Because the space charge is external:

$$\bar{I}/A = \{-\sum_i [D_i (z_i F)^2 c_i A/RTd] - (j\omega\epsilon A/d)\}\Delta\bar{\phi}$$

and

$$Z(j\omega) = [(1/R) + j\omega C]^{-1} = [(A\sigma/d) + (j\omega\epsilon A/d)]^{-1} = -\Delta\bar{\phi}/\bar{I}$$

Consequently, the proper equivalent circuit for the high-frequency "geometric" impedance is, unequivocally, parallel with $\tau = RC$, as given above in Eqn. 1.

APPENDIX 2. LEAST-SQUARES FITTING OF NON-IDEAL (SUNKEN) SEMICIRCLES TO POORLY REPRESENTED IMPEDANCE PLANE PLOTS

The interval where fitting must be done is found in an interactive way, by defining the frequency limits of points belonging to the semicircle in question. Minimum and maximum real impedances occurring within this interval are then marked in the plot (see points a and b in Fig. 2). The impedance range thus indicated could be changed when it seemed to be not appropriate.

By starting then from an initial guess of semicircle parameters, an error function of the type

$$\mathrm{RSS} = \sum_i \{(x_i - x_0)^2 + (y_i - y_0)^2]^{1/2} - R\}^2$$

must be minimized, where x_0, y_0 and R correspond to the centre coordinates and radius, respectively, of the semicircle, while RSS means residual sum of square errors. This kind of error function implies that deviations between measured and calculated points are considered in the direction of actual semicircle radius. This approximation is more exact than the usual assumption of "vertical" errors, because in impedance plots all measured points are biased by both real and imaginary error components.

Minimization of the error function was done by a first-order gradient method specially developed in this work for solving semicircle fitting. The procedure generally provided correct results when the semicircle section represented by measured points was not smaller than about 30°.

The resulting parameters rendered possible the calculation of solution and membrane bulk resistances, the parameter α describing the ideality of the semicircle, and the value of ω_{max} together with statistical characteristics of the results.

REFERENCES

1 E. Pungor and K. Tóth, Analyst, 95 (1970) 625.
2 Instruction Manual, Cyanide Ion Activity Electrode (model 94-06), Orion Research, Cambridge, MA, 1967.
3 Aomi, T., Denki Kagaku, 46 (1978) 343.
4 M. Gratzl, L. Gryzelko, J. Kömives, K. Tóth and E. Pungor, in E. Pungor (Ed.), Ion-Selective Electrodes-4, Elsevier and Akadémiai Kiadó, Budapest, 1985, 417 pp.
5 L. Gryzelko, M. Gratzl, L. Ernyei, K. Tóth and E. Pungor, Magy. Kémiai Foly., 92 (1986) 1.
6 M. Gratzl, J. Kömives, L. Gryzelko, K. Tóth and E. Pungor, Magy. Kémiai Foly., 92 (1986) 71.
7 E. Pungor, M. Gratzl, L. Pólos, K. Tóth, M. F. Ebel, H. Ebel, G. Zuba and J. Wernisch, Anal. Chim. Acta, 156 (1984) 9.
8 R. P. Buck, D. E. Mathis and R. K. Rhodes, J. Electroanal. Chem., 80 (1977) 245.
9 R. K. Rhodes and R. P. Buck, J. Electroanal. Chem., 86 (1978) 349.
10 R. P. Buck, Ion-Selective Electrode Rev., 4 (1982) 3.
11 E. Pungor, J. Havas, K. Tóth and G. Madarász, Hung. Patent 152106 (1964).
12 N. D. Cogger, Techn. Report 012/84, Solartron Instruments, Schlumberger, U.K.
13 E. Lindner, K. Tóth and E. Pungor, Anal. Chem., 54 (1982) 202.
14 M. Gratzl, E. Lindner and E. Pungor, Anal. Chem., 57 (1985) 1506.
15 R. P. Buck, J. Membr. Sci., 17 (1984) 1.

Analytica Chimica Acta, 189 (1986) 229—236
Elsevier Science Publishers B.V., Amsterdam — Printed in The Netherlands

INDIRECT DETERMINATION OF SURFACTANTS BY ADSORPTIVE STRIPPING VOLTAMMETRY[a]

B. PIHLAR*, B. GORENC and D. PETRIČ

Department of Chemistry, Faculty of Natural Sciences and Technology, E. Kardelj University, 61001 Ljubljana (Yugoslavia)

(Received 19th March 1986)

SUMMARY

The effect of some anionic, cationic and nonionic surface-active substances on the suppression of adsorptive accumulation of the bis(dimethylglyoximato)nickel(II) complex, $Ni(DMG)_2$, is described. Competitive adsorption of surfactants can be used to determine surfactants commonly used in commercial detergents. Triton X-100 shows the most pronounced effect on the peak height. The shape of the calibration curve depends on the concentration and on the adsorption potential. Highest sensitivity is obtained when equilibrium between $Ni(DMG)_2$ in solution and on the electrode surface is attained rapidly. Under these conditions, the detection limit is 1 $\mu g\ l^{-1}$ Triton X-100. Calibrations are linear over 1—2 orders of magnitude.

Surfactants are probably the commonest organic pollutants in the aqueous environment. At low concentrations, they are usually determined by spectrophotometry [1—4] and electrochemical techniques [5—17].

Electrochemical methods for the determination of surface-active substances are based on adsorption phenomena in the electrode/electrolyte interphase, because surfactants are mostly electro-inactive in aqueous media. Inhibition or promotion of the charge-transfer process and the change in the double-layer capacity caused by specific adsorption of surfactants are the commonest basis for voltammetry, which has found wide application in their determination [5—11, 17], as well as in the study of the structural and ionic characteristics and behaviour of surface-active substances in the environment [12—15]. Polarographic measurement of surfactants based on the suppression of the maxima of oxygen [6] or mercury(II) [8] can be considered as indirect methods. The Kalousek commutator technique [12, 13] or a.c. voltammetry [7, 11, 14], both based on capacitive phenomena, can be treated as direct methods, giving a signal proportional to the increase in concentration of the surfactant.

Recently, adsorptive stripping voltammetry has become popular [16, 18], and because of its wide application, it is promising for compounds with surface-active properties [14—17]. The power of this approach was recognized

[a]This paper is dedicated to the memory of Professor Lado Kosta (1921—1986).

0003-2670/86/$03.50

by the development of a highly sensitive voltammetric method for the determination of nickel [19] which is based on the adsorptive preconcentration of the bis(dimethylglyoximato)nickel(II) complex on a hanging mercury drop electrode (HMDE). As previously described, surface-active substances affect the adsorption of $Ni(DMG)_2$ by competitive coverage of the electrode surface [19].

The purpose of the present work was to investigate the inhibitory effect of different groups of surface-active substances on the adsorptive accumulation of $Ni(DMG)_2$. The main aim was to establish if it is possible to exploit the competitive adsorption of surfactants for the determination and/or differentiation of substances with surface-active properties via measurement of the nickel voltammetric peak current.

EXPERIMENTAL

Apparatus and reagents

A microprocessor-controlled polarographic analyzer (PAR model 374) and a static mercury drop electrode (PAR model 303) were used. The differential pulse cathodic stripping mode of operation was used at a fast scan rate (8 mV s^{-1}) with a medium drop size (electrode area of 0.014 cm^2), if not otherwise stated. In the preconcentration step, the solution was stirred at 750 rpm with a magnetic stirrer. The circuitry of the commercial SMDE was modified in the sense that during the preconcentration step purging with gas was discontinued and stirring of the solution was done with the magnetic stirring bar only. Dissolved oxygen was removed by purging with argon (99.999%).

The supporting electrolyte solution was 0.1 M ammonia buffer, pH 9.2, prepared by measuring out appropriate amounts of 25% ammonia and 30% hydrochloric acid solutions (both Suprapur; Merck). To the buffer solution, an appropriate amount of DMG (butan-2,3-dioxime) and a standard solution of nickel(II) were added. A 0.1 M solution of DMG was prepared by dissolving an appropriate amount of the reagent (Merck) in 96% ethanol. The optimal concentration of DMG in the cell was about 1×10^{-4} M, as described before [19]. A nickel standard solution (1.0 g l^{-1}) was prepared from a Titrisol ampoule (Merck). The concentration of nickel(II) in the cell was 10 μg l^{-1} if not otherwise stated.

Standard solutions of surfactants (10 mg l^{-1}) were prepared by dissolution and dilution of commercial products, as received, in deionized water. Polyethyleneglycol (PEG) of mean molecular weight 400 and 4000 (Merck) and Triton X-100 (polyethyleneglycol mono(*p*-(1,1,3,3-tetramethylbutyl)-phenyl) ether; Merck) were studied as typical nonionic surfactants. Two types of alkylbenzene sulphonates, PDS (4-phenyldodecane sulphonate; Fluka) and tetrapropylenebenzene sulphonate (TBS; Merck), and Aerosol OT (dioctyl ester of sodium sulphosuccinic acid; BDH) were investigated as anionic surfactants commonly used in commercial detergents. Aerosol OT was more

sparingly soluble in water than the other surfactants; it was dissolved in absolute ethanol and then diluted with water to the appropriate concentration. From the group of cationic surface-active substances, tetramethylammonium hydroxide (10% solution; Merck), tetramethylammonium tetrafluoroborate (Merck) and Cetrimide (hexadecyltrimethylammonium bromide; Fluka) were used.

All reagents and standard solutions were prepared with deionized water obtained from a Milli-Q System (Millipore), and stored in glass bottles. Standards of lower concentration were prepared by appropriate dilution daily.

Procedure for the investigation of parameters

The electrolyte solution (10 ml) containing 0.1 M ammonia buffer, 1.0×10^{-4} M DMG and 10 $\mu g\ l^{-1}$ nickel were transferred to the cell and the measurement procedure was started. The initial potential was set between 0 and −0.9 V vs. Ag/AgCl, the purging time to 5 min, deposition time to 120 s and equilibration time to 15 s. The voltammograms were recorded in the differential pulse mode at a fast scan rate in the cathodic direction from the initial potential to −1.1 V. The peak corresponding to the reduction of the adsorbed $Ni(DMG)_2$ appears at about −0.95 V.

In the presence of surface-active substances, a substantial decrease of the peak current, I_p, was obtained because of the competitive coverage of the electrode surface. To evaluate the effect of concentration and the influence of specific adsorption of different surfactants, the dependence of I_p on the concentration and on the potential of accumulation was investigated under the same experimental conditions as before.

Recommended procedure for determination of surfactants in natural and waste waters

To 10 ml of sample, 1.0 ml of solution containing 1.0 M ammonia buffer, 1.0×10^{-3} M DMG and 200 $\mu g\ l^{-1}$ Ni(II) was added and measurements were started with the initial potential set to −0.7 V. Measurement at different accumulation potentials gives some information on the ionic type of surfactant present in the sample.

The concentration of the surface-active substances in the sample was evaluated from a calibration graph obtained under the same conditions with Triton X-100 as a calibration standard.

RESULTS AND DISCUSSION

For the study of the suppression of the $Ni(DMG)_2$ peak, it is important to know the basic principles of the voltammetric method, and to understand the influence of all parameters on the sensitivity of the measurements. The method is based on the adsorptive enrichment of the planar bis(dimethylglyoximato)nickel(II) complex at the electrode surface [19]. The amount of charge, and thus the peak height, I_p, is proportional to the surface concentra-

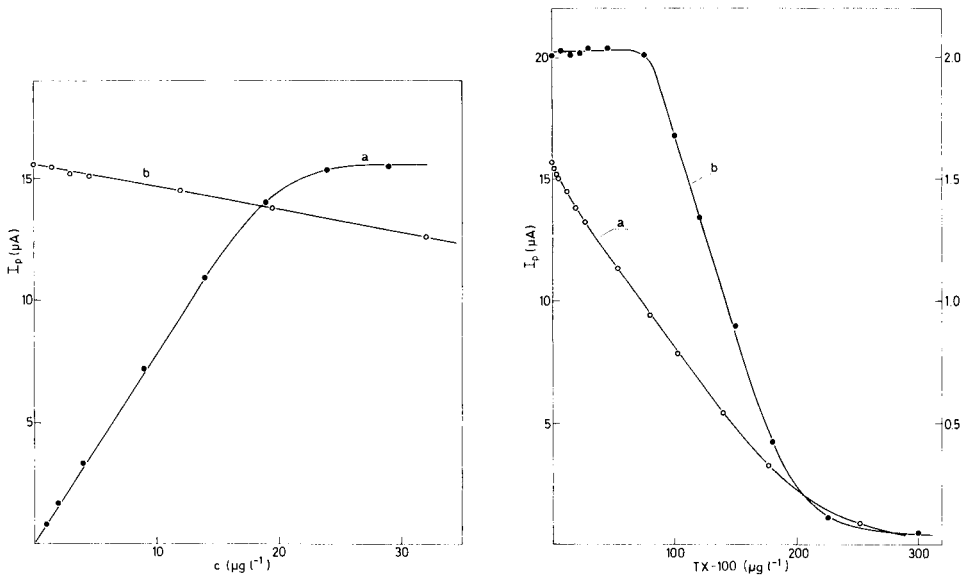

Fig. 1. Dependence of the peak height of $Ni(DMG)_2$ on the concentration of Ni(II) (curve a), and the influence of Triton X-100 at 29 μg l^{-1} Ni(II) (curve b). Conditions: 0.1 M NH_3/NH_4Cl buffer containing 1.0×10^{-4} M DMG; preconcentration for 2 min at −0.7 V; electrode area 1.4 mm^2.

Fig. 2. Relationship between I_p and concentration of Triton X-100 with different amounts of Ni(II): (a) 29 μg l^{-1}; (b) 3.2 μg l^{-1}. Conditions as for Fig. 1.

tion of $Ni(DMG)_2$ in the reaction zone. As can be seen from curve (a) on Fig. 1, the dependence of the peak height on the concentration of nickel(II) in solution has the shape of an isotherm. For the given experimental conditions, I_p is linearly proportional to the nickel(II) concentration in the range between 0 and 15 μg l^{-1}. If the electrode is more than about 75% covered, the surface accumulation of $Ni(DMG)_2$ becomes slower, reaching maximal coverage at about 30 μg l^{-1} Ni(II) (in 2 min of preconcentration).

Curve (b) in Fig. 1 shows the suppressive effect of the non-ionic surfactant Triton X-100 on the peak height. As can be seen, the $Ni(DMG)_2$ peak height decreases under these conditions nearly linearly with increasing concentration of the surfactant. This indicates that the adsorption of Triton X-100 proceeds very quickly, despite the low concentration. It is evident that the presence of Triton X-100 at the μg l^{-1} level can easily be detected. However, it must be noted that such a high sensitivity for Triton X-100 is obtained only at a high concentration of nickel, i.e., when the surface concentration of $Ni(DMG)_2$ approaches its maximal value. This is logical, because only under these condition can the adsorption of $Ni(DMG)_2$ proceed quickly enough to reach equilibrium at a given time-scale, and any significant displacement of the $Ni(DMG)_2$ chelate on the electrode surface results immediately in an appropriate decrease of the peak height.

Figure 2 shows the suppressive effect of Triton X-100 for two different concentrations of nickel. At lower concentrations of nickel (curve b), there is a clearly defined "dead" range, in which the peak height remains unaffected. This 'dead' zone decreases in width as the concentration of nickel in solution increases, and it disappears completely with attainment of equilibrium between the surface concentration of $Ni(DMG)_2$ and its concentration in the solution (curve a, Fig. 2). This effect cannot be explained by the difference in the strength of the adsorptive properties of Triton X-100 and $Ni(DMG)_2$. Obviously, Triton X-100 is the stronger surfactant, otherwise the $Ni(DMG)_2$ peak would not be suppressed at all, but at lower concentrations of Ni(II), Triton at low concentrations behaves as the weaker surfactant under equal experimental conditions. A probable reason for this anomalous behaviour lies in lack of attainment of the adsorption equilibrium of $Ni(DMG)_2$; at Ni(II) concentrations in solution below 25 $\mu g\ l^{-1}$, equilibrium is not reached between the solution and the surface concentration of $Ni(DMG)_2$, under the constant hydrodynamic and timing conditions used. Therefore, at low concentrations of Triton X-100, the adsorption of $Ni(DMG)_2$ is the predominant process. As the surfactant concentration increases, a point is reached at which the strength of the adsorptive properties of Triton prevails, and adsorption of $Ni(DMG)_2$ is inhibited.

From the viewpoint of the determination of nickel by adsorption stripping voltammetry, this anomalous behaviour at low nickel concentrations is convenient, because I_p was affected only at higher concentrations of surfactants. Moreover, the appearance of the "dead" region is not a real drawback for the measurement of surface-active substances via inhibition of the $Ni(DMG)_2$ peak because there is still a moderate range with a nearly linear relationship between I_p and the concentration of the surfactant (Fig. 2).

The influence of the preconcentration potential in the range between 0 and −0.9 V on the peak height was studied at different concentrations of surfactants, as well as at different concentration of nickel(II). The dependence of I_p on the potential of accumulation at two different concentrations of nickel and Triton X-100 is presented in Fig. 3. The peak height of $Ni(DMG)_2$ in the absence of surfactant (curve a) is constant when the adsorption potential was between −0.2 and −0.8 V. At more positive potentials, the adsorption of $Ni(DMG)_2$ is inhibited by the adsorption of chloride and the oxidation of mercury, and at more negative potentials than −0.8 V, $Ni(DMG)_2$ is reduced on arrival at the electrode surface. The inhibition of $Ni(DMG)_2$ adsorption by Triton X-100 is potential-dependent (curves b and c, Fig. 3). As Triton X-100 is a nonionic surfactant, the suppression is more pronounced around the electrocapillary maximum. The concentration of nickel(II) has no significant effect on the dependence of the inhibition by Triton on the adsorption potential, and the relationship has the same course and magnitude at low concentrations (curve b), as well as at concentrations of nickel(II) where adsorptive equilibrium was attained (curve c).

The suppressive effect of polyethyleneglycols also depends on the molecular

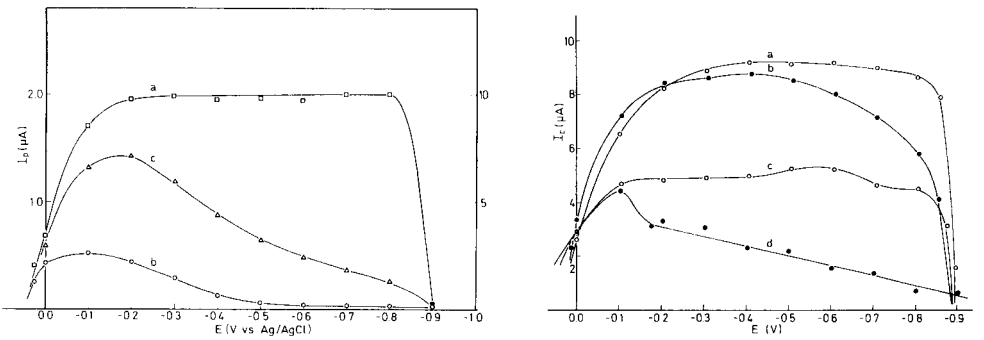

Fig. 3. Dependence of peak current on adsorption potential for 3.2 μg l^{-1} Ni(II): (a) in the absence of Triton X-100; (b) in the presence of 300 μg l^{-1} Triton X-100; (c) in the presence of 29 μg l^{-1} Ni and 250 μg l^{-1} Triton X-100. Conditions as for Fig. 1, apart from Ni(II) concentration.

Fig. 4. Relationships between peak current and adsorption potential for 10 μg Ni l^{-1} without and with surfactant: (a) without surfactant; (b) 200 μg l^{-1} PEG-400; (c) 200 μg l^{-1} PEG-4000; (d) 200 μg l^{-1} Triton X-100. Conditions as for Fig. 1, apart from adsorption potential.

weight of the surfactant. Figure 4 illustrates the dependence of I_p on the adsorption potential in the presence of PEG-400 (curve b), PEG-4000 (curve c) and Triton X-100 (curve d); PEG-4000 acts as a stronger surfactant than PEG-400, but both are weaker than Triton X-100. A similar dependence of tensammetric peak heights on the molecular weight of PEGs was described by Batycka and Łukaszewski [14]. In contrast to Triton X-100 (curve d),

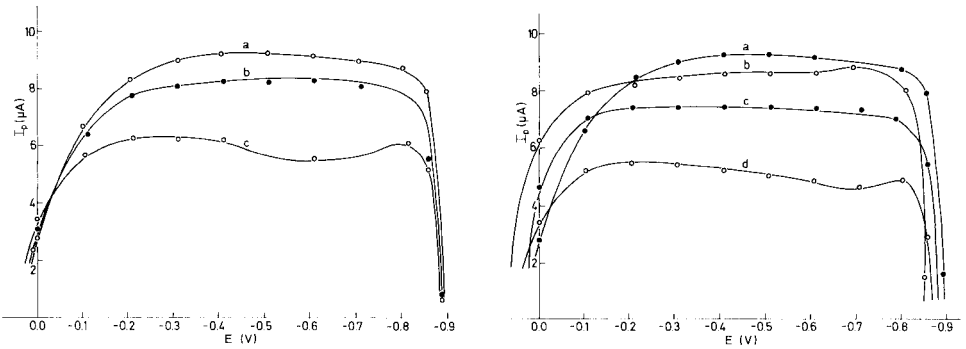

Fig. 5. Dependence of peak current on the adsorption potential with and without surfactant: (a) without surfactant; (b) 200 μg l^{-1} TBS; (c) 200 μg l^{-1} Aerosol OT. Conditions as for Fig. 4.

Fig. 6. Dependence of peak current on adsorption potential without and with surfactant: (a) without surfactant; (b) 200 μg l^{-1} tetramethylammonium tetrafluoroborate; (c) 200 μg l^{-1} tetramethylammonium hydroxide; (d) 200 μg l^{-1} Cetrimide. Conditions as for Fig. 4.

the excess of electric charge on the electrode has an insignificant influence on the adsorption of PEGs (curve b and c) in the observed range of accumulation potentials.

Of the anionic surfactants tested, only Aerosol OT inhibits the adsorption of $Ni(DMG)_2$. Figure 5 shows the relationship between I_p and accumulation potential in the presence of TBS (curve b) and Aerosol OT (curve c). In this potential range at a similar concentration, PDS showed no marked influence on the adsorption of $Ni(DMG)_2$.

The cationic surfactants investigated also had a much weaker inhibitory effect on I_p than the nonionic agents. The suppression was most pronounced for Cetrimide (Fig. 6, curve d). Of the two tetramethylammonium surfactants tested, the hydroxide (curve c) inhibited $Ni(DMG)_2$ adsorption more than the tetrafluoroborate (curve b). The accumulation potential with these surfactants exhibits no significant influence on I_p, except for Cetrimide, where there is a small minimum around −0.7 V. Despite the relatively small change in the extent of inhibition at −0.7 and −0.8 V, there is a significant difference in the dependence of I_p on the concentration of Cetrimide, when accumulation is done at each of these potentials (Fig. 7). With adsorption at −0.8 V (curve b), the linear range is much wider than that obtained with accumulation at −0.7 V (curve a). Therefore, the importance of correct selection of the preconcentration potential cannot be underestimated.

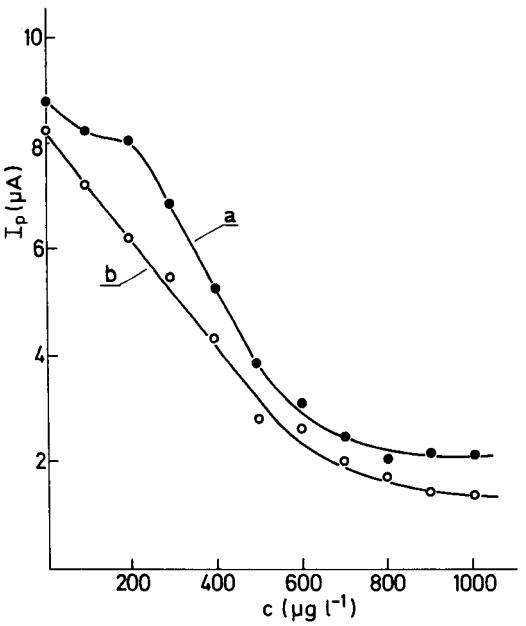

Fig. 7. Dependence of the $Ni(DMG)_2$ peak height on the concentration of Cetrimide. Adsorption potential: (a) −0.7 V; (b) −0.8 V. Other conditions as for Fig. 4.

Analytical application

The results presented above show that the suppression of $Ni(DMG)_2$ adsorption by surfactants could be applied for the voltammetric determination of surface-active substances. The method is very sensitive, but not selective, i.e., it is not possible to differentiate between anionic, cationic and nonionic groups of surfactants. However, with an appropriate adjustment of the accumulation potential and the concentration of nickel(II), it is possible to improve the selectivity when a mixture of surfactants with different properties is investigated.

The precision of results obtained by this indirect method depends mainly on the reproducibility of the $Ni(DMG)_2$ peak height, and is usually below 2% (r.s.d.). The reproducibility of the electrode surface renewal, and of the stirring during the preconcentration step, are the most important parameters influencing the precision of the results.

The recommended procedure given under Experimental enables strong surfactants like Triton X-100 to be determined in the concentration range between 10 and 200 $\mu g\ l^{-1}$. To improve the sensitivity, the concentration of nickel(II) in the cell can be increased to about 30 $\mu g\ l^{-1}$, at which level, the detection limit for Triton X-100 was 1 $\mu g\ l^{-1}$.

The application of the method is not restricted to a stationary electrode. With appropriate adjustment of the concentration of nickel(II), measurements are possible with a dropping mercury electrode. The method might also be automated by adaptation of the flow-injection procedure for the determination of nickel, recently described by Eskilsson et al. [20].

This work was supported by the Research Community of Slovenia.

REFERENCES

1 J. Longwell and W. D. Maniece, Analyst, 80 (1955) 167.
2 H. L. Webster and J. Halliday, Analyst, 84 (1959) 552.
3 C. Hennequin and A. Lerenard, Analusis, 3 (1975) 177.
4 P. Berth, J. Heidrich and G. Jakobi, Tenside Deterg., 17 (1980) 228.
5 G. S. Buchanan and J. C. Griffith, J. Electroanal. Chem., 5 (1963) 204.
6 K. Linhart, Tenside Deterg., 9 (1972) 241.
7 H. Jehring, Elektrosorptionsanalyse mit der Weschelstrompolarographie, Akademie Verlag, Berlin, 1974.
8 Z. Kozarac, V. Žutić and B. Ćosović, Tenside Deterg., 13 (1976) 260.
9 Z. Kozarac, B. Ćosović and M. Branica, J. Electroanal. Chem., 68 (1976) 75.
10 J. P. Hart, W. F. Smyth and B. J. Birch, Analyst, 104 (1979) 853.
11 M. J. Rosen, X. Hua, P. Bratin and A. W. Cohen, Anal. Chem., 53 (1981) 232.
12 B. Ćosović and D. Hršak, Tenside Deterg., 16 (1979) 262.
13 Z. Kozarac, D. Hršak, B. Ćosović and J. Vržina, Environ. Sci. Technol., 17 (1983) 268.
14 H. Batycka and Z. Łukaszewski, Anal. Chim. Acta, 162 (1984) 207, 215.
15 Z. Łukaszewski, H. Batycka and W. Zembrzuski, Anal. Chim. Acta, 175 (1985) 55.
16 R. Kalvoda, Anal. Chim. Acta, 138 (1982) 11; Anal. Chim. Acta, 162 (1984) 197.
17 N. K. Lam and M. Kopanica, Anal. Chim. Acta, 161 (1984) 315.
18 J. Wang, Int. Lab., 15 (1985) 68.
19 B. Pihlar, P. Valenta and H. W. Nürnberg, Fresenius Z. Anal. Chem., 307 (1981) 337.
20 H. Eskilsson, C. Haraldsson and D. Jagner, Anal. Chim. Acta, 175 (1985) 79.

Analytica Chimica Acta, 189 (1986) 237—243
Elsevier Science Publishers B.V., Amsterdam — Printed in The Netherlands

LIQUID-STATE MERCURY(II) ION-SELECTIVE ELECTRODE BASED ON *N*-(O,O-DIISOPROPYLTHIOPHOSPHORYL)THIOBENZAMIDE

WALENTY SZCZEPANIAK* and JOLANTA OLEKSY

Faculty of Chemistry, A. Mickiewicz University, ul. Grunwaldzka 6, 60-780 Poznań (Poland)

(Received 2nd May 1986)

SUMMARY

A liquid ion-exchange electrode containing a complex of mercury(II) with *N*-(O,O-diisopropylthiophosphoryl)thiobenzamide in carbon tetrachloride is described. The electrode shows excellent sensitivity and good selectivity. The slope of the calibration graph is 29.0 mV/pHg^{2+} in the pHg^{2+} range 2—15.2 in mercury(II) ion buffers. The electrode can be used for determination of 5×10^{-5}—10^{-2} M Hg(II) in the presence of 10^{-2} M Cu(II), Ni(II), Co(II), Zn(II), Pb(II), Cd(II), Mn(II), Fe(III), Cr(III), Bi(III) or Al(III) ions and in the presence of 10^{-3} M Ag(I) ions. It can be also used for end-point detection in titrations with EDTA of 10^{-3}—10^{-4} M mercury(II) at pH 2.

Few papers describing mercury(II) ion-selective electrodes with liquid or solid membranes have been published. Solid-membrane electrodes based on mercury(II) chalcogenides [1—3] have low ohmic resistance and are easily made. These electrodes are useful for end-point detection in the titration of mercury(II), but their lack of reproducible response with time makes them unattractive for direct potentiometric monitoring or for investigations of complex formation. Liquid-membrane electrodes based on the mercury(II) complex with dithizone [4] or 1-(2-pyridylazo)-2-naphthol [5] do not provide suitable selectivity coefficients in relation to Ag^+ and Fe^{3+}, which are usually present in real samples. Thus, further investigations of new electrode systems are justified in attempts to obtain an electrode with better parameters. Systems based on other mercury(II) chelates dissolved in suitable organic solvents offer such possibilities.

In this paper, the complex of a phosphorylated thiobenzamide [PTB; HL; *N*-(O,O-diisopropylthiophosphoryl)thiobenzamide] with mercury(II) is proposed as the active substance in a liquid-exchange electrode sensitive to mercury(II) ions. The PTB forms a mercury(II) complex of the type HgL_2

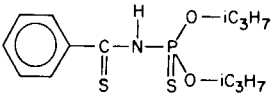

(HL)

0003-2670/86/$03.50

[6]. This complex is very stable (HgL_2, $\log \beta = 35.35$) compared to other metals such as Ag(I) (AgL, $\log \beta = 16.31$) and Ni(II) (NiL_2, $\log \beta = 8.39$) [6]. Furthermore, PTB has a high extraction coefficient into carbon tetrachloride over a wide pH range (from 3.5 M sulfuric acid). Only Ag(I) and Cu(II) are also extracted from acidic medium. Complexes of Co(II), Ni(II), Cd(II), Pb(II) and Zn(II) are extracted from alkaline solutions and Fe(III) is not extracted at all.

EXPERIMENTAL

Liquid ion-exchanger and reagents

The PTB was prepared by reaction of benzonitrile with diisopropyldithiophosphoric acid [7]. The crude compound was purified by liquid adsorption chromatography on a silica-gel column followed by recrystallization from hexane. The melting point of the purified compound was 58—59°C. A 10^{-2} M solution of the mercury(II) complex with PTB in carbon tetrachloride was used as the liquid ion-exchanger. It was prepared by shaking 10^{-2} M PTB solution in carbon tetrachloride with excess of 10^{-2} M mercury(II) nitrate in 10^{-2} M nitric acid, separation of the phases and drying of the organic phase over sodium sulfate.

All reagents used were of analytical grade. Standard solutions of mercury(II) were prepared by serial dilution with 10^{-2} M nitric acid (down to 10^{-5} M) from a 0.1 M stock solution or by preparing metal buffers for more dilute solutions.

Construction of the electrode

A modified teflon body, similar to one described earlier [8], was used in the electrode construction. The different design was necessary because a different internal reference electrode was used. The simplified scheme of the electrode is shown in Fig. 1. A silanized filter disc (Sartorius type SM-113-06) saturated with ion-exchanger solution was used as the liquid membrane. The internal electrode was a silver/silver chloride electrode with salt bridge. The internal solution was 10^{-2} M mercury(II) nitrate in nitric acid. The potential was measured vs. a double-junction silver/silver chloride electrode with a 1 M KNO_3 salt bridge.

The measuring cell was

Ag/AgCl	1 M KCl	1 M KNO_3	internal solution	liquid membrane	test solution	1 M KNO_3	1 M KCl	AgCl/Ag

The e.m.f. was measured (±0.1 mV) with a N-512 pH meter (ELPO, Poland) connected to a V-544 digital voltmeter (Meratronik, Poland) and a G_1B_1 recorder (Carl Zeiss, Jena, G.D.R.).

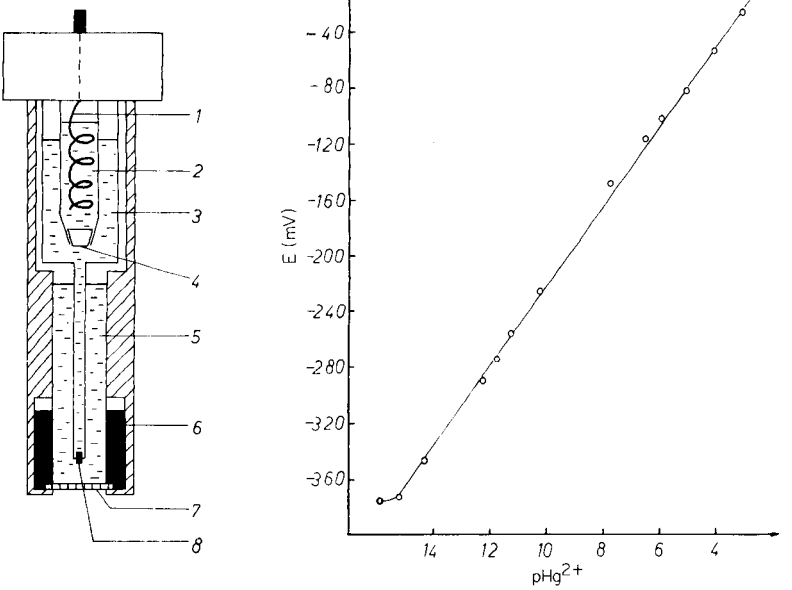

Fig. 1. Diagram of the electrode: (1) Ag/AgCl; (2) 1 M KCl; (3) 1 M KNO_3; (4) glass joint; (5) internal solution; (6) ion-exchanger reservoir; (7) membrane; (8) asbestos fibre junction.

Fig. 2. The calibration curve in mercury(II) ion buffers.

RESULTS AND DISCUSSION

Problem of an internal reference electrode

Because of high stability of chloromercury complexes a conventional silver/silver chloride electrode cannot be used as the internal electrode. In previous electrodes, this problem was avoided by having a conducting material directly in contact with the membrane [4, 5]. In the present case, the internal resistance was high, so that this type of construction (hydrophobic graphite saturated with ion-exchanger) was unsuitable. Thus, the possibility of using other internal electrodes was examined. Silver, platinum, Ag(Hg), Au(Hg) and a half-cell with salt bridge Ag/AgCl|1 M KCl|1 M KNO_3 were tested. The best results (stable and reproducible potential) were obtained with the half-cell and so it was used in the construction of the electrode.

Calibration and response time of the electrode

The electrode response at Hg^{2+} concentrations below 10^{-5} M was examined in mercury(II) ion buffers based on the equilibria of the mercury(II) chloride, bromide and acetate complexes. The composition of these solutions is presented in Table 1. The ionic strength was 0.1 M (KNO_3) in all solutions.

The e.m.f./log c relationship was found to be linear over the concentration range pHg^{2+} = 2—15.2 with a correlation coefficient of 0.9993 (Fig. 2). The slope of the calibration graph is 29.0 mV/decade change in concentration, which is very close to the theoretical Nernstian slope.

The response time of the electrode depends on the concentration of the solution investigated. It is ca. 30 s for 10^{-2} and 10^{-3} M solutions and ca. 1 min for more dilute solutions.

Effect of pH and various cations

The influence of pH on the electrode potential was tested over the range 1—4 for 10^{-3} and 10^{-4} M mercury(II) nitrate. The ionic strength was adjusted to 1.0 by the addition of KNO_3. Changes in the electrode potential for pH > 2.5 result from the changes in the Hg^{2+} ion concentration. However, the decrease in the electrode potential for pH < 2 is probably connected with changes in liquid-junction potential. This effect depends clearly on the salt bridge solution (Fig. 3a). When the electrode potential was corrected for the liquid-junction potential estimated from the Henderson equation, the e.m.f./pH relationship was linear (within ±5 mV) over the pH range 1.0—2.0 (Fig. 3b). Thus, hydrogen ions even at 0.1 M concentration do not participate directly in the creation of the electrode potential connected with the ion-exchange reaction across the membrane/aqueous solution interface. They only cause changes in liquid-junction potential or in the concentration of Hg^{2+}.

The electrode can be used at pH 1.5—4 (at constant pH for a given set of solutions).

Table 2 presents the selectivity coefficients for the electrode which were determined by mixed solution method [11]. For this purpose, the electrode potentials were measured for solutions containing only Hg^{2+} ions (10^{-4} M) and solutions with Hg^{2+} ions (10^{-4} M) and interfering ions Me^{z+} (10^{-2} M). The values of the selectivity coefficients show that the electrode has high selectivity for mercury(II) ion relative to many divalent cations, as well as to Fe^{3+}, Al^{3+}, Cr^{3+} and Bi^{3+}. Only Ag^{+} ions interfere significantly.

TABLE 1

Composition of the mercury(II) ion buffers used for calibration of the electrode

Ligand	Concn.[b] (10^{-3} M)	pH	pHg^{2+} [a]	Ligand	Concn.[b] (10^{-3} M)	pH	pHg^{2+} [a]
Acetate	1.0	4.5	5.9	Chloride	6.0	2.0	11.8
Acetate	3.0	4.5	6.5	Chloride	10.0	2.0	12.2
Acetate	1.0	5.5	7.7	Bromide	1.0	2.0	14.3
Chloride	1.0	2.0	10.2	Bromide	3.0	2.0	15.2
Chloride	3.0	2.0	11.2	Bromide	6.0	2.0	15.9

[a] pHg^{2+} was calculated at $c_{tot.}$ = 10^{-3} M Hg(II), I = 0.1 M (KNO_3), log β_{HgCl^+} = 6.74, log β_{HgCl_2} = 13.22, log β_{HgBr^+} = 9.05, log β_{HgBr_2} = 17.3 [9], log $\beta_{Hg(AcO)_2}$ = 8.43 [10]. [b] Equilibrium concentration of free ligand.

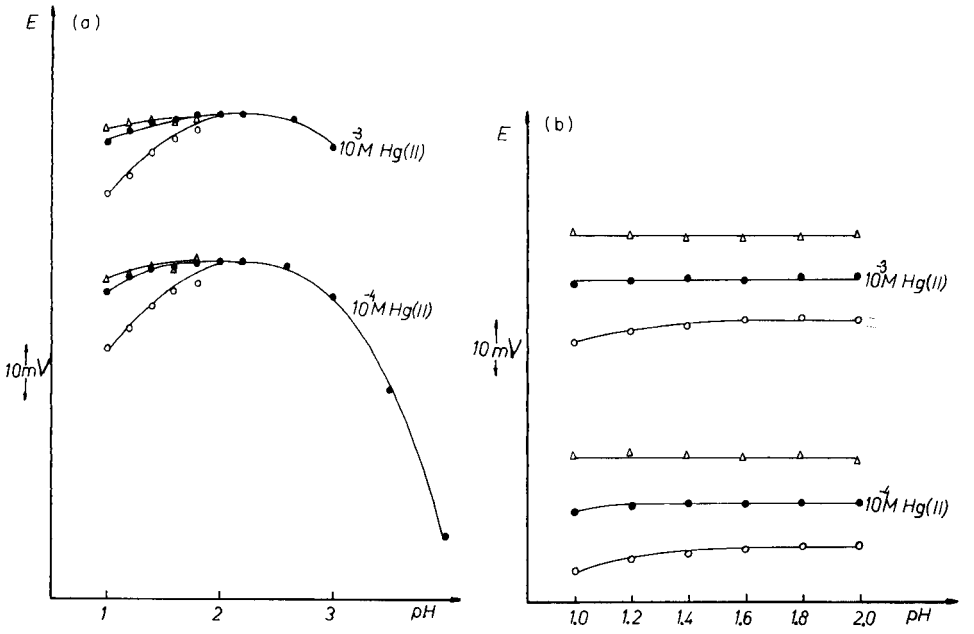

Fig. 3. Effect of pH for various salt bridge solutions: (○) 0.1 M KNO_3; (●) 1 M KNO_3; (△) 2 M KNO_3. (a) Experimental values of the electrode potential; (b) the electrode potential corrected for the liquid-junction potential estimated from the Henderson equation.

TABLE 2

Selectivity coefficients at pH 2.0 and ionic strength 0.2 M (KNO_3)[a]

Cation	$K^{pot}_{Hg^{2+}/Me^{z+}}$	Cation	$K^{pot}_{Hg^{2+}/Me^{z+}}$	Cation	$K^{pot}_{Hg^{2+}/Me^{z+}}$
Fe^{3+}	3.9×10^{-4}	Zn^{2+}	1.4×10^{-3}	Sr^{2+}	5.7×10^{-4}
Al^{3+}	3.4×10^{-4}	Co^{2+}	2.4×10^{-3}	Ba^{2+}	9.1×10^{-4}
Cr^{3+}	3.5×10^{-4}	Pb^{2+}	2.5×10^{-3}	Mn^{2+}	2.5×10^{-3}
Bi^{3+}	6.2×10^{-4}	Cd^{2+}	1.0×10^{-3}	Tl^{+}	$< 2.4 \times 10^{-2}$
Cu^{2+}	1.9×10^{-3}	Ca^{2+}	1.2×10^{-3}	Ag^{+}	0.96
Ni^{2+}	1.2×10^{-3}	Mg^{2+}	4.0×10^{-4}		

[a]Measured for 10^{-4} M Hg^{2+} and 10^{-2} M Me^{z+}.

Analytical application

The electrode described can be used for the determination of mercury(II) ions in unbuffered solutions by direct potentiometry in the concentration range 10^{-5}—10^{-2} M. Figure 4 presents calibration graphs in the presence of various interfering ions at constant concentration. It is possible to determine 5×10^{-5}—10^{-2} M Hg(II) ions in the presence of 10^{-2} M Cu(II), Ni(II), Zn(II), Co(II), Pb(II), Cd(II), Mn(II), Ca(II), Sr(II), Ba(II), Fe(III), Al(III), Bi(III) or Cr(III) and in the presence of 10^{-3} M Ag(I) ions.

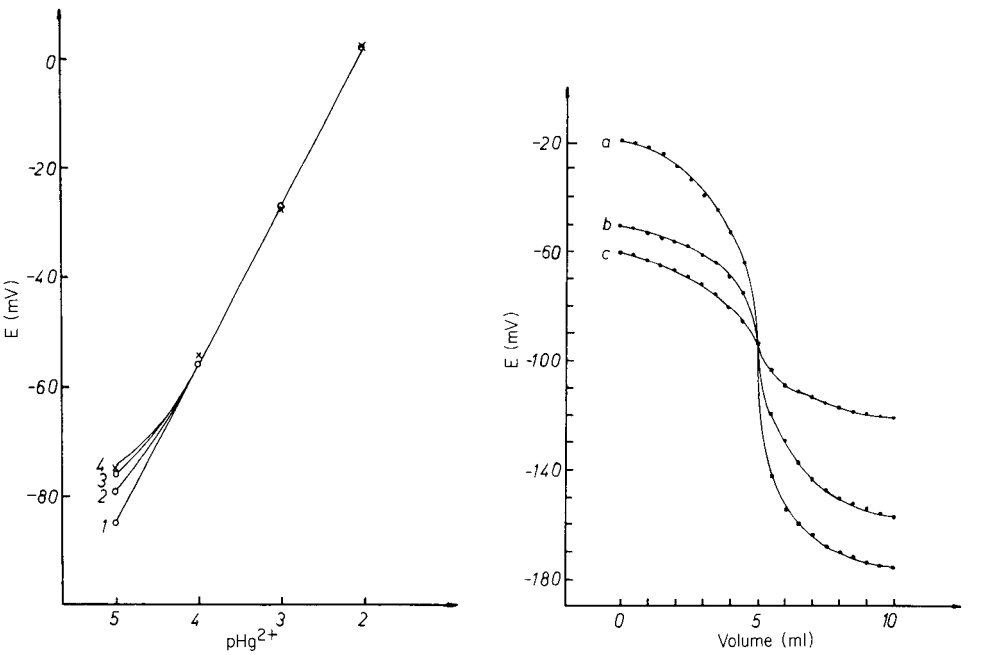

Fig. 4. Calibration graphs in solutions containing interfering ions at a concentration of 10^{-2} M (pH 2): (1) Hg(II) and Hg(II) with Mg(II), Sr(II), Ba(II) or Ca(II); (2) Hg(II) with Fe(III), Al(III), Bi(III) or Cr(III); (3) Hg(II) with Cu(II), Ni(II), Zn(II), Co(II), Pb(II), Cd(II) or Mn(II); (4) Hg(II) with 10^{-3} M Ag(I) (×).

Fig. 5. Potentiometric titration of Hg(II) with EDTA solution of one order higher molarity at pH 2.0 in nitric acid: (a) 10^{-3} M Hg(II); (b) 10^{-4} M Hg(II); (c) 5×10^{-5} M Hg(II).

TABLE 3

A statistical evaluation of mercury(II) determination by potentiometric titration with EDTA

Hg(II) content[a] (mg)	Average value ± confidence interval (95%)[b] (mg)	Relative standard deviation[b] (%)
0.50	0.51 ± 0.03	5.2
5.02	5.02 ± 0.05	0.8
10.03	10.03 ± 0.06	0.5

[a]In 50 ml of solution. [b]$n = 5$.

The application of the electrode for end-point detection in the titration of mercury(II) was also examined. Figure 5 presents examples of potentiometric titration curves for Hg(II) solutions titrated with EDTA at pH 2. This concentration of H^+ ions eliminates the influence of many cations which form complexes with EDTA at higher pH. The end-points were determined

numerically as inflection points of the approximate spline function [12] on the experimental points. The determination of mercury(II) by these potentiometric titrations was statistically evaluated (Table 3). Satisfied reproducibility was achieved for mercury(II) solutions at concentrations $\geqslant 10^{-4}$ M. The titration of 5×10^{-5} M Hg(II) was possible but the reproducibility was poor.

This work was financially supported by Problem MR.I.32/I.10.

REFERENCES

1 J. Růžička and C. G. Lamm, Anal. Chim. Acta, 53 (1971) 206.
2 M. Neshkova and H. Sheytanov, in E. Pungor (Ed.), Conference on Ion-selective Electrodes, Akademia Kiado, Budapest, 1977, p. 503.
3 G. A. East and I. A. Da Silva, Anal. Chim. Acta, 148 (1983) 41.
4 J. Růžička and J. Chr. Tjell, Anal. Chim. Acta, 51 (1970) 1.
5 V. V. Cosofret, P. G. Zugravescu and G. E. Baiulescu, Talanta, 24 (1977) 461.
6 V. F. Toropova, G. A. Lazareva, F. M. Batyrshina and M. G. Zimin, Zh. Anal. Khim., 37 (1982) 1739.
7 A. N. Pudovik, R. A. Cherkasov, M. G. Zimin and N. G. Zabirov, Izv. Akad. Nauk USSR, (1979) 861.
8 K. Ren and W. Szczepaniak, Chem. Anal. (Warsaw), 21 (1976) 1365.
9 J. Inczedy, Równowagi Kompleksowania w Chemii Analitycznej (The Complexes Formation Equilibria in Analytical Chemistry), PWN, Warsaw, 1979.
10 V. P. Gladyshev, S. A. Levickaya and L. M. Filipova, Analiticheskaya Khimya Rtuti (Analytical Chemistry of Mercury), Nauka, Moskva 1974.
11 Commission on Analytical Nomenclature, Pure Appl. Chem., 48 (1976) 129.
12 K. Ren and A. Ren-Kurc, Talanta, in press.

Analytica Chimica Acta, 189 (1986) 245—252
Elsevier Science Publishers B.V., Amsterdam — Printed in The Netherlands

USE OF A NITRATE-SELECTIVE ELECTRODE FOR PERRHENATE AND PERCHLORATE

M. GEISSLER* and R. KUNZE

Research Institute for Non-Ferrous Metals, VEB Mansfeld Kombinat "W. Pieck", Lessingstraße 41, 9200-Freiberg (German Democratic Republic)

(Received 19th May 1986)

SUMMARY

The nitrate-selective membrane electrode based on tributyloctadecylphosphonium nitrate can be used to quantify perrhenate and perchlorate after appropriate conditioning of the membrane. Near-Nernstian responses are obtained for 10^{-3}—10^{-6} M perrhenate and 10^{-2}—4×10^{-6} M perchlorate. Iron(II), copper(II) and chloride do not interfere in moderate amounts; other interferences are discussed. Rhenium leaches are analysed after suitable sample preparation. The electrode is useful in following the potentiometric titration of perrhenate with nitron.

Several nitrate-selective electrodes have been described [1]; almost all are based on a poly(vinyl chloride) membrane containing a suitable ion-exchanger and mediator/solvent. Tributyloctadecylphosphonium nitrate has been used as the ion-exchanger [2—4]. Perrhenate-sensitive electrodes have been based on the perrhenate salts of tetraoctylammonium [5], tetraphenylarsonium [6] and tetradecylammonium [7] ions. A liquid-membrane perrhenate-selective electrode based on chromium(III) stearate has been described [8]. Various electrodes responding to perchlorate ions have also been reported [9—11]. In this report, the behaviour of the nitrate-selective electrode described earlier [2, 3] towards perrhenate and perchlorate is discussed.

EXPERIMENTAL

Apparatus and reagents

A digital pH-meter (MV-870; VEB Präcitronic, Dresden) and a potentiograph (E-536; Metrohm Herisau) were used. The nitrate-sensitive membrane electrode was a Sensitrode filled with 0.05 M copper(II) nitrate as inner electrolyte and having a copper Sensitrode as inner reference electrode (VEB Kombinat Keramische Werke Hermsdorf, Hermsdorf, G.D.R.). The external reference was a saturated calomel electrode (KE-10; Research Institute Meinsberg, Waldheim, G.D.R.). These electrodes were inserted into solutions directly.

0003-2670/86/$03.50

All chemicals used were of analytical-reagent grade. Deionized water was used throughout.

Nitron formate solution (0.1 M) was prepared by dissolving 8 g of nitron in some water by addition of 35 ml of formic acid (1.193 g ml^{-1}) at room temperature and diluting to 200 ml with deionized water. The solution was filtered through a 1G4 sintered-glass frit to remove any residue and diluted to 250 ml in a volumetric flask with water. The nitron formate solution thus prepared was at pH 3; it was stored in a dark glass flask.

Procedures

Membrane electrode preparation. Before starting measurements, the electrode was preconditioned in 1×10^{-4} M ammonium perrhenate for 30 min. If the electrode had been previously conditioned in 1×10^{-3} M potassium nitrate [12], it had to be conditioned again as described above for measurements of perrhenate (and vice versa). The nitrate Sensitrode could be used as a perchlorate electrode if it was conditioned in 1×10^{-4} M sodium perchlorate for 30 min.

Procedure for rhenium in leaches. An aliquot (1—5 ml) of the rhenium leach was diluted with about 80 ml of deionized water, acidified with sulfuric acid (1 + 1), heated to 70°C and oxidized with saturated potassium permanganate solution until the pink colour persisted. After 20 min, the excess of permanganate was reduced with saturated oxalic acid solution, 20 ml of 0.37 M iron(III) chloride and 50 ml of water were added, and 30 min later hydroxides were precipitated by the addition of 20 ml of a zinc oxide suspension (200 g l^{-1}). After vigorous shaking, the mixture was transferred to a 250-ml calibrated flask, diluted to volume and left overnight. The colourless supernatant liquid (green solutions are not usable) was filtered through paper and 25 ml of the filtrate was placed in a 50-ml calibrated flask and diluted to volume after addition of 5 ml of 1 M sodium sulfate. This solution was used for the measurement of perrhenate as described above. The standard addition method was used to evaluate the concentration of perrhenate in these leaches. Two portions of the original leach were taken through the above procedure with and without standard addition.

Determination of the titration factor. The titration factor was evaluated by titrating a precisely measured volume of 0.0537 M ammonium perrhenate (10 mg ml^{-1} Re) with the nitron formate solution. The standard ammonium perrhenate solution was prepared by weighing ammonium perrhenate (99.99%, dried at 105°C) and dissolving in the appropriate volume of deionized water in a volumetric flask.

RESULTS AND DISCUSSION

The nitrate Sensitrode is a membrane electrode prepared by mixing dissolved poly(vinyl chloride) and tributyloctadecylphosphonium nitrate in a mixture of *o*- and *p*-nitrophenyl-n-hexyl ether. The trigonal planar nitrate

(the radius, r, of the complex ion is 0.189 nm) can be exchanged by the tetrahedral perrhenate ($r \approx 0.25$ nm) or perchlorate ion ($r = 0.236$ nm). This ion-exchange is done simply by preconditioning of the electrode membrane in ammonium perrhenate or perchlorate solution. Nitrate solution is used as the internal electrolyte in all cases. The ion-exchange processes described are reversible.

Response of the electrode to perrhenate and perchlorate

Figure 1 shows the potential dependence of the nitrate Sensitrode on perrhenate concentration in 0.1 M sodium sulfate. The calibration plots are linear at both pH 3 and pH 6, with a working range of 10^{-3}—10^{-6} M perrhenate. The lower limit of detection for perrhenate calculated from the curves is 4×10^{-7} M. The calibration curves for pH 3 and pH 6 are essentially parallel with a potential difference of 4—6 mV. The slopes of the linear portions are super-Nernstian, being 63.5 mV per decade at pH 3 and 62.0 mV per decade at pH 6. It can be seen from Fig. 1 that the measured points deviate from the lines for concentrations of 10^{-3} and 10^{-2} M perrhenate at both pH 3 and pH 6. It was therefore necessary to calculate the activities. From the tables published by Kielland [13], it was assumed that the k value for perrhenate is the same as that for permanganate or perchlorate, i.e., $k = 3.5$. At a total ionic strength $I = 0.2$ and $k = 3.5$, the individual activity coefficient $f_i(ReO_4^-)$

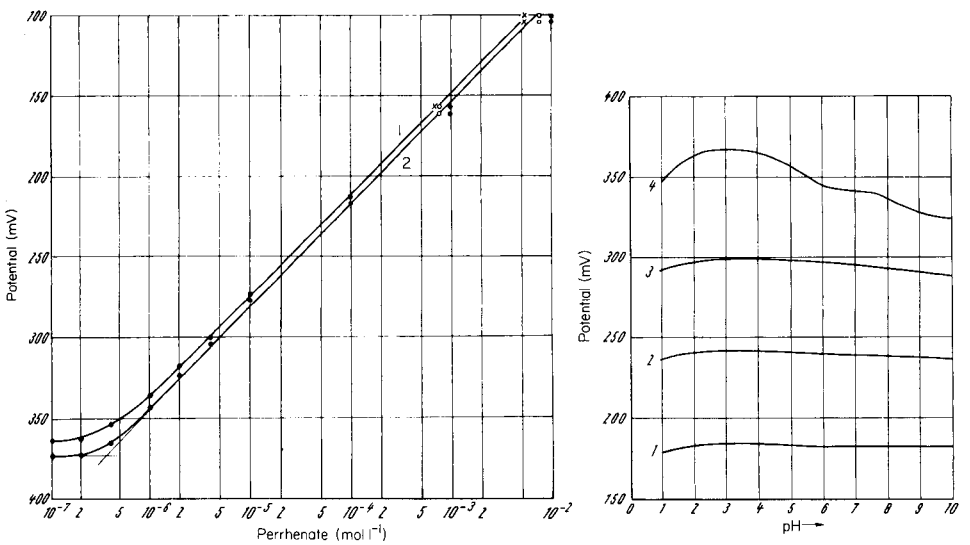

Fig. 1. Calibration curves for perrhenate: (1) pH 3; (2) pH 6. Corrected points: (○) $f_i(ReO_4^-) = 0.76$; (×) $f_i(ReO_4^-) = 0.55$.

Fig. 2. Potential/pH diagram: (1) 10^{-3}; (2) 10^{-4}; (3) 10^{-5}; (4) 10^{-6} M perrhenate, all in 0.1 M sodium sulfate. Adjustment of pH with H_2SO_4 or NaOH (glass electrode). Potential response time 3 min.

presented in the Kielland tables is 0.76. The activities calculated with this activity coefficient for the concentrations mentioned above are 7.6×10^{-4} and 7.6×10^{-3} M perrhenate, respectively. The measured points for 7.6×10^{-4} M perrhenate then fit the lines well, but not those for 7.6×10^{-3} M perrhenate. From the equation $\log f_{\pm} = -0.5093 z_+ z_- I^{1/2}$, the mean activity coefficient $f_{\pm}$ can be calculated. The value obtained for $I = 0.2$ is $f_{\pm} = 0.55$ and the measured points for 5.5×10^{-3} M perrhenate are then near the calibration lines (Fig. 1). Obviously, the individual activity coefficient for perrhenate lies in the range 0.55—0.76.

The potential response of the Sensitrode is influenced by pH. Figure 2 shows the potential/pH diagram in the pH range 1—10 for four levels of perrhenate activity. These curves demonstrate that the electrode potentials are independent of pH between 6 and 7.5.

Measurements over a period of 24 h gave mean potential values $\bar{E}_1 \pm \Delta\bar{E}_1 = 166 \pm 0.4$ mV and $\bar{E}_2 \pm \Delta\bar{E}_2 = 221 \pm 0.2$ mV for perrhenate concentrations of 1.07×10^{-3} M and 1.07×10^{-4} M, respectively, at pH 6; $\Delta\bar{E}$ is the confidence interval calculated for the level of significance $P = 0.95$ and for 24 degrees of freedom. The results were checked for drift. The test quantity PG for drift testing is defined [14] by

$$PG = [\sum(E_j - E_{j+1})^2]/(N-1)s^2$$

where E_j are the potential values, N is the number of values and s the standard deviation. The values calculated were $PG_1 = 0.2576$ and $PG_2 = 0.073$ for the concentrations mentioned above; these are much less than the theoretical value $W = 1.3552$ ($P = 0.95$) [14] needed to ensure that the potential values of long-term measurements are free from drift.

Practical response-time curves [15] of the Sensitrode for different concentration changes are shown in Fig. 3. Obviously, the response time depends on the concentration of the solution to which the electrode was previously exposed. When the concentration is high, the response time is below 2 min (Fig. 3, curves 3 and 4).

Figure 4 shows the calibration curve for perchlorate in 0.1 M sodium sulfate. The working range is 10^{-2}—4×10^{-6} M, and the limit of detection is 3.7×10^{-7} M perchlorate. The Nernstian slope is 56 mV per decade.

Interferences

Important interfering ions for this determination of perrhenate were tested; molybdate, tungstate, vanadate, Fe^{3+}, Cu^{2+} and chloride are present in rhenium leaches. Table 1 lists the tolerable concentrations for chloride at pH 6 and for copper(II) and iron(III) at pH 3 in the measurement of low concentrations of perrhenate. Interfering ion concentrations higher than those shown produce high potential values with chloride and low values with iron and copper.

According to the mixed solution method [16], the selectivity coefficients $k_{i,j}^{pot}$ were calculated from $k_{i,j}^{pot} = a_i/a_j^{z_i/z_j}$ for molybdate, tungstate and vanadate at pH values of 3, 6 and 9. The selectivity coefficients found are listed

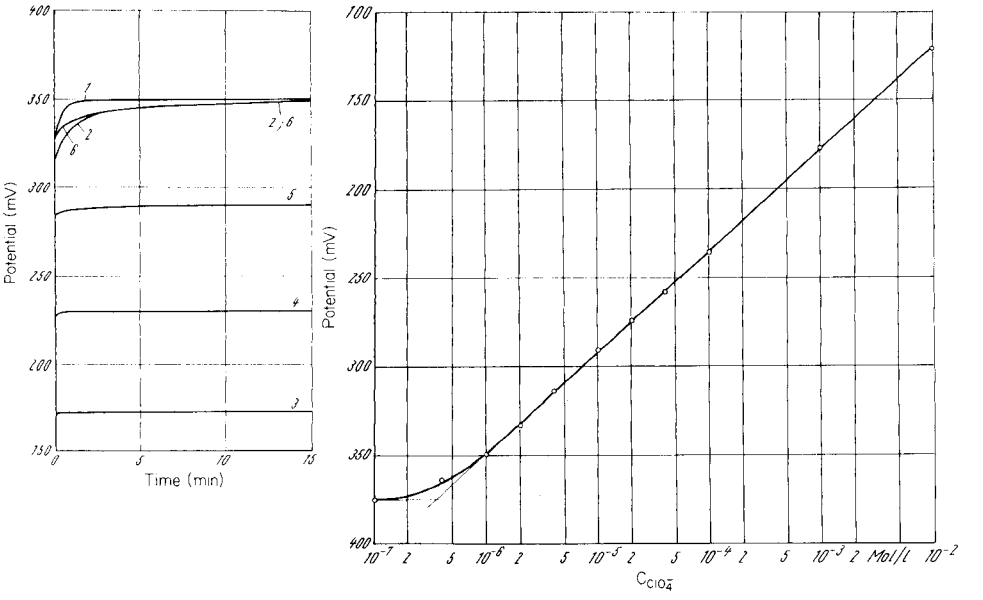

Fig. 3. Practical response-time curves for perrhenate. Change of perrhenate concentrations c_1/c_2 (mol l^{-1}): (1) $0/10^{-6}$; (2) $10^{-3}/10^{-6}$; (3) $10^{-6}/10^{-3}$; (4) $10^{-3}/10^{-4}$; (5) $10^{-4}/10^{-5}$; (6) $10^{-5}/10^{-6}$.

Fig. 4. Calibration curve for perchlorate.

TABLE 1

Permissible concentrations for chloride, Fe^{3+} and Cu^{2+}

Interfering ion j	C_j (M)	$C_{ReO_4^-}$ (M)	pH
Cl^-	5.6×10^{-3}	1.07×10^{-6}	6
Fe^{3+}	3.6×10^{-3}	4.08×10^{-6}	3
Cu^{2+}	3.2×10^{-3}	4.28×10^{-6}	3

in Table 2. These coefficients emphasize that the interferences diminish as the pH is increased. At pH 3, the three ions mentioned interfere badly, especially tungstate. The interferences of all three ions are similar at pH 6, whereas tungstate interferes comparatively less at pH 9.

Application to rhenium-containing leaches

The direct potentiometric determination of perrhenate with the conditioned Sensitrode was investigated in rhenium leaches which were black-brown in colour. The composition of the leaches is complicated, consisting of ca. 10 g l^{-1} Re, 20—60 g l^{-1} sulfate, 5—15 g l^{-1} Mo, W and V each, organic

TABLE 2

Selectivity coefficients for vanadate, molybdate and tungstate

Interfering ion j	a_j (M)	Selectivity coefficient		
		pH 3	pH 6	pH 9
Vanadate[a]	7.63×10^{-3}	3.79×10^{-1}	3.29×10^{-4}	3.86×10^{-4}
Molybdate[b]	3.48×10^{-4}	4.59×10^{-3}	2.47×10^{-4}	—
Tungstate[a]	1.47×10^{-2}	—[c]	1.23×10^{-4}	1.86×10^{-5}
	1.47×10^{-3}	—[c]	1.03×10^{-4}	—

[a] As the sodium salt. [b] As the ammonium salt. [c] The curves could not be utilized.

carbon and residues of solvents, at pH ≈ 8. These metals are all in anionic form in this medium and the appropriate cation is the ammonium ion. Naturally, it is not possible to measure perrhenate by direct potentiometry in such a complicated leach, but only in the filtrate after the separation of the major components, as described under Experimental.

The results obtained for three rhenium leaches are compared in Table 3 with the values found by the spectrophotometric dimethylglyoxime method [17] after the same separation procedure. The agreement of the results is satisfactory for this complicated matrix. When the content of rhenium is bigger than 10 g l^{-1}, then the potentiometric method gives a larger scatter but the spectrophotometric method is also not without problems.

Potentiometric precipitation titration

Perrhenate can be precipitated by nitron [4,5-dihydro-2,4-diphenyl-5-(phenylimino)-1H-1,2,4-triazolium hydroxide] from 0.02 M sulfuric acid at 80°C with a 5% (w/v) nitron acetate solution in excess [18]. After cooling in ice water and settling for about 2 h, the precipitate is washed nitron-free, dried and weighed. The nitron perrhenate is best formed at higher temperature but the solubility of the compound must be lowered by cooling. An attempt was made to use the conditioned nitrate Sensitrode to follow the precipitation of perrhenate with nitron at 5 and 20°C. Figure 5 shows the titration curve obtained for 50 mg of rhenium in 100 ml of solution with 0.1 M nitron formate [11] at 5°C in 0.1 M sodium sulfate adjusted to pH 3 by addition of formic acid; the potentiograph was adjusted so that the titrant flow was not greater than 0.5 ml min^{-1}. Under these conditions, it was possible to titrate 30—100 mg ml^{-1} rhenium with nitron formate solution; the results obtained at 5 and 20°C were similar. When the concentration of the nitron formate solution was less than 0.1 M, the titration curves found were very flat and even more unsymmetrical. In such cases, straightforward graphic determination of the inflection point was inexact, and Gran plots were applied.

TABLE 3

Results for the potentiometric and spectrophotometric determination of rhenium

Sample no.	Rhenium found (g l^{-1})[a]	
	Potentiometry	Spectrophotometry
2	12.9 ± 1.7	12.8 ± 0.6
5	8.7 ± 0.3	8.4 ± 0.3
7	9.9 ± 0.1	9.4 ± 0.3

[a]Mean and confidence interval (P = 0.95) for 8 determinations.

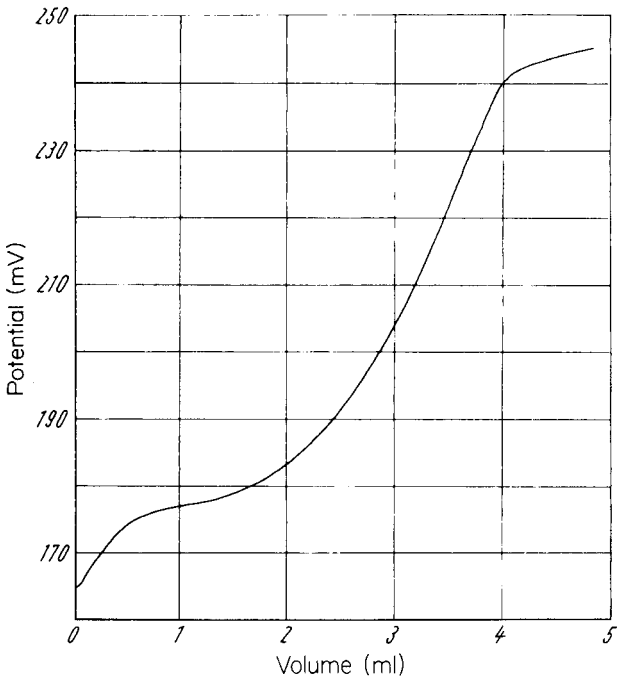

Fig. 5. Titration curve recorded for the precipitation of perrhenate with nitron formate at 5°C. For detail, see text.

REFERENCES

1 J. Koryta and K. Štulík, Ion-selective Electrodes, 2nd edn., Cambridge University Press, 1983.
2 J. Siemroth, I. Hennig and P. Hartmann, Wirtschaftspatent 127 372 Int. Cl. 3 (51) G 01 N 27/30, 1977.
3 U. Grünke, P. Hartmann and J. Siemroth, Hermsdorfer Techn. Mitt., 48 (1977) 1547.
4 H.-P. Vielmeyer, I. Dahse and U. Grünke, Wirtschaftspatent 210 352, Int. Cl. 3 (51) G 01 N 27/30, 1982.
5 W. N. Golubev and T. A. Filatova, Electrochim., 10 (1974) 1123.

6 W. A. Zarinskij, O. M. Petruchin, V. M. Trepalina and L. K. Shpigun, Zh. Anal. Khim., 31 (1976) 1191; W. A. Zarinskij, L. K. Shpigun, V. M. Trepalina and J. V. Volobureva, Zavod. Lab., 43 (1977) 941.
7 Sh. K. Norov, W. W. Palzevskij and E. S. Gureev, Zh. Anal. Khim., 31 (1977) 2394.
8 M. M. Mansurov, G. L. Semenova, Ch. M. Jakubov and A. A. Pendin, Zh. Anal. Khim., 40 (1985) 7, 1267.
9 A. C. Wilson, Talanta, 23 (1976) 387.
10 F. Jasmin, Iraqi J. Sci., 20 (1979) 430.
11 K. Hiiro, A. Kawahara and T. Tanaka, Anal. Chim. Acta, 110 (1979) 321.
12 M. Geißler and R. Kunze, Fresenius Z. Anal. Chem., 314 (1983) 560.
13 J. Kielland, J. Am. Chem. Soc., 59 (1937) 1675.
14 W. Gottschalk, Analytiker-Taschenbuch, Akademie-Verlag Berlin 1980, Bd. 1, p. 69.
15 G. G. Guilbault, Pure Appl. Chem., 51 (1981) 1907.
16 E. Pungor and K. Toth, Anal. Chim. Acta, 47 (1969) 291.
17 B. T. Kenna, Anal. Chem., 33 (1961) 1130.
18 W. Prodinger, Organische Fällungsmittel in der Quantitativen Analyse. Die chemische Analyse, Bd. 37, 3, Auflage, Ferdinand Enke, Stuttgart, 1954.

Analytica Chimica Acta, 189 (1986) 253—262
Elsevier Science Publishers B.V., Amsterdam — Printed in The Netherlands

COMBINED USE OF ELECTROANALYTICAL METHODS TO DERIVE CALIBRATION PLOTS FOR SPECIES DIFFICULT TO STANDARDIZE

PAOLO UGO, SALVATORE DANIELE and GIAN-ANTONIO MAZZOCCHIN

Department of Spectroscopy, Electrochemistry and Physical Chemistry, University of Venezia, Dorsoduro 2137, 30123 Venezia (Italy)

GINO BONTEMPELLI*

Department of Analytical, Inorganic and Metallorganic Chemistry, University of Padova, via Marzolo 1, 35131 Padova (Italy)

(Received 10th April 1986)

SUMMARY

A simple method is described for the derivation of calibration graphs for electroactive analytes which are difficult to standardize from a calibration for an easily standardized reference species dissolved in the same medium. The method is based on evaluation of the ratios between the current-signals recorded for the analyte and for the reference solution by rotating-disk-electrode voltammetry and by an electroanalytical technique based on stationary electrodes which provides purely diffusion-controlled responses (e.g., chronoamperometry or normal-pulse voltammetry). This approach can be applied to all electroactive species which undergo diffusion-controlled processes, regardless of the degree of reversibility involved. Reliability tests, done with electroactive organic species dissolved in dimethyl sulphoxide, show that both accuracy and precision are within ±5%. The method is applied to the determination of hydrogen and oxygen solubilities in dimethyl sulphoxide and acetonitrile, respectively, as an example of quantitative evaluations of species which are difficult to standardize.

Quantitative analysis by electroanalytical techniques such as voltammetry is usually achieved by comparing the response obtained for the required analyte in the sample with similar signals provided by exactly known amounts of the same species. This procedure is standard usage for the determination of many compounds but it cannot be applied to evaluate the concentration of electroactive species for which a standard sample is not available for comparison. For instance, the method can be awkward to apply to analytes which are difficult to handle (e.g., gaseous solutes) or to substances which cannot be prepared in pure form (e.g., by-products of a new synthetic route or metabolites of a drug). This difficulty cannot be overcome by resorting simply to the usual internal standard method because the signals depend on the characteristics of the electroactive species (e.g., diffusion coefficients and number of electrons involved) which can differ markedly from one substance to another, especially in organic media. Standardization procedures can, of course, be avoided in quantitative electro-

0003-2670/86/$03.50

analysis by using bulk electrolysis but these are generally time-consuming and can seriously affect the bulk equilibrium conditions, which would be particularly misleading when dissolved gases have to be determined.

In the present paper, a method is proposed for evaluating the concentration of analytes which are difficult to standardize. The method is based on combined use of two types of electroanalytical measurements, which are applied both to the solution of the "unstandardizable" analyte and to solutions containing known amounts of a different easily-standardizable electroactive species in the same medium. This method, which actually involves conversion of calibration curves, is applied to the determination of the hydrogen and oxygen solubilities in dimethyl sulphoxide (DMSO) and acetonitrile, respectively, as typical examples. The satisfactory agreement of the results found with literature data [1, 2] indicates the effectiveness of the proposed procedure.

EXPERIMENTAL

Chemicals

All the chemicals used were of reagent-grade quality. The purity of the compounds used to test the reliability of the procedure (with the exception of perchloric acid) was examined by thin-layer chromatography and elemental analysis; compounds which gave more than 2% relative errors from the theoretical carbon or hydrogen values were rejected.

Reagent-grade solvents (DMSO and acetonitrile) were purified by recommended procedures [3] and were stored over 0.4-nm molecular sieves under a nitrogen atmosphere.

The supporting electrolyte, tetrabutylammonium perchlorate (TBAP), was recrystallized from methanol and dried under vacuum at 50°C. Stock solutions of anhydrous perchloric acid in DMSO were obtained by anodic oxidation on a platinum electrode of hydrogen gas bubbled through the solvent containing 0.1 M TBAP.

Nitrogen used to remove dissolved oxygen from the working solutions, as well as the oxygen and hydrogen used in solubility measurements, were previously passed through concentrated sulphuric acid to remove traces of water and then equilibrated to the vapour pressure of the solvent.

Apparatus and procedure

Chronoamperometric, normal-pulse voltammetric (n.p.v.) and rotating-disk-electrode (RDE) voltammetric experiments were done in an H-shaped three-electrode cell with cathodic and anodic compartments separated by a sintered glass disk. Perchloric acid was electrogenerated in this cell from hydrogen by using a platinum gauze as the anode and a nickel spiral as the counter electrode (where the solvent discharge occurred).

Linear-sweep voltammetric measurements (l.s.v.) were conducted in a different three-electrode cell in which the working electrode was surrounded

by a platinum spiral counter electrode. Its potential was probed by a Luggin capillary-reference electrode compartment, the position of which was made adjustable by mounting it on a syringe barrel.

An aqueous saturated calomel electrode (SCE) was always used as the reference electrode. It was connected to the cell by a salt-bridge containing the medium relevant to the test solution. Glassy-carbon or platinum disks, mirror-polished with graded alumina powder prior to each set of experiments, were used as working electrodes.

In the n.p.v. tests at solid electrodes, the diffusion layer was renewed at the end of each pulse with a synchronized knocker. In the chronoamperometric, l.s.v. and RDE voltammetric tests, the electroanalytical unit was a three-electrode system assembled with MPI System 1000 equipment or an Amel 552 potentiostat in conjunction with an Amel 568 digital logic-function generator. For n.p.v. experiments, a Tacussel PRT-30-01 potentiostat was used with a Tacussel VAP-4 pulsed control unit. The rotating disk electrode was a Tacussel RDI controlled by a Tacussel Controvit unit. In all cases, an Amel 863 x-y recorder was employed.

In the controlled-potential electrolyses, an Amel 552 potentiostat was used and the associated coulometer was an Amel 731 integrator.

In all measurements, the cells were thermostated at 25.0 ± 0.2°C in a constant-temperature bath.

THEORETICAL CONSIDERATIONS

The current-response provided by all dynamic electroanalytical techniques for a generalized diffusion-controlled redox process is conditioned by the characteristics typical of the electroactive species (diffusion coefficient, D, number of electrons transferred, n, and, in some cases, degree of reversibility), as well as by its bulk concentration, C. In particular, when an electroanalytical technique capable of giving current-signals independent of the degree of reversibility is applied (e.g., chronoamperometry or n.p.v.), the currents recorded at the same electrode on solutions of two different species depend only on the different values of D, n and C. Thus, for instance, the diffusion-controlled current for chronoamperometric measurements is given by the Cottrell equation:

$$i_{chr} = F\,A\,\pi^{-1/2}\,t^{-1/2}\,n\,D^{1/2}\,C \qquad (1)$$

where the symbols have their usual significance.

Consequently, by comparing the signal obtained for an unstandardizable analyte (X) with that relative to an easily-standardized reference species (R), the unknown concentration of X can be calculated from

$$C_X = [i_{chr}(X)/i_{chr}(R)]\,(n_R/n_X)\,(D_R/D_X)^{1/2}\,C_R \qquad (2)$$

This relationship shows that determination of the diffusion coefficient ratio makes it possible to evaluate the analyte concentration C_X from C_R,

provided that n_R and n_X are known independently (as is frequently verified in experimental practice). Therefore, the entire calibration curve relative to a standardizable reference species can easily be converted to that appropriate to an unstandardizable analyte.

In order to determine the diffusion coefficient ratio, the single D values can be measured independently by an electrochemical method. Such measurements, however, require prior knowledge of both the real electrode area (which measurement involves time-consuming procedures) and the concentration of the electroactive species which is of course unknown for the unstandardizable analyte X.

These difficulties can be overcome by a combined use of two electroanalytical techniques capable of providing current-responses which exhibit different dependences on the diffusion coefficients. A dependence on $D^{1/2}$ is displayed by all current-signals controlled by semi-infinite linear diffusion (e.g., by chronoamperometry or n.p.v.), whereas for electroanalytical techniques involving forced convection (like RDE voltammetry) the limiting current depends on $D^{2/3}$ [4], regardless of the degree of reversibility characterizing the process:

$$i_{RDE} = K_{RDE}\, F\, A\, \omega^{1/2}\, \nu^{-1/6}\, n\, D^{2/3}\, C \tag{3}$$

Therefore, by conducting parallel measurements by chronoamperometry and RDE voltammetry on solutions of the analyte X and of the reference species R, species R being dissolved in the same medium at a known concentration C_R, the diffusion coefficient ratio can easily be evaluated from the following combination of the recorded currents:

$$(D_R/D_X)^{1/6} = [i_{RDE}(R)/i_{chr}(R)]\,[i_{chr}(X)/i_{RDE}(X)] \tag{4}$$

provided that t and ω in the chronoamperometric and RDE tests, respectively, are the same for both the analyzed solutions.

By combining Eqns. 4 and 2, the following relationship is obtained:

$$C_X = (n_R/n_X)[i_{chr}(X)/i_{chr}(R)]^4\,[i_{RDE}(R)/i_{RDE}(X)]^3\, C_R \tag{5}$$

which allows C_R to be converted to the unknown C_X without direct knowledge of the single D values being necessary. The same relationship is of course derived when Eqn. 2 is derived by comparing RDE signals instead of chronoamperometric ones (i.e., when Eqn. 3 instead of Eqn. 1, is used to obtain Eqn. 2). Moreover, if RDE limiting currents are coupled with diffusion-controlled signals displayed by an electroanalytical technique different from chronoamperometry (like n.p.v.), equations similar in all respects to Eqn. 5 are obtained, except that i_{chr} is replaced by the relevant diffusion current (e.g., i_{NPV}).

In principle, C_R can also be converted to C_X by coupling RDE voltammetry with other electroanalytical methods giving signals partially controlled by the charge-transfer rate like l.s.v., a.c.v. or differential pulse voltammetry (d.p.v.). This type of coupling implies, however, that the αn values relevant

to both R and X are known independently if they undergo irreversible processes, while a dependence on n different from that given in Eqn. 5 is expected for Nernstian reactions. Thus, when both R and X are involved in reversible processes, the use of l.s.v. leads to the following equation:

$$C_X = (n_R/n_X)^3 [i_p(X)/i_p(R)]^4 [i_{RDE}(R)/I_{RDE}(X)]^3 C_R \quad (6)$$

where i_p is the peak-current recorded in l.s.v. experiments.

It should be emphasized that the above considerations are valid only for diffusion-controlled processes; they cannot be applied to electrochemical reactions involving pure kinetic control (e.g., CE or catalytic processes). This is because the rate control arising from a homogeneous reaction imposes a dependence of i_{RDE} on $D^{1/2}$ instead of $D^{2/3}$ [4]. Consequently, in these cases, the diffusion coefficient ratio cannot be evaluated through a relationship similar to Eqn. 4, unless it is possible to single out a suitable time-window in which the kinetic control can be removed for both the coupled techniques.

RESULTS AND DISCUSSION

Reliability of the proposed method

The method proposed is based on evaluating the ratio between the current-signals recorded by both RDE voltammetry and chronoamperometry on two solutions in the same medium, one containing a known amount of a reference species (R) and the other an analyte (X) at unknown concentration. From these ratios a "conversion factor" can be obtained (see Eqn. 5) which allows the calibration curve for the unstandardizable analyte to be derived from that for the reference standard. As reported above, in these measurements, chronoamperometry can be replaced by other techniques like n.p.v. or l.s.v.

In order to test the reliability of this method, it was applied to evaluate the concentration of some electroactive analytes in DMSO by using ferrocene (Fc) as the reference species (R). The concentrations found in this way were then compared with those estimated for the relevant analytes either by accurate weighing or by coulometric measurements (the latter in the case of the electrogenerated perchloric acid). The electroactive species used as analytes were *p*-benzoquinone, *o*-dinitrobenzene, anhydrous perchloric acid and 1-naphthylamine. All these compounds exhibited cyclic voltammetric behaviour (see Fig. 1) that agreed well with that reported in the literature [5—8], even though in some cases [6, 8] the aprotic solvents used were different from DMSO. As can be seen from Fig. 1, the first reduction step for *p*-benzoquinone and *o*-dinitrobenzene, as well as the reduction of perchloric acid, occur through appreciably reversible uncomplicated one-electron processes. In contrast, a chemical reaction appears to be coupled with the oxidation of 1-naphthylamine. Even though aromatic amines generally undergo one-electron anodic processes [9], both one-electron

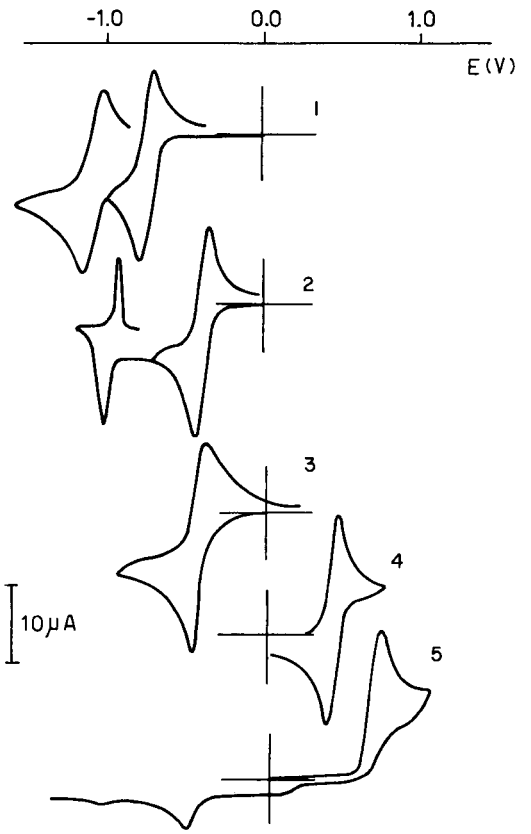

Fig. 1. Cyclic voltammograms recorded with a platinum disk electrode in DMSO solutions containing 0.1 M TBAP and 2.5×10^{-3} M analyte: (1) *a*-dinitrobenzene; (2) *p*-benzoquinone; (3) perchloric acid; (4) ferrocene; (5) 1-naphthylamine. Scan rate 0.1 V s^{-1}.

and two-electron oxidations have been proposed for 1-naphthylamine [8, 10], depending on the nature of the medium used. Notwithstanding, this species was chosen for the purpose of gaining insight on this subject.

None of the reliability tests were conducted by direct insertion in Eqn. 5 of the current ratios obtained in single measurements obtained for the analyte and reference solutions. In order to smooth the experimental uncertainty, the current was recorded in both these solutions at different values (four at least) of the time-conditioning parameter characterizing each of the electroanalytical techniques used (i.e., $\omega^{1/2}$ for RDE, $t^{-1/2}$ for chronoamperometry, $\tau^{-1/2}$ for n.p.v., $v^{1/2}$ for l.s.v.). By plotting currents against the relevant time-conditioning parameter, linear plots were obtained; the slopes of these plots, evaluated by the least-squares method, are normalized currents little affected by the uncertainty inherent in single measurements. These slopes, instead of currents, were then inserted in Eqn. 5. The C_X values thus obtained are reported in Table 1 where they are compared with those calculated as reported above.

TABLE 1

Comparison of analyte concentrations found by the proposed procedure with those evaluated by weighing or coulometry

Analyte	Concentrations[a] (mmol l^{-1}) found by coupling RDE voltammetry with the indicated technique			Calculated concentrations (mmol l^{-1})
	Chronoamperometry	N.p.v.	L.s.v.	
p-Benzoquinone	3.10 ± 0.15	3.03 ± 0.12	3.12 ± 0.15	3.01[b]
1-Naphthylamine	1.66 ± 0.08	1.56 ± 0.07	1.55 ± 0.08	1.60[b]
o-Dinitrobenzene	2.02 ± 0.10	2.08 ± 0.08	1.96 ± 0.09	2.09[b]
$HClO_4$	3.78 ± 0.18	3.65 ± 0.15	3.70 ± 0.16	3.60[c]

[a]Mean values of five independent replicate determinations, with standard deviation. [b]By weighing. [c]By controlled-potential coulometry.

The concentrations reported are mean values of five independent replicate determinations, with the standard deviation within each set of measurements. Inspection of Table 1 indicates that the suggested procedure allows both the accuracy and precision to come within ±5%. Of course, when the currents obtained in single measurements were inserted directly in Eqn. 5, lesser accuracies and precisions were obtained for the determination of CX (within ±12%). Obviously, the detection limit for the method will be that appropriate to the less sensitive of the two electroanalytical techniques used.

As far as the number of electrons involved in the oxidation of 1-naphthylamine is concerned, full agreement between the expected and found concentrations of this compound was obtained only by assuming that it undergoes a one-electron process ($n_X = 1$); when $n_X = 2$ was used, the C_X value obtained was half that expected on the basis of accurate weighing. In this connection, it must be emphasized that this type of analysis can be used (by rearranging Eqn. 5) effectively for determining n values when the analyte concentrations C_X are known. A quite similar procedure for the evaluation of n was recently proposed [11], but it involved the use of microelectrodes which are not widely available.

A further observation on the anodic process of 1-naphthylamine relates to the chemical reaction following the charge transfer which is apparently involved (see Fig. 1). For such a process, a peak-current function higher by about 10% than that relative to ferrocene would be expected in l.s.v. experiments if the electrode step were reversible [12]. However, the concentration data by l.s.v. agree well with the calculated data. This finding can be accounted for if a quasi-reversible charge-transfer step is accepted; such a step is supported by the observed $E_p - E_{p/2}$ value which is higher than 48 mV [13] (about 60 mV at 0.1 V s^{-1}). Consequently, the peak decrease caused by the relatively slow electrode reaction probably balances to some extent the peak increase produced by the following chemical reaction.

Determination of the solubility of hydrogen and oxygen

As an example of the ability of the proposed method to provide rapid but satisfactorily accurate performance, the procedure was applied to the determination of the solubility of hydrogen and oxygen in DMSO and acetonitrile respectively. In many cases, the problem of evaluating the concentration of gaseous species is difficult because standardization is not easy. Gas solubilities can be measured by volumetric or gas-chromatographic methods [1, 2]; some electroanalytical procedures have also been applied [14, 15]. All these approaches involve the use of calibration curves based on volumetric measurements, which are generally time-consuming and easily affected by experimental errors in unpractised hands.

The present solubility determinations were done with 1 M TBAP solutions in the desired solvent which were saturated by bubbling the gas directly into the thermostated electrochemical cell. The concentration of the dissolved gas was estimated by comparing the current-responses measured by RDE voltammetry and chronoamperometry (or n.p.v. or l.s.v.) on these saturated solutions with those obtained by the same electroanalytical techniques on a reference solution containing a known amount of ferrocene. Dissolved oxygen was measured by using glassy-carbon electrodes, while platinum electrodes were used for dissolved hydrogen. Reproducible responses were obtained with the platinum electrodes only when they were polished prior to each experiment by using either alumina powder or electrochemical activation as suggested elsewhere [15]. In both cases, however, after the polished electrodes had been dipped in the hydrogen-containing DMSO solutions, progressive poisoning became apparent within a few minutes, probably because of adsorption effects on the platinum surface [15, 16]. This prevented the determination of hydrogen solubility by n.p.v. which requires quite a long electrode/solution contact time.

The dissolved-gas concentrations were calculated on the basis of Eqn. 5. The values obtained (Table 2) agree quite well with literature data [1, 2], even though the electroanalytical measurements here described were made in the presence of a large amount of supporting electrolyte. This agreement

TABLE 2

Comparison of solubility data for hydrogen and oxygen obtained by the proposed procedure with those reported in the literature

Gas	Solvent	Solubility[a] (mmol l^{-1}) found by coupling RDE voltammetry with the indicated technique			Literature data (mmol l^{-1})
		Chronoamperometry	N.p.v.	L.s.v.	
O_2	Acetonitrile	8.0 ± 0.3	8.0 ± 0.2	8.1 ± 0.3	8.1 [2]
H_2	DMSO	1.1 ± 0.1	—	0.9 ± 0.1	1.07 [1]

[a]Mean values of five independent replicate determinations with standard deviation.

strongly suggests that the salt effect [1] is negligible in the case of the neutral analytes considered here. Confirmation of this wiew was obtained by verifying that there was no appreciable change in solubility when the measurements were conducted at different concentrations of the supporting electrolyte (0.05—1 M).

It must be emphasized that these solubility measurements, although their precision is not very high, offer the advantage of avoiding the troublesome standardization steps based on volumetric methods.

CONCLUSIONS

The electroanalytical procedure proposed appears to be a rapid and effective means of deriving calibration curves for species which are not easily standardized. The main drawback is its relatively low precision, particularly if single measurements are used. Less accurate and precise but faster analytical procedures are, however, quite frequently preferable to time-consuming methods even when they provide high precision and accuracy.

The described method can be applied to all electroactive species which undergo diffusion-controlled electrochemical processes, regardless of the degree of reversibility involved in the electrode reaction. It cannot be used when the analyte undergoes a kinetically controlled process (e.g., CE or catalytic); This can be established by checking the trend of the plots of current against analyte concentration and/or against the time-conditioning parameter characterizing the electroanalytical technique chosen [4]. Even in these unfavourable cases, however, reliable results may be obtained, in principle, if the electroanalytical measurements are made in a time-scale such that the kinetic complication does not affect the relevant response [4]. A further advantage offered by the procedure is that the two different electroanalytical techniques do not require that the same electrode be used; e.g., measurements at a dropping mercury electrode could be combined with RDE measurements.

The applicability of this procedure may be profitably extended even to analytes which are easily standardized. In such cases, the number of electrons involved in the relevant redox process can be calculated quickly by solving Eqn. 5 for n_X rather than for C_X, as was indicated for 1-naphthylamine.

We thank Mr. M. Tescari of the University of Padova for skilful technical assistance in assembling the electroanalytical instrumentation. The financial aid of the Italian National Research Council (C.N.R.) and of the Ministry of Public Education is gratefully acknowledged.

REFERENCES

1 C. L. Young (Ed.), I.U.P.A.C. Solubility Data Series, Vol. 5/6, Pergamon Press, New York, 1981.
2 J. M. Achord and C. L. Hussey, Anal. Chem., 52 (1980) 601.
3 J. F. Coetzee (Ed.), I.U.P.A.C. Recommended Methods for Purification of Solvents, Pergamon Press, Oxford, 1982.
4 A. J. Bard and L. R. Faulkner, Electrochemical Methods, Wiley, New York, 1980.
5 I. M. Kolthoff and T. B. Reddy, J. Am. Chem. Soc., 108 (1961) 980.
6 J. Q. Chambers and R. N. Adams, J. Electroanal. Chem., 9 (1965) 400.
7 S. Daniele, P. Ugo, G. A. Mazzocchin and G. Bontempelli, Anal. Chim. Acta, 173 (1985) 141.
8 N. Vettorazzi, J. J. Silber and L. Sereno, J. Electroanal. Chem., 125 (1981) 459.
9 C. K. Mann and K. K. Barnes, Electrochemical Reactions in Nonaqueous Systems, M. Dekker, New York, 1970.
10 N. Vettorazzi, J. J. Silber and L. Sereno, J. Electroanal. Chem., 158 (1983) 89.
11 A. S. Baranski, W. R. Fawcett and C. M. Gilbert, Anal. Chem., 57 (1985) 166.
12 R. S. Nicholson and I. Shain, Anal. Chem., 36 (1964) 706.
13 D. H. Evans, J. Phys. Chem., 8 (1972) 1160.
14 J. W. Barrett and P. D. Summer, Hong Kong Baptiste College Academic Journal, 8 (1981) 1.
15 W. C. Barrette Jr. and D. T. Sawyer, Anal. Chem., 56 (1984) 653.
16 R. F. Lane and A. T. Hubbard, J. Phys. Chem., 81 (1977) 734.

Analytica Chimica Acta, 189 (1986) 263—275
Elsevier Science Publishers B.V., Amsterdam — Printed in The Netherlands

INVERSVOLTAMMETRISCHE SPURENBESTIMMUNG VON ANTIMON(III) UND ANTIMON(V) IN AQUATISCHEN UMWELTPROBEN NACH SELEKTIVER EXTRAKTION

M. METZGER und H. BRAUN*

Kernforschungszentrum Karlsruhe, Laboratorium für Isotopentechnik, Postfach 3640, D-7500 Karlsruhe (Bundesrepublik Deutschland)

(Eingegangen den 5 August 1985)

SUMMARY

(Stripping Voltammetry of Traces of Antimony(III) and Antimony(V) in Natural Waters After Selective Extraction)

The biological activity of antimony depends on the oxidation state. The Sb(III) and Sb(V) states can be distinguished, even in the ng l^{-1} range, by coupling extraction with ammonium pyrrolidinedithiocarbamate into methyl isobutyl ketone (APDC/MIBK), or *N*-benzoyl-*N*-phenylhydroxylamine (BPHA) into chloroform, with anodic stripping voltammetry (a.s.v.). After complex formation with APDC in acetate-buffered medium, Sb(III), but not Sb(V), is extracted into MIBK and quantified by a.s.v. Antimony(V) is quantified in the aqueous phase after removal of Sb(III) by extraction with BPHA into chloroform from the medium acidified with nitric acid. The applicability of the proposed separation/a.s.v. method is demonstrated for samples of rain, snow and water from a dredging operation. The stability of the two antimony species is examined for natural waters with Sb(III) and Sb(V) added; possibilities of stabilization are described. The procedures should be suitable for speciation of antimony in relatively unpolluted waters.

ZUSAMMENFASSUNG

Antimon weist in Abhängigkeit von der Oxidationsstufe unterschiedliche biologische Aktivitäten auf. Durch Kopplung der Extraktionssysteme Ammoniumpyrrolidindithiocarbamat/Methylisobutylketon (APDC/MIBK) bzw. *N*-Benzoyl-*N*-Phenylhydroxylamin (BPHA)/Chloroform mit der inversvoltammetrischen Methode kann in wäßrigen Systemen auch noch im ng l^{-1}-Bereich zwischen Sb(III) und Sb(V) unterschieden werden. Nach Komplexierung mit APDC im acetat/essigsauren Medium läßt sich Sb(III) im Gegensatz zu Sb(V) selektiv in MIBK extrahieren und voltammetrisch nachweisen. Zur Bestimmung von Sb(V) wird im salpetersauren Medium Sb(III) mit BPHA komplexiert und quantitativ in Chloroform extrahiert. Die wäßrige Phase wird dann bezüglich der in ihr verbleibenden Sb(V)-Spezies analysiert. Die Anwendbarkeit der Trennverfahren in Kombination mit der voltammetrischen Bestimmungsmethode wird an Regen, Schnee und Baggerseewasser gezeigt. Die Stabilität beider Antimon-Spezies in natürlichen, mit Sb(III) und Sb(V) versetzten Wässern wird untersucht. Stabilisierungsmöglichkeiten werden beschrieben. Die gekoppelten Verfahren sind zur Antimon-Spezifizierung in natürlichen und wenig belasteten aquatischen Systemen geeignet.

0003-2670/86/$03.50

Für die meisten umweltrelevanten Metalle ist der analytische Nachweis sowohl in biologischen als auch in Umweltproben auch im unteren Spurenbereich (ng l^{-1}) quantitativ zufriedenstellend durchführbar. Da die Wirkungen der Metalle in Bezug auf Ökologie, Physiologie sowie Toxikologie von den Verbindungsformen der Elemente abhängen, gewinnt die analytische Identifizierung und Quantifizierung solcher Metallspezies zunehmend an Bedeutung. Antimon, ein Element welches sich toxikologisch ähnlich wie Arsen verhält, weist in Abhängigkeit von der Oxidationsstufe unterschiedliche biologische Aktivitäten auf. Es tritt in seinen Verbindungen fast ausschließlich in der Oxidationsstufe (III) und (V) auf, wobei dreiwertige Verbindungen in der Regel toxischer sind als fünfwertige [1].

Ziel der vorliegenden Arbeit war es, durch optimale Kopplung der voltammetrischen Analysenmethode mit einem substanzspezifischen Trennverfahren die Bedingungen zu erarbeiten, die es gestatten, Aussagen über die quantitative Verteilung beider Antimon-Wertigkeitsstufen in aquatischen Umweltproben zu machen. Zur Gesamt-Antimonbestimmung in wäßrigen Systemen hat sich neben der Atomabsorptionsspektrometrie das voltammetrische Bestimmungsverfahren bewährt. Unter Anwendung der inversen Wechselstromvoltammetrie läßt sich Antimon an einer rotierenden Glas-Kohlenstoffelektrode, auf der ein Quecksilberfilm elektrolytisch abgeschieden wurde, bei sehr guter Nachweisempfindlichkeit bestimmen [2]. Wegen der durchzuführenden Probenvorbereitung (Oxidation, Reduktion) läßt sich die Substanzspezifität der Meßmethode zur direkten Unterteilung des Gesamt-Sb-Gehaltes nicht ausnutzen. Zur selektiven Bestimmung der Wertigkeitsstufen wird deshalb die Kopplung mit einem substanzspezifischen Trennverfahren notwendig. Eine geeignete Trennmethode ist die Flüssigextraktion.

Antimon zeigt in Abhängigkeit von der Oxidationsstufe in Gegenwart einer Reihe Komplexbildner unterschiedliches Komplexbildungsverhalten. Mit einem geeigneten Lösungsmittel läßt sich dann die jeweilige Antimonspezies selektiv aus der Matrix in eine andere Phase überführen. In der Literatur wird die Anwendung verschiedener Komplexbildner beschrieben, wie Triphenyltetrazoliumchlorid [3], Dithizon [4], Natriumdiethyldithiocarbamat [4], *N*-Benzoyl-*N*-Phenylhydroxylamin [5], Ammoniumpyrrolidindithiocarbamat [4, 6] und Dibenzylammoniumdibenzyldithiocarbamat [7].

Aufgrund der guten Kombinationsfähigkeit mit der gewählten Bestimmungsmethode und aus spurenanalytischen Gründen wurde zur Lösung der Problemstellung ein Ammoniumpyrrolidindithiocarbamat/Methylisobutylketon (APDC/MIBK) bzw. *N*-Benzoyl-*N*-Phenylhydroxylamin/Chloroform (BPHA/$CHCl_3$)-Extraktionssystem angewendet.

EXPERIMENTELLES

Geräte und Reagentien

Die inversvoltammetrischen Untersuchungen wurden mit einem Metrohm Polarecord E506, VA Kontroller E608 und einer rotierenden Scheibenelek-

trode E628/1 durchgeführt. Als Arbeitselektrode wurde eine Glas-Kohlenstoffelektrode EA289/1 mit einer elektrochemisch aktiven Oberfläche von 7 mm^2 eingesetzt. Hilfs- und Referenz-elektrode, jeweils Ag/AgCl in gesättigter KCl-Lösung, waren mit der Probenlösung durch ein Zwischenelektrolytgefäß, gefüllt mit 0,1 M $HClO_4$/0,005 M HCl, verbunden. Das Probenvolumen des Voltammetrier/gefäßes betrug 20 ml. Meßmethode war die getastete phasen/selektive Wechselstromvoltammetrie der 1. Oberwelle mit einer Wechselspannungsfrequenz von 37,5 Hz AC_{2T}, Phasenwinkel 0°.

Alle Reagentien hatten, soweit erhältlich, die Qualität Suprapur (Merck). Zur Herstellung der Lösungen wurde mehrfach deionisiertes Wasser verwendet.

APDC-Lösung. Pyrrolidin-1-dithiocarbonsäure Ammoniumsalz (0,5 g) werden in 100 ml Wasser gelöst und zur Reinigung zweimal mit je 20 ml Methylisobutylketon ausgeschüttelt.

BPHA-Lösung. *N*-Benzoyl-*N*-phenylhydroxylamin (2 g) werden in 100 ml Chloroform gelöst.

Kaliumdichromatlösung. Kaliumdichromat (0,8 g) werden in 75 ml Wasser gelöst und mit 25 ml 14 M HNO_3 versetzt.

Pufferlösung pH 4,5. Natriumacetat (8,2 g) werden in 93,5 ml Wasser gelöst und mit 6,5 ml Essigsäure versetzt. Nach Zugabe von 2 ml APDC-Lösung wird die Pufferlösung zur Reinigung zweimal mit je 10 ml Methylisobutylketon ausgeschüttelt.

Antimon(V)-Stammlösung. Antimonmetall (0,5 g) werden in 10 ml 14 M HNO_3 gelöst und zur Trockene eingedampft. Der Rückstand wird in 100 ml 10 M HCl gelöst und mit Wasser auf 500 ml verdünnt.

Antimon(III)-Stammlösung. Der Inhalt einer Ampulle mit handelsüblicher Antimon(III)-Lösung, die 1 g Sb als $SbCl_3$ enthält, wird mit 100 ml 10 M HCl versetzt und mit Wasser auf 1000 ml verdünnt.

Standardlösungen werden durch Verdünnung der Stammlösungen in 1 M HCl bereitet.

Präparation der Quecksilberfilmelektrode

Auf der mit $Al(OH)_3$-Pulver (Metrohm EA276A) polierten Glas-Kohlenstoffelektrode wird aus einer 0,01 M HCl/1 $\times$ 10^{-4} M Hg-Lösung für die Dauer von 120 s bei einem kathodischen Anreicherungspotential von -1 V unter gleichzeitiger Elektrodenrotation und Stickstoffeinleitung ein Hg-Film abgeschieden. Nach Einstellung der Rotation und Stickstoffeinleitung wird die Elektrode anodisch bis $-0{,}1$ V im AC_{2T}-Modus polarisiert und der Polarisationszyklus dreimal wiederholt. Zur Konditionierung wird die Quecksilberfilmelektrode in 1,2 M HCl/0,014 M Ascorbinsäure-Lösung wechselweise bei $-0{,}4$ und $-0{,}1$ V, $-0{,}4$ und $+0{,}2$ V sowie abschließend bei $-0{,}6$ und $-0{,}1$ V polarisiert. Nach Zugabe von 10 ng Sb(III) wird die Einsatzfähigkeit der Elektrode überprüft.

Inversvoltammetrischer Bestimmungsvorgang

Die vorbereitete Probelösung wird ins Voltammetriergefäß, in welchem 1,6 ml 10 M HCl vorgelegt werden, überführt und mit Wasser auf 20 ml verdünnt. Die Lösung wird für ca. 60 s entlüftet und die präparierte Hg-Filmelektrode wird eingebracht. Die Elektrode wird unter Rotation für die Dauer von 80 s bei einem Anreicherungspotential von —0,52 V polarisiert. Gleichzeitig wird Stickstoff in die Lösung eingeleitet. Nach Einhaltung einer Beruhigungsphase von 10 s wird dann mit einer in anodischer Richtung zunehmenden Spannung unter gleichzeitiger getasteter Registrierung des Wechselstromanteils der Oberwelle 1 (AC_{2T}-Modus) bis —0,1 V polarisiert (10 mV s^{-1}). Diese Reinigungsspannung von —0,1 V bleibt für 10 s angelegt, und der Meßvorgang wird wiederholt. Oftmals bildet sich das Sb-Signal erst nach dem zweiten oder dritten Polarisationszyklus aus. Während der Beruhigungs- und Strippingphase wird die Elektrodenrotation sowie die Stickstoffeinleitung augehalten.

Nach Optimierung der Abscheideparameter Elektrolysezeit, Wechselspannungsamplitude, Empfindlichkeit und gegebenenfalls Elektrolysepotential wird der Polarisationszyklus bis zur Registrierung reproduzierbarer Voltammogramme wiederholt. Nach 2—3 maliger Standardaddition mit Sb(III)-Lösung, die jeweils während der Reinigungsphase durchgeführt wird, lassen sich die registrierten Oberwellenvoltammogramme auswerten.

Die optimalen Versuchsbedingungen zur voltammetrischen Antimon-Bestimmung sind in Tabelle 1 zusammengefaßt.

Verfahrensweise

Gesamtantimon-Bestimmung. Die Untersuchungslösung (<30 ng Sb) wird in einem Quarztiegel auf 5 ml verdünnt und mit 0,5 ml Kaliumdichromatlösung versetzt. Die Lösung wird zunächst für die Dauer von 2 Min und nach Zugabe von 0,8 ml 10 M HCl und 0,5 ml 10 %iger Ascorbinsäurelösung für weitere 4 Min unter mäßigem Sieden erhitzt.

Antimon(III)-Bestimmung. Durch Zugabe von Pufferlösung wird die Probe auf pH 4,5 eingestellt und mit 1 ml APDC-Lösung versetzt. Anschließend wird mit 10 ml MIBK extrahiert, die wäßrige Phase verworfen und die organische Phase mit wenig Wasser gewaschen. In einem Quarztiegel werden 1—2 ml organische Phase auf ein Volumen von 0,5 ml eingeengt, abgekühlt und mit

TABELLE 1

Optimale Bedingungen für die voltammetrische Antimon-Bestimmung

Parameter	Einstellung	Parameter	Einstellung
Modus	AC_{2T}	Wechselspannungsamplitude	20 mV
Anreicherungspotential	—0,52 V	Pulsfolgezeit	0,4 s
Reinigungspotential	—0,1 V	Elektrodenrotation	1500 U min^{-1}
Spannungsänderungs-geschwindigkeit	10 mV s^{-1}	Linearitätsbereich	0—100 ng Sb
		Nachweisempfindlichkeit	0,2 ng Sb

0,2 ml Kaliumdichromatlösung und 1,5 ml Wasser versetzt. Die organische Phase wird vorsichtig verflüchtigt und in die abgekühlte Lösung 6 ml 1,4 M HCl gegeben. Nach Zugabe von 0,5 ml 10 %iger Ascorbinsäurelösung wird für die Dauer von 4 Min unter leichtem Sieden erhitzt.

Antimon(V)-Bestimmung. Üblicherweise wird die Antimon(V)-Konzentration durch Subtraktion des Sb(III)-Gehaltes vom Sb-Gesamtgehalt ermittelt. Zur direkten Bestimmung von Sb(V) wird die Untersuchungslösung durch Zugabe von Wasser auf ein Volumen von 25 ml gebracht und mit 50 μl 14 M HNO_3 angesäuert. Nach Zusatz von 2 ml BPHA-Lösung wird anwesendes Sb(III) in die organische Phase extrahiert. Ein Aliquot der mit wenig Chloroform gewaschenen wäßrigen Phase wird in einen Quarztiegel überführt und entsprechend der "Gesamtantimon-Bestimmung" weiter behandelt.

ERGEBNISSE UND DISKUSSION

Unter Verwendung der Quecksilberfilmelektrode wurde die wechselstromvoltammetrische Antimonbestimmung in einem 1,2 M HCl/0,014 M Ascorbinsäure-Grundelektrolyten durchgeführt. Unter den gewählten Bedingungen wird Antimon nur in der Oxidationsstufe (III) erfaßt. Nach früheren Untersuchungen liegt Antimon in wäßrigen Matrizes meist in elektrochemisch inaktiver Bindungsform vor [2]. Eine entsprechende Probenvorbereitung wird deshalb notwendig. Hierbei hat es sich bewährt, die Probelösung zunächst oxidativ mit einem Kaliumdichromat/Salpetersäure-Gemisch zu behandeln. Anschließend wird durch Zusatz von Ascorbinsäure vorhandenes Antimon in das elektrochemisch aktive Sb(III) überführt.

Aufgrund der erreichbaren Nachweisempfindlichkeit von 20 ng l^{-1} läßt sich die Meßmethode für die Sb-Spezifizierung in natürlichen aquatischen Systemen nach vorausgegangener APDC/MIBK-bzw. BPHA/$CHCl_3$-Extraktion anwenden.

Selektive Extraktion von Sb(III) und Sb(V)

APDC/MIBK-Extraktionssystem. Unter bestimmten Bedingungen bildet Sb(III) im Gegensatz zu Sb(V) mit APDC eine stabile Komplexverbindung. Aus wäßrigen Matrizes läßt sich diese als $Sb(APDC)_3$ in ein geeignetes organisches Lösungsmittel extrahieren. Als Lösungsmittel wurde MIBK eingesetzt, welches sich nach Kamada und Yamamoto [4] für die Sb(III)-Extraktion besonders eignet. Die voltammetrische Untersuchung, die nach Ausführung der Extraktion vorgenommen wurde, erwies sich sowohl für die wäßrige als auch für die organische Phase als besonders schwierig. Durch entsprechende Probenvorbereitung gelang es, die Bestimmung des extrahierbaren Sb(III)-Anteils bei sehr guter Nachweisempfindlichkeit durchzuführen.

Die wäßrige Phase und damit die in ihr verbleibende Sb(V)-Spezies ist für die Voltammetrie unzugänglich. Grund hierfür ist die im stark sauren Medium stattfindende Zersetzung [8] des nicht zur Sb(III)-Komplexierung verbrauchten APDC-Anteils. Infolge der gebildeten Zersetzungsprodukte kommt

es beim Anlegen des Elektrolysepotentials zur irreversiblen Belegung der Quecksilberoberfläche. Die Elektrode wird so für eine weitere Verwendung unbrauchbar. Die voltammetrischen Untersuchungen beschränken sich damit auf die Sb(III)-Erfassung in der organischen Phase. Hierbei ergaben sich zunächst prinzipielle Schwierigkeiten.

Beim Einbringen der Elektrode in die Untersuchungslösung bildete sich an deren Oberfläche ein dünner Film des organischen Lösungsmittels. Das Diffusionsverhalten der Sb(III)Ionen in Richtung Elektrode wird durch den zusätzlichen Phasenübergang bei Anlegen des Elektrolysepotentials stark beeinträchtigt. Außerdem kommt es durch die veränderte Oberflächenspannung zu einer lokalen Mikrotropfenbildung des ursprünglich über die gesamte Glas-Kohlenstoff-Stirnfläche verteilten Quecksilbers. Die Elektrode läßt sich so nicht mehr weiter einsetzen. Die auftretenden Schwierigkeiten konnten beseitigt werden, indem vor Durchführung der Analyse die MIBK-Phase vollständig entfernt wurde. Dabei hat sich folgendes Vorgehen als günstig erwiesen. Nach Ausführung der Extraktion wird ein Aliquot der organischen Phase in einem Quarztiegel bei Temperaturen unterhalb des Siedepunktes soweit eingeengt, daß der Boden des Tiegels gerade noch bedeckt bleibt. Es darf dabei nicht zur Trockne eingedampft werden, da dann bei Ausführung der Messung kein Antimon mehr nachgewiesen werden kann. Anschließend wird in Gegenwart von Dichromat/HNO_3-Lösung die organische Phase gerade vollständig verdampft. Untersuchungen haben gezeigt, daß Antimon erst nach vollständiger Entfernung der organischen Phase quantitativ in die anorganische Phase übergeht. In Gegenwart von Ascorbinsäure wird Antimon im salzsauren Medium in die elektrochemisch aktive Sb(III)-Form überführt und anschließend bestimmt.

Die betrachteten Sb-Spezies weisen in Abhängigkeit vom pH-Wert der Lösung ein unterschiedliches Extraktionsverhalten auf. Die Untersuchungen ergaben, daß in einem stark salzsauren Medium (pH < 1) sowohl Sb(III) als auch Sb(V) in Gegenwart von APDC in die organische Phase extrahiert wird. Da APDC in einem solch sauren Medium äußerst instabil ist, läßt sich dieses Verhalten durch die Extrahierbarkeit gebildeter Sb-Chlorokomplexe erklären. Aufgrund abnehmender Chlorokomplexbildungs-Tendenz bei gleichzeitiger Zunahme der Sb/APDC-Komplexstabilität unterlag der extrahierbare Sb-Anteil bei Anwesenheit beider Antimon-Oxidationsstufen im Bereich pH 1—2 erheblichen Streuungen. Dagegen läßt sich im pH-Bereich 2—5 Sb(III) auch in Gegenwart von Sb(V) selektiv und quantitativ in die organische Phase überführen.

Bei den weiteren Untersuchungen wurde die Sb(III)-Extraktion im acetatessigsauren Medium bei pH 4,5 ausgeführt. Eine vorübergehende Trübung der organischen Phase nach Durchführung der Extraktion hat keinen Einfluß auf den weiteren Bestimmungsablauf.

Unter den gesetzten Bedingungen bildet APDC mit einer Reihe Metallionen stabile Komplexverbindungen. Die APDC-Konzentration wurde deshalb mit 5 mg absolut so gewählt, daß die quantitative Komplexierung von 200 ng

Sb(III) auch noch bei signifikanter Erhöhung der üblicherweise in der Untersuchungsmatrix vorhandenen Metallgehalte gewährleistet ist. Wird die zu extrahierende Lösung zweimal für jeweils 20 s ausgeschüttelt, so wird Sb(III) vollständig in die organische Phase überführt.

Höchste Anforderungen müssen an die Reinheit des verwendeten organischen Lösungsmittels gestellt werden. Da in den zu untersuchenden Proben für Sb(III) äußerst geringe Konzentrationen erwartet werden, muß eine quasi blindwertfreie Versuchsdurchführung möglich sein. Mit einem Sb-Blindwert bis zu 0,2 ng ml^{-1} entspricht handelsübliches MIBK nicht ohne weiteres den bezüglich Reinheit gestellten Ansprüchen. MIBK wurde deshalb zusätzlich durch Destillation gereinigt. Bei einer anschließenden Analyse konnte kein Antimon mehr nachgewiesen werden.

Nach Extraktionsdurchführung betrug die MIBK-Löslichkeit im acetatessigsauren Medium 1,5% bei 20°C. Bei der Auswertung wird immer das gesamte eingesetzte MIBK-Volumen berücksichtigt. Die Löslichkeit ist deshalb von untergeordneter Bedeutung. Bis zu einem Phasenverhältnis $V_{pH\,4,5}/V_{MIBK}$ von 6 konnten gleichbleibend gute Analysenergebnisse erzielt werden.

Wie aus Tabelle 2 ersichtlich, lassen sich nach Durchführung der beschriebenen Probenvorbereitung auch geringe Sb(III)-Gehalte mit guter Genauigkeit bestimmen. Die Extraktion wurde jeweils mit einem Phasenvolumenverhältnis V_W/V_0 von 5:1 ausgeführt. Auch in Gegenwart eines 20-fachen Sb(V)-Überschusses konnte der vorgelegte Sb(III)-Anteil mit einer guten Wiederfindungsrate bestimmt werden. Die voltammetrische Bestimmung erfolgte nach der Standardadditionsmethode. Bei einer Lösung, deren Sb(III)-Gehalt 0,5 ng ml^{-1} betrug, konnte die Bestimmung mit einer relativen Standardabweichung von 10% bei 4 Einzelmessungen durchgeführt werden. Mit der beschriebenen Methode lassen sich Sb(III)-Gehalte bis zu 30 ng l^{-1} erfassen.

Nach Erfassung des Gesamt-Sb-Gehaltes läßt sich durch Subtraktion des Sb(III)-Gehaltes der Sb(V)-Anteil ermitteln. Damit sind durch Anwendung des APDC/MIBK-Extraktionssystems die Voraussetzungen für eine selektive Sb(III)-Bestimmung im ng l^{-1}-Bereich gegeben.

TABELLE 2

Selektive Sb(III)-Bestimmung nach APDC/MIBK-Extraktion und Sb(V)-Bestimmung nach BPHA/$CHCl_3$ Extraktion

APDC/MIBK-Extraktion			BPHA/$CHCl_3$-Extraktion		
Vorgegeben (ng)		Gefunden Sb(III) (ng)	Vorgegeben (ng)		Gefunden Sb(V) (ng)
Sb(III)	Sb(V)		Sb(III)	Sb(V)	
50	50	51	0	50	52
25	500	23	12,5	37,5	36
20	0	19	25	25	25
10	10	11	37,5	12,5	12
5	15	5	50	0	0
0	20	0			

BPHA/Chloroform Extraktionssystem. Die komplexierenden Eigenschaften von BPHA lassen sich für die selektive Sb(III)/Sb(V)-Extraktion ausnutzen. Das unterschiedliche Komplexierungsverhalten der Sb-Spezies wurde bereits 1966 von Lyle and Shendrikar [9] beschrieben. Im Gegensatz zu Sb(V) bildet Sb(III) im salzsauren Medium ein stabiles Metall-Chelat, welches sich quantitativ in eine Chloroform-Phase überführen läßt. Nach Han-Wen et al. [5] ist dieses Extraktionssystem auch für die spurenanalytische Sb-Spezifizierung anwendbar.

Im Hinblick auf die weitere Probenvorbereitung wurde die salpetersaure Probenlösung mit einer Lösung von BPHA in Chloroform versetzt und der gebildete Sb(III)-BPHA-Komplex in die Chloroformphase extrahiert. Im Gegensatz zum APDC/MIBK-Extraktionssystem läßt sich die extrahierbare Sb(III)-Spezies voltammetrisch nicht bestimmen. Beim Aufkochen der organischen Phase zersetzt sich BPHA nach Zusatz von Dichromat-Lösung unter Bildung des entsprechenden Oxidationsproduktes. Der entstehende braune Niederschlag läßt keine weitere Aufarbeitung der Probe zu. Damit kann nur die in der wäßrigen Phase verbleibende Sb(V)-Spezies analysiert werden. Zwar besitzt BPHA eine geringe Löslichkeit in der wäßrigen Phase, aber schon Spuren des Chelators reichen aus, um den voltammetrischen Nachweis durch Unterdrückung des Antimon-Reoxidationssignals zu stören. Deshalb ist es unbedingt notwendig, nach Extraktionsdurchführung gelöstes BPHA aus der wäßrigen Phase durch Waschen mit Chloroform zu entfernen. Ein Aliquot der wäßrigen Phase läßt sich dann nach beschriebener Aufoxidation und Reduktion analysieren.

Die Extraktionsbedingungen wurden so gewählt, daß eine selektive Antimon-Trennung für die üblicherweise auftretenden Antimon-Gehalte in natürlichen Wässern gewährleistet bleibt. Gute Extraktionsergebnisse wurden in Gegenwart von 40 mg BPHA auch noch bei Phasenvolumenverhältnissen V_W / V_0 von 15:1 erzielt. Extraktionszeiten von zweimal 20 s sind ausreichend, um Sb-BPHA quantitativ in die organische Phase zu überführen. Die verwendeten Chemikalien BPHA und Chloroform wiesen keine nachweisbaren Sb-Blindwerte auf.

Die Anwendbarkeit des BPHA-Chloroform-Systems zur selektiven Sb(III)-Extraktion im unteren Spurenbereich wurde untersucht. Wie aus Tabelle 2 zu entnehmen ist, läßt sich Sb(III) in verschiedenen Sb(III)/Sb(V)-Konzentrationsverhältnissen vollständig und selektiv nach Komplexierung mit BPHA in die organische Phase überführen. Die angegebenen Antimon-Gehalte beziehen sich jeweils auf ein Probevolumen von 25 ml. Die nicht chelatisierte Sb(V)-Spezies kann nach entsprechender Probenvorbereitung mit guter Wiederfindungsrate voltammetrisch bestimmt werden. Bei einer Sb(V)-Konzentration von 0,5 ng ml^{-1} betrug die relative Standardabweichung 11% (4 Einzelmessungen). Durch Subtraktion des in der wäßrigen Phase verbleibenden Sb(V)-Anteils von Sb-Gesamtgehalt läßt sich die Konzentration an Sb(III) ermitteln.

Stabilität der Antimon-Spezies in wäßrigen Matrizes

Um Aussagen über die Sb-Speziesverteilung in natürlichen Wässern machen zu können, mußte zuvor die Frage der Stabilität beider Oxidationsstufen geklärt werden. Dazu wurde Baggerseewasser pH 7 mit Sb(III)-Lösung versetzt, so daß die Sb-Konzentration 1 ng ml^{-1} betrug. Durch Verwendung von Seewasser wird eine mögliche Sb-Umwandlung, hervorgerufen durch vorhandene oxidierend wirkende Stoffe, berücksichtigt. Zur Stabilisierung von Sb(III) wurde ein Teil der Lösung durch HCl-Zugabe auf pH 1 gebracht und in einem weiteren Aliquot durch Zusatz von Weinsäure eine Konzentration von 0,3% eingestellt.

In regelmäßigen Zeitabständen wurde dann durch APDC/MIBK-Extraktion der extrahierbare Sb(III)-Anteil bestimmt. Um Verluste durch Adsorption an den Gefäßwandungen auszuschließen, wurde jeweils der Gesamtantimon-Gehalt überprüft.

Die Ergebnisse der Stabilitätsuntersuchungen sind in Abb. 1 dargestellt. Bei dem im natürlich Zustand belassenen Seewasser konnte die Ausgangskonzentration nach 4 h wiedergefunden werden. Durch eine Umwandlung in Sb(V) kam es bei längeren Standzeiten zur Abnahme der nachweisbaren Sb(III)-Spezies, bis schließlich nach 48 h kein Sb(III) mehr extrahiert werden konnte. Bei der Gesamtgehaltsbestimmung konnte Sb selbst nach 4 Wochen quantitativ wiedergefunden werden. In der salzsauren Probe war es möglich, Sb(III) nach 12 Tagen vollständig zu extrahieren und nachzuweisen. Die Acidität der Probenlösung hat damit einen wesentlichen Einfluß auf die Umwandlungsrate von Sb(III) in Sb(V). Aufgrund der Bildung von stabiler Aquoantimonoweinsäure $H[C_4H_2O_6Sb(OH_2)]$ konnte in der mit Weinsäure versetzten Lösung Sb(III) ebenfalls noch nach 12 Tagen quantitativ nachgewiesen werden. Damit läßt sich in Gegenwart von Weinsäure die Sb-Umwandlung auch für längere Standzeiten verhindern.

Die beschriebene Methode soll u.a. zur Antimon-Spezifizierung in Regen-

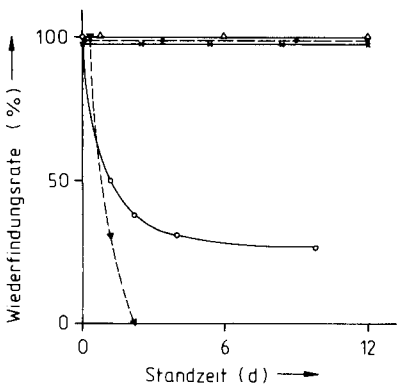

Abb. 1. Abhängigkeit der Sb(III)-Stabilität von der Standzeit ($C_{Sb(III)}$ = 1 ng ml^{-1}). Seewasser: (▾) unversetzt; (•) pH 1,1; (×) Weinsäure. Regenwasser: (○) unversetzt; (△) Weinsäure.

wasser herangezogen werden. Da sich die Acidität des Untersuchungsmediums unmittelbar auf die Antimon-Umwandlung auswirkt, wurde das Sb(III)-Verhalten in Regenwasser untersucht. In Regenwasser mit einem pH-Wert von 4,2 wurde durch Sb(III)-Zugabe eine Konzentration von 1 ng ml^{-1} eingestellt. Zur Stabilisierung von Sb(III) wurde ein Teil der Lösung mit Weinsäure (Konzentration von 0,3%) versetzt. Die gemessenen Sb(III)-Gehalte in Abhängigkeit von der Standzeit sind in Abbildung 1 mit aufgeführt. In Gegenwart von Weinsäure läßt sich auch in diesem Medium Sb(III) während der gesamten Versuchsdauer von 10 Tagen quantitativ nachweisen. In der nichtstabilisierten Lösung nimmt der Sb(III)-Anteil zunächst erheblich ab. Nach 4 Tagen lassen sich nur noch 30% der Sb(III)-Ausgangskonzentration nachweisen. Bei längeren Standzeiten stellt sich ein Gleichgewicht zwischen Sb(III) und Sb(V) ein, und der Sb(III)-Gehalt ändert sich nur noch wenig. Weitere Untersuchungen an synthetischen Lösungen, pH 4, haben gezeigt, daß für diese Gleichgewichtseinstellung die Acidität der Probenlösung ausschlaggebend ist.

Bekanntermaßen neigen Verbindungen des fünfwertigen Antimons in saurer Lösung in solche des dreiwertigen überzugehen. Um diese Möglichkeit mit in die Betrachtungen einzuschließen, wurde Seewasser durch HCl-Zugabe auf pH 1 gebracht und mit Sb(V) eine Konzentration von 2 ng ml^{-1} eingestellt. Selbst nach Standzeiten von 3 Wochen konnte kein extrahierbarer Sb(III)-Anteil nachgewiesen werden. Bei der Gesamtgehaltsbestimmung wurde Antimon quantitativ wiedergefunden.

Aufgrund dieser Untersuchungsergebnisse ist ein selektiver Sb(III)/Sb(V)-Nachweis nur dann möglich, wenn die Spezifizierung unmittelbar nach der Probenahme erfolgt. Wird für die Probenahme längere Zeit benötigt (z.B. Sammeln von Regenwasser) oder kann die Bestimmung nicht unmittelbar nach der Probenahme durchgeführt werden, empfiehlt es sich, die Lösung zur Stabilisierung von Sb(III) mit Weinsäure zu versetzen.

ANWENDUNGSBEISPIELE

In Verbindung mit dem voltammetrischen Analysenverfahren wurden die beschriebenen Extraktionsmethoden zur selektiven Sb(III)- und Sb(V)-Bestimmung auf verschiedene aquatische Systeme angewendet. Neben Schnee- und Regenproben aus Gebieten unterschiedlicher Schwermetallbelastung wurde Oberflächenwasser eines Baggersees untersucht. Zur Entnahme von Schnee wurde die obere Schicht einer ca. 0,5 m^2 großen Schneefläche entfernt und verworfen. Die Probe wurde anschließend gleichmäßig über die gesamte Fläche verteilt entnommen. Die Regenwässer wurden nach der Bergerhoff-Methode gesammelt. Baggerseewasser wurde ca. 0,2 m unter dem Wasserspiegel entnommen. Die wäßrigen Matrizes wurden sofort nach der Probenahme zur Abtrennung partikulärer Bestandteile durch Membranfilter von 0,45-μm Porenweite filtriert.

Die untersuchten Wässer wiesen die für diese Matrizes üblichen Antimon-

TABELLE 3

Bestimmung von Gesamtantimon, Sb(III) und Sb(V) in natürlichen Wässern

Wasser	Sb-Gesamt ($ng\ ml^{-1}$)	APDC/MIBK Sb(III) ($ng\ ml^{-1}$)	BPHA/$CHCl_3$ Sb(V) ($ng\ ml^{-1}$)
Schnee I	0,15	<0,04	0,14
Schnee II	0,22	<0,05	—
Schnee III	0,35	<0,08	—
Regen I	0,36	<0,06	—
Regen II	0,87	<0,1	0,8
Seewasser	0,10	<0,03	—

gehalte auf [10]. Die Ergebnisse der Spezies-Untersuchungen sind in Tabelle 3 zusammengefaßt. In den betrachteten Matrizes konnte kein mit APDC/MIBK extrahierbarer Sb(III)-Anteil nachgewiesen werden. Der in den Wässern enthaltene Sb-Gehalt wird demnach nur durch die Anwesenheit von Sb(V) hervorgerufen. Eine vergleichbare Antimonverteilung ergab die für einige Proben durchgeführte BPHA/Chloroform-Extraktion. Auch hierbei stimmte der in der wäßrigen Phase verbleibende Sb(V)-Anteil mit dem Sb-Gesamtgehalt der Probe überein. Vorliegende Aussagen über eine Sb-Spezies-Verteilung in aquatischen Systemen [5] werden damit bestätigt.

Um gelöste organische Stoffe und Metallspezies zu berücksichtigen, welche die Komplexierung und Extraktion beeinträchtigen können, wurden einige Proben mit Sb(III) versetzt. Nach Ausführung der APDC/MIBK-Extraktionen wurde der Sb(III)-Anteil bestimmt. In Tabelle 4 sind die Ergebnisse der Untersuchungen zusammengestellt. Danach konnten die vorgelegten Sb(III)-Gehalte quantitativ in die organische MIBK-Phase extrahiert werden.

In Abb. 2 sind die Voltammogramme zur selektiven Sb(III)-Bestimmung in Regenwasser nach Ausführung der APDC/MIBK-Extraktion vor und nach entsprechender Aufstockung mit einer Eichlösung dargestellt.

Zusätzliche Untersuchungen wurden angestellt, um den Auswascheffekt beider Antimon-Spezies durch Einwirkung von "saurem Regen" auf die von einer Müllverbrennungsanlage emittierten Reingasstäube zu zeigen. Eine

TABELLE 4

Wiederfindung von Sb(III) in natürlichen Wässern

Wasser	Sb(III) ($ng\ l^{-1}$)		Gesamt gefunden
	Gefunden	Addiert	
Regen	<0,1	0,28	0,3
Seewasser	<0,03	0,90	0,9
Schnee	<0,05	0,20	0,19
Schnee	<0,05	0,50	0,5

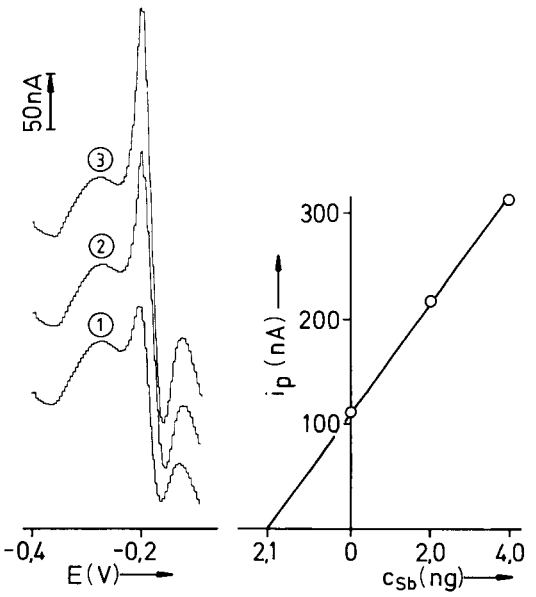

Abb. 2. Voltammogramme zur Bestimmung von Sb(III) nach APDC/MIBK-Extraktion: (1) Probe; (2) Probe + 2 ng Sb(III); (3) Probe + 4 ng Sb(III). Untersuchungsmatrix, Sb(III)-versetztes Regenwasser; Anreicherungspotential −0,52 V, Wechselspannungsamplitude 20 mV, Spannungsänderungsgeschwindigkeit 10 mV s^{-1}, Elektrodenrotation 1500 min^{-1}, Anreicherungszeit 240 s.

Spezifizierung der eluierbaren Antimon-Menge war wegen der hohen Gehalte an ebenfalls auslaugbaren und mit APDC Komplexierenden Schwermetalle wie Cd, Ni, Cu, Pb etc. nicht möglich. Dies zeigt gleichzeitig auch die Grenzen der Anwendungsmöglichkeiten.

Die beschriebene Extraktionsmethode in Kopplung mit der voltammetrischen Meßmethode ist ohne zusätzliche Trennverfahren nur zur Antimon-Spezifizierung in natürlichen bzw. wenig belasteten aquatischen Systemen geeignet. Die Untersuchungen geben einen Hinweis darauf, daß Antimon in natürlichen aquatischen Systemen bevorzugt in der weniger toxischen Oxidationsstufe Sb(V) auftritt. Um generelle Aussagen über die Sb-Wertigkeitsverteilung in natürlichen Wässern zu machen, bedarf es noch einer Reihe weiterer Untersuchungen. Das Vorhandensein nicht extrahierbarer Antimon-Spezies muß bei weiteren Betrachtungen mit berücksichtigt werden.

LITERATUR

1 B. Venugopal und T. D. Luckey, Metal Toxicity in Mammals, 2nd. Ed., Vol. 2, Plenum Press, New York, 1979.
2 H. Braun und M. Metzger, Z. Anal. Chem., 241 (1985) 241.
3 A. Alexandrov, E. Blasius und W. Neumann, J. Radioanal. Chem., 43 (1978) 169.
4 T. Kamada und Y. Yamamoto, Talanta, 24 (1977) 330.

5 S. Han-Wen, S. Xiao-Quan und Ni. Zhe-Ming, Talanta, 29 (1982) 589.
6 K. S. Subramanian und J. C. Meranger, Anal. Chim. Acta, 124 (1981) 131.
7 H. D. Seltner, H. R. Linder und B. Schreiber, Int. J. Environ. Anal. Chem., 10 (1981) 7.
8 A. Hulanicki, Talanta, 14 (1967) 1371.
9 S. J. Lyle und A. D. Shendrikar, Anal. Chim. Acta, 36 (1966) 286.
10 A. H. Abu-Hilal und J. P. Riley, Anal. Chim. Acta, 131 (1981) 175.

Analytica Chimica Acta, 189 (1986) 277—283
Elsevier Science Publishers B.V., Amsterdam — Printed in The Netherlands

DETERMINATION OF FOLIC ACID BY ADSORPTIVE STRIPPING VOLTAMMETRY AT THE STATIC MERCURY DROP ELECTRODE

DEN-BAI LUO

Department of Chemistry, South-Central Institute for National Minorities, Wuhan (People's Republic of China)

(Received 24th October 1985)

SUMMARY

Folic acid can be determined at nanomolar concentrations by controlled adsorptive accumulation of folic acid on a static mercury drop electrode held at —0.3 V vs. Ag/AgCl followed by reduction of the surface species. In 0.1 M sulfuric acid, a cathodic scan gives peaks at —0.47 V and —0.75 V vs. Ag/AgCl; the latter peak provides greater sensitivity. Differential-pulse stripping is shown to be superior to normal-pulse and d.c. stripping. After a 5-min preconcentration, the detection limit is about 1×10^{-10} M folic acid. The adsorptive stripping response is evaluated with respect to concentration dependence, preconcentration time and potential, solution acidity and the presence of gelatin and bromide. The relative standard deviation at the 5×10^{-8} M level is 1.2%. This method is applied to the determination of folic acid in pharmaceutical tablets.

Folic acid (PteGlu, pteroylglutamic acid) is a compound of great biological importance [1]. Folic acid deficiency is characterized mainly by growth failure and anemia. It is widely distributed in animals and plants. Simple and sensitive methods for its determination are required for pharmaceutical, clinical and food analysis. Published methods for the determination of folic acid include spectrophotometry based on its reaction with Folin-Ciocalteu reagent [2] and chromatographic procedures [3, 4], but these are not sensitive enough for the determination of folic aicd at submicromolar concentrations. Polarography based on reduction of folic acid on a mercury drop electrode [5, 6], oscillographic polarography on a solid electrode [7] and oscillopolarographic titration [8] have been suggested for determination of folic acid in drugs. The detection limit of the d.c. polarographic method [5] is about 0.1 μg ml^{-1} for a diffusion current of 1 nA.

Interest in adsorptive stripping voltammetry which provides very sensitive determinations of compounds with surface-active properties has recently increased. Various important reducible and oxidizable compounds have been measured following their adsorptive accumulation onto mercury [9—12] or solid [13—15] electrodes, yielding detection limits in the 10^{-8}—8×10^{-11} M range. No previous application of stripping voltammetry to the determination of folic acid seems to have been reported.

0003-2670/86/$03.50

In the present paper a voltammetric method is described for trace measurement of folic acid based on its adsorptive accumulation at the static mercury drop electrode. The analyte is first preconcentrated by controlled adsorption onto the working electrode and the accumulated species is then stripped by reduction in a sulfuric acid supporting electrolyte. A detection limit of about 1×10^{-10} M folic acid is obtained after 5-min preconcentration. This method is applied to the determination of folic acid in pharmaceutical tablets and urine samples.

EXPERIMENTAL

Instrumentation and solutions

An EG & G Princeton Applied Research (PAR) Model 174 polarographic analyzer was used with a Model 303 static mercury drop electrode, an Ag/AgCl (saturated KCl) reference electrode and a platinum wire auxiliary electrode. Instrumental parameters were as follows: medium drop size; potential scan rate, 10 mV s^{-1}; pulse amplitude, 50 mV; pulse repetition, 0.5 s. A PAR Model RE-0089 X-Y recorder was used for the collection of experimental data. The sample cell was PAR Model 0057. A magnetic stirrer (PAR Model 305) set to the MANUAL, SLOW position and a star-head stir bar provided the convective transport during the preconcentration.

Stock solutions (2×10^{-4} M) of folic acid (standard reagent, Medical and Biological Preparation Inspection Institute, Ministry of Public Health, People's Republic of China) were prepared by dissolving 4.41 mg in 10 ml of 0.01 M borax solution and diluting to 50 ml with distilled-deionized water. All solutions were prepared with distilled-deionized water; analytical-grade reagents were used.

Procedures

Sample preparations. Solutions of tablets were prepared by dissolving a single tablet in 20 ml of 0.01 M borax solution in a 100-ml flask, and diluting to the mark with water. After 30 min, 10 μl of the clear supernatant solution was added to the supporting electrolyte in the cell.

For urine, four 2.5-ml portions of the sample were placed in four 150-ml beakers and 10, 20 or 30 μl of 2×10^{-4} M folic acid was added to three of the beakers, to provide a standard additions series. Then 15 ml of water was added to each beaker and the sample solutions were boiled gently for about 3 min. After cooling, the sample solutions were transferred to 25-ml flasks, 1.25 ml of 2 M sulfuric acid was added and the solutions were diluted to the mark. A portion (10 ml) of these solutions was transferred to the cell.

Stripping voltammetry. The supporting electrolyte solution (usually 10 ml of 0.1 M sulfuric acid) was degassed with nitrogen for 8 min (and for 30 s before each adsorptive stripping cycle). The preconcentration potential (usually −0.30 V) was applied to the electrode for a selected time, while the solution was stirred at a reproducible rate. The stirring was then stopped,

and after a 15-s rest period, the voltammogram was recorded by applying a negative-going differential-pulse scan. The scan was terminated at −0.95 V, and the adsorptive stripping cycle was repeated using a new mercury drop. All data were obtained at ambient temperature.

RESULTS AND DISCUSSION

Factors affecting the adsorptive stripping response

The cyclic voltammograms of 3×10^{-5} M of folic acid in 0.1 M sulfuric acid are shown in Fig. 1. Two sharp cathodic peaks (I_c and II_c) were observed at −0.55 V and −0.83 V vs. Ag/AgCl, respectively. The heights of these peaks increased with prolongation of the period during which the HMDE was kept at −0.30 V before scanning. The subsequent scans produced smaller but unchanged peaks. At a slower scan rate (20 mV s^{-1}), a small broad "diffusion peak" overlapping with the peak I_c was observed at about −0.50 V. Two small anodic peaks appeared at −0.45 V and −0.76 V, respectively. At higher scan rate (100 mV s^{-1}), the height of peak I_a slightly increased and peak II_a disappeared. These results indicate that the reduction of folic acid in sulfuric

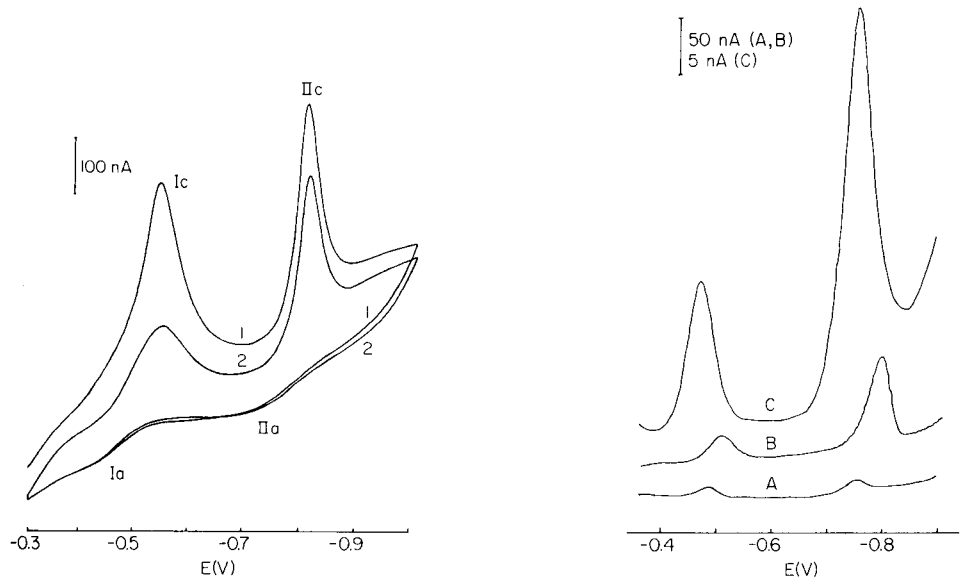

Fig. 1. Cyclic voltammograms for 3×10^{-5} M folic acid in an unstirred 0.1 M sulfuric acid solution (scan rate, 50 mV s^{-1}). Peaks Ia/Ic and IIa/IIc correspond, respectively, to the anodic waves (a) and the cathodic waves (c). Accumulation time at −0.30 V: (1) 20 s; (2) 0 s.

Fig. 2. Linear scan (A), normal pulse (B) and differential pulse (C) stripping voltammograms for 3×10^{-8} M folic acid in 0.1 M sulfuric acid. Preconcentration for 2 min at −0.30 V; scan rate, 10 mV s^{-1}.

acid solution undergoes two steps and the electrochemical processes are irreversible [16].

The spontaneous adsorption process can be utilized as an effective preconcentration step prior to pulse voltammetric measurement. The adsorptive stripping response strongly depends on the composition of the chosen supporting electrolyte. Various electrolytes (sodium hydroxide, sulfuric acid, acetate and borate buffers) were examined for the adsorptive stripping study. In acetate buffer, two peaks appeared, analogously to the behavior in sulfuric acid; there was only one peak in borate buffer, pH 8.25, which varied in height and potential with change of pH. Differential-pulse stripping for 2×10^{-7} M folic acid after preconcentration for 30 s at −0.3 V in 0.1 M sulfuric acid produced two well-defined peaks (I and II) at −0.47 and −0.75 V vs. Ag/AgCl, respectively. The current of peak II was seven times larger than that of peak I, thus peak II was preferred for analytical purposes (unless otherwise stated). Peak currents of 56, 57, 55, 57 and 45 nA were obtained for solutions in 0.02, 0.1, 0.3, 0.7, and 1.3 M sulfuric acid, respectively, with peaks moving slightly to more positive potentials. The optimum range of sulfuric acid was from 0.02 to 0.7 M. A 13-fold enhancement of peak current was obtained in 0.1 M H_2SO_4 for 5×10^{-8} M folic acid after preconcentration for 2 min at −0.30 V, thus 0.1 M sulfuric acid was used in subsequent work. The detailed behavior of adsorptive stripping of folic acid in acetate and borate buffer media will be reported elsewhere.

Figure 2 shows a comparison of stripping voltammograms for a 3×10^{-8} M folic acid using the three conventional potential waveforms available with the instrumentation used. Clearly, the differential-pulse mode offers a much better signal/noise ratio than normal-pulse stripping, thus it was preferred for subsequent work.

The amount of folic acid adsorbed on the electrode is a function of deposition time in a well-stirred 0.1 M sulfuric acid solution. Figure 3 shows that the current for peak I (curve a) increases linearly with preconcentration time, while for the peak II (curve b) the current increases nonlinearly. The plot of i vs. $t^{1/2}$ for peak II is linear after 60 s. The stripping response also

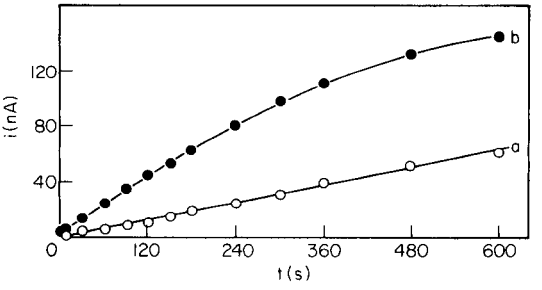

Fig. 3. Effect of preconcentration time (t) on the differential-pulse stripping response for 5×10^{-8} M folic acid. Curves (a) and (b) correspond, respectively, to peaks I and II. Other conditions as in Fig. 2.

depends on the preconcentration potential. Potentials of −0.20, −0.30, −0.40, −0.50, −0.60 and −0.65 V yielded peak currents of 17.4, 15.7, 14.4, 14.2, 13.8 and 11.1 nA, respectively (5×10^{-8} M folic acid; 30-s preconcentration). A preconcentration potential of −0.30 V was used in subsequent work.

Organic compounds forming compounds with mercury (e.g., sulfur-containing compounds) on deposition at a suitably positive potential may give cathodic peaks on application of negative potential scans. Various non-sulfur compounds, such as flavin or porphyrins, also yield cathodic stripping responses. For these compounds, preconcentration may involve adsorptive accumulation without the formation of mercury compounds [17]. In order to understand the nature of the accumulation of folic acid, three experiments were done with 5×10^{-8} M folic acid in 0.1 M sulfuric acid under the following conditions: (i) no deposition at −0.30 V but a 15-s rest before stripping; (ii) open circuit for 2 min (the cell was disconnected from the PAR 174 polarographic analyzer) followed by a 15-s rest at −0.30 V; (iii) deposition at −0.30 V for 2 min followed by a 15-s rest. The resulting stripping peak currents were 3.5, 16.5 and 49.6 nA, respectively. If the stripping responses resulted from the formation of a mercury salt of folic acid during preconcentration, the peak currents from the first and second experiments should be equal, and the peak current from the third experiment should be thirteen times larger than that from the second (calculated from Fig. 3b), not just three times. Moreover, when the preconcentration potential is as negative as −0.65 V, oxidation of mercury is not possible in 0.1 M sulfuric acid. Therefore, during preconcentration, folic acid is simply adsorbed on the electrode, and this adsorption is more efficient in closed circuit.

Quantitative evaluation is based on the linear correlation between the stripping peak current and concentration. For example, a linear relation was obtained for eight different concentrations of folic acid covering the range 4×10^{-10}—11.2×10^{-9} M after a preconcentration period of 5 min (other conditions as for Fig. 2). A least-squares treatment of the data yielded a slope of 1.16 nA/10^{-9} M (correlation coefficient, 0.997). The precision was estimated by eight successive measurements of 5×10^{-8} M folic acid (60-s preconcentration at −0.30 V). The mean peak current found was 24.2 nA, with a range of 24.0—24.8 nA and a relative standard deviation of 1.2%. For peak I, the mean peak current was 6.2 nA, with a range of 5.9—6.5 nA and a relative standard deviation of 3%. These values compare favorably with those reported for adsorptive stripping measurements at solid electrodes [13, 14]. Besides the reproducible area and self-cleaning properties of the static mercury drop electrode, this improvement can be attributed to the stability of folic acid in the supporting electrolyte. For a period of 3 h, the peak height and shape remained unchanged for a 5×10^{-8} M folic acid.

The signal enhancement associated with the adsorptive preconcentration resulted in very much lower detection limits compared to those obtained by conventional voltammetric measurements. Measurement of 9.6×10^{-9} M

folic acid was used to evaluate the detection limit, defined as twice the height of the baseline ripples. A value of 1×10^{-10} M was estimated following 5-min preconcentration. The detection limit calculated from data for peak I was about 7×10^{-10} M.

Interferences

Practical applications of adsorptive stripping voltammetry can suffer from interferences caused by surface-active compounds. The effect of gelatin on the folic acid stripping response is shown in Fig. 4A; even 1 mg l^{-1} gelatin depresses the folic acid peak current by 10% of its initial value, while 5 mg l^{-1} causes an 80% decrease. The suppression effect depends on the preconcentration period (Fig. 4A); the decrease in peak current is accompanied by a gradual broadening of the peak and shifting of the peak potential to more negative values. The likely explanation is that the surfactant competes with folic acid for the surface of the electrode, affecting the rate of charge transfer and also the amount of surface coverage by folic acid.

Anions reacting with mercury ions (e.g., bromide) can cause depression of the adsorptive stripping response [12]. Sodium bromide was added to a 5×10^{-8} M solution of folic acid to investigate the effect of bromide on the peak current of folic acid (Fig. 4B); only 8% and 13% peak current depressions were observed in 5×10^{-3} M NaBr solution after preconcentration for 30 and 90 s, respectively.

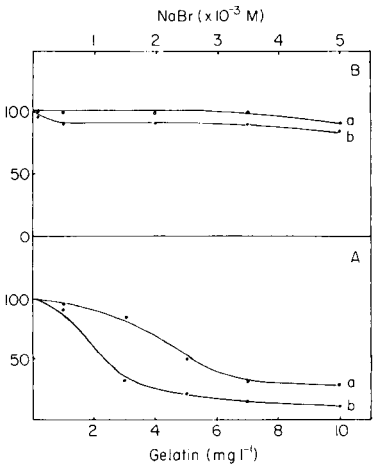

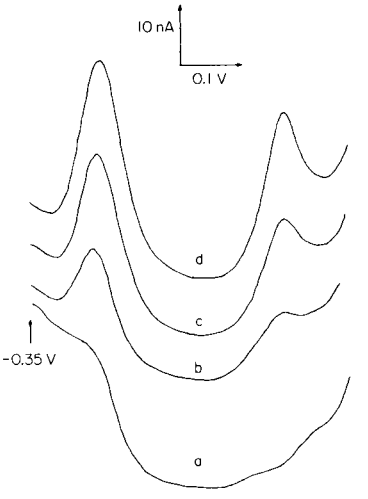

Fig. 4. Effect of gelatin (A) and sodium bromide (B) on the folic acid (5×10^{-8} M) stripping peak. Preconcentration period: (a) 30 s; (b) 90 s. Other conditions as in Fig. 2; 100 indicates the measurement with no interference present.

Fig. 5. Stripping voltammograms for standard additions to a urine sample in 0.1 M sulfuric acid: (a) urine sample; (b—d) additions of folic acid in concentration steps of 8×10^{-8} M. Preconcentration for 30 s (without stirring); other conditions as in Fig. 2.

Applications of the method

Single tablets (Changchow Medicine Works, Kiangsu Province), nominally containing 5 mg of folic acid per tablet, were used for folic acid determination. Quantitation was based on standard additions. The result obtained was 5.05 ± 0.24 mg (95% confidence limit, n = 4). Well-defined peaks were obtained and no interference was observed.

Figure 5 demonstrates the possibility of applying the method to measurement of folic acid in urine. The heights of both peaks I and II increased in a linear fashion after the addition of known amounts of folic acid to the urine.

In conclusion, the adsorptive stripping voltammetric method described possesses immediate value for pharmaceutical and food analysis. Further studies on the electroanalytical chemistry of folic acid and its derivatives are continuing in this laboratory.

REFERENCES

1 A. White, P. Handler, E. L. Smith, R. L. Hill and I. R. Lehman, Principles of Biochemistry, 6th edn., McGraw-Hill, New York, 1978, pp. 1349—1352.
2 G. R. Rao, G. Kanjilal and K. R. Mohan, Analyst, 103 (1978) 993.
3 H. R. S. Iyer and B. K. Apte, Indian J. Pharm., 31 (1969) 58.
4 W. H. Tafolla, A. C. Sarapu and G. R. Dukes, J. Pharm. Sci., 70 (1981) 1273.
5 L. Rozanski, Analyst, 103 (1978) 950.
6 M. Jozan, Acta Pharm. Hung., 50 (1980) 153.
7 A. V. Belyi, R. L. Galagan, L. M. Belaya and T. V. Gurzhii, Farm. Zh., 6 (1981) 45.
8 Z. D. Qiao, D. H. Pan and H. Gao, Yaoxue Tongbao, 17 (1982) 522.
9 C. F. Kolpin and H. S. Swofford, Jr., Anal. Chem., 50 (1978) 916.
10 A. Webber, M. Shah and J. Osteryoung, Anal. Chim. Acta, 154 (1983) 105.
11 J. Wang, D. B. Luo and P. A. M. Farias, J. Electroanal. Chem., 185 (1985) 61.
12 J. Wang, D. B. Luo, P. A. M. Farias and J. S. Mahmoud, Anal. Chem., 57 (1985) 158.
13 H. Y. Cheng, L. Falat and R. L. Li, Anal. Chem., 54 (1982) 1384.
14 E. N. Chaney and R. P. Baldwin, Anal. Chem., 54 (1982) 2556.
15 J. Wang and B. A. Freiha, Anal. Chem., 55 (1983) 1285.
16 E. Laviron, J. Electroanal. Chem., 52 (1974) 355; 63 (1975) 245.
17 J. Wang, Stripping Analysis: Principles, Instrumentation and Applications, Verlag Chemie International, Deerfield Beach, FL, 1985, p. 58.

Analytica Chimica Acta, 189 (1986) 285—292
Elsevier Science Publishers B.V., Amsterdam — Printed in The Netherlands

LIQUID-PHASE POLYMER-BASED RETENTION, A NEW METHOD FOR SEPARATION AND PRECONCENTRATION OF ELEMENTS

K. E. GECKELER and E. BAYER*

Institute of Organic Chemistry, University of Tübingen, D-7400 Tübingen 1 (Federal Republic of Germany)

B. YA. SPIVAKOV, V. M. SHKINEV and G. A. VOROB'EVA

Vernadsky Institute of Geochemistry and Analytical Chemistry, Academy of Sciences, Moscow 117 975 (U.S.S.R.)

(Received 24th June 1986)

SUMMARY

A method based on the retention of inorganic ions by water-soluble polymeric reagents (liquid-phase polymer-based retention) in a membrane filtration cell is suggested for the separation and preconcentration of various elements. The preseparated elements remain in the aqueous solution, which is convenient for most instrumental methods of completing the analysis. The water-soluble poly(ethyleneimine) and its thiourea and methylated derivatives are shown to be useful for retention of different inorganic ions and their separation from elements not bound to the polymeric reagent.

Preconcentration techniques are often required in inorganic analysis, especially in trace analysis to separate elements to be determined from the interfering constituents of the sample and to improve the sensitivity of the method [1, 2]. Liquid—liquid extraction, sorption, precipitation and other methods, based on two-phase distributions, are used in most cases for the separation of inorganic species contained in dissolved solid matrices, industrial fluids or natural waters. Although many such methods have been developed and successfully used, their application can cause problems. Some problems can be connected with heterogeneous reactions and interphase transfer. Other problems can arise if aqueous solutions are preferred for the subsequent procedure rather than organic solvents or solid concentrates. In such cases, additional procedures are needed, e.g., back-extraction, desorption, dissolution of solid concentrates, etc., which complicate the analysis and can result in contamination of the sample from the reagents added.

Two-phase systems can be avoided by application of separation methods based on membrane processes, which are among the most promising techniques for enrichment of various species from solutions [3]. Use of chemically inert solid membranes makes it possible to achieve separations in the homogeneous aqueous phase, and these processes are easily handled and automated. To date, membrane separations have been relatively seldom used in

0003-2670/86/$03.50

analytical chemistry. Ultrafiltration has been applied to study copper complexation in swamp water and to estimate distribution of species between solution and solid particles [4—6]. Reverse osmosis can also be used [7].

Higher efficiency and selectivity of membrane separations can be achieved by using water-soluble polymeric reagents in combination with membrane filtration [8—11]. Different polymeric reagents with chelating groups have been synthesized for use in the retention of metal ions in homogeneous aqueous phases [8, 9]. This method, based on separation of inorganic ions bound to the polymer from uncomplexed ions, has been recommended for recovery of metals from diluted solutions. The technique can easily be used for analytical purposes, because in this case the equipment and procedures are simple. Also, more diverse and expensive but stronger complexing reagents can be applied [11].

First attempts to apply complexation in combination with ultrafiltration for the concentration of copper(II) and nickel ions have been described [12]. However, the term used does not stress the most important ingredient of the system, the polymeric reagent, and the process itself is diafiltration rather than ultrafiltration.

The method described here is based on the application of a new class of polymeric reagents in liquid phase in conjunction with membrane filtration and therefore it may be termed liquid-phase polymer-based retention (LPR).

This paper shows the possibility of separation and enrichment of different inorganic ions by the LPR method and describes a procedure pertinent to analytical purposes.

EXPERIMENTAL

Reagents and radionuclides

Acid, base and salt solutions were prepared from analytical-grade reagents. Poly(ethyleneimine) (P), poly(ethyleneimine-methylthiourea) (P-TU) and permethylated poly(ethylenimine) sulfate (P-PMS), used in retention studies, had a molecular mass in the range 30 000—40 000 g mol^{-1}. The reagents were dissolved in water and membrane-filtered prior to use. Individual radionuclides ^{65}Cu, ^{110m}Ag, ^{198}Au, ^{65}Zn, ^{203}Hg, ^{76}As, ^{54}Mn, ^{59}Fe, ^{60}Co, ^{109}Pd, ^{197}Pt were applied to study the distribution of these elements between the cell solution and the filtrate. To examine the behavior of several elements simultaneously, the mixture used contained ^{24}Na, ^{39}K, ^{134}Cs, ^{65}Cu, ^{198}Au, ^{69m}Zn, ^{115}Cd, ^{115m}In, ^{76}As, ^{51}Cr, ^{75}Se, ^{60}Co.

Equipment

The unit used for retention studies consisted of a filtration cell with a magnetic stirrer, a membrane with an exclusion rating of 10 000 (Amicon PM-10), a reservoir, a selector and a regulator (Fig. 1). The pressure of nitrogen was kept constant (300 kPa) during membrane filtration.

Radiometric measurements of individual isotopes were made with an

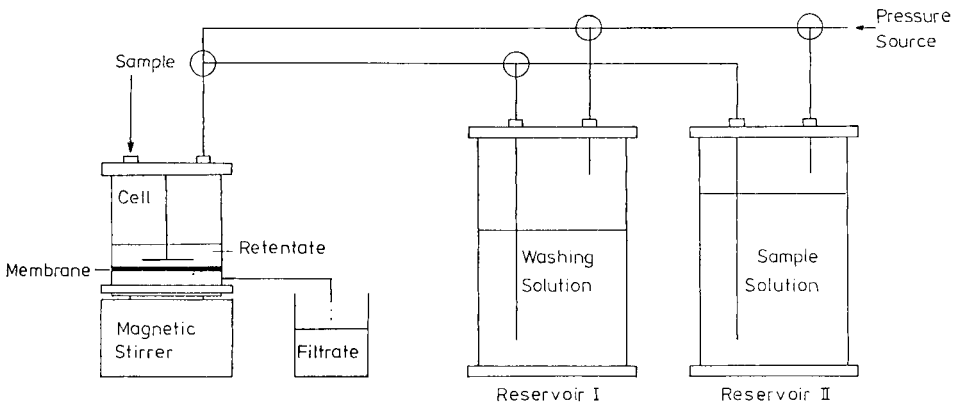

Fig. 1. Instrumental arrangement for the LPR method.

NRG-603 automatic γ-counter (Tesla). Simultaneous measurements of γ-activities of several elements were made with a Ge(Li) detector connected to a multichannel LP-4900 analyzer (Nokia). The γ-spectra were computer-processed with a program developed by V. P. Kolotov and V. V. Atrashkevich at the Vernadsky Institute. Concentrations of Ni, Mg, and in some cases of Cu, Zn, Cd, Hg, Co were measured by atomic absorption spectrometry on a Beckman 1248 spectrometer.

Procedure

An aliquot of a nitrate or chloride solution of one or several elements was placed in the filtration cell containing the polymeric reagent solution. The total constant volume was 2 or 4 ml in the cell; the reagent concentration was between 1 and 5% and the element concentration between 10^{-4} and 10^{-6} mol l^{-1}. The pH of the cell and reservoir solution were adjusted to the same value. The system was pressurized, and the cell solution was stirred for 5 min and then washed with the reservoir solution. The filtrate fractions were collected and subjected to radiometric or atomic absorption measurements, as was the cell solution before and after each filtration run. The retention values, calculated from the concentration measurements of filtrate and retentate, were compared to ensure that no adsorption phenomena had occured during the experiment.

RESULTS AND DISCUSSION

In previous studies devoted to polymer-based retention, large volumes of feed metal solutions were passed into the filtration unit to show the possibility of metal recovery from dilute solutions [11]. The loading capacities of the polymers with respect to metal ions were the main characteristics examined, to estimate the applicability of the reagents on a preparative scale. Such a procedure can also be used for the preconcentration of elements from

samples with large volumes, e.g., in the analysis of waters or very dilute fluids. However, when this procedure is used, interfering components of the test solution partly remain in the cell after the filtration run, even when they do not interact with the reagent. A small sample can be more convenient to handle, especially when the problem consists in separation of elements to be determined from interfering matrix constituents (relative preconcentration) rather than in their enrichment (absolute preconcentration).

That is why a new procedure is suggested in which the sample is placed directly in the polymer-containing cell solution and then washed with water. The pH is adjusted to a value at which the elements of interest are retained and other species removed. A combination of two procedures is also of interest: a sample with large volume is passed through a smaller volume of polymer solution in the cell and then washed to achieve both absolute and relative preconcentration.

The loading capacity of the polymers is not as important for the separation of trace elements to be determined as their ability completely to retain the required elements in the course of one filtration run. It can easily be shown that the retention of any species, not bound to the polymer and therefore not rejected by the membrane, is described by an exponential function:

$$R = C_r C_0^{-1} = \exp(-V_f V_0^{-1})$$

where C_r is the species concentration in the retentate (cell solution after a filtrate volume of V_f has been passed), C_0 is the initial species concentration in the cell, V_0 is the volume of cell solution, and V_f is the volume of filtrate.

The retention of such species can be expressed as $\log R = -0.43\,Z$, where $Z = V_f/V_0$. Thus, theoretically the concentration of unrejected species in the cell can be made 10^3 times lower at $Z = 7$ or more than 10^4 times lower at $Z = 11$, etc. In other words, if element A is completely retained in the cell ($R_A \rightarrow 1$), it can be separated from element B with a maximum separation factor ($\beta = R_A/R_B$) expressed as $\log \beta = 0.43\,Z$. The separation factor β expressed as a ratio of distribution coefficients for two species, used in methods based on two-phase distributions, cannot be applied to homogeneous phase distribution. For that reason, the separation factor in LPR separations should be expressed as the ratio of retention values.

Separation of various ions with two neutral polymeric reagents with different complexing groups (P and P-TU), and with one polymer with anion-exchange groups (P-PMS) was examined. The data in Fig. 2 show that polymer P, a relatively weak complexing agent, can be used for metal separations by the LPR method in neutral solutions. At pH 6 this reagent quantitatively retains several divalent metals (Cu, Zn, Cd, Hg, Mn, Co, Ni). Manganese(II) is also completely retained at pH > 8, which is very interesting because extraction of this element from aqueous solution is a difficult problem for any separation method. Copper(II), which forms the most stable complexes with P, can be separated from other elements at lower pH values ($\geqslant 3$). Alkali and

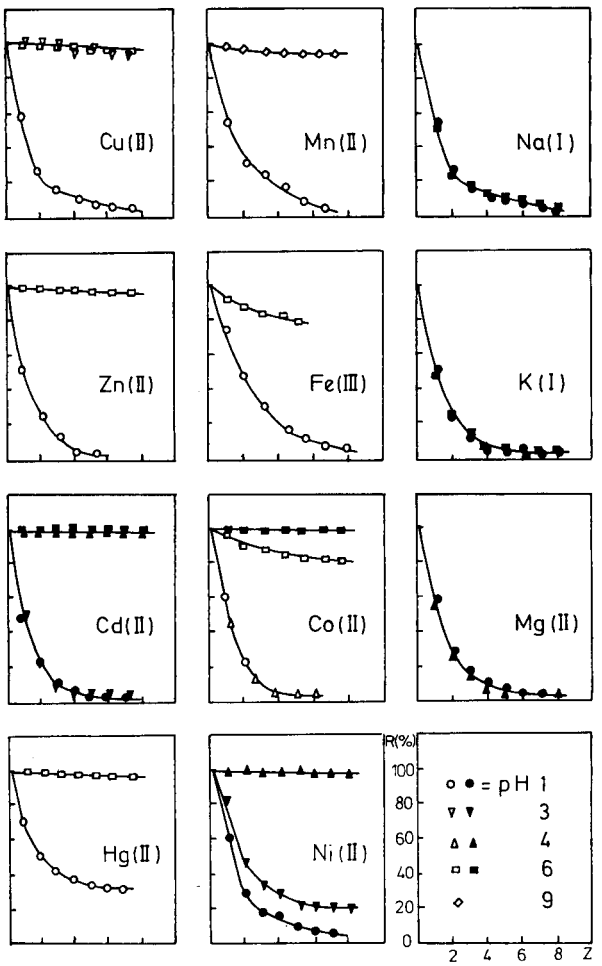

Fig. 2. Retention of metal ions by 1% (w/w) P at different pH values in the absence (filled symbols) and presence of 0.15 M $NaNO_3$ (open symbols) as a function of the ratio of filtrate volume to cell solution volume (Z). The pH symbols are defined in the bottom right hand corner.

alkaline-earth elements are completely washed out into the filtrate at any pH value (Fig. 2).

The sulfur-containing P-TU derivative is an effective reagent for separation of mercury and noble metals from other elements. A 3% (w/w) solution of P-TU quantitatively retains Hg(II), Ag(I), Au(III), Pd(II), Pt(IV) from chloride solution at pH 1 and separates these elements not only from alkali metal ions but also from non-ferrous metal ions such as Co(II), Zn(II), Cd(II) and In(III) (Fig. 3). Under these conditions, chromium(VI), which is present as an oxo anion in solution, is also removed from the cell. For the elements Hg, Ag, Au, Pd added to the solution containing P-TU, prior

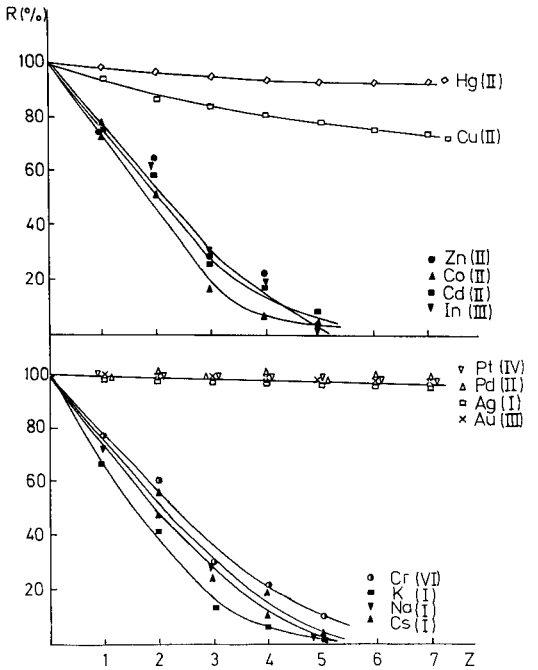

Fig. 3. Retention of metal ions by 3% (w/w) P-TU from 0.15 M NaCl at pH 1 as a function of Z.

stirring for less than 5 min is enough for complex formation and separation from uncomplexed elements. In the case of platinum(IV), complete retention is achieved if the cell solution is stirred for 2 h before the filtration is started. This is necessary because of the kinetic inertness of hexachloroplatinate(IV).

Chromate ions are readily retained by the anion-exchange reagent, P-PMS, during the filtration. Selenium(IV) is also retained in the cell containing 4% P-PMS at pH 8.5, most probably as selenite. The reagent also retains partly some divalent metal cations (Cu, Zn, Cd, Co) which can interact with the unmethylated nitrogen atoms of the base polymer. This decreases the reagent selectivity to anionic forms of elements. However, it also shows the possibility of simultaneous retention of various elements by means of bifunctional reagents. Alkali metal cations as well as other ions which do not interact with any reagent groups, are completely washed out into the filtrate (Fig. 4).

The retention of inorganic ions by the LPR method is influenced by several factors. The influence of solution pH is illustrated in Fig. 2. This factor affects both the complexation reaction and the flow rate through the membrane. In the presence of poly(ethyleneimine) and its derivatives, the flow rate drops dramatically at pH 11. The flow rate also decreases with the polymer concentration, but the latter factor generally favours retention because of the better complexation ability of polymer reagents.

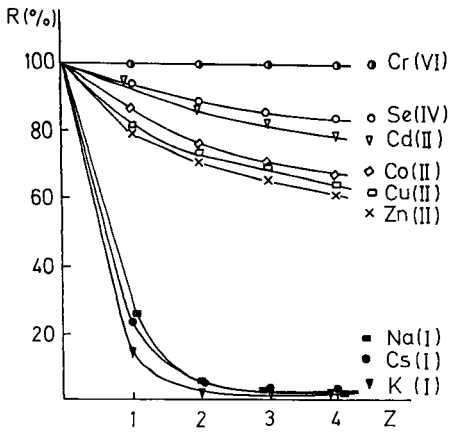

Fig. 4. Retention of metal ions and oxo anions by 4% P-PMS from 0.01 M NaCl at pH 8.5.

Neutral salts (e.g., sodium chloride or nitrate) do not have a significant effect on retention with a strong complexing reagent such as P-TU. The salts have a stronger effect on the retention of metal ions with the poly(ethyleneimine) reagent. This can be seen from the data on the cobalt retention presented in Fig. 2. Neutral salts have the greatest influence on the retention of anions with P-PMS. The effect could be due to competition of the salt anions for the anion-exchange reagent and to the effect of the salts on the conformation of the polymer molecules in solution [13]. The last factor can be important for any type of polymer.

The efficiency of the LPR method also depends on the pressure applied, type of membrane and other factors which should be taken into consideration to obtain rapid and effective separations.

A combined procedure can be applied for the enrichment of some elements from a large sample volume and subsequent separation from other elements initially present in the sample. To demonstrate this, a model fluid containing Hg(II), Cd(II), Cu(II) and 3% NaCl (concentration in sea water) was passed from reservoir II to the cell containing 1% P-TU at pH 6. After 10-fold preconcentration, the cell solution was washed from reservoir I with a 10-fold volume of distilled water referred to the cell solution volume. After this procedure, 98% of the mercury, cadmium and copper remained in the cell while the sodium concentration decreased to 3 mg l^{-1}. Then cadmium and copper were quantified by flame atomic absorption spectrometry and mercury by the cold-vapour atomic absorption technique.

It should be stressed, in conclusion, that the LPR separation is expected to be easily combined with inductively-coupled plasma spectrometric, electrochemical, spectrophotometric and other methods of analysis.

This work was supported in part by the Deutsche Forschungsgemeinschaft.

REFERENCES

1 Yu. A. Zolotov and N. M. Kuz'min, Preconcentration of Trace Elements, Khimiya, Moscow, 1983.
2 A. Mizuike, Enrichment Techniques for Inorganic Trace Analysis, Springer, Berlin, 1983.
3 S.-T. Hwang and K. Kammermeyer, Membranes in Separations, Wiley, New York, 1975.
4 J. K. Tuschall and P. L. Brezonik, Anal. Chim. Acta, 149 (1983) 47.
5 M. R. Hoffman, E. S. Yost, S. J. Eisenreich and W. S. Maier, Environ. Sci. Technol., 15 (1981) 655.
6 R. J. Smith, Anal. Chem., 48 (1976) 74.
7 M. Takagi, T. Hayashita and K. Ueno, 4th Annual Meeting of Japan Society of Membrane Science, Tokyo, 1982.
8 K. Geckeler, G. Lange, H. Eberhardt and E. Bayer, Pure Appl. Chem., 52 (1980) 1883.
9 E. Bayer, H. Eberhardt and K. Geckeler, Angew. Makromol. Chem., 97 (1981) 217.
10 K. Geckeler, V. N. R. Pillai and M. Mutter, Adv. Polym. Sci., 39 (1981) 65.
11 B. Ya. Spivakov, K. Geckeler and E. Bayer, Nature, 315 (1985) 313.
12 Q. T. Nguyen, Y. Jyline and J. Neel, Desalination, 36 (1981) 277.
13 A. S. Polinskii, V. S. Pshezhetskii and V. A. Kabanov, Polymer Science U.S.S.R., 25 (1983) 81.

Analytica Chimica Acta, 189 (1986) 293—299
Elsevier Science Publishers B.V., Amsterdam — Printed in The Netherlands

COMPARISON OF LIQUID CHROMATOGRAPHIC SEPARATIONS OF GEOMETRICAL ISOMERS OF SUBSTITUTED PHENOLS WITH β- AND γ-CYCLODEXTRIN BONDED-PHASE COLUMNS

C. ALLEN CHANG* and QIHUI WU

Department of Chemistry, University of Texas at El Paso, El Paso, TX 79968-0513 (U.S.A.)

(Received 6th June 1986)

SUMMARY

The capacity factors (k') of several substituted phenols were measured by using β- and γ-cyclodextrin bonded-phase columns with mobile phases varying from the classical normal-phase conditions (e.g., heptane/2-propanol) to the reversed-phase conditions (e.g. water/2-propanol). The cyclodextrin columns have unusual selectivities in both normal- and reversed-phase separations because of their large number of hydroxyl functional groups and their ability to form inclusion complexes with substrates. The occurrences of minima in plots of log k' vs. percent organic modifier for various substituted phenols are considered to result from solute/solvent competition for interaction with the stationary phase and from the relative hydrophobicity of the stationary and mobile phases.

Tailor-made column-packing materials in liquid chromatography are desirable because of their different physical and chemical properties that help to provide highly selective separations. Often these packing materials are prepared with silica because of its pressure resistance and easy surface modification. Thus, simple bonded phases such as octadecylsilica (ODS), and amine and cyano bonded phases have been widely used [1]. More delicate molecular design on surfaces has already demonstrated its promise for a new generation of columns. Among the columns recently developed are the cyclodextrin-bonded phase [2], the amino acid ester-bonded phase (Pirkle columns) [3], and possibly the metal complex-bonded phases [4]. All the second-generation bonded-phase columns have common characteristics, i.e., the functional groups or molecules derivatized on the surface are more complex and capable of multipoint interactions with the analytes, thus making separations more selective.

The use of a β-cyclodextrin-bonded phase column has been reported for the separation of geometrical isomers of mono- and di-substituted benzenes as well as their organometallic derivatives [5]. Because of its capabilities to form both H-bonding and inclusion complexes with analytes, the β-cyclodextrin column can be used in both normal- and reversed-phase chromatography [6, 7]. In particular, the hydrogen-bonding interaction is con-

0003-2670/86/$03.50

sidered to be more significant in determining the separation selectivities in the normal-phase mode, whereas the inclusion process is thought to be more significant in the reversed-phase mode. This paper deals with the results of studies on the retention and separation of various substituted phenols in both normal- and reversed-phase modes with both the β- and γ-cyclodextrin (β-CD and γ-CD) bonded-phase columns. β-Cyclodextrin and γ-CD are cyclic carbohydrates containing seven and eight glucose units and having cavity sizes of about 7 Å and 8.5 Å in diameter, respectively. For comparison, results of separation of these phenols on a less-structured Partisil PXS-ODS column are also included.

EXPERIMENTAL

Apparatus

A Beckman Model 332 gradient liquid chromatography system was used for the separations. This system was equipped with two Altex Model 110A pumps, a Model 210 sample injector valve, and a Model 420 system controller. A Waters Model 440 absorbance detector (254 nm) and a Houston Instrument Omniscribe Model D5000 recorder were also used. In some studies, a Micromeritics (Norcross, GA) Model 786 variable-wavelength (200—600 nm) detector with a deuterium lamp was also used with a Linear Model 555 single-channel recorder.

Pressure-Lok series C-160 25-μl syringes (Precision Sampling, Baton Rouge, LA) were used for sample injection.

Columns and chemicals

The β-CD and γ-CD bonded-phase columns (5-μm particle size, 25-cm × 4.6-mm i.d.) were obtained from Advanced Separation Technologies (Whippany, NJ). The Partisil PXS-ODS column (10-μm particle size, 25-cm × 4.6-mm i.d.) was obtained from Whatman (Clifton, NJ).

The *o*-, *m*-, and *p*-isomers of four substituted phenols (cresol, chlorophenol, nitrophenol, and aminophenol) were from Aldrich (Milwaukee, WI). High-performance liquid chromatographic-grade solvents were from Fisher (Fairlawn, NJ).

Chromatographic procedures

Before the separation experiments, the columns were pre-equilibrated with the mobile phase for at least 3 h. After pre-equilibration, a flow rate of 1 ml min^{-1} was set for the chromatographic processes. Samples consisted of 3-μl aliquots of mixtures of solutes, each at 1—2 μg μl^{-1}, dissolved in the eluent. Back-pressures of <1000 psi and 3000 psi were usually observed in the course of the normal-phase and reversed-phase chromatography, respectively. All data points were collected by averaging more than three reproducible separations. Published methods were used to evaluate t_0 for the β-CD and γ-CD columns [8].

RESULTS AND DISCUSSION

The three bonded-phase columns all have mixed surface coverage of functional groups, partly because of the difficulty of controlling the extent of surface derivatization reaction [9]. The β-CD and the γ-CD packings have alkyldiol and unreacted silanol groups in addition to the bound cyclodextrin molecules. The Partisil PXS-ODS column has both silanol and octadecyl groups. The octadecyl groups on the silica surface form less structured regions that are hydrophobic; these can be regarded as similar to the environment that the cyclodextrin cavity creates.

Elution order

Table 1 lists the capacity factors of several substituted phenols on β-CD, γ-CD, and Partisil PXS-ODS columns with different mobile-phase compositions. The elution orders for both the β-CD and γ-CD columns are the same (except for a few minor differences) in the normal-phase separation of phenols with 2-propanol/heptane mixtures as mobile phases. For example, with 2-propanol/heptane (20:80, v/v) the orders are *ortho* < *meta* < *para* for cresol, *meta* < *para* < *ortho* for chlorophenol, *ortho* < *meta* < *para* for nitrophenol, and *ortho* < *meta* < *para* for aminophenol. As the percentage of 2-propanol increases, most of the elution orders remain unchanged except for nitrophenol isomers, where the order becomes *meta* < *ortho* < *para*. In contrast, the elution order is quite different when a Partisil PXS-ODS column is used. The capacity factors for these phenol derivatives are all much smaller for the ODS column than for the CD columns. This indicates that the interactions between analytes and β-CD/γ-CD columns are stronger, presumably because of their greater number of hydroxyl groups. When the capacity factors of analytes are compared for β-CD and γ-CD columns, the k' values for the β-CD column are smaller for cresols, chlorophenols and nitrophenols, but greater for aminophenols. This is similar to what was observed when substituted anilines were separated on CD columns [10].

Remarkably, the elution order of these isomers in the reversed-phase mode is essentially the same as seen in normal-phase mode, again with a few minor exceptions, particularly when the percentage of 2-propanol in water is low. Thus the common expectation is not observed, i.e., those isomers which are eluted sooner in normal-phase operation are not necessarily eluted later in reversed-phase chromatography. The unusual elution behavior seen with the cyclodextrin columns may result from the formation of inclusion complexes, which takes molecular size into account and is more subtle and selective than conventional reversed-phase separation. Thus, compounds that form stronger inclusion complexes with cyclodextrin molecules and are least soluble in the reversed-phase mobile phase have greater retention times. However, the inclusion process seems to be the dominant factor in affecting the retention of solutes.

Figure 1A and B shows the normal- and reversed-phase separations of

TABLE 1

Capacity factors of selected substituted phenol isomers on β-CD, γ-CD, and Partisil PXS-ODS columns with different mobile-phase compositions

[Detection at 254 nm; flow rate 1.0 ml min^{-1}; t_0 = 2.91 min (β-CD), 2.96 min (γ-CD) and 3.0 min (PXS-ODS). Relative errors are within 2%.]

Column	Sample	Capacity factors with varying contents of 2-propanol (%)									
		In heptane					In water				
		20	40	60	80	100	80	60	40	20	10
β-CD	*o*-Cresol	0.42	0.21	0.11	0.07	0.05	0.01	0.01	0.12	0.74	1.08
	p-Cresol	0.57	0.24	0.13	0.07	0.05	0.02	0.03	0.15	0.86	1.61
	o-Chloro[a]	0.70	0.33	0.20	0.12	0.09	0.04	0.07	0.17	1.15	2.24
	p-Chloro[a]	0.66	0.28	0.16	0.10	0.07	0.02	0.03	0.14	1.35	2.50
	o-Nitro[a]	1.11	1.00	0.76	0.59	0.43	0.32	0.39	0.69	2.14	3.00
	m-Nitro[a]	2.04	0.77	0.44	0.37	0.22	0.08	0.04	0.14	1.07	1.96
	p-Nitro[a]	5.53	2.23	1.28	0.94	0.77	0.34	0.41	0.85	3.05	4.32
	p-Amino[a]	9.34	2.92	1.42	0.84	0.52	0.02	0.01	0.04	0.25	0.31
γ-CD	*p*-Cresol	0.57	0.23	0.14	0.08	0.06	0.03	0.02	0.06	0.53	0.97
	p-Chloro[a]	0.71	0.32	0.14	0.09	0.07	0.02	0.02	0.05	0.56	1.08
	p-Amino[a]	5.99	1.99	0.98	0.54	0.35	0.13	0.13	0.11	0.21	0.28
PXS-ODS	*p*-Cresol	0.20	0.11	0.09	0.09	0.07					
	p-Chloro[a]	0.17	0.12	0.09	0.06	0.05					
	p-Nitro[a]	0.24	0.20	0.11	0.09	0.09					

[a]Phenol derivative.

twelve substituted phenols under appropriate isocratic mobile-phase conditions on a γ-CD column. The normal-phase separation seems to give better resolution, i.e., nine out of twelve compounds can be separated, although the later peaks are quite broad. When the normal-phase chromatograms are compared for separations on γ-CD (Fig. 1A), β-CD (Fig. 1C), and Partisil PXS-ODS (Fig. 1D) under simple optimized isocratic elution conditions with 2-propanol/heptane mixtures as mobile phases, it is seen that none of the three column types completely separates the test mixture. Yet, any one of the columns can separate most of the compounds and therefore, can be used for practical applications.

Effect of mobile-phase composition and retention mechanism

The effect of mobile-phase composition is seen not only when the elution order of a particular series of compounds is concerned but also when the capacity factors (k') for a particular compound are measured at different mobile phase composition. Figure 2 shows log k' values for the geometrical isomers of nitrophenol plotted as a function of mobile-phase composition. The data include normal-phase operation with heptane/2-propanol mixtures through to 100% 2-propanol, followed by reversed-phase mode with 2-propanol/water mixtures. In the normal-phase region, the log k' values decrease

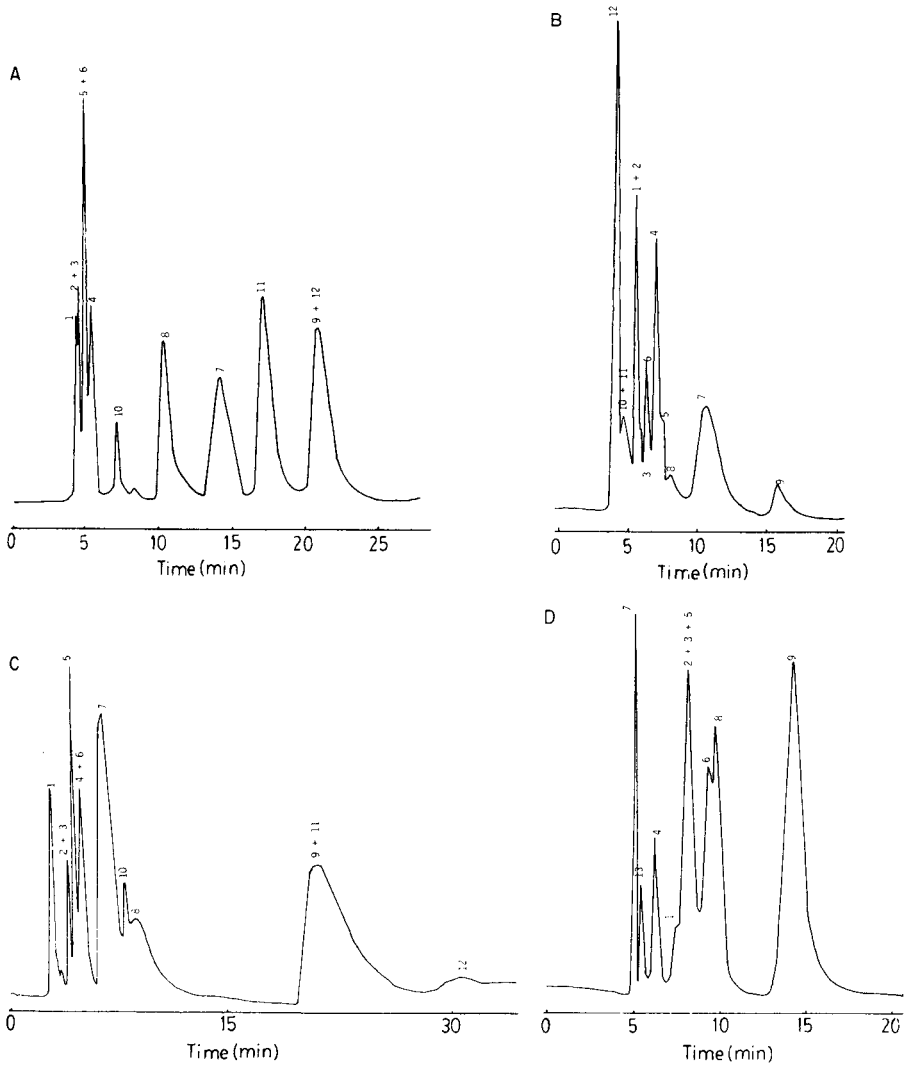

Fig. 1. Chromatograms for mixtures of several substituted phenol isomers on different columns with different eluents: (A) γ-CD column with 2-propanol/heptane (20:80); (B) γ-CD column with 2-propanol/water (10:90); (C) β-CD column with 2-propanol/heptane (20:80); (D) Partisil PXS-ODS column with 2-propanol/heptane (2:98). Peak identification: (1) *o*-cresol; (2) *m*-cresol; (3) *p*-cresol; (4) *o*-chlorophenol; (5) *m*-chlorophenol; (6) *p*-chlorophenol; (7) *o*-nitrophenol; (8) *m*-nitrophenol; (9) *p*-nitrophenol; (10) *o*-aminophenol; (11) *m*-aminophenol; (12) *p*-aminophenol; (13) phenol.

as expected as the solvent strength is increased with *m*-nitrophenol showing more solvent dependence. As the water content is increased in the 2-propanol mixtures to generate the reversed-phase mode, the log k' values initially decrease as the percent water increases, reaching minima around 70% 2-propanol in water. The log k' values then increase with increasing water

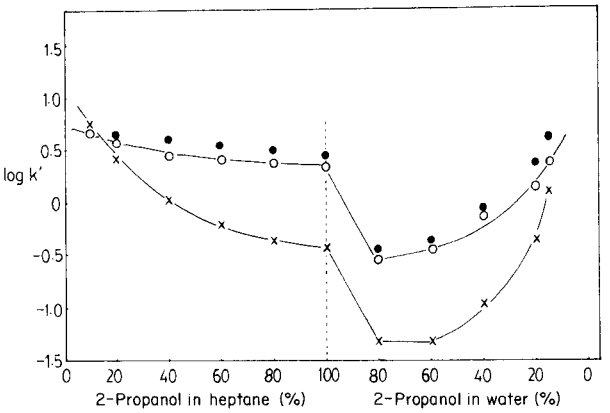

Fig. 2. Plots of log k' values on a γ-CD column as a function of mobile-phase composition: (○) *o*-nitrophenols; (×) *m*-nitrophenols; (●) *p*-nitrophenols.

content, i.e., the expected reversed-phase behavior. The unusual observation of minima does not occur when methanol is used as the organic solvent. The log k' values always increase when higher water content is added into methanol at any composition.

The observation of minima can be rationalized because 2-propanol forms a stronger inclusion complex with the cyclodextrin molecules than methanol and so competes against the substituted phenol for cyclodextrin. With a mobile-phase composition of 100% 2-propanol, the substituted phenols simply interact with the packing material surface through H-bonding and other minor forces. When water is added, the strength of phenol/cyclodextrin H-bonding is further decreased because of the better hydrophilicity of water. However, the inclusion of the analytes is not favored when the 2-propanol content is still high because of the favorable mass action of 2-propanol. The reversed-phase behavior occurs only when the cavities of cyclodextrin molecules become available and are more hydrophobic than the bulk mobile phase. This condition facilitates formation of inclusion complexes with the analytes. The same explanation has been offered for similar observations when substituted anilines are separated [10].

Finally, for practical normal-phase separation, it is recommended that the content of strong organic modifier (e.g., 2-propanol) be kept low so that the maximum number of interactions between the bonded phase and the substrates can be achieved for better resolution. In the reversed phase separation, the water concentration should be kept high to facilitate formation of the inclusion complexes.

Acknowledgement is made to the National Institute of Health-Minority Biomedical Research Support Program, the Texas Advanced Technology Research Program, and the Robert A. Welch Foundation of Houston, Texas for financial support of this research. Thanks are also due to Professor D.W. Armstrong for the gift of cyclodextrin bonded-phase columns.

REFERENCES

1 L. R. Snyder and J. J. Kirkland, Introduction to Modern Liquid Chromatography, 2nd edn., Wiley, New York, 1979.
2 D. W. Armstrong, J. Liq. Chromatogr., 7(S-2) (1984) 353.
3 W. H. Pirkle, J. M. Finn, J. L. Schreiner and B. C. Hamper, J. Am. Chem. Soc., 103 (1981) 3964.
4 C. A. Chang, C. -S. Huang and C. -F. Tu, Anal. Chem., 55 (1983) 1390.
5 C. A. Chang, H. Abdel-Aziz, N. Melchor, Q. Wu, K. H. Pannell and D. W. Armstrong, J. Chromatogr., 347 (1985) 51.
6 C. A. Chang, Q. Wu and D. W. Armstrong, J. Chromatogr., 354 (1986) 454.
7 C. A. Chang, Q. Wu and L. Tan, J. Chromatogr., 361 (1986) 199.
8 W. L. Hinze, T. E. Richl, D. W. Armstrong, W. DeMond, A. Alak and T. Ward, Anal. Chem., 57 (1985) 237.
9 D. W. Armstrong, U.S. Patent, No. 4,539,399, Sep., 1985.
10 C. A. Chang and Q. Wu, J. Chromatogr., 371 (1986) 269.

ıalytica Chimica Acta, 189 (1986) 301—311
sevier Science Publishers B.V., Amsterdam — Printed in The Netherlands

ÉPARATION CHROMATOGRAPHIQUE DES LANTHANIDES EN EUX GROUPES BASÉE SUR DES DIFFÉRENCES DANS LA INÉTIQUE DE DÉCOMPOSITION DES COMPLEXES ANTHANIDES-MACROCYCLES

MERCINY, J. F. DESREUX et J. FUGER*

ıboratoire de Chimie Analytique et Radiochimie, Université de Liège au Sart Tilman, 4000 Liège (Belgique)

:eçu le 10 Juin 1986)

ÉSUMÉ

La séparation des lanthanides en deux groupes, basée sur des vitesses de décomplexa-ɔn différentes des entités LnDOTA (DOTA = acide 1,4,7,10-tétraazacyclododécane-*N*′,*N*″,*N*‴-tétraacétique) est réalisée sur une colonne d'échangeur d'ions cationique sul-nate (forme H^+). Les terres yttriques, du terbium au lutétium inclus, sont éluées, par ɔl 1,25 M, en tête de chromatogramme, sous forme de complexes Ln-DOTA-H; les lan-anides légers, du lanthane au samarium inclus, sont élués sous forme d'ions tripositifs, queue de chromatogramme, par une solution plus concentrée d'acide chlorhydrique. est possible, en partant d'un mélange en quantités égales de complexes Eu-DOTA et d-DOTA de récupérer, en tête d'élution, 40% de gadolinium exempt d'europium et, en ı d'élution, 47% d'europium exempt de gadolinium.

JMMARY

(*Chromatographic separation of lanthanides into two groups based on kinetic differ-ɔces in the decomposition of macrocycle/lanthanide complexes*)

The separation of the lanthanides in two groups, based on differences in decomplexa-ɔn rates of the LnDOTA entities (DOTA = 1,4,7,10-tetraazacyclododecane-*N*,*N*′,*N*″,*N*‴-traacetic acid), is achieved on a sulphonate cation-exchange column (H^+ form). The trium earths, from terbium to lutetium, are eluted first as Ln-DOTA-H species with 25 M HCl; the light lanthanides, from lanthanum to samarium inclusive, are eluted as ıcomplexed ions at the end of the chromatogram, with more concentrated hydrochloric id. Given an equimolar mixture of the Eu-DOTA and Gd-DOTA complexes as starting lution, 40% of the gadolinium can be recovered free from europium at the start of ıtion and 47% of the europium free from gadolinium at the end of the elution.

Le macrocycle polyaza-polycarboxylique DOTA (acide 1,4,7,10-tétraaza-ɔclododécane *N*,*N*′,*N*″,*N*‴-tétraacétique ou H_4Y) forme avec les lanthanides ivalents des complexes de chélation, de stoechiométrie 1:1, dont la stabilité t particulièrement élevée ($K = 10^{28}$ mol l^{-1} pour le gadolinium à 25°C [1]). a cinétique de formation et de décomposition de ces complexes a égale-ent été étudiée [2] dans le cas du gadolinium notamment: à pH 2,85, la action de chélation est de second ordre vis-à-vis de l'ion métallique et de la

)03-2670/86/$03.50

concentration en ligand et la constante de vitesse est de l'ordre de 2×10^{-2} M^{-1} s^{-1}. La dissociation de GdDOTA est bien plus lente encore, même en milieu très acide: la réaction est de second ordre vis-à-vis de la concentration en acide et en chélatant avec une constante de vitesse de l'ordre de 10^{-5} M^{-1} s^{-1}. A pH 1,15, la demi-vie de GdDOTA est de 21 jours, une valeur exceptionnellement élevée pour des polyaminopolyacétates de lanthanides.

Des travaux récents de Brücher et Laurency [3, 4] tendraient à prouver que ces cinétiques sont différentes d'un lanthanide à l'autre: elle serait de plusieurs ordres de grandeur supérieure pour le cérium par rapport au gadolinium [3] ce qui, par ailleurs, est souvent le cas pour les complexes des lanthanides avec les acides polyaminopolyacétiques [4, 5].

La technique chromatographique, au moyen d'échangeurs d'ions, semble particulièrement bien adaptée à l'étude de phénomènes aussi lents, grâce, notamment, à la facilité de garder constantes les conditions expérimentales, même pendant des temps très longs. C'est donc cette technique et plus particulièrement l'élution chromatographique sur colonne d'échangeur cationique sulfonate que nous avons choisie pour aborder l'étude de ces systèmes.

Un examen préalable du comportement du chélatant libre (H_4Y) et des complexes LnYH sur ce type d'échangeur s'avère nécessaire pour l'interprétation des résultats.

PARTIE EXPÉRIMENTALE

Les caractéristiques de la colonne sont 9,8-mm de diamètre (soit une section de 0,75 cm^2), 1,75-mm de hauteur d'échangeur (poids, m = 6,18 g), et un volume libre, V_1 de 5,67 ml. L'échangeur utilisé est Dowex 50-X8 (400 mesh, forme protonée; capacité 4,817 méq g^{-1}).

Protocole expérimental

Les complexes sont préparés par attaque directe des oxydes de lanthanides, préalablement calcinés à 1200° C, par une quantité stoechiométrique de complexant à l'ébullition.

Les 5 ml de solution de complexant ou de complexe (0,3 mmol pour le complexant seul comme pour les complexes LnYH, ou 0,15 mmol de GdYH et 0,15 mmol de EuYH pour les essais de séparation Eu/Gd) sont déposés au sommet de la colonne et cette dernière rincée par 10—15 ml d'eau désionisée introduite en plusieurs fois. On amène alors la solution chlorhydrique éluante de différentes molarités et règle le débit d'élution. Les différentes fractions d'élution sont analysées par titrage acide-base en ce qui concerne le complexant (après élimination de HCl par évaporation à sec), et par fluorescence-x dans le cas des lanthanides.

RÉSULTATS

Étude de la fixation de l'acide tétraazacyclododécanetétraacétique sur un échangeur cationique sulfonate

Trois solutions de concentrations différentes, 1,167, 1,986 et 3,62 M en HCl ont été utilisées pour l'élution; les autres variables expérimentales relatives à l'échangeur, la colonne et les conditions d'élution sont décrites dans la section qui précède. La mesure, sur les chromatogrammes, du volume correspondant à la sortie du maximum de concentration de l'acide H_4Y nous permet de calculer le coefficient de distribution K_d et, par conséquent, la constante d'échange $K_{éch}$ correspondant à l'équilibre

$$n\text{R—H} + \text{H}_4\text{Y} \rightleftharpoons (\text{R—H})_n\text{H}_4\text{Y} \qquad (1)$$

n étant égal au nombre de pôles de fixation de l'entité éluée. En effet, $K_d = (V_m - V_l)/m$, et avec le volume libre V_l égal à 5,67 ml et la masse de résine m égale à 6,18 g, $K_d = (V_m - 5{,}67)/6{,}18$, V_m étant égal au volume d'élution correspondant à la sortie du maximum de concentration. D'autre part $K_{éch} = K_d[H^+]_s^n/[H^+]_r^n = K_d$ (molarité de HCl)^n/(capacité de la résine)^n.

Un exemple de chromatogramme obtenu est représenté à la Fig. 1 et les résultats sont repris dans le Tableau 1; ils permettent de conclure à la fixation du complexant par deux pôles, la constante d'échange de cette espèce vis-à-vis des protons étant égale à 1,43 g ml^{-1}.

Il est évident que l'obtention, en fonction de la concentration en HCl de l'éluant, d'une valeur constante de $K_{éch}$ pour une valeur donnée de n fournit ce nombre n de pôles de fixation de l'entité éluée.

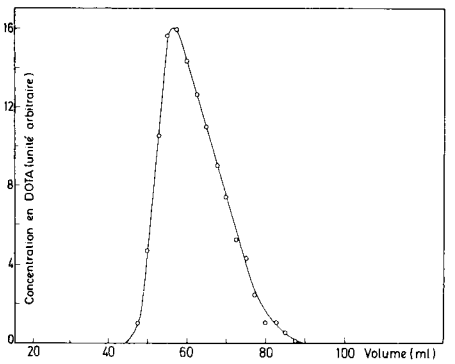

Fig. 1. Elution de DOTA par HCl 1,986 M. Vitesse d'élution, 0,7 ml min^{-1}; V_m = 56,5 ml; K_d = 8,22; N (nombre de plateaux) = $8(V_m/\beta)^2 = 8(56{,}5/19)^2 = 71$.

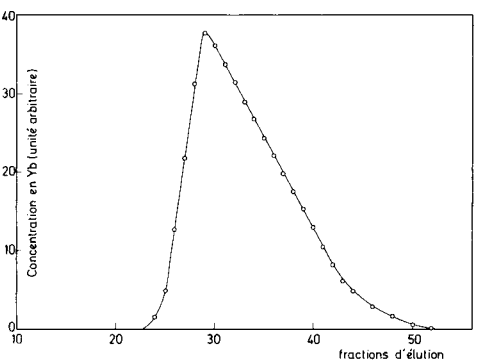

Fig. 2. Elution du complexe YbYH par HCl 1,251 M. Vitesse d'élution, 1,2 ml min^{-1}; V_m = 29 fractions d'élution = 99,1 ml; K_d = 15,15; N = 45. Détection par fluorescence-x.

TABLEAU 1

Fixation et élution de l'acide tétraazacyclododécanetétraacétique sur un échangeur cationique sulfonate Dowex 50-X8

HCl (M)	V_m (ml)	K_d (ml g^{-1})	$K_{éch}$		
			$n = 1$	$n = 2$	$n = 3$
1,167	160,5	25,04	6,00	1,46	0,36
1,986	56,5	8,22	3,28	1,40	0,57
3,62	21,3	2,53	1,84	1,43	1,06
			Moyenne: 1,43 g ml^{-1}		

Étude du comportement des complexes lanthanides-DOTA (LnYH) sur un échangeur cationique sulfonate

Le comportement des complexes LnYH, pour les terres yttriques en tout cas, est semblable à celui du complexant libre: nous avons pu montrer, en suivant le même protocole expérimental que celui qui vient d'être décrit, qu'ils sont retenus sur un échangeur cationique sulfonate, qu'ils sont élués par une solution de HCl et qu'ils se comportent comme des entités bipolaires. La réaction peut se décrire par

$$2R{-}H + LnHY \rightleftharpoons (R{-}H)_2LnYH \qquad (2)$$

L'allure du chromatogramme représenté sur la Fig. 2 et qui a trait à l'élution du complexe YbYH est la même pour les autres lanthanides, du lutétium au terbium inclus. De même, les résultats repris dans le Tableau 2, également dans le cas du complexe YbYH, conduisent aux mêmes conclusions pour les lanthanides précités (les valeurs de K_d obtenues en milieu HCl 1,251 M sont reprises dans le Tableau 3).

Les constantes de protonation du ligand macrocyclique DOTA ont été publiées par Desreux et al. [6]: les pK valent respectivement 1,71, 1,88, 4,18, 4,24, 9,23 et 11,08 en milieu KCl 1 M à la température de 25°C. Dans les mêmes conditions de milieu, la valeur de la constante de formation des complexes Ln-DOTA est de l'ordre de 10^{28} mol l^{-1} [1]. La valeur de la constante de formation apparente, en milieu HCl 1,251 M est par conséquent égale à $K'_c = 10^{28} \times 10^{-32,3}/[H^+]^6$, ou encore égale à $10^{-0,5}$ mol l^{-1}, ce qui signifie que le complexe devrait être détruit dans ce milieu de forte acidité (d'autant plus si l'on fait intervenir la compétition entre le complexant et la résine pour les ions Ln^{3+}). C'est grâce à la cinétique de décomplexation très lente de ces entités qu'elles subsistent intactes pendant le temps nécessaire à l'élution sans subir de décomposition sensible (seule la traînée assez marquée des pics d'élution, inexistante dans le cas du complexant libre, pourrait traduire une très légère décomplexation).

Ce qui précède n'aurait que peu d'intérêt (les valeurs de K_d sont trop semblables pour envisager une séparation chromatographique) si le comportement

TABLEAU 2

Fixation et élution du complexe YbYH sur échangeur cationique sulfonate Dowex 50-X8

HCl (M)	V_m (ml)	K_d (ml g^{-1})	$K_{éch}$ (Yb^{3+}/H^+)		
			$n = 1$	$n = 2$	$n = 3$
1,251	99,1	15,15	3,93	1,02	0,26
1,000	158,8	24,82	5,15	1,07	0,22
1,54	69,0	10,27	3,28	1,05	0,33
			Moyenne: 1,05 g ml^{-1}		

TABLEAU 3

Coefficient de distribution des complexes LnYH sur un échangeur cationique sulfonate dans le cas des terres yttriques[a]

Eléments	K_d (ml g^{-1})	Eléments	K_d (ml g^{-1})
Lutétium	18,40	Holmium	15,56
Ytterbium	15,15	Dysprosium	15,94
Thulium	16,36	Terbium	15,62
Erbium	17,10		

[a]Échangeur Dowex 50-X8; éluant HCl 1,251 M; vitesse d'élution 1,2 ml min^{-1}; temps de séjour sur la colonne environ 100 min; analyse des fractions d'élution par fluorescence-x.

des terres cériques, du lanthane au samarium inclus, n'était fondamentalement différent de celui des terres yttriques. La Fig. 3 représente le chromatogramme obtenu lors de l'élution du complexe NdYH dans les mêmes conditions expérimentales d'acidité de l'éluant et de vitesse d'élution. Après percolation d'environ 150 ml d'éluant, on décèle, dans l'éluat, la présence de l'acide H_4Y seul, exempt de toute trace de néodyme. Son coefficient de distribution, dans ces conditions, est égal à 23,4 ml g^{-1}, valeur identique à celle que l'on obtient en le déposant seul au sommet de la colonne et nettement supérieure à celle des complexes LnYH (environ égale, en moyenne, à 17 ml g^{-1}). Après passage de plus de 400 ml d'éluant, ce qui correspondrait à un K_d supérieur à 64 ml g^{-1}, on ne décèle toujours aucune trace de lanthanide dans l'éluat: il faut changer la force élutive et travailler en milieu 5 M en HCl pour assister enfin à la désorption du néodyme.

L'interprétation est simple: le complexe NdYH est détruit par la forte acidité de l'éluant suivant la réaction

$$NdYH + 3H^+ \rightleftharpoons Nd^{3+} + H_4Y \qquad (3)$$

comme permettent de le prévoir la constante de formation du complexe et la fonction de distribution de l'acide macrocyclique. L'acide libre est élué tandis que l'ion tripositif reste fixé sur la résine; nous avons déterminé la constante

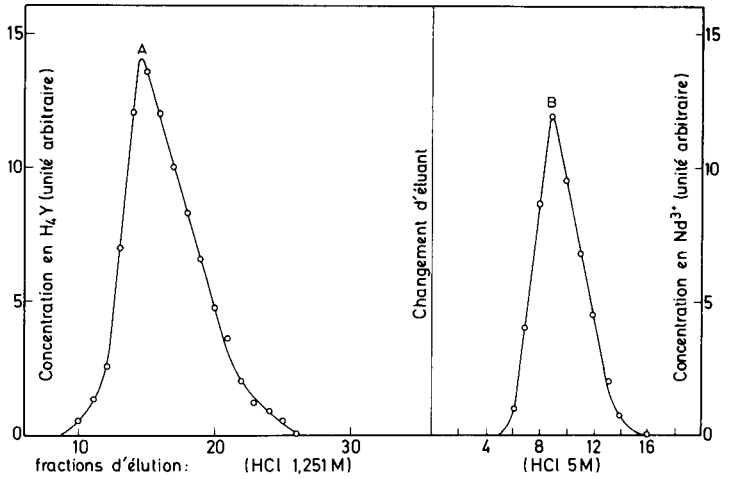

Fig. 3. Elution du complexe NdYH sur échangeur cationique sulfonate (vitesse d'élution 1,2 ml min^{-1}). Pics: (A) sortie de H_4Y seul élué par HCl 1,251 M (détection par titrage acide-base); (B) sortie de Nd^{3+} élué par HCl 5 M (détection par fluorescence-x).

d'échange de l'ion Nd^{3+} vis-à-vis des protons sur le type d'échangeur utilisé: elle vaut 7,3 g^2 ml^{-2}, ce qui signifie qu'il faudrait, en milieu HCl 1,251 M et sur une colonne de 6,17 g de résine, attendre le passage de 2600 ml d'éluant pour assister à la sortie du maximum de concentration (V_m) du pic d'élution de ce cation.

Cette différence de comportement entre le néodyme et les terres yttriques implique une très nette différence dans les cinétiques de décomplexation des entités LnYH. Les autres terres cériques, du lanthane au samarium inclus, ont un comportement identique à celui du néodyme: leur complexe avec DOTA est détruit pendant le séjour sur la colonne et ce, dans des limites assez larges de débit d'élution correspondant à des temps de séjour allant de 600 min à 60 min. Le fait, d'ailleurs, que le coefficient de distribution du complexant libre soit le même en présence ou en l'absence de cation métallique prouve que cette décomplexation s'effectue très vite, sur les premiers plateaux de la colonne, sans quoi la sortie du complexant serait avancée.

Il devient ainsi possible de séparer de façon très efficace les lanthanides en deux groupes distincts en mettant à profit cette différence dans les cinétiques de décomplexation. En milieu HCl 1,251 M, sur une colonne contenant 6,17 g d'échangeur, on assiste à la sortie des complexes LnYH des terres yttriques après passage de 100 ml d'éluant environ alors qu'il faudrait attendre 2600 ml pour assister à l'élution des ions trivalents des terres cériques. Il est évidemment plus simple après passage des complexes des terres yttriques de désorber les terres cériques par un éluant de plus forte acidité. Un exemple de séparation réalisée sur le couple holmium/néodyme est donné sur la Fig. 4.

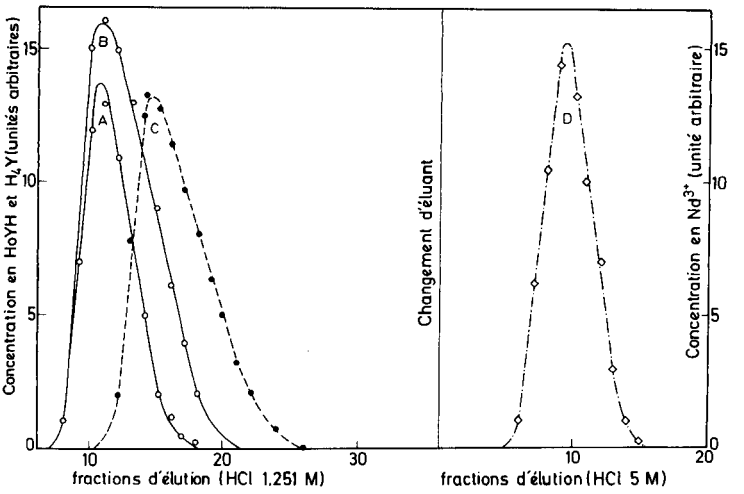

Fig. 4. Séparation holmium/néodyme sur échangeur cationique sulfonate. Conditions: voir Partie Expérimentale; vitesse d'élution 1,2 ml min^{-1}; 5 ml de solution contenant 0,3 mmol de HoYH et 0,3 mmol de NdYH. Pics: (A) sortie de HoYH élué par HCl 1,251 M; (B et C) analyse des fractions d'élution par pHmétrie (B, titrage de HoYH; C, titrage de H_4Y provenant de la destruction du complexe NdYH); (D) sortie de Nd^{3+} par HCl 5 M.

Comportement des complexes GdYH et EuYH sur échangeur cationique sulfonate

Ainsi qu'on pouvait s'y attendre, les complexes EuYH et GdYH ont un comportement intermédiaire entre celui des complexes des terres yttriques et des terres cériques. Fixés au sommet de la colonne de résine, ils sont élués en partie sous forme de complexes par la solution chlorhydrique, comme dans le cas des terres yttriques mais, au cours de cette élution, subissent également le processus de décomplexation de manière plus lente cependant que les terres cériques. Le chromatogramme d'élution prend ainsi l'allure de la Fig. 5: après passage d'environ 100 ml d'éluant, l'europium et le gadolinium sont élués sous forme de complexes LnYH, mais en partie seulement; le reste, passé à l'état d'ions tripositifs, est élué lentement par la solution de HCl 1,251 M pour être enfin totalement désorbé par une solution 2 M en HCl. La rampe continue que l'on observe entre la 10ème et la 40ème fraction d'élution peut s'interpréter par le fait que la décomplexation s'effectue tout au long du trajet du complexe sur la colonne et que la cinétique de décomplexation est d'autant plus faible que la concentration en complexe est faible. Ainsi, au sommet de la colonne, la quantité de complexe est importante et dès lors importante aussi la quantité d'ions tripositifs libérés. Dans la zone inférieure, nettement plus pauvre en complexe, on trouve également moins d'ions tripositifs.

Comme on le voit également sur cette figure, bien que l'on soit parti de quantités égales de EuYH et GdYH, les premières fractions d'élution sont nettement enrichies en gadolinium, les dernières en europium. Cela signifie

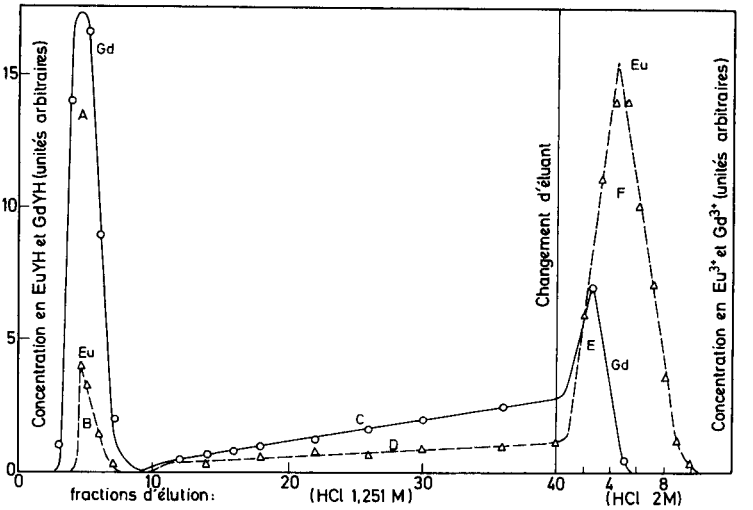

Fig. 5. Elution des complexes GdYH et EuYH sur échangeur cationique sulfonate. Conditions: voir Partie Expérimentale; 5 ml de solution contenant 0,15 mmol de EuYH et 0,15 mmol de GdHY; vitesse d'élution 1,2 ml min^{-1} (temps de séjour de 100 min des complexes sur la colonne). Pics: (A) GdYH 45% de la quantité initiale; (B) EuYH 9% de la quantité initiale; (E) Gd^{3+} 35% de la quantité initiale; (F) Eu^{3+} 75% de la quantité initiale. Traînées: (C) Gd^{3+}; (D) Eu^{3+}.

que les cinétiques de décomplexation sont différentes pour ces deux cations, le comportement du gadolinium le rapprochant des terres yttriques, celui de l'europium des terres cériques.

Le rapport entre la quantité de complexe LnYH et d'ions tripositifs Ln^{3+} est évidemment fonction du temps de séjour du complexe sur la colonne, autrement dit du débit d'élution (à K_d et masse de résine constants).

Le Tableau 4 rend compte de l'évolution du rapport $LnYH/Ln_{total}$ en fonction du temps de séjour sur la colonne ou encore du débit d'élution. Nous montrerons que l'exploitation de ces résultats peut conduire à une séparation incomplète mais très efficace des deux métaux Eu et Gd.

DISCUSSION

Un essai de visualisation des phénomènes est réalisé sur la Fig. 6. La colonne est divisée en zones, numérotées 1 à 27 de façon tout à fait arbitraire. Ces zones ne correspondent pas à la notion conventionnelle de plateaux qui sont chacun une portion de la colonne où il y a équilibre entre phases. Les deux lanthanides sont fixés au sommet de la colonne, sous forme de complexes EuYH et GdYH: nous admettons qu'ils occupent entièrement la première zone. Lorsque l'élution par HCl commence, trois phénomènes se déroulent simultanément: (1) les deux lanthanides sont élués, à même vitesse (les coefficients de distribution sont égaux), sous forme de complexes LnYH;

TABLEAU 4

Pourcentage de désorption des entités EuYH et GdYH en milieu HCl 1,251 M en fonction du temps de séjour sur la colonne[a]

Temps (min)	Pourcentage $LnYH/Ln_{total}$	
	EuYH	GdYH
30	37,5	75,0
100	9,0	45,0
180	2,0	31,0
280	0	23,0

[a]Les temps sont mesurés à la sortie du maximum de concentration des pics d'élution des complexes.

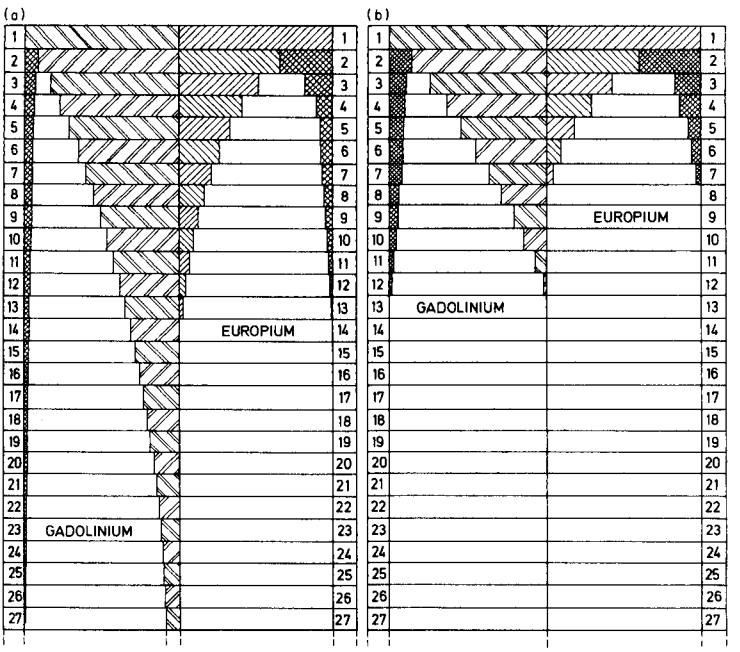

Fig. 6. Comportement des complexes EuYH et GdYH élués par une solution de HCl 1,251 M sur la colonne d'échangeur cationique sulfonate: visualisation de l'élution et de la décomplexation simultanées des entités LnYH. Vitesse d'élution: (a) 1,2 ml min^{-1}; (b) 0,12 ml min^{-1}. Les traits réseaux représentent la répartition des ions tripositifs sur les différentes zones. Ces ions sont considérés comme immobiles et cette répartition n'évolue donc pas en fonction du temps (en première approximation en tout cas). Les traits hachures représentent la migration des complexes LnHY sur la colonne de résine; ces complexes sont mobiles. Par conséquent, lorsque n est occupé, toutes les autres zones ($n-1$, $n-2$, $n-3 \ldots n+1$, $n+2$, $n+3 \ldots$) sont libérées ou inoccupées.

(2) à cause de la forte acidité de l'éluant, ces mêmes complexes sont détruits, à des vitesses différentes pour chacun des lanthanides et variables en fonction de la concentration en complexe, c'est-à-dire de la position sur la colonne; (3) les ions tripositifs des lanthanides ainsi libérés se fixent sur l'échangeur et, en première approximation, s'immobilisent. En effet, le K_d des ions Ln^{3+}, en milieu HCl 1,25 M et sur ce type d'échangeur est de l'ordre de 450 ml g^{-1}.

Pour fixer les idées, prenons l'exemple de la zone 8 de la Figure 6A: il reste, dans cette zone, 17% de l'europium initial sous forme de complexe EuYH, le solde du métal étant réparti sur les plateaux 2 à 8 sous forme d'ions Eu^{3+}. De même, dans cette même zone, on trouve 50% du gadolinium sous forme de GdYH, le reste s'étant décomplexé pendant le trajet pour l'atteindre et se trouvant donc dans les zones 2—8 sous forme de Gd^{3+}. On peut ainsi se rendre compte qu'au-delà de la zone 13, dans l'exemple choisi, on trouve 31% environ du gadolinium initial, réparti sous forme de GdYH et Gd^{3+}, totalement exempt d'europium. Une séparation des deux cations est donc possible si le complexe EuYH est totalement détruit pendant son séjour sur la colonne ou encore si la fin de la colonne se situe au-delà de la zone 14 dans l'exemple choisi. En d'autres termes, il s'agit de régler le débit d'élution, en fonction de la valeur du K_d de EuYH, de la concentration en HCl de l'éluant et de la masse de résine pour que le temps de séjour de EuYH sur la colonne soit suffisant pour provoquer sa totale décomplexation.

Un examen comparatif de Fig. 6A et B montre encore que, sur le plan de la séparation, les performances sont d'autant meilleures et la marge de manoeuvre d'autant plus large que la vitesse d'élution sera rapide. On voit

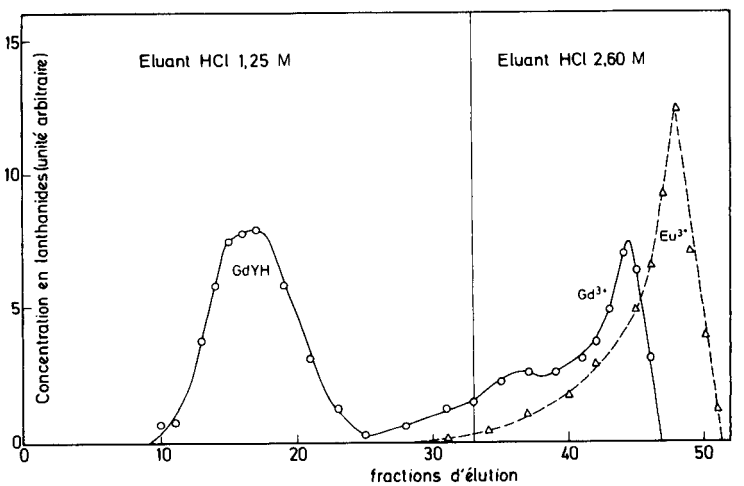

Fig. 7. Séparation europium/gadolinium. Conditions expérimentales: 78 g d'échangeur Dowex 50-X8 (400 mesh, forme protonée) de capacité égale à 4,817 méq g^{-1}; diamètre, 18 mm; hauteur de résine, 980 mm; volume libre, 67,5 ml; fractionnement, 120 ml; vitesse d'élution, 0,15 ml s^{-1}. Temps de séjour du Gd sur la colonne (mesuré à la sortie du maximum du pic d'élution), 4 h.

aussi qu'en tête de colonne, le rapport Eu/Gd sera d'autant plus élevé que la vitesse d'élution est rapide.

Il semble donc qu'il y ait intérêt à fixer la vitesse d'élution à sa valeur la plus élevée possible (tenant compte des pertes de charge de la colonne) et à ajuster la masse de résine, en fonction de la valeur de K_d(EuYH), pour que le complexe séjourne au moins 4 h sur la colonne comme le montre le Tableau 4.

Les résultats présentés sur la Fig. 7 rendent compte des performances que l'on peut espérer de ce procédé de séparation de l'europium et du gadolinium, basé sur la différence dans les cinétiques de décomplexation des entités EuDOTAH et GdDOTAH. Dans les conditions expérimentales reprises en légende de la Fig. 7, le complexe Gd-DOTAH (40% de la quantité initiale) est élué en tête du chromatogramme, totalement exempt d'europium. On observe ensuite une traînée d'un mélange Eu^{3+}/Gd^{3+} correspondant à la décomplexation des entités EuDOTAH et GdDOTAH au cours de leur migration sur la colonne. Enfin, après la fraction 46, le gadolinium est entièrement extrait de la colonne et disparaît de l'éluat. Les fractions 47, 48, 49 et 50, quant à elles, contiennent l'ion Eu^{3+} (47% de la quantité initiale) totalement exempt de gadolinium.

J. F. D. est Chercheur Qualifié du Fonds National de la Recherche Scientifique (Bruxelles).

BIBLIOGRAPHIE

1 M. F. Loncin, J. F. Desreux et E. Merciny, Inorg. Chem., 25 (1986) 2646.
2 A. Lopez-Mut, E. Merciny et J. F. Desreux, ouvrage inédit.
3 E. Brücher, communication personnelle.
4 E. Brücher et G. Laurency, J. Inorg. Nucl. Chem., 43 (1981) 2089.
5 G. A. Nyssen et D. W. Margerum, Inorg. Chem., 9 (1970) 1814.
6 J. F. Desreux, E. Merciny et M. F. Loncin, Inorg. Chem., 20 (1981) 987.

Analytica Chimica Acta, 189 (1986) 313—321
Elsevier Science Publishers B.V., Amsterdam — Printed in The Netherlands

DETERMINATION DE L'ETAIN DANS LES SEDIMENTS ET LES BOUES DE STATIONS D'EPURATION PAR SPECTROMETRIE D'ABSORPTION ATOMIQUE AVEC GENERATION D'HYDRURES

M. LEGRET* et L. DIVET

Laboratoire Central des Ponts et Chaussées, B.P. 19, 44340 Bouguenais (France)

(Reçu le 6 juin 1986)

SUMMARY

(Determination of tin in sediments and sewage sludges by atomic absorption spectrometry with hydride generation.)

The conditions for the determination of tin in sediments and sewage sludges by atomic absorption spectrometry with hydride generation are evaluated. Hydride generation is achieved in a 0.4 M nitric acid/0.2 M tartaric acid solution. The effects of hydrochloric, nitric, sulfuric and hydrofluoric acids are discussed. Matrix effect and interferences from other trace elements are studied. Seven sample decomposition procedures are compared. Refluxing with a (1 + 3) nitric acid/hydrochloric acid mixture was the preferred procedure for decomposing such samples.

RESUME

On a déterminé les meilleures conditions opératoires pour la détermination de l'étain dans les sédiments et les boues de stations d'épuration par spectrométrie d'absorption atomique avec génération d'hydrures. La génération d'hydrures est effectuée dans un milieu contenant de l'acide nitrique 0,4 M et de l'acide tartrique 0,2 M. Les effets des acides chlorhydrique, nitrique, sulfurique et fluorhydrique ont été étudiés. Les perturbations dues aux matrices complexes et à la présence de certains éléments trace ont été évaluées. Sept méthodes différentes de mise en solution des échantillons ont été comparées. La méthode de minéralisation par reflux à l'aide d'un mélange d'acide nitrique et d'acide chlorhydrique concentrés (1 + 3) permet une détermination satisfaisante de l'étain dans ces milieux.

La spectrométrie d'absorption atomique avec génération d'hydrures est la méthode la plus largement utilisée actuellement pour le dosage des traces d'étain dans les milieux naturels. La limite de détection obtenue est généralement suffisante pour la plupart des échantillons. Cette méthode a connu de nombreux développements afin de permettre la détermination de l'étain dans les échantillons géologiques [1] mais surtout dans les eaux [2, 3], et notamment l'eau de mer et les organismes marins [4, 5] en raison des problèmes posés par l'utilisation des peintures antisalissures contenant des composés organostanniques.

Par ailleurs, les sols sont le milieu récepteur de nombreux déchets dont les boues de curage des cours d'eau et les boues de stations d'épuration des eaux

0003-2670/86/$03.50

usées. Il est donc nécessaire de pouvoir déterminer les teneurs en micropolluants de ces milieux, dont l'étain, afin de préserver la qualité de l'environnement. Dans ce travail, on a cherché à établir les meilleures conditions opératoires pour le dosage de l'étain dans les sédiments et les boues de stations d'épuration. Les perturbations dues à ces matrices et aux éléments traces présents dans ces milieux ont été étudiées. Enfin, on a comparé l'influence de différentes méthodes de mise en solution des échantillons sur la détermination de l'étain.

PARTIE EXPÉRIMENTALE

Matériel et réactifs

Les essais ont été réalisés à l'aide d'un spectrophotomètre Perkin-Elmer, modèle 272, équipé d'un générateur d'hydrures MHS-20. L'hydrure généré dans le réacteur est entrainé par un courant d'argon dans une cellule à fenêtres de quartz de 166 mm de longueur et 14 mm de diamètre. La cellule est chauffée par un four électrique règlable entre 100 et 1000°C; elle est traversée par le rayonnement d'une lampe sans électrode Perkin-Elmer contenant de l'argon sous faible pression et alimentée par une source extérieure (Perkin-Elmer EDL power supply).

L'eau utilisée est purifiée sur une installation de déminéralisation Maxy comportant deux colonnes de résines échangeuses d'ions (Modèle Recherche). Les concentrations des acides utilisés sont les suivantes: acide nitrique à 65% (d = 1,40); acide chlorhydrique à 30% (d = 1,16); acide sulfurique à 96% (d = 1,84); acide fluorhydrique à 48% (d = 1,16); acid perchlorique à 70% (d = 1,67); acide acétique à 96% (d = 1,06). Tous les réactifs sont de qualité pure pour analyse (Merck Suprapur ou Pro-Analysis).

La solution réductrice est constituée par une solution à 30 g l^{-1} de borohydrure de sodium dans la soude à 10 g l^{-1}.

Etalonnage et conditions opératoires

Les solutions étalons ont été préparées à partir d'une solution Merck Titrisol d'étain (1 g d'étain) diluée à 1 l dans une solution d'acide chlorhydrique 0,15 M pour obtenir une solution mère à 1 g l^{-1}. Les différentes solutions étalons sont obtenues à partir de la solution mère par dilution dans l'acide chlorhydrique 0,15 M. Le volume d'échantillon à analyser introduit dans le réacteur est de 10 ml. Lors de la réaction de génération d'hydrures, il est ajouté un volume de 10 ml de solution de borohydrure de sodium.

Le débit d'argon est maintenu à environ 400 ml min^{-1}. Les paramètres de règlage de l'appareil sont indiqués dans le Tableau 1. Les mesures d'absorbance ont été effectuées en hauteur de pic et sans correction d'absorption non specifique, celle-ci étant sans effet lors de nos essais.

Toutes les solutions ont été préparées en double. Les résultats présentés sont la moyenne de deux essais après déduction du blanc.

TABLEAU 1

Conditions opératoires pour la génération d'hydrures

Raie (nm)	Bande passante (nm)	Temps de purge I (s)	Temps de réaction (s)	Temps de purge II (s)	Température de la cellule (°C)
286,3	0,7	10	15	50	900

Méthodes de minéralisation

Méthode 1. Peser 1 g d'échantillon sec dans une capsule en porcelaine. Introduire la capsule dans un four à moufle froid. La température est amenée à 550°C et maintenue 3 h. Transférer le résidu dans une capsule en téflon, introduire 10 ml d'acide chlorhydrique concentré et 10 ml d'acide fluorhydrique concentré. Amener à sec. Répéter l'opération une autre fois. Terminer l'attaque avec 10 ml d'acide chlorhydrique concentré. Reprendre le résidu par 4 ml d'acide nitrique concentré et quelques ml d'eau déminéralisée. Après dissolution à chaud du résidu, filtrer sur filtre Whatman 40, transvaser le filtrat dans une fiole jaugée de 100 ml et ajuster le volume avec de l'eau déminéralisée.

Méthode 2. Peser 1 g d'échantillon sec dans un ballon de 100 ml. Ajouter 3 ml d'eau déminéralisée puis 7,5 ml d'acide chlorhydrique concentré et 2,5 ml d'acide nitrique concentré (eau régale). Couvrir le ballon et laisser reposer 12 h à température ambiante. Faire bouillir à reflux pendant 2 h. Laisser refroidir lentement, rincer le réfrigérant en récupérant le liquide dans le ballon. Filtrer sur filtre Whatman 40, transvaser le filtrat dans une fiole jaugée de 100 ml et ajuster le volume avec de l'eau déminéralisée.

Méthode 3. Peser 1 g d'échantillon sec dans une capsule en téflon. Ajouter 25 ml d'acide nitrique concentré. Chauffer progressivement jusqu'à 120°C. Après réduction sensible du volume, retirer la capsule de la plaque chauffante et laisser refroidir. Ajouter successivement 25 ml d'acide nitrique concentré et 10 ml de peroxyde d'hydrogène à 30% (p/v). Chauffer jusqu'à consistance pâteuse. Laisser refroidir. Reprendre le résidu par 4 ml d'acide nitrique concentré et quelques ml d'eau déminéralisée. Après dissolution à chaud du résidu, filtrer sur filtre Whatman 40. Transvaser le filtrat dans une fiole jaugée de 100 ml et ajuster le volume avec de l'eau déminéralisée.

Méthode 4. Peser 1 g d'échantillon dans une capsule en téflon. Ajouter 15 ml d'acide fluorhydrique concentré et 10 ml d'acide nitrique concentré. Porter sur plaque chauffante, pendant 2 h, puis ajouter 2 ml d'acide perchlorique concentré et évaporer à sec. Reprendre le résidu par 4 ml d'acide nitrique concentré et quelques ml d'eau déminéralisée. Après dissolution à chaud du résidu, filtrer sur filtre Whatman 40. Transvaser le filtrat dans une fiole jaugée de 100 ml et ajuster le volume avec de l'eau déminéralisée.

Méthode 5. Peser 1 g d'échantillon sec dans un ballon de 100 ml. Ajouter 10 ml d'acide nitrique concentré et 5 ml d'acide sulfurique concentré. Faire

bouillir à reflux pendant 5 h. Laisser refroidir lentement, rincer le réfrigérant en récupérant le liquide dans le ballon. Filtrer sur filtre Whatman 40, transvaser le filtrat dans une fiole jaugée de 100 ml et ajuster le volume avec de l'eau déminéralisée.

Méthode 6. Peser 200 mg d'échantillon sec dans une bombe en téflon. Ajouter 5 ml d'acide nitrique concentré. Chauffer dans un étuve à 140°C pendant 3 h. Après refoidissement, filtrer sur filtre Whatman 40, transvaser le filtrat dans une fiole jaugée de 100 ml et ajuster le volume avec de l'eau déminéralisée.

Méthode 7. Peser 1 g d'échantillon sec dans un erlenmeyer de 100 ml. Ajouter 15 ml d'un mélange d'acide nitrique et d'acide chlorhydrique concentrés (3:1 v/v). Laisser reposer pendant 16 h. Filtrer sur filtre Whatman 40, transvaser le filtrat dans une fiole jaugée de 100 ml et ajuster le volume avec de l'eau déminéralisée.

RESULTATS ET DISCUSSION

Influence des acides sur le dosage de l'étain

La présence d'un acide est nécessaire dans le milieu réactionnel pour générer l'hydrogène naissant par décomposition du borohydrure de sodium. Une partie de l'acide est utilisée pour neutraliser la soude contenue dans la solution de borohydrure. Les acides couramment utilisés sont les acides acétique, nitrique, chlorhydrique et sulfurique. On a étudié l'influence de ces acides sur la détermination de 50 ng d'étain, afin de se situer dans la partie linéaire de la courbe d'étalonnage, pour des concentrations d'acide comprises entre 0,05 et 1 mol l^{-1}.

En présence d'acide acétique on a constaté un dédoublement des pics et une mauvaise reproductibilité des essais. Les résultats obtenus avec les autres acides sont présentés dans le Tableau 2. L'absorbance est maximum pour une concentration d'acide voisine de 0,1 M. Néanmoins, avec des acides chlorhydrique et sulfurique le signal décroît très rapidement de part et d'autre de cette concentration. En effet, la quantité d'acide introduite doit être suffisante pour générer l'hydrure mais un excès d'acide peut ralentir la distillation de l'hydrure par formation de mousse [3]. L'acide nitrique donne les meilleurs résultats. Le signal est moins sensible aux variations de la concentration

TABLEAU 2

Influence des acides sur le dosage de l'étain (50 ng)

Acide	Signal exprimé en absorbance				
	0,05[a]	0,1[a]	0,3[a]	0,6[a]	1[a]
HNO_3	198	214	220	195	138
HCl	198	234	119	119	58
H_2SO_4	208	221	182	96	46

[a]Concentration en acide en mol l^{-1}.

en acide, il est plus reproductible et les pics obtenus sont plus fins. La concentration optimale est voisine de 0,4 M.

Il a été montré que la détermination des métaux lourds par spectrométrie d'absorption atomique [6] pouvait être gênée par la présence des acides utilisés pour la mise en solution des échantillons et subsistant dans les solutions à doser. Après évaporation il peut en effet subsister des quantités faibles d'acides, notamment de l'acide fluorhydrique utilisé généralement pour la mise en solution des échantillons contenant des silicates. On a donc étudié l'influence de cet acide sur le dosage de l'étain pour des concentrations comprises entre 0,006 et 0,3 mol l^{-1} (soit entre 0,02 et 1% v/v d'acide concentré). Les résultats présentés dans le Tableau 3 ont été obtenus en présence de 50 ng d'étain et dans un milieu nitrique 0,4 M. Il apparaît que l'acide fluorhydrique provoque un diminution très importante du signal et pour des concentrations très faibles (—35% pour 0,006 M); il est donc nécessaire de l'éliminer parfaitement par évaporation lors de mises en solution.

Interférences dues aux matrices complexes

Les molécules d'hydrures formées dans le générateur sont ensuite dissociées dans un four, il y a donc volatilisation de l'analyte et séparation de la matrice. Bien que, en principe, on ne devrait pas observer d'interférences certaines perturbations du dosage sont possibles. Les perturbations sont de deux ordres [7] : d'une part, en phase vapeur, la mesure risque d'être majorée par absorption moléculaire par d'autres espèces volatiles formées à partir de tiers éléments; d'autre part, en solution dans le générateur la réaction de réduction peut être empêchée (présence d'agents oxydants) ou être incomplète (vitesse de la réaction de réduction trop lente). Enfin, les réactions de précipitations de tiers-éléments en présence de borohydrure de sodium peuvent bloquer l'analyte.

Afin d'étudier l'influence d'une matrice complexe sur le dosage de l'étain, on a préparé une solution synthétique, en milieu nitrique 0,03 M correspondant à la mise en solution de 1 g de sédiment sec dans 100 ml. La composition de ce sédiment est la suivante: Fe_2O_3 8%; Al_2O_3 20%; MgO 8%; CaO 7%; Na_2O 3%; K_2O 3%. La partie restante est constituée par la silice et les matières organiques qui sont généralement éliminées au cours de la minéralisation et ne sont donc pas présentes dans les solutions à doser. Tous ces éléments ont été introduits sous forme de nitrate. Des quantités variables d'étain ont été

TABLEAU 3

Influence de l'acide fluorhydrique sur le dosage de l'étain (50 ng) en milieu nitrique 0,4 M

Concentration (mol l^{-1})	0,006	0,015	0,030	0,060	0,150	0,300
Signal[a]	143	143	121	104	88	24

[a]En absorbance.

introduites dans cette solution qui correspondent aux teneurs généralement rencontrées dans les sédiments et les boues, soit entre 0,5 et 100 mg kg^{-1}. Après dilution des solutions afin de se situer dans le domaine analytique, les dosages ont été effectués en présence d'acide nitrique 0,4 M. Les concentrations en étain ont été déterminées d'une part par rapport à une courbe d'étalonnage simple et d'autre part par la méthode des ajouts dosés. Les écarts entre les valeurs trouvées et les valeurs théoriques introduites sont présentés dans le Tableau 4. L'interférence de la matrice devient notable sur le dosage pour les teneurs en étain inférieures à 5 mg kg^{-1}; les valeurs trouvées sont inférieures aux valeurs théoriques et les écarts avec ces valeurs sont supérieurs à 40% pour les teneurs inférieures à 1 mg kg^{-1}. La méthode des ajouts dosés permet de réduire ces écarts à des valeurs inférieures à 10%.

L'utilisation de divers réactifs complexants a été proposée [7] pour réduire les interférences constatées lors des déterminations par spectrométrie d'absorption atomique avec génération d'hydrures. Dans ce travail on a employé un milieu réactionnel contenant de l'acide nitrique 0,4 M et de l'acide tartrique 0,2 M. Les résultats obtenus avec ce milieu sont présentés dans le Tableau 4. On constate que l'ajout d'un agent complexant, l'acide tartrique, permet de réduire légèrement les perturbations, l'écart entre la valeur mesurée et la valeur théorique est de 28% pour une teneur en étain d 1 mg kg^{-1}. La présence de ce réactif améliore également la résolution des pics d'absorption ainsi que la sensibilité de la méthode (35 ng d'étain pour 0,100 d'absorbance au lieu de 65 ng en milieu nitrique seul). On utilisera donc ce milieu pour la suite des essais.

Etude des effets inter-éléments

Pour compléter l'étude des perturbations rencontrées lors du dosage par génération d'hydrure on a envisagé l'influence de la présence d'éléments à l'état de traces dans la matrice complexe et susceptibles d'interférer sur la détermination de l'étain [5]. On a préparé trois solutions contenant la matrice définie précédemment dans lesquelles ont été ajoutées des quantités variables de As, Cd, Co, Cr, Cu, Ni, Pb et Se correspondant à un sédiment,

TABLEAU 4

Interférences dues a une matrice complexe sur la détermination de l'étain

Milieu	Valeur théorique (mg kg^{-1})					
	0,5	1	5	10	50	100
Ecarts (%)[a]						
Acide nitrique 0,4 M	−60	−44	−5	−6	−3	−4,6
Ajouts dosés	−10	−8	+8	−3	+5	0,0
Acide nitrique 0,4 M Acide tartrique 0,2 M	−48	−28	−6	+2	−3	+4,1

[a]Par rapport à la valeur théorique.

M1, contenant les teneurs naturelles en métaux [8] et à deux sédiments, **M2** et **M3**, moyennement et fortement pollués [9] . Les teneurs en éléments traces des trois matrices étudiées sont présentées dans le Tableau 5.

Les dosages ont été effectués en présence d'acide nitrique 0,4 M et d'acide tartrique 0,2 M. Les concentrations en étain ont été déterminées par rapport à une courbe d'étalonnage simple et par la méthode des ajouts dosés. Les écarts entre les valeurs trouvées et les valeurs théoriques introduites sont présentés dans le Tableau 6.

En présence d'éléments traces, les perturbations dues à la matrice sont sensibles pour des teneurs en étain inférieures à 10 mg kg^{-1}. Les écarts avec la valeur théorique varient entre 15 et 82% selon les matrices et la concentration en étain. Les interférences sont plus importantes avec la matrice **M3** fortement chargée en métaux et d'une manière générale plus importantes qu'en absence de métaux traces. Il existe donc des effets inter-éléments lors de la génération d'hydrures qui bloquent la volatilisation de l'étain. Dans le domaine de concentration sensible aux interférences, il est nécessaire d'effectuer les dosages par la méthode des ajouts dosés.

En conclusion, on effectuera les déterminations d'étain sur une prise d'essai de 10 ml dans un milieu contenant de l'acide nitrique 0,4 M et de

TABLEAU 5

Teneurs en éléments traces des matrices complexes étudiées

Matrice	Teneur (mg kg^{-1})							
	As	Cd	Co	Cr	Cu	Ni	Pb	Se
M1	10	1	10	100	100	100	100	0,1
M2	20	20	20	100	100	100	100	2
M3	100	100	500	500	500	500	500	10

TABLEAU 6

Effets inter-éléments lors du dosage de l'étain

Matrice		Valeur théorique (mg kg^{-1})					
		0,5	1	5	10	50	100
Ecarts (%)[a]							
M1	Méthode directe	−71	−43	−26	−6	−12	+3
	Ajouts dosés	−5	+1	+2	+2	−3	+4
M2	Méthode directe	−72	−38	−15	−2	−5	+1
	Ajouts dosés	−4	−11	+5	−6	+8	+14
M3	Méthode directe	−82	−56	−20	−4	−3	−2
	Ajouts dosés	+2	+2	−2	+12	+3	−2

[a]Par rapport à la valeur théorique.

l'acide tartrique 0,2 M. La génération d'hydrures est obtenue par ajout de 10 ml d'une solution de borohydrure de sodium à 30 g l^{-1} dans la soude à 10 g l^{-1}, la cellule de mesure étant chauffée à 900°C. Dans ces conditions, le domaine analytique s'étend entre 5 et 100 ng d'étain dans la prise d'essai; la concentration caractéristique, pour 1% d'absorbance, est de 1,6 ng.

Comparaison de différentes méthodes de minéralisation

Pour effectuer le dosage de l'étain par génération d'hydrures il est d'abord nécessaire de mettre en solution les échantillons de sédiment ou de boue. De nombreuses méthodes ont été décrites pour la détermination de divers éléments, notamment As, Se et Sb, par génération d'hydrures [10—12] ou pour la détermination des métaux lourds dans les sédiments et les boues [13].

Sept méthodes de minéralisation pour le dosage de l'étain ont été comparées dans quatre échantillons réels différents, dont deux sédiments (A et B) une boue de station d'épuration (C), et une roche (D). Pour comparer ces différentes méthodes (voir Partie Expérimentale) on retiendra la méthode la plus efficace pour extraire la quantité maximale d'étain contenu dans l'échantillon et qui donne la dispersion la plus faible sur les valeurs obtenues.

Les résultats obtenus avec ces méthodes sur les quatre échantillons sont présentés dans le Tableau 7. Les minéralisations ont été réalisées en double et les résultats présentés sont la moyenne des deux essais. Les valeurs obtenues sont très différentes selon les méthodes employées. Néanmoins, pour l'ensemble des échantillons, les méthodes 2 et 4 donnent les résultats les plus élevés.

Compte tenu des difficultés d'utilisation au laboratoire des acides fluorhydrique et perchlorique concentrés et des risques d'interférences dues à l'acide fluorhydrique, on retiendra plus particulièrement la méthode 2 qui utilise un mélange d'acides nitrique et chlorhydrique concentré à reflux, méthode par ailleurs utilisée pour la détermination des métaux lourds, notamment dans les boues. Des essais complémentaires ont été réalisés pour vérifier la reproductibilité de cette méthode. On a effectué dix minéralisations de l'échantillon C et déterminé la teneur en étain.

TABLEAU 7

Comparaison de différentes méthodes de minéralisation (1—7) pour la détermination de l'étain dans les sédiments et les boues

Echantillon	Teneur (mg kg^{-1})						
	1	2	3	4	5	6	7
A	0,3	16,2	2	20,6	11,5	0,9	7,4
B	0,5	1,4	0,2	7,9	0,9	6,3	1,9
C	155	218	23	154	54	53	143
D	59	63	11	59	34	18	14

La moyenne des mesures est de 207,7 mg kg^{-1} avec un écart-type de 11,9. D'après ces valeurs, il apparaît que cette méthode est suffisamment reproductible et elle est donc satisfaisante pour la détermination de l'étain dans les sédiments et les boues.

Conclusion

La spectrométrie d'absorption atomique avec génération d'hydrures est une méthode qui permet le dosage de l'étain dans les sédiments et les boues de stations d'épuration.

Le milieu réactionnel qui donne le meilleur signal est une solution contenant de l'acide nitrique 0,4 M et de l'acide tartrique 0,2 M. L'ajout d'acide tartrique permet d'améliorer la sensibilité de la méthode ainsi que la résolution des pics d'absorption. La présence d'acide fluorhydrique peut diminuer fortement le signal et il est nécessaire de bien éliminer cet acide par évaporation lors des mises en solution. Dans une matrice complexe de type sédiment le signal peut être diminué à partir d'une teneur en étain de 5 mg kg^{-1} dans l'échantillon ou de 10 mg kg^{-1} en présence de certains éléments traces; pour les teneurs inférieures il est donc nécessaire d'utiliser la méthode des ajouts dosés pour obtenir en résultat satisfaisant. Enfin, la méthode de mise en solution des échantillons par reflux à l'aide d'un mélange (1 + 3) d'acide nitrique et d'acide chlorhydrique concentrés permet une détermination satisfaisante de l'étain dans ces milieux.

BILIOGRAPHIE

1 K. S. Subramanian, Int. Lab., 19 (1981) 32.
2 M. Camail, B. Loiseau, A. Margaillan et J. L. Vernet, Analusis, 11 (1983) 358.
3 R. Pinel, I. G. Gandjar, M. Z. Benabdallah, A. Astruc et M. Astruc, Analusis, 12 (1984) 404.
4 V. F. Hodge, S. L. Seidel et E. D. Goldberg, Anal. Chem., 51 (1979) 1256.
5 W. Maher, Anal. Chim. Acta, 138 (1982) 365.
6 M. Legret, L. Divet et D. Demare, Anal. Chim. Acta, 175 (1985) 203.
7 M. Pinta, Spectrométrie d'Absorption Atomique, Tome 1, Masson, O.R.S.T.O.M., Paris, 1979, p. 262.
8 J. M. Martin et M. Meybeck, Mar. Chem., 7 (1979) 173.
9 D. Robbe, P. Marchandise, Ch. Tome et G. Ruban, Campagne 1981 de l'Inventaire National du Degré de Pollution des Eaux Superficielles. Interprétation des Résultats Obtenues sur les Sédiments, Ministère de l'Urbanisme et du Logement, rapport LPC, 1984, p. 113.
10 D. D. Nygaard et J. M. Lowry, Anal. Chem., 54 (1982) 803.
11 S. Kempton, R. M. Sterritt et J. N. Lester, Talanta, 29 (1982) 675.
12 N. G. Van der Veen, H. J. Keukens et G. Vos, Anal. Chim. Acta, 171 (1985) 285.
13 P. Marchandise, J. L. Olie, D. Robbe et M. Legret, Environ. Technol. Lett., 3 (1982) 157.

Analytica Chimica Acta, 189 (1986) 323—328
Elsevier Science Publishers B.V., Amsterdam — Printed in The Netherlands

SPECTROPHOTOMETRIC DETERMINATION OF CHLORHEXIDINE WITH BROMOCRESOL GREEN BY FLOW-INJECTION AND MANUAL METHODS

J. MARTINEZ CALATAYUD* and P. CAMPÍNS FALCÓ

Departamento de Química Analítica, Facultad de Química, Universidad de Valencia, Burjasot, Valencia (Spain)

(Received 13th February 1986)

SUMMARY

A spectrophotometric study of the chlorhexidine/bromocresol green/Triton X-100 system is reported; at pH 5.3, both 2:1 and 1:1 bromocresol green/chlorhexidine complexes are formed. In the manual spectrophotometric method, Beer's law is obeyed for chlorhexidine concentrations of 2.9—32.2 μg ml^{-1} (r.s.d. 0.4—1.3%); the molar absorptivity is 12 500 l mol^{-1} cm^{-1}. In the flow-injection method, the calibration graph is linear for the chlorhexidine range 23.0—83.9 μg ml^{-1} (r.s.d. 0.8%); the injection is ca. 60 h^{-1}. Benzocaine, acetylsalicylic acid, ascorbic acid and sucrose are tolerated at 10^{-2}—10^{-3} M levels. Hibitane 5% was analyzed successfully.

Chlorhexidine(I) is a bactericidal drug used in several pharmaceutical formulations. Titration in non-aqueous medium is suitable for the determination of relatively large amounts of the drug [1]. A lengthy spectrophotometric procedure [2] based on reaction with standardized hypobromite has been recommended for smaller amounts. A spectrophotometric assay based on differences between the absorbances before and after reaction with bromothymol blue [3] has been criticized as yielding large errors [4, 5]. Other ion-pair complexes between chlorhexidine and dyes have been reported. The ion-pair with bromocresol green provides a molar absorptivity of 11 100 l mol^{-1} cm^{-1} at 410 nm and chlorhexidine in the range 2.5—30 μg ml^{-1} can be determined [5]. Methyl orange has been used similarly [4]. Both these methods involve liquid—liquid distribution into chloroform. These reaction systems have not been studied in detail.

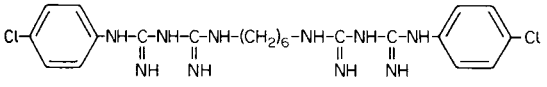

(I)

This paper deals with a simple and fast procedure for determining chlorhexidine in pharmaceutical preparations based on chlorhexidine/bromocresol green systems; a non-ionic surfactant is added to avoid the extraction procedure. A chemical study of the system is described and spectrophotometric determinations (classical and flow-injection procedures) are reported.

0003-2670/86/$03.50

EXPERIMENTAL

Reagents and apparatus

Chlorhexidine hydrochloride (donated by ICI Farma) was titrated potentiometrically with perchloric acid in anhydrous acetic acid medium [1]; its purity was found to be 99.30% (r.s.d. 0.3%, n = 5). Other chemicals were bromocresol green (Merck, indicator), Triton X-100 (Probus), sucrose (Baker), ascorbic acid (Merck), benzocaine (Probus) and acetylsalicylic acid (prepared here from salicylic acid and acetic anhydride). Other reagents were of analytical grade.

Succinate buffer solution was prepared from succinic acid and sodium hydroxide at ionic strengh 0.5 M; the pH was checked potentiometrically.

A Crison Model 501 digital potentiometer was used with a Radiometer G20-28 glass electrode and a calomel methanol-KCl saturated electrode (saturated KCl in methanol). A Crison model 517 potentiometer with an Ingold combined electrode was also used.

A Shimadzu u.v.-visible spectrophotometer with 1-cm cells served for conventional measurement. For the flow-injection method, a Coleman model 55 spectrophotometer was used with an 18-μl flow cell (1-cm path length). The basic flow-injection apparatus was a Tecator 5020 with 0.5-mm i.d. tubing. The recorder was a Unicam 45-AR model.

Procedures

Stoichiometry of the chlorhexidine/bromocresol green system. Bromocresol green solution (5 ml), previously buffered to pH 5.35 with the succinate buffer, was added to different volumes of 7.92×10^{-4} M chlorhexidine. The solution was diluted to 10 ml with deionized water and centrifuged. The absorbance of the clear supernatant liquid was measured at 615 nm against deionized water. In other tests, a constant amount of chlorhexidine (5 ml of 2.23×10^{-5} M, pH 5.35) and increasing volumes of 3.63×10^{-4} M bromocresol green were mixed and measured in the same way.

Conventional spectrophotometric determination of chlorhexidine. Succinate buffer solution (5 ml), 5.54×10^{-4} M bromocresol green (5 ml) and 2.5% (v/v) Triton X-100 (2 ml) were added to the chlorhexidine solution (8.5—25.0 μg ml^{-1}). After dilution to 25 ml, absorbance was measured at 630 nm against a similar solution without chlorhexidine.

Flow-injection method. The flow manifold was a single-channel system. The carrier was 7.26×10^{-5} M bromocresol green containing 0.06% (v/v) Triton X-100 buffered to pH 5.00 with the succinate buffer (20 ml of buffer to 100 ml of bromocresol green/Triton X-100 solution). The sample volume was 60 μl, the concentration of chlorhexidine injected being in the range 23.0—83.9 μg ml^{-1}. The reaction coil was 92 cm long and the flow rate 3.14 ml min^{-1}. Absorbances were recorded at 630 nm. For hibitane (5%), 0.30 ml of the sample was diluted to 200 ml with deionized water and 60-μl portions were injected.

RESULTS AND DISCUSSION

Qualitative tests were made with chlorhexidine and several dyes (methyl orange, bromocresol green, thymol blue and bromocresol purple) in presence of non-ionic surfactants (Triton X-100, Emulsogen EL, Nemol K10/30, Emulsogen LP, Emulsogen MS and gum arabic) over the pH range 5—6. Comparisons against the corresponding blank solution (without chlorhexidine) showed that reaction with bromocresol green in presence of Triton X-100 provided the greatest color contrast and sensitivity.

Study of the chlorhexidine/bromocresol green/Triton X-100 system

Triton X-100 added to an aqueous bromocresol green solution modified the acidity constant of the dye from $pK_a = 4.66$ to about 5.7; this increase is similar to that obtained when the polarity of the solvent is decreased [6]. The addition of chlorhexidine to a bromocresol green/Triton X-100 mixture produced hyperchromic and hypochromic effects on the 615- and 420-nm absorption bands of bromocresol green. A study of the influence of pH (Fig. 1) showed that the best pH range is 5.20—5.60; pH 5.35 was selected as the working pH value. Acetate, phthalate, citrate, succinate and citric/phosphate buffers were tested; the succinate buffer was best.

The absorbance at 630 nm depended strongly on the amount of Triton X-100 when its concentration was less than 0.2% (v/v). The chlorhexidine/bromocresol green system remained in solution for more than 1 week when

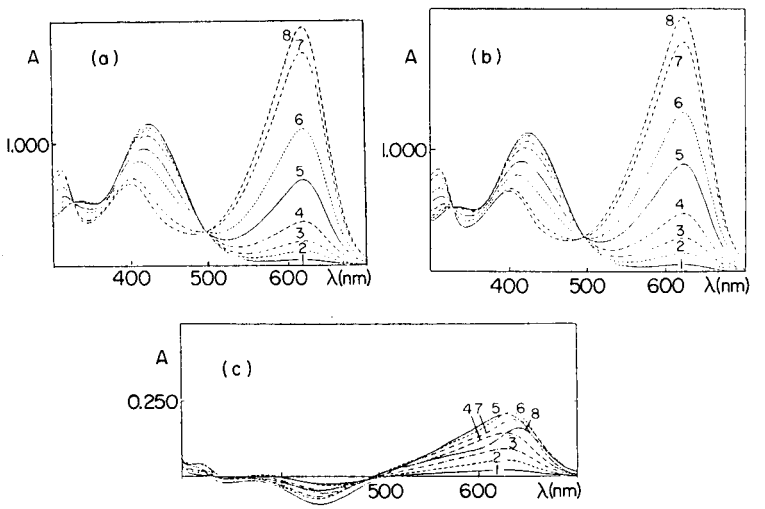

Fig. 1. Influence of pH: (1) 3.96; (2) 4.36; (3) 4.65; (4) 4.92; (5) 5.28; (6) 5.60; (7) 6.00; (8) 6.20. (a) 6.72×10^{-5} bromocresol green and 0.1% Triton X-100; (b) 6.72×10^{-5} bromocresol green, 1.47×10^{-5} M chlorhexidine and 0.1% Triton X-100. (c) spectra (b) plotted against (a). Spectra (a, b) measured against deionized water. Acetate buffer used at I = 0.1 M.

0.2% Triton X-100 was present; absorbances at 630 nm were constant for more than 24 h.

Several methods were used in attempts to elucidate the stoichiometry of the reaction. Job's method for mixtures of bromocresol green (BG) and chlorhexidine (C), without surfactant, suggested the formation of 1:1 and 2:1 complexes. These stoichiometries were also observed when Triton X-100 was present and the Yoe—Jones [7] and Asmus [8] methods were applied. For the former procedure, the chlorhexidine concentration was kept constant (2.0×10^{-5} M) and bromocresol green was added; the plot of absorbance vs. BG/C concentrations started to curve at the 1:1 ratio but constant absorbance was not attained until the BG/C concentration mole ratio was $\geqslant 2.9$. The reverse order of addition also did not produce clear results. Clearer information was obtained from the Asmus method, as modified by Klausen and Langmyhr [9]. Straight lines were observed for $m = n = 1$ when the BG/C mole ratios were less than 1.51, but straight lines were obtained only for $m = 1$ and $n = 2$ when the molar ratios exceeded 1.72. The stability constants of the ion-pairs calculated from the Asmus method were about 6×10^{-5} and 9×10^{-10}, respectively. The formation of both complexes (1:1 and 2:1) within the narrow pH range used suggests ion-pair formation with mono-anionic bromocresol green and diprotonated chlorhexidine. The 1:1 system would require another anion, and chloride was detected (with silver ion) after the complex had been dissolved in nitric acid; chloride was not detected in the 2:1 complex. The obtained ion-pair precipitates are thought to be $(CH_2)(BG)(Cl)$ and $(CH_2)(BG)_2$.

Spectrophotometric determination of chlorhexidine

Manual procedure. The determination was based on the more stable 2:1 compound. Beer's law was obeyed at 630 nm, with 0.2% Triton X-100 in the range 2.9—32.2 $\mu g\ ml^{-1}$ chlorhexidine; the molar absorptivity was of 12 500 l $mol^{-1}\ cm^{-1}$ ($r = 0.99994$). The optimum range for chlorhexidine was 8.5—25.0 $\mu g\ ml^{-1}$, from the Ringbom method. Beer's law was also obeyed with 0.1 and 0.5% Triton X-100 was added; the molar absorptivities changed slightly but the linearity range was not increased. The reproducibility of the method was checked for different sets of conditions. For solutions containing 19.7 μg ml chlorhexidine (7.76×10^{-5} M bromocresol green and 0.1% Triton X-100), the relative standard deviation (r.s.d.) was 0.4%, and for solutions with 20.2 $\mu g\ ml^{-1}$ (1.11×10^{-4} M bromocresol green and 0.2% Triton X-100), the r.s.d. was 0.7% ($n = 10$).

The tolerance of the method for possible concomitants was investigated for solutions containing 2.53×10^{-5} M chlorhexidine (1.11×10^{-4} M bromocresol green, 0.2% Triton X-100). The results are given in Table 1.

Spectrophotometric determination of chlorhexidine in Hibitane 5%, after suitable dilution, gave a result of 2.13×10^{-5} M ($n = 5$), i.e., 4.7% compared with a nominal content of 5%. Titration with perchloric acid in acetic acid medium gave a result of 4.6%.

TABLE 1

Effects of other compounds

Compound	Manual method		Flow-injection method	
	Conc. ($\times 10^{-3}$ M)	Abs.[a]	Conc. ($\times 10^{-3}$ M)	Peak height (cm)
—	—	0.330	—	9.4
Benzocaine	2.53	0.328	8.10	9.3
Acetylsalicylic acid	2.53	0.332	4.05[b]	9.4
Ascorbic acid	2.53	0.328	4.05[b]	9.5
Sucrose	2.53	0.329	8.10	9.3

[a]Average absorbance for $n = 3$. [b]Sample buffered with the succinate buffer (10 ml per 50 ml of sample) prior to injection.

Flow-injection procedure. Preliminary tests were made with several bromocresol green and Triton X-100 concentrations in the carrier stream and different sample volumes. The highest peaks were obtained with BG/C mole ratios around 1. The different flow-injection parameters (flow rate, reaction-coil length and sample volume) were studied for a carrier solution containing 50 ml of 5.15×10^{-5} M bromocresol green, 2.5 ml of 12.5% (v/v) Triton X-100, 100 ml of succinate buffer (pH 5.35, $I = 0.5$ M) diluted to 500 ml with deionized water. Different volumes (30, 60, 100 and 140 μl) of 7.9×10^{-5} M chlorhexidine solution were directly injected into the carrier stream. The reaction coil was varied from 42 to 167 cm and the flow rate from 1.71 to 5.55 ml min^{-1}. The r.s.d. values were in the range 0.5—2.4% ($n = 5$). Maximum peak heights were obtained for sample volumes of 60, 100 and 140 μl for coil lengths of 92 and 142 cm, and flow rates in the range 2.61—3.14 ml min^{-1}. The dependence for 60-μl injections is shown in Fig. 2. Peak heights were much smaller when 30 μl was injected and split peaks were obtained with short coil lengths (especially for 140-μl injections). The selected parameters were sample volume 60 μl, coil length 92 cm, and flow rate 3.14 ml min^{-1} in order to obtain a high injection rate.

The chemical parameters optimized for the manual method were revised for the flow-injection procedure because kinetic behaviour is important in the latter. The best pH interval was found to be 4.80—5.15 and the pH selected was 5.00 (succinate buffer). Changes in the bromocresol green concentration between 5.15×10^{-5} and 1.42×10^{-4} M showed that constant peak heights were obtained for BG/C mole ratios of 0.72—1.27; when the ratio was increased to 2, the peak heights decreased considerably. This suggests that better results were obtained when the 1:1 complex was formed. The best Triton X-100 concentration was 0.6% (v/v).

The calibration graph was linear over the range 23.0—83.9 μg ml^{-1} chlorhexidine when 7.3×10^{-5} M bromocresol green and 0.06% Triton X-100 were

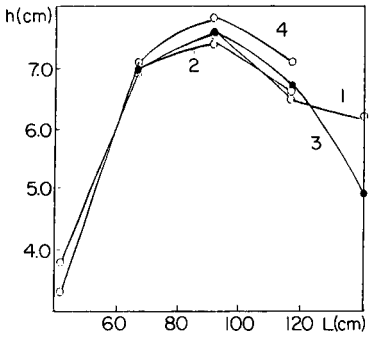

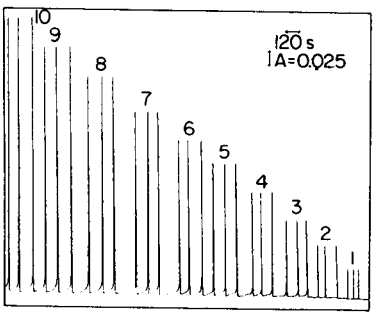

Fig. 2. Effects of coil length and flow rate: (1) 1.71, (2) 2.61, (3) 2.73, (4) 3.14 ml min^{-1}. Injected volume 60 μl. See text for details.

Fig. 3. Peaks obtained in a calibration run for chlorhexidine. Peaks 1—10 correspond to 4.1, 5.1, 6.1, 7.2, 8.1, 9.1, 10.1, 11.6, 13.0 and 14.5 × 10^{-5} M chlorhexidine, respectively.

used. A typical calibration run is shown in Fig. 3. For 60-μl injections of 8.1 × 10^{-5} M (46.0 μg ml^{-1}) chlorhexidine, the r.s.d. was 0.8% (n = 20) and the injection rate was about 60 h^{-1}. The effects of other substances are listed in Table 1 (8.1 × 10^{-5} M chlorhexidine and 7.26 × 10^{-5} M bromocresol green). The chlorhexidine content of Hibitane 5% was found to be 4.7% by this procedure.

Conclusion

Both methods described for chlorhexidine are fast and simple. The linear range for the manual procedure (2.9—32.2 μg ml^{-1}) is slightly better than that of the extraction procedure and the molar absorptivity is larger. The linear range is extended when the flow-injection method is applied (23.0—83.9 μg ml^{-1}). Tolerance for other substances is similar in both methods.

REFERENCES

1 British Pharmacopoeia, 1980, Volume 1, p. 100.
2 A. Holbrook, J. Pharm. Pharmacol., 10 (1958) 370.
3 J. B. Lowry, J. Pharm. Sci., 68 (1979) 110.
4 G. Andermann, M. O. Buhler and M. Erhart, J. Pharm. Sci., 69 (1980) 215.
5 S. Pinzauti, E. La Porta, M. Casini and C. Betti, Pharm. Acta Helv., 54 (1982) 334.
6 E. Bishop (Ed.), Indicators, Pergamon Press, Oxford, 1972, p. 104.
7 J. H. Yoe and A. L. Jones, Ind. Eng. Chem. Anal. Ed., 16 (1944) 111.
8 H. Asmus, Z. Anal. Chem., 178 (1960) 104.
9 K. S. Clausen and F. J. Langmyhr, Anal. Chim. Acta, 28 (1963) 501.

Analytica Chimica Acta, 189 (1986) 329—337
Elsevier Science Publishers B.V., Amsterdam — Printed in The Netherlands

MICRODIFFUSION AND SPECTROPHOTOMETRIC DETERMINATION OF FLUORIDE IN BIOLOGICAL SAMPLES

BORIS CULIK

Meereszoologie, Institut für Meereskunde, Düsternbrooker Weg 20, 2300 Kiel 1 (Federal Republic of Germany)

(Received 3rd June 1986)

SUMMARY

Routine separation of fluoride from large numbers of biological samples (soft and hard tissues) is achieved by microdiffusion from perchloric acid and absorption by sodium hydroxide on filter paper in disposable polypropylene vials. Spectrophotometry with a modified lanthanum/alizarin complexone reagent allows rapid determination of fluoride. Up to 80 samples can be processed per day. Recoveries are in the range 88—102%. Results obtained by spectrophotometry and with the fluoride-sensitive electrode agree within 3—10% for various samples of krill and shrimp products.

Routine analysis of large numbers of biological samples for fluoride content required the development of a cheap, rapid, easy and accurate method of extraction and determination. This paper describes improved procedures for microdiffusion and spectrophotometry, their accuracy and recovery; their performance is compared with that of other methods for the same purpose.

Extraction techniques described for similar purposes [1—6] tend to be cumbersome and time-consuming: procedures based on reverse extraction [2, 3], pyrohydrolysis [4] and diffusion or steam distillation [5]. Preliminary experiments showed that these methods are unsuitable for the extraction of fluoride from large numbers of biological samples. Microdiffusion techniques have repeatedly been described in the literature [5—9], but most of them require rather lengthy preparatory steps [5—7], and the preparation of individual diffusion cells is also a disadvantage [8, 9].

The spectrophotometric determination of fluoride with alizarin complexone (alizarin fluorine blue; alizarin-3-methylimino-*N*,*N*-diacetic acid) as its cerium or lanthanum complex [10—13] has practically been displaced by potentiometry with the fluoride-selective electrode [2, 8, 9] since its introduction by Frant and Ross [14]. This is surprising, because the spectrophotometric method offers major advantages of speed in handling large numbers of samples with low fluoride concentrations for which the electrode requires long equilibration times. Although the accuracy of the alizarin complexone method has been questioned [8], it will be shown that both methods give similar results.

0003-2670/86/$03.50

EXPERIMENTAL

Apparatus and reagents

Polypropylene vials with lids (30 × 30 mm) were obtained from Semadeni Company (cat. no. 2.2061; 3072 Ostermundigen, Switzerland), as were polypropylene test tubes (16 × 100 mm). The filter paper used was hardened and ash-free (Whatman 541). A Beckman model 29 spectrophotometer was used with 50-mm pathlength glass cuvettes.

Other equipment included a Metrohm Dosimat Model E535 burette, a fluoride-selective electrode (Model 96-01; Orion Research, Cambridge, MA), a pH/mV meter programmable for standard addition (Model pMX; WTW Company, D-8120 Weilheim), a laboratory stirrer, and a stripchart recorder (Servogor, Model RE-511).

All reagents were of analytical grade. Twice-distilled water was used throughout.

The alizarin complexone reagent was prepared as follows. A 10^{-3} M solution of alizarin-3-methylimino-*N*,*N*-diacetic acid (Merck) was made by dissolving the dye with a few drops of ammonia and diluting to 1 l with water; any suspended matter was filtered off. This solution can be stored in a brown glass container for about 14 days. A portion (200 ml) of the alizarin complexone solution was mixed with 200 ml of 10^{-3} M lanthanum nitrate (Merck), 50 ml of acetate buffer (2 M, pH 4.5, made from 82.4 g of sodium acetate and 208 ml of anhydrous acetic acid in water, adjusted to pH 4.5 and diluted to 500 ml), and finally 400 ml of acetone. This mixture was prepared daily.

Silver perchlorate solution (40%) was prepared by dissolving 22.5 g of silver oxide in 100 ml of boiling perchloric acid (70%). For the total ionic strength adjustment buffer (TISAB), 58 g of sodium chloride, 57 ml of anhydrous acetic acid and 4 g of CDTA (cyclohexanediaminotetraacetic acid; Merck) in 500 ml of water was adjusted to pH 5.5 and diluted to 1 l with water. The stock fluoride solution (1000 μg g^{-1}) was prepared from dried (110°C) sodium fluoride and diluted as required to yield working standards (10 μg g^{-1}).

Procedures

Microdiffusion method. Prepare the lids of the polypropylene vials by inserting a tightly-fitting round filter paper. Impregnate it with 100 μl of 1 M sodium hydroxide. Weigh the freeze-dried, homogenized sample into the bottom of the vial; use ca. 100 mg for soft tissue material, and less than 10 mg for skeletal samples. Add 2 ml of chilled perchloric acid (70%) to the sample and immediately cover the vial with the prepared lid. Place all the vials on a tray and cover with a second tray of the same size, placing a weight on top to prevent the lids from lifting. Digest in an oven at 60°C for 18—24 h.

The filter paper is squeezed between the lid and the rim of the vial and so acts as a seal (Fig. 1). If the sample contains a high chloride concentration,

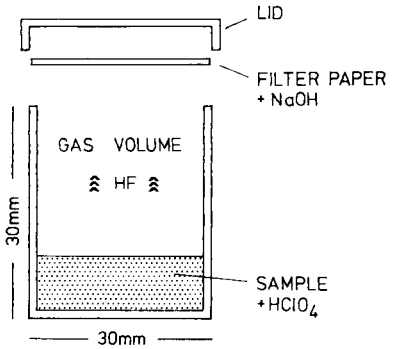

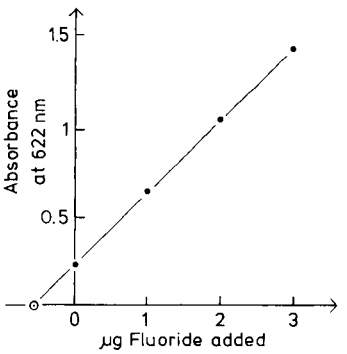

Fig. 1. Polypropylene vial used in microdiffusion. The impregnated filter paper is squeezed in place between the lid and the rim of the vial.

Fig. 2. Graphical extrapolation of fluoride content of a krill product after standard addition. (○) Extrapolated value.

the filter paper is attacked and blackens. To prevent this, the diffusion has to be repeated by adding ca. 10 µl of silver perchlorate (40%) for each milligram of chloride to the sample just before the perchloric acid. The time allowed for diffusion must then be doubled to 36—48 h [7].

Spectrophotometry. Fold the dry filter paper after the microdiffusion and insert it into a polypropylene test tube. Add 2 ml of water to dissolve the absorbed salts. Leave the filter paper in the test tube, add 100 µl of the 10^{-3} M alizarin complexone (prepared as described above at pH 4.5) as a pH indicator and shake well. Add about 70 µl of perchloric acid (10%) until the colour changes from red to yellow (pH 4.5). This is the back-extract. Add 5 ml of the mixed lanthanum/alizarin complexone reagent, stopper and shake. The total volume of all samples and standards is 7.17 ml.

Prepare standards for the calibration graph. Prepare six polypropylene test tubes by adding 100 µl of 1 M sodium hydroxide and 1.5, 1.7, 1.8, 1.85, 1.88 and 1.89 ml of water, respectively. Add 100 µl of the 10^{-3} M alizarin complexone and proceed as described above, after addition of 0.4, 0.2, 0.1, 0.05, 0.02 and 0.01 ml of standard fluoride solution (10 µg g^{-1}), respectively.

Prepare a blank solution in a polypropylene vial with 0.3 ml of 1 M sodium hydroxide, 5.7 ml of water and 0.3 ml of 10^{-3} M alizarin complexone. Add ca. 210 µl of perchloric acid (10%) until the colour change from red to yellow is observed. Add 15 ml of the mixed reagent. The composition of this blank is the same as that of the samples and standards, the large volume being needed for calibration of the spectrophotometer.

Keep all solutions in the dark for 60 min for complete colour development. Using 5-cm cuvettes, measure the absorbance against the blank in the double-beam spectrophotometer at 622 nm.

Comparison with the fluoride-selective electrode

After the microdiffusion, proceed as described above (under Spectrophotometry) until the back-extract is obtained. Place a 1-ml subsample of this solution into a polypropylene vial slightly larger than the electrode tip and add 1 ml of TISAB. To ensure good mixing, the vial itself is attached to a laboratory stirrer and rotated at about 50 rpm. Monitor the millivolt reading on the chart recorder and record the value when the reading is stable within 0.1 mV min^{-1}. Calibrate the electrode for the fluoride range of the samples using the programmable pH/mV meter. A more detailed description of the technique is available [13].

Determine fluoride in another 1-ml subsample by the above spectrophotometric method.

Comparison with other methods

Samples of shrimp (*Crangon crangon*) homogenate were sent to three independent laboratories. (a) D. Fremstad and K. Nagy (SINTEF, Division of Applied Chemistry, Trondheim, Norway) extracted the samples with buffer solution for 24 h and finally used the fluoride-selective electrode. (b) K. Cammann and T. Weiss (Division of Analytical Chemistry, Ulm University, F.R.G.) extracted fluoride by, (1) ashing in a nickel crucible or by, (2) microdiffusion, again completing the determination with the fluoride-selective electrode. (c) G. Siebert (Universitäts- und Poliklinik für Zahn-, Mund- und Kieferkrankheiten, Würzburg, F.R.G.) extracted the samples [15] and completed the determination by a gas-chromatographic method [16].

RESULTS

Recovery

The described spectrophotometric method provides good sensitivity, giving linear calibration for the range 0—4 μg of fluoride in the solution finally measured. Typical calibration parameters at 622 nm are a slope of 0.434 with an intercept of 0.0006 and correlation coefficient 0.999.

Recoveries for the microdiffusion/spectrophotometric procedure were tested on penguin (*Pygoscelis adeliae*) liver homogenate as organic matrix (1.2 $\mu g\, g^{-1}$ fluoride, dry weight). Fluoride (1 μg as sodium fluoride) was added to each sample before microdiffusion. The recovery was calculated from the difference between the expected and measured fluoride values (Table 1) and ranged from 88 to 102% (average 94%).

The recoveries relevant to only spectrophotometry were estimated by the following procedure [17]. A krill product was used as the organic matrix; after microdiffusion, the filter papers were processed by the spectrophotometric procedure as described above. After the reading had been taken, the solutions were poured back into the test tubes and 1 μg of fluoride (100 μl of 10 $\mu g\, g^{-1}$ standard) was added; 60 min later a second reading was taken against a reagent blank to which 100 μl of water had been added. After these

TABLE 1

Recovery from a penguin liver homogenate by the proposed method

Liver sample (mg)	Fluoride (μg)				Recovery (%)
	In sample	Total[a]		Difference	
		Calc.	Measured		
110	0.132	1.132	1.038	−0.094	92
100	0.120	1.120	0.990	−0.130	88
200	0.240	1.240	1.125	−0.115	91
200	0.240	1.240	1.115	−0.125	90
310	0.372	1.372	1.406	+0.034	102
300	0.360	1.360	1.390	+0.030	102

[a] After addition of 1 μg of fluoride before microdiffusion.

steps had been repeated 3 times, the absorbances measured were plotted against micrograms of fluoride added (Fig. 2). The fluoride content of the sample was calculated after the first reading (i.e., without fluoride added) and by extrapolation of the standard additions plot. This was repeated for 10 samples of the unhomogenized krill product. Table 2 shows the results of the first reading compared to the extrapolated values. The correlation between the 4 readings is in all cases greater than 0.99, which gives an indication of the reliability of the reagent. The mean value for the first reading was 318 ± 25 $\mu g\ g^{-1}$ whereas extrapolation after standard addition resulted in 358 ± 33 $\mu g\ g^{-1}$. A paired *t*-test (p = 95%) showed that the difference is significant. Recovery for the colour reagent was therefore on average 91.6% with a range of 87.5—98.6%.

The influence of silver perchlorate (40%) during microdiffusion, which is required for the precipitation of chloride, was tested on samples of krill product. Pairs of samples of comparable weight were extracted with and without the addition of silver perchlorate (Table 3). A paired *t*-test (p = 95%) showed that if the time allowed for diffusion was doubled (36—48 h), the addition of silver perchlorate had no negative influence on recovery. On the contrary, the addition of silver perchlorate to large sample weights increased recovery because destruction of the filter paper during diffusion was prevented.

Comparison of the spectrophotometric and potentiometric methods

In order to compare the results obtained by both procedures, 1 ml of the "back-extract" was analyzed by spectrophotometry and with the fluoride-selective electrode. The organic matrix was shrimp homogenate (*Crangon crangon*) and krill homogenate (*Euphausia superba*). The results obtained with the fluoride-selective electrode (Table 4) were 3—10% higher. The difference between the two methods was more important for low fluoride concentrations. It is doubtful if this difference can be attributed to more

TABLE 2

Comparison of fluoride concentrations in samples of a krill product (unhomogenized)

Sample weight (mg)	r^a	Fluoride ($\mu g\ g^{-1}$)[b]		Difference	
		Standard addition	Direct reading	($\mu g\ g^{-1}$)	(%)
11.9	0.9999	384	346	38	9.9
12.9	0.9997	429	375	54	12.6
20.2	0.9997	306	275	31	10.1
21.3	0.9997	312	287	25	8.0
44.4	0.9990	343	302	41	11.9
45.6	0.9989	343	307	36	10.4
97.5	0.9988	355	323	32	9.0
110.0	0.9981	399	345	54	13.5
112.2	0.9972	358	353	5	1.4
115.0	0.9973	295	269	26	8.8
$\bar{X}$	0.9988	358 ± 33	318 ± 25	30	8.4

[a]Correlation of standard addition plot. [b]Dry weight.

TABLE 3

Influence of silver perchlorate on fluoride recovery

Without silver perchlorate			With silver perchlorate			
No.	Sample[a] (mg)	Fluoride ($\mu g\ g^{-1}$)	No.	Sample[a]	$AgClO_4$ (ml)	Fluoride ($\mu g\ g^{-1}$)
1	4.9	352	2	4.7	0.02	287
3	11.9	311	4	12.9	0.05	337
5	21.3	276	6	20.2	0.10	291
7	45.6	319	8	44.4	0.20	311
9	97.5	299	10	112.2	0.50	344
11	115.0	270	12	110.0	0.50	324
$\bar{X}$	—	304 ± 32	$\bar{X}$	—	—	316 ± 25

[a]Dry weight.

reliable electrode readings at low concentrations as claimed by Dabeka et al. [8]. The present experiments showed that electrode readings were generally too high at low fluoride concentrations, because of slow or incomplete electrode equilibration. Standard addition to the samples eliminates this problem.

Comparison with results from other laboratories

Shrimp meal homogenate was sent to three independent laboratories, where it was analyzed by different methods (see Experimental). Table 5 shows the results obtained and should be compared to the upper part of

TABLE 4

Comparison of the alizarin complexone method with the fluoride-selective electrode

Material	Sample weight (mg)	Fluoride ($\mu g\ g^{-1}$)[a]		Difference	
		Alizarin complexone	Electrode	($\mu g\ g^{-1}$)	(%)
Shrimp	199.6	30.3	33.8	3.5	10
meal	216.7	30.7	32.9	2.2	7
Krill	51.1	1242	1277	35	3
meal	52.4	1209	1244	35	3

[a]Dry weight.

TABLE 5

Results of shrimp meal analyses obtained by three independent laboratories

Laboratory	Fluoride ($\mu g\ g^{-1}$)[a]		n
	Mean	Range	
(a)	33.9	30.0—38.8	6
(b) 1	34.5	34, 35	2
2	39.5	38, 41	2
(c)	24.7	24.4, 24.9	2

[a]Dry weight.

Table 4. The comparison proves that microdiffusion followed by the spectrophotometric fluoride determination is accurate and provides acceptable results.

DISCUSSION

During the development of the microdiffusion technique, several methods were tested. These tests showed that it is not necessary to fix the filter paper at an angle to the acidic phase [7], which means that it can be used as a seal. An important factor is the distance between the surface of the acidic phase and the filter paper in the lid. The height of the vessel should not exceed 30 mm. Because the diffusion takes place between the surfaces of the acidic phase and the filter paper, these should be as large as possible. The diameter of the vessels used here (30 mm) should be regarded as a minimum. The utilization of filter paper to hold the alkaline phase saves much time; it is no longer necessary to let the alkaline phase dry on the lid prior to microdiffusion, nor to dissolve it with the risk of spilling afterwards [8, 9].

In comparison with other extraction methods, microdiffusion offers a practical alternative. Routine extractions were done previously in this

laboratory by reverse extraction involving organic and aqueous phases [3, 13]. Although this technique is suitable for the analysis of large numbers of samples, it has to be ensured that the tissues analyzed have a low fat content. This means that fat extraction is necessary for several tissues involved in fat storage (e.g., bone marrow), and the results obtained can be difficult to interpret. Furthermore, the separation of phases in the test tubes requires skill, and includes several sources of errors. Fluoride isolation by microdiffusion requires no previous fat extraction, allows the analysis of subsamples weighing from <10 mg up to 500 mg and enables the fluoride-containing filter paper to be recovered without further steps such as removal of the organic phase or washing of the extract.

The modified alizarin complexone reagent in combination with microdiffusion yields recoveries above 90%. The reliability of the method is good as shown by correlation coefficients of >0.99 for calibration curves and standard addition experiments. The advantage over analysis with the fluoride-selective electrode is that for a whole batch of samples the time for colour development is 60 min, whereas up to 20 min is needed for potential readings of individual samples to become stable within 1 mV min^{-1}. The spectrophotometric procedure allows analysis of up to 80 samples per day and preparation of the same number of samples for microdiffusion, while only 20 samples per day can be handled with the potentiometric method. The results obtained by the two methods differ only by 3—10% and are similar to those obtained by other laboratories. The spectrophotometric method is therefore preferred in routine analyses of biological samples and the electrode is utilized only for liquid samples such as urine and seawater [18].

This work was supported by a grant from the "Deutsche Forschungsgemeinschaft" (MZ-AD 24/6) and by a stipend from the "Studienstiftung des deutschen Volkes".

REFERENCES

1 J. A. Cooke, M. S. Johnson and A. W. Davison, Environ. Poll., 11 (1976) 257.
2 T. Soevik and O. R. Braekkan, J. Sci. Food Agric., 32 (1981) 467.
3 P. Venkateswarlu, Anal. Chem., 46 (1974) 878; Anal. Biochem., 68 (1975) 512.
4 G. Troll, A. Farzaneh and K. Cammann, Chem. Geol., 20 (1977) 295.
5 L. Singer and W. D. Armstrong, Anal. Biochem., 10 (1965) 495; Anal. Chem., 26 (1954) 904.
6 R. J. Hall, Analyst, 85 (1960) 560; 88 (1963) 76.
7 J. Bäumler and E. Glinz, Mitt. Geb. Lebensmittelunters. Hyg., 55 (1964) 250.
8 R. W. Dabeka, A. D. McKenzie and H. B. S. Conacher, J. Assoc. Off. Anal. Chem., 62 (1979) 1065.
9 R. W. Dabeka and A. D. McKenzie, J. Assoc. Off. Anal. Chem., 64 (1981) 1021.
10 R. Belcher, M. A. Leonard and T. S. West, J. Chem. Soc., (1959) 3577.
11 R. Belcher and T. S. West, Talanta, 8 (1961) 853, 863.
12 K. Kremling, Fluoride, in K. Grasshoff (Ed.), Methods of Seawater Analysis, Verlag Chemie, Weinheim, 1976.

13 A. Keck, Dissertation, Christian-Albrechts Universität Kiel, (1984).
14 M. S. Frant and J. W. Ross, Science, 154 (1966) 1553.
15 G. Siebert and K. Trautner, Z. Ernährungswiss., 24 (1985) 54.
16 J. A. Freesen, F. H. Cox and M. J. Witter, Pharm. Weekblad, 103 (1968) 909.
17 J. C. Duinker, Marine Chemistry, Institut für Meereskunde, personal communication, (1983).
18 B. Culik, Polar Biol., (1987) in press.

Analytica Chimica Acta, 189 (1986) 339—351
Elsevier Science Publishers B.V., Amsterdam — Printed in The Netherlands

PREDICTING RETENTION DATA BY TARGET FACTOR ANALYSIS AND MULTIPLE REGRESSION ANALYSIS

DARRYL G. HOWERY*, GERALD D. WILLIAMS[a] and NELSON AYALA[a]

Department of Chemistry, The City University of New York, Brooklyn College, Brooklyn, NY 11210 (U.S.A.)

(Received 9th September 1983)

SUMMARY

Target factor analysis is used to predict gas-chromatographic retention indices from a training-set data matrix for 13 solutes and 15 stationary phases. In the target-combination approach, sets of data vectors are target-tested in combination and the resulting coefficients for the best model are used for predictions. Retention indices for 42 solutes and 24 stationary phases are predicted to better than 1% even with a three-factor model. In the target free-float approach, values for missing retention indices on target test vectors are predicted. Predictions from sets of target-test data selected by chemical intuition are compared to those obtained from sets of target-test data selected by using models from the combination step. The target-combination approach and multiple-regression approach are overall of similar utility for predicting new data.

Factor analysis, a mathematical method for studying matrices of data, has been used extensively to model chromatographic retention data [1—4]. Weiner and Howery [5] demonstrated the feasibility of using target factor analysis to predict gas-chromatographic retention indices with key sets of typical vectors from the data matrix, and extended the approach by using key sets of basic parameters for solutes, predicting the retention indices of five esters on 23 stationary-phase solvents [6]. Here, several methods are presented for predicting retention indices from a minimum of experimental data. Two approaches based on target factor analysis are explored. A third approach based on multiple regression is described for comparative purposes. Although chromatographic data are used to illustrate the approaches, each of the methods described has broad utility for predicting many kinds of chemical data.

EXPERIMENTAL

Retention indices (RI) were obtained from McReynolds' compilation [7]. The data matrix, on which all of the predictive calculations were based, was

[a]Present address: Department of Chemistry, University of Virginia, Charlottesville, VA 22901, U.S.A.

0003-2670/86/$03.50

chosen to include the minimum amount of data needed to span a broad range of solute and solvent properties. The data matrix for the training set consists of retention indices at 120°C for 13 solutes and 15 solvents. The prediction-set data involve 42 solutes and 24 solvents, both sets of which were selected also to incorporate a wide range of chromatographic behavior. All of the solutes and solvents, with designations, are listed in Table 1.

The methodologies of factor analysis and of multiple regression have been detailed in the monographs of Malinowski and Howery [1] and of Draper and Smith [8]. Factor analysis was performed by a modified version of the computer program FACTANAL [9] in FORTRAN-IV. Stepwise multiple regression was performed by the SAS package of programs [10]. Additional program modules for predicting data were written as needed. All computations were done on an IBM model 370/165 digital computer.

Three methods were used to predict retention indices. The first method is based on the combination step of target factor analysis; the second method, on the target testing step of target factor analysis; and the third method, on multiple regression. In each case, the data required to predict new retention indices consist solely of known retention indices. A physico-chemical model for the data is not required.

Target-combination approach

The target-combination approach involves the following procedure. First, the abstract solution for the data matrix of the training set is calculated using principal factor analysis and the correct number of factors is evaluated. Then, sets of typical vectors from the data matrix are tested in a target-combination procedure to identify the key (best) sets of typical vectors. The key combination sets are those which reproduce the data with the smallest root-mean-square (r.m.s.) error for a given number of factors. These key combination sets are particularly important in the present discussion because target-combination predictions are based on the key sets. All combinations of typical vectors were tested to find the best models. Malinowski [11] developed a short-cut method for finding key sets which gives equally useful results. Finally, the coefficient column matrix obtained for a key combination set is used to predict new retention data. Predictions are only possible when the complete set of key retention indices for a new molecule is known. Because several combination sets usually give nearly equivalent r.m.s. errors, predictions can be based on any one of these best sets with no significant loss of accuracy.

Mathematically, the target-combination approach can be summed up in two equations. First, combinations of sets of typical vectors are target-tested according to

$$\mathbf{R}_{\text{typical}}\,\mathbf{C}_{\text{typical}} = \mathbf{D}_{\text{typical}} \qquad (1)$$

In Eqn. 1, matrix $\mathbf{R}_{\text{typical}}$ is the row matrix consisting of a specified com-

TABLE 1

Solutes and stationary-phase solvents studied

Symbol	Name	Symbol	Name
Solutes in the data matrix			
1	1-butanol	8	butyl ethyl ether
2	2-methyl-1-pentanol	9	propylene oxide
3	butraaldehyde	10	ethane
4	isovaleraldehyde	11	octane
5	3-methyl-2-pentanone	12	toluene
6	propyl formate	13	*m*-diethyl benzene
7	2-methyl-2-butyl acetate		
Solvents in the data matrix			
A	Apiezon L	I	Pluronic F88
B	Carbowax 20M	J	polyphenyl ether (5 ring)
C	di-2-ethyl-hexyl sebacate	K	sucrose acetate isobutyrate
D	diisodecyl phthalate	L	TMP Tripelargonate
E	Flexol 8N8	M	tricresyl phosphate
F	Hallcomid M18	N	Triton X-305
G	Igepal CO 880	O	UCON 50-HB-2000
H	isooctyldecyl adipate		
Solutes predicted			
1P	methanol	22P	ethyl vinyl ether
2P	iso-butanol	23P	ethylene oxide
3P	3-methyl-1-pentanol	24P	furan
4P	heptanol	25P	tetrahydropyran
5P	cyclopentanol	26P	butane
6P	2-propanol	27P	tetradecane
7P	acetaldehyde	28P	cyclohexane
8P	2,2-dimethylpropanol	29P	1-pentene
9P	acrolein	30P	benzene
10P	acetone	31P	*m*-xylene
11P	2-pentanone	32P	ethylbenzene
12P	1,3-butadione	33P	*p*-dichlorobenzene
13P	cyclopentanone	34P	methylene chloride
14P	2,3-butadione	35P	carbon tetrachloride
15P	ethyl formate	36P	2-chloroethanol
16P	t-butyl acetate	37P	3-hydroxy-2-butanone
17P	allyl acetate	38P	bis-(2)-ethoxyethyl ether
18P	propyl propionate	39P	acetonyl acetate
19P	methylal	40P	trioxane
20P	isopropyl methyl formate	41P	paraldehyde
21P	isopentyl ether	42P	water
Solvents predicted			
AP	Apiezon J	MP	neopentyl glycol succinate
BP	Apiezon M	NP	Oronite NIW
CP	Carbowax 400	OP	Pluronic F68
DP	Carbowax 1000	PP	Pluronic L63
EP	dibutyl tetrachlorophthalate	QP	Pluronic L81
FP	diethylene glycol adipate	RP	Pluronic P84

TABLE 1 (*continued*)

Symbol	Name	Symbol	Name
GP	di-2-ethylhexyl adipate	SP	polyphenyl ether (6 ring)
HP	dioctyl phthalate	TP	SE 52
IP	Dow-Corning 550 Fluid	UP	sucrose octaacetate
JP	ethylene glycol sebacate	VP	Tergitol NPX
KP	Hallcomid M18 OL	WP	UCON LB 1715
LP	Kroniflex THFP	XP	Versilube F-50

bination set of typical vectors, $C_{typical}$ is the target-transformed column coefficient matrix, and $D_{typical}$ is the data matrix resulting from target combination. A key set of typical vectors is identified when the r.m.s. error between $D_{typical}$ and the original data matrix is the smallest obtained. Then, by using the coefficient matrix for a key set, new data can be calculated from

$$R_{new}\ C_{typical} = D_{predicted} \tag{2}$$

In Eqn. 2, R_{new} is a row matrix of known retention indices involving the set of new-row molecules and the key column molecules. For example, the row in R_{new} for a new-row molecule solute x consists of the retention index for solute x on the first key solvent, the retention index for solute x on the second key solvent, and so forth.

Target free-float approach

A second method of target factor analysis for predicting data involves target-testing of individual test vectors (rather than target-testing sets of vectors). Here, advantage is taken of the fact that a test vector requires a minimum of n test data points for an n-factor test. The remaining test points, said to be free-floated, are predicted from the least-squares target transformation vector. As an example, data on retention indices available for four of the original 13 solutes on a new solvent not in the original data matrix are considered. Then, a test vector can be constructed with these four known test points, the remaining nine test points being free-floated (left blank) on the test vector. Target transformation of this vector using four (or fewer) factors gives a complete predicted vector having predicted values for the nine free-floated points. However, the target free-float approach must be used with discretion. For an n-factor target test having fewer than n input test points, the procedure is impossible, for mathematical reasons. If n test points are input for n factors, the values of the input points are predicted exactly, implying a successful test and therefore accurate predictions. However, the validity of the predicted values for the free-floated points in this special case depends strongly on the molecules represented in the test points. If the test data include molecules which span the range of the properties of the complete set of test molecules, then the predicted values will probably

be trustworthy. But, if the test values represent only one of the kinds of molecules in the complete set, there is little probability that the predicted values will be worthy of consideration. If some of the free-floated values actually are known, then the reliability of the predicted values can be better gauged. The safest course in practice is to have the number of test points exceed as much as possible the number of factors. If data for a wide variety of molecules are predicted accurately, then the values for the missing points can be accepted with little hesitation.

To gain insight into the target free-float approach, the test data for the target vectors were selected in two ways. In the first set of calculations, the test molecules were chosen according to the results of the target-combination step. Three target-combination models labeled models 2, 10 and 40 (because the models produced r.m.s. errors of about 2, 10 and 40 RI units, respectively, in the target-combination step) were used to identify the test molecules. For example, if a particular set of typical vectors for three molecules gives in target-combination an r.m.s. error of say 9.9, then test data for those three molecules could be input on a test vector to evaluate the model 10 model. In the second set of calculations, three models based on chemical intuition, termed here the good, in-between and bad models, were used to pick the test molecules. Test molecules which, from chemical reasoning, are expected to span best the properties of all of the test molecules were used in the good model. Test molecules which were expected to be neither good nor bad representatives of the complete set of test molecules, were selected rather arbitrarily to form the inbetween model. The third model was deliberately chosen to be a bad model having test molecules spanning only a minor portion of the properties of the entire set of test molecules. Though different chemists would undoubtedly choose different sets of models by chemical intuition, the sets chosen here were used to demonstrate in a rough way the kinds of predictions expected for representative selections of test data.

Multiple-regression approach

The third main approach to data prediction utilizes linear multiple regression. In this technique, a vector of data (the dependent variable) is modeled with a particular set of typical vectors (the independent variables). The set of least-squares coefficients calculated for that model is then used to predict new retention indices. To illustrate this approach and to compare it with the target-combination approach, retention indices were predicted for the 42 new solutes and the 24 new solvents in Table 1. Two regression models called the "specific" model and the "global" model were explored.

In the specific-model procedure, each vector of the data matrix is modeled with all possible sets of the remaining vectors from the data matrix, n at a time. For each typical vector, the set of independent typical vectors which gives the best least-squares fit is calculated. Each specific, best model is then used to predict new data, the predictions for each model being based on a

different regression model. For example, the coefficient matrix for the best regression model for column 1 in the data matrix is used to predict additional new elements in column 1, corresponding to the set of new-row molecules. Averaging the r.m.s. errors for the predictions for each typical vector furnishes an overall r.m.s. error which serves to evaluate the usefulness of the specific regression model.

In the global-model procedure, results from the specific-model calculations are used to establish a single model to describe all of the data. Here, all of the typical vectors in a data matrix are modeled as nearly as possible by the same set of typical vectors. To identify the vectors in the global model, those vectors represented with the highest frequencies are selected after considering all of the specific regression models. For example, those four key vectors which occur the greatest number of times, summing over all of the specific models, constitute the four-factor global model. To predict with the key vectors (which cannot model themselves), a modification to the procedure is used. For each of the four vectors in the global model, the vector which occurs with the fifth highest frequency is substituted for that key vector in order to make the predictions for the key vector. The global model is not the best model for any one of the typical vectors, but rather is the most representative regression model for the entire data matrix. Thus, a global regression model is similar to, though mathematically not the same as, a key target-combination set.

RESULTS AND DISCUSSION

When the original 13 × 15 data matrix was factor-analyzed, the reproduction results summarized in Table 2 were obtained. The experimental error in the data is estimated to be within the range ±3 RI units, though a few data may have errors as large as 5 RI units. Taking into account the r.m.s. error, the percentage of reproduced data points having errors less than the upper limit of the experimental error and the largest error, Table 2 shows that use of four factors gives a reasonably good model while five factors give a definitely acceptable solution. The factor indicator function, based on Malinowski's theory of error for abstract factor analysis [12], has a broad minimum at four factors, while the real error based on the theory best approximates the experimental error for five factors. The correct factor size is considered as five, although predictions for four factors should also be acceptable.

Target-combination predictions

In Table 3 are listed for 2–5 factors the molecules represented in the key combination sets and the associated r.m.s. errors. Small numbers of key typical vectors model very accurately the training-set data matrix. In fact, the r.m.s. errors for the target-combination models are almost as small as those obtained with the least-squares principal factors (see Table 2). The

TABLE 2

Summary of reproduction step

Factors	R.m.s. error[a]	Absolute errors >5 RI units (%)	Largest error[a]	Indicator function[a]	Real error[a]
1	31.82	86.7	145.0	0.2503	36.0
2	10.84	50.8	52.4	0.1091	13.2
3	5.36	27.7	27.7	0.0683	6.8
4	2.78	8.2	12.9	0.0456	3.7
5	2.05	2.1	7.8	0.0461	2.9
6	1.46	0.0	4.4	0.0473	2.3

[a]Data are given in RI units.

TABLE 3

Key combination sets of typical vectors

No. of factors	Solutes		Solvents	
	R.m.s. error[a]	Key typical molecules[b]	R.m.s. error[a]	Key typical molecules[b]
2	12.02	6,10 or 11	11.03	C,O
3	5.86	2,9,10 or 11	5.63	C,J,O
4	2.94	1,4,10 or 11,12	3.02	A,B,E,J
5	2.32	1,4,6,10 or 11,12	2.28	A,B,F,K,M
6	1.68	1,4,6,7,10 or 11,12	1.70	A,B,D,F,M,O

[a]RI units. [b]See Table 1 for designations.

extensive nature of McReynolds' compilation [7] made it possible to test the target-combination approach for a variety of solutes and solvents. By using the key sets of solute vectors and of solvent vectors from Table 3, data for 42 new solutes and for 24 new solvents were predicted. Results are summarized in Tables 4 and 5. For models utilizing 2—5 factors, the mean value of the absolute errors, the r.m.s. error, the percentage of errors exceeding 10 RI units, and the largest error are furnished in the tables for solutes and solvents. The statistics in Table 4 apply to the complete set of 42 solutes and 24 solvents, while those in Table 5 apply to smaller sets. In order to evaluate the results realistically, predictions involving the key molecules, which from the nature of the method are predicted very accurately, are not included in the statistics. In a few cases, the exact number of which is given in the penultimate column in Table 4, experimental values were not reported by McReynolds. In a few other cases (last column of Table 4) predictions could not be made because at least one key retention index was not available. Data for water in particular and for a few other solutes were predicted with large r.m.s. errors. Results for a reduced predictor set are tabulated in Table 5. Molecules which in the full-set study (Table 4) gave the largest

TABLE 4

Summary of predictions for the full set using the target-combination approach

No. of factors	Mean absolute error[a]	R.m.s. error[a]	Absolute errors >10 RI unit (%)	Largest error[a]	Missing values[b]	No. of omitted molecules[c]
Predictions for 42 new solutes[d]						
2	12.8	18.9	42.2	140	9	1
3	9.3	14.3	33.3	158	9	1
4	6.7	10.2	21.0	62	4	3
5	6.0	9.4	15.9	58	8	1
Predictions for 24 new solvents[d]						
2	12.1	19.9	40.2	99	2	0
3	7.3	9.9	33.2	28	0	2
4	5.6	8.0	17.1	27	2	0
5	4.8	6.5	12.5	18	1	3

[a]RI units. [b]Experimental values for retention indices not available. [c]Predictions not possible (at least one key value not available). [d]Predictions of key test data not included in calculations.

TABLE 5

Summary of predictions for the reduced set using the target-combination approach

No. of factors	No. of molecules[a]	Mean absolute error[b]	R.m.s. error[b]	Absolute error >10 RI unit (%)	Largest error[b]	Missing values[c]
Predictions for new solutes[d]						
2	31	10.6	14.1	38.7	48	5
3	36	7.7	10.2	28.8	34	8
4	38	5.2	6.8	14.3	28	6
5	37	4.7	6.4	10.8	26	8
Predictions for new solvents[d]						
2	17	8.6	12.4	32.6	42	1
3	20	6.2	8.3	26.7	28	0
4	21	5.1	7.2	14.8	26	2
5	24	4.8	6.5	12.5	18	1

[a]Molecules having excessively large errors are deleted (see text and Table 4). [b]RI units. [c]Experimental values for retention indices not available. [d]Predictions of key data not included in calculations.

r.m.s. errors (typically greater than 10 RI units) were excluded from the calculations. The number of molecules studied in each case is given in the second column of Table 5. Typically, the molecules deleted are those such as water which has properties not completely spanned by the molecules in the original data matrix. Comparison of the associated r.m.s. errors in Tables 4

and 5 shows, as expected, that predictions for the reduced set are considerably better.

The results in the two tables indicate that retention indices for a wide range of solute and solvent types can be predicted to better than 1% even with a three-factor model. Predictions with a five-factor model are only slightly better than those with a four-factor model. The number of typical vectors used for predictions depends on the accuracy desired and the quantity of data available. The greater the number of typical vectors used, the more accurate will be the predictions. However, the quantity of key data required increases directly with an increase in the number of factors, imposing practical limitations. Considering the diversity of properties of the molecules in the predictor set, the target-combination approach appears to be a useful predictive method.

Starting with relatively small matrices of known data, large amounts of data can be predicted stepwise using target combination. For example, if the training-set data matrix has r rows and c columns, then in the first step, data for expanded portions of the matrix involving $c1$ new columns and the original r rows and involving $r1$ new rows and the original c columns can be predicted by using Eqn. 2. Then, data for the remainder of the expanded matrix, involving the $r1$ rows and the $c1$ columns, can be predicted by using either set of data calculated in the first step. The entire process can be repeated starting with the now-complete expanded matrix as the training-set matrix to predict matrices involving a new set of $r2$ additional rows and $c2$ additional columns, and so forth. If the new molecules are similar to the molecules in the original training-set matrix, the stepwise approach can be utilized for large-scale predictions.

Target free-float predictions

Four examples of target tests for prediction using the target free-float approach are given in Table 6. The experimental values of the retention indices for the 13 solutes on a solvent, dioctyl phthalate, are shown in the second column of the table. For each test, the molecules for which test values were input are indicated by asterisks on the predicted vectors. Test molecules for the first two tests were selected according to key sets from the target-combination results. Input values for the last two tests were selected more arbitrarily by chemical intuition. Each test was run for four factors. The first test, having test molecules indicated by a combination set with r.m.s. error of about 2, gives perfect predictions for the test data because the number of test points equals the number of factors. In addition, the free-floated points are predicted quite accurately. The second test, involving another combination set with r.m.s. error of about 2, but with an added test value, predicted all five test points fairly accurately (though not precisely), lending credence to the predictions of the remaining points. In the last two examples, the number of test points equals the number of factors so that the test values are predicted exactly. However, the free-floated points

TABLE 6

Details of four target free-float tests for predicting retention indices on dioctyl phthalate, using four factors

Solute[a]	I[b]	Predicted vectors (RI units)[c]			
		TC(2)	TC(2)	CI(g)	CI(i)
1	782	782.0*	781.9*	776.4	782.0*
2	956	958.4	957.9	956.0*	976.9
3	683	680.8	679.0	678.5	683.0*
4	747	747.0*	746.6*	747.0*	760.5
5	842	844.5	842.0	845.5	863.9
6	693	696.7	696.0*	692.8	693.0*
7	854	857.0	855.0	859.5	884.8
8	718	720.3	719.7	724.8	755.9
9	558	563.1	563.1	558.0*	550.7
10	200	200.0*	200.2	202.5	216.4
11	800	800.0	800.8*	810.0	865.5
12	860	854.3	859.1*	850.2	860.0*
13	1132	1132.0*	1135.9	1132.0*	1160.9

[a]See Table 1 for designations. [b]Experimental value of the retention index for the solute on dioctyl phthalate [7]. [c]All points on the test vectors, except those for the starred (*) solutes, were free-floated. Models to select test molecules were TC(2), a target-combination set with r.m.s. error of 2, and CI(g) and CI(i), good and inbetween chemical-intuition sets, respectively.

are predicted more accurately when the test molecules are selected from a good-model intuition set (third example) than when an inbetween-model intuition set is used (fourth example).

Many target tests of the type shown in Table 6 were done. Some of the results from the target free-float approach are summarized in Table 7. For three and four factors using both n and $n+1$ test points, the six ways of selecting test points (the 2, 10 and 40 models from combination-based sets, and the good, inbetween and bad models from intuition-based sets) are compared for predictive capabilities. The average of the r.m.s. errors for predicting the retention indices of nine representative new solutes and of six representative new solvents are given in the table. Predictions from the 2 model are usually better than those from the good model, as expected. Comparing the combination-based results, the reliability of predictions becomes progressively poorer when the 10 model and the 40 model are used. The r.m.s. error for a specified combination set is a useful qualitative indicator of the validity of predictions using that set of molecules for target free-float predictions. Comparing the intuition-based results, the predictions usually become poorer when the inbetween model and bad models are used, though several exceptions were obtained for the particular sets used here. For example, results for the four-factor, five-point inbetween model for solvents gave quite accurate predictions. Adding an additional test point to

TABLE 7

Summary of r.m.s. errors (RI units) in predictions by the target free-float approach

No. of factors	No. of test points	R.m.s. errors[a]					
		By target combination			By chemical intuition		
		Model[b]	Solutes	Solvents	Model[c]	Solutes	Solvents
3	4	2	10.4	14.8	g	17.3	10.0
4	4	2	7.4	6.8	g	33.4	8.4
4	5	2	6.9	5.5	g	7.7	5.4
3	4	10	16.4	18.5	i	53.5	23.6
4	4	10	21.9	34.8	i	258.2	37.8
4	5	10	13.8	11.2	i	16.4	6.5
3	4	40	24.2	58.6	b	11.4	37.6
4	4	40	87.9	1258	b	59.0	4527
4	5	40	30.9	18.5	b	54.9	39.5

[a]Average of the r.m.s. errors for nine solutes (1P, 5P, 9P, 11P, 15P, 20P, 28P, 30P and 33P in Table 1) and six solvents (AP, DP, HP, PP, TP and UP in Table 1). [b]R.m.s. error for combination set used to select test molecules. [c]Chemical-intuition set used to select test molecules: g, good; i, inbetween; b, bad.

the four-factor tests generally improved the predictions, especially for the intuition-based sets. Increasing the factor size from three to four does not necessarily improve the predictions. For example, the four-factor, five-point predictions are poorer in three of the four cases than the three-factor, four-point predictions when the 40 model and the bad models are used.

The target free-float approach is closely related to the target-combination approach. In fact, if the molecules represented in a target test and in a target-combination set are exactly the same, then the predicted values using the two approaches are identical. Thus, the target free-float method for this special case serves as a simpler alternative to the target-combination approach. The r.m.s. error for a specified combination set furnishes a measure of the validity of predictions, information not obtainable from the corresponding target test.

Multiple-regression predictions

Some results from the predictions of retention indices using both the specific regression model and the global regression model are shown in Table 8. The average of the r.m.s. errors over all of the predicted data vectors and the largest error are listed for solutes and for solvents using two- and four-factor regression models. The specific model, as expected, is considerably more accurate than the global model, especially for the solvents. In three of the four cases in the table, the error is reduced somewhat when a four-factor model is used. With the solvent-specific model, the two-factor solution is slightly better than the four-factor model. Comparison of the r.m.s. errors in prediction for target combination (Table 4) and for multiple

TABLE 8

Summary of predictions using two multiple-regression approaches

No. of factors	Specific model		Global model		
	R.m.s. error[a]	Largest error[a]	R.m.s. error[a]	Largest error[a]	Key molecules[b]
Predictions for 42 new solutes					
2	12.8	108	23.5	125	E,N
4	10.3	67.6	16.5	109	A,F,G,K
Predictions for 24 new solvents					
2	6.4	23.9	22.4	102	7,10
4	7.8	27.4	15.5	100	1,4,7,10

[a]RI units. [b]See Table 1 for designations.

regression (Table 8) shows that the global model gives the least accurate predictions. For two factors, the specific regression model overall is considerably more accurate than the target-combination model, yet for four factors the two approaches give essentially equivalent predictions. The target-combination approach and the specific multiple-regression approach appear to be of similar utility when more accurate predictions are required.

The key molecules identified by target combination and by multiple regression are satisfyingly similar. Five of the 12 key molecules listed for the global regression model (right-hand column of Table 8) are also identified as key molecules in target combination (2- and 4-factor models in Table 3). Another three pairs of key molecules involve compounds with similar chemistry. The key sets listed in the tables are not unique, because many other sets model the data almost as well as the key sets. Data for a particular key molecule can usually be replaced with data for a molecule of similar structure without risking significant loss of predictive accuracy [2]. Such redundancy of data is consistent in most cases with chemical knowledge, though the mathematical methods sometimes indicate unexpected equivalencies of data vectors.

This work was supported in part by a PSC-BHE grant from the Faculty Research Award Program of The City University of New York. We also appreciate the use of the facilities of the Computer Center of C.U.N.Y.

REFERENCES

1 E. R. Malinowski and D. G. Howery, Factor Analysis in Chemistry, Wiley, New York, 1980, Chap. 9.
2 R. B. Selzer and D. G. Howery, J. Chromatogr., 115 (1975) 139.
3 G. Dahlmann, H. J. K. Koser and H. H. Oelert, J. Chromatogr. Sci., 17 (1979) 307.
4 R. F. Hirsch, R. J. Gaydosh and J. R. Chretian, Anal. Chem., 52 (1980) 723.

5 P. H. Weiner and D. G. Howery, Anal. Chem., 44 (1972) 1189.
6 D. G. Howery, in B. R. Kowalski (Ed.), Chemometrics: Theory and Applications, ACS Symp. Ser. 52, American Chemistry Society, Washington, DC, 1977, p. 73.
7 W. O. McReynolds, Gas Chromatographic Retention Data, Preston Technical Abstracts, Niles, IL, 1966.
8 N. R. Draper and H. Smith, Applied Regression Analysis, 2nd edn., Wiley, New York, 1981.
9 E. R. Malinowski, D. G. Howery, P. H. Weiner, J. M. Soroka, P. T. Funke, R. B. Selzer and A. Levinstone, FACTANAL, Program 320, Quantum Chemistry Program Exchange, Indiana University, Bloomington, IN, 1976.
10 A. J. Barr, J. H. Goodnight, J. P. Sall and J. T. Hewig, Statistical Analysis System, Statistical Analysis System Institute, Raleigh, NC, 1976.
11 E. R. Malinowski, Anal. Chim. Acta, 134 (1982) 129.
12 E. R. Malinowski, Anal. Chem., 49 (1977) 612.

Analytica Chimica Acta, 189 (1986) 353—363
Elsevier Science Publishers B.V., Amsterdam — Printed in The Netherlands

ERROR-FREE STORAGE COMPRESSION OF BINARY-CODED INFRARED SPECTRA

M. J. ADAMS* and I. BLACK

Department of Spectrochemistry, The Macaulay Institute for Soil Research, Craigiebuckler, Aberdeen AB9 2QJ (Great Britain)

(Received 4th December 1985)

SUMMARY

Microcomputer systems are increasingly being used to acquire and store digital spectral data, and computerised data bases and spectral libraries are valuable in the identification of sample spectra. Access to the original recorded data is essential, so problems of storing large volumes of spectral data arise. To alleviate such problems partly, error-free data-compression schemes based on Huffman shift coding are tested on infrared spectra. The results indicate that substantial savings, up to 70%, of the digital memory requirements can be achieved by using error-free coding techniques. Part of this saving is attributed to data compression of oversampled regions of digitised spectra. Compressed spectral data can not only be stored more efficiently but also provide increased data-transfer rates between computer systems.

In recent years, there has been a dramatic increase in the use of microprocessors and microcomputers in spectrometric laboratories, mainly for instrument control, data recording and processing, usually with dedicated computer/spectrometer systems. There has also been an increasing awareness and use of computer networks and data bases for the storage of spectral data [1]. With the decreasing cost of computer memory units and the increasing sophistication of microcomputer operating systems, this computerised storage and inter-computer transfer of spectral data will certainly increase. In spectroscopy laboratories, there is often a demand for a system of storing spectral data which allows efficient use of available computer memory and fast access and data-transfer rates. For example, in mass spectrometry and infrared spectrometry, several schemes have been proposed that reduce the data to a file of binary values indicating the presence or absence of a component in a pre-defined region. Such techniques produce peak "hit" lists which can provide a useful data base for sample identification by pattern recognition methods [2, 3]. Where large amounts of data are produced for reference and archival storage, it may be required that no information be lost in storage, i.e. the spectrum as originally recorded, including any noise, be saved. Large amounts of computer storage media can then quickly be filled and sophisticated management systems are required to manipulate the large library of data.

0003-2670/86/$03.50

In this laboratory, various data-compression algorithms have been examined in attempts to achieve increased storage efficiency. The results obtained with an error-free compression scheme as applied to a series of infrared spectra are reported below. Error-free compression of data is based on the premise that not all the possible digital levels in a recorded spectrum occur equally often, and that an overall compression in required memory space can be achieved by assigning shorter binary code words to the more frequently occurring values. Most data-compression techniques were originally developed for the bandwidth compression of video signals and have since been successfully applied to the processing of digital imagery and can be effectively used to store spectral data.

DATA RECORDING AND STORAGE

The steps involved in digital recording of a spectrum have been discussed by many authors. Willson and Edwards [4], in their review of sampling and smoothing of spectra, recommended a procedure which ensures efficient data recording without aliasing. In general, to achieve the recording resolution necessary to reproduce faithfully any fine structure present in the original spectrum, large parts of the spectrum will be oversampled. It is the effect of this that can be reduced by error-free compression.

The computerised spectrometer in this infrared laboratory has been described elsewhere [5]. Briefly, the system consists of a type 580B spectrometer (Perkin-Elmer) interfaced to an Apple microcomputer via a serial RS232C interface. The computer has 48K RAM, twin disk drives (140K capacity each) and a serial link to a Data General Eclipse computer for the bulk storage of recorded spectra. Infrared spectra are recorded at a spectral resolution of, typically, 2 cm^{-1} in the range 4000--2000 cm^{-1} and a resolution of 1 cm^{-1} in the range 2000—180 cm^{-1}. Thus a spectrum is described by 2821 data points on a 0—2000 transmission scale, i.e., 11-bit resolution. Whilst many such spectral recordings can be stored on floppy disk media for immediate access by laboratory staff, the inefficient storage techniques used by microcomputer systems soon make this system unworkable and recourse to a larger, bulk storage device is required. In the present case, this is achieved with the aid of the Apple—Eclipse link.

Most microcomputer users apply BASIC as the computer language to develop data-logging and manipulation programs. This language is usually interpreted by the computer and exhibits slow program execution rates compared with the higher, usually compiled, languages of PASCAL and FORTRAN. Saving a numeric array of integer values, (e.g., a spectrum) on disks can take a long time when the usual disk operating system and nested loops within BASIC programs are used. Reading such files is similarly slow. Integers are generally stored as 16-bit (two-byte) words within a microcomputer and as ASCII data, one character per byte, in disk-based text files. Thus, a 2821-point spectrum of 11-bit values occupies in excess of

5.5 kbytes of RAM within the computer and more than 14 kbytes of disk storage. A single floppy disk in an Apple system can, therefore, store about nine such sequential-access BASIC text files. If the data are transferred between the computer and disk unit as a binary file, easily accomplished from BASIC and the disk operating system, then the 5.5 kbytes of RAM per spectrum is mirrored in the same amount of disk storage and about 20 spectra can be saved on a single disk. Further savings can be made by storing each data point not as a two-byte integer but as a fractional byte word of fixed bit length. The transmission values of the infrared spectra discussed here are scaled in the range 0—2000 and can be represented by 11 bits. Storing the blocks of 11-bit data values sequentially in memory can achieve a 30% reduction in memory requirements and a spectrum will occupy less than 4 kbytes of memory. To achieve even greater savings in computer memory, more sophisticated compression techniques must be applied. Sequential fractional-byte storage can still be used but with variable word length dependent on the probability of occurrence of each value.

If the probability of each of the N possible digital values or levels, i, is given by P_i, then an entropy value, H, can be associated with these levels and is given by

$$H = -\sum_{i=1}^{N} P_i \log_2 P_i \tag{1}$$

and, if the data sample points are independent of each other, then H bits represents the lower limit of the average length of the binary code words used to describe the spectrum.

If binary code words of equal length are assigned to the spectral data with N possible values then the code word size, R_0, for each sample point is given, from Eqn. 1, by

$$R_0 = \log_2 N \text{ bits} \tag{2}$$

It is the aim of error-free compression schemes to reduce the average length, R_1, of the binary code words, from R_0 bits to that given by the limit H.

The implementation of an error-free data-compression scheme requires two fundamental steps. First, a new spectral form or representation is generated from the original recorded data so that an individual element, or data point, is less correlated to adjacent elements and, secondly, that each element be assigned a binary code word. This code word is given by the probability of occurrence of the value of the element. One such technique which specifies this assignment of code words with unequal length was developed by Huffman [6].

IMPLEMENTATION OF THE HUFFMAN COMPRESSION SCHEME

The first requirement for error-free data compression is to derive from the original data a less self-correlated spectrum. The method applied must be exactly reversible, i.e., the original data must be obtainable from the new spectrum without error. One simple means of achieving lower correlation is accomplished by subtracting each spectral value from its predecessor in the original spectrum. That this technique indeed produces point values less dependent upon each other than the original data can be illustrated with the aid of a correlation diagram.

Figure 1 illustrates infrared spectra of samples from a test set used to evaluate the efficiency of error-free data-compression. All spectra were recorded from solid samples, prepared as KBr disks, or as films dried down from suspensions, at the spectral resolution discussed above, providing 2821-point data arrays of 11-bit transmission values. Figure 1(a) is of iron 8-quinolinolate and Fig. 1(c) of a synthetic iron phosphate. For the purpose of this discussion, Fig. 1(a) may be considered an intense spectrum typical of an organic crystalline sample and Fig. 1(c) as typical of a less well characterised inorganic mineral exhibiting diffuse broad-band spectral features. Figures 1(b) and (d) are the corresponding point-difference data. These derived spectra exhibit the distinctive characteristics of first-derivative data, i.e., zero-crossing points corresponding to maxima and minima in the original data and a dramatic increase in the apparent noise. The correlation diagrams are obtained by plotting the value of each point, or element, against its predecessor and are shown in Fig. 2 for the two test spectra. Elongation along the diagonal through the first and third quadrants implies a tendency for high values to follow high and low values to follow low. Bracewell [7] discussed this interdependence between sequential data and described the quantitative evaluation of a correlation coefficient. He suggested, for simplicity, that the correlation diagram be divided into quadrants,

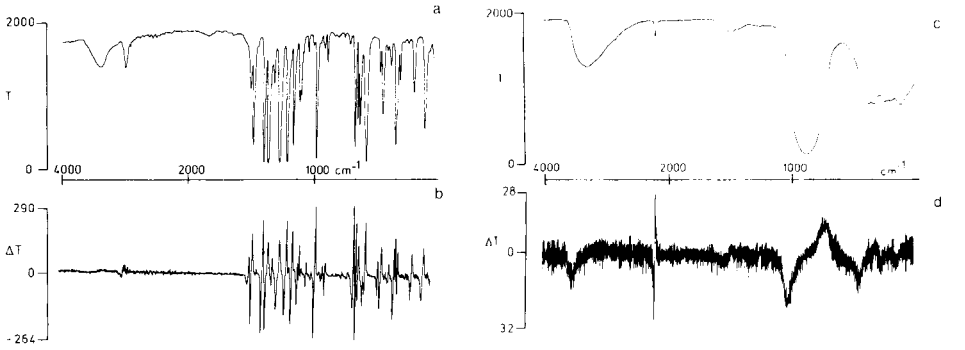

Fig. 1. The infrared spectra of (a) iron 8-quinolinolate and (c) a synthetic iron phosphate. Both spectra were recorded from KBr disk samples. The corresponding point-difference first-derivative spectra are illustrated in (b) and (d).

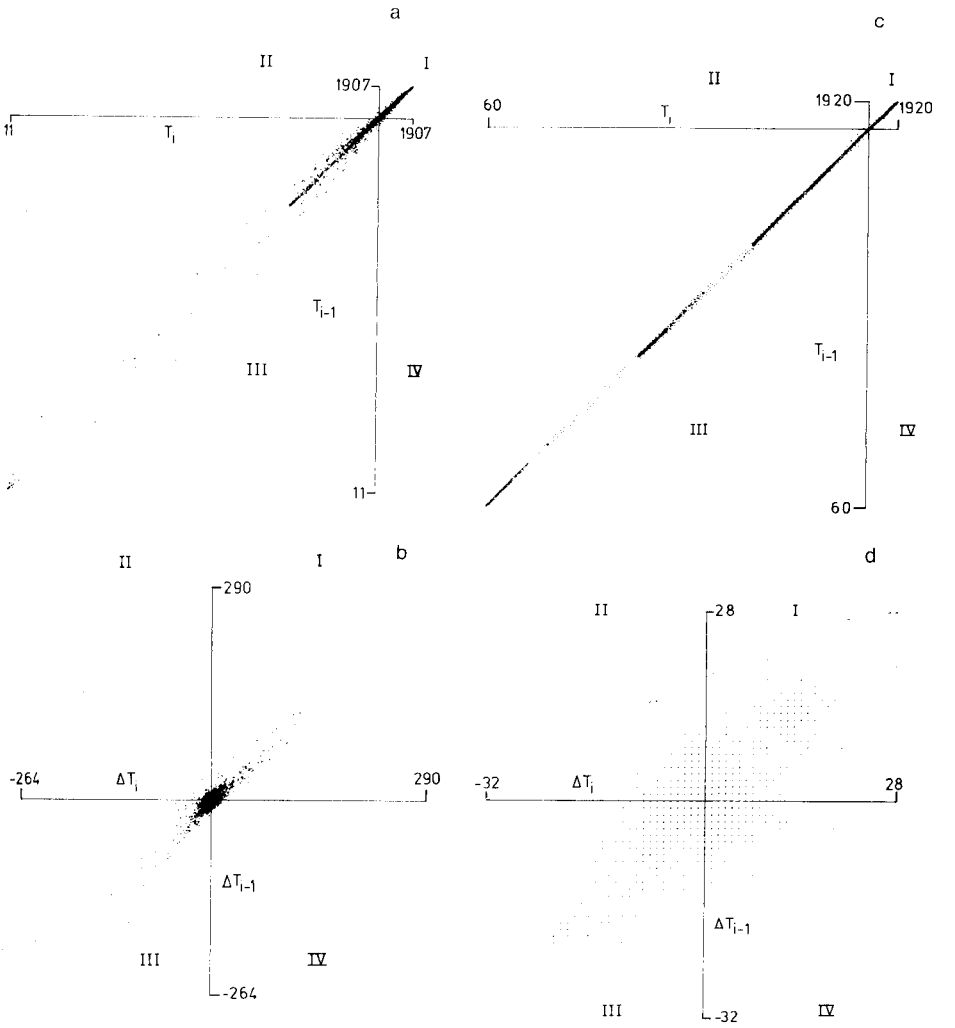

Fig. 2. Correlation diagrams for the original spectral data of the 8-quinolinolate (a) and iron phosphate (c) and for the first-derivative data, (b) and (d).

meeting at the median point, and counting the number of data points in each quadrant. To obtain the correlation coefficient, the difference between the number of data points in the first and third quadrants and those in the second and fourth is divided by the total number of points. For the 8-quinolinolate spectra, this value is 0.97 for the original data and 0.40 for the derivative. The corresponding values for the iron phosphate spectra are 0.99 and 0.15, respectively. The lower correlation of the derivative data is apparent from the diagrams.

Following the representation of the original data by the point-difference, or derivative, spectrum, the next step is the assignment of a binary code word to each possible value. To achieve a reduction in the average length of

code word, this assignment should be related to the entropy or frequency of occurrence of the derivative values. Rosenfeld and Kak [8] presented an excellent account of the technique of Huffman code-word selection and assignment. The scheme derives from the probability distribution of the data. The frequency distribution diagrams for the test spectra are shown in Fig. 3 and are related to the correlation diagrams, in that they can be considered as projections of the correlation data on to a single, point value axis. From these distribution data, a binary tree is constructed, the roots of which are the data-point values. An algorithm for the scheme is given in Fig. 4 and the formation of a typical binary tree in Fig. 5. The Huffman code is derived from the node path through the tree. The formation of such a tree, and subsequent analysis for code-word assignment and decoding is implemented easily in machine code in a microcomputer system. It can be appreciated from Fig. 5 that a string of binary digits can be decoded in only one way, i.e., a Huffman code is a uniquely decodable code. To decode compressed data, the bit stream is examined from the most significant bit until a root value is reached.

The major disadvantage of Huffman coding is the number of code words required. For a spectrum recorded at 11-bit resolution, the original data can have 2048 levels and the less correlated derivative data can have 4096 values. Using the algorithm in Fig. 4 to generate the code words produces a very large binary tree of $2N - 1$ nodes, where N is the number of levels. Furthermore, the code words corresponding to the infrequent values will be very long. These large code words can be avoided if the scheme is modified to use Huffman shift codes. The use of shift codes to mark low probability

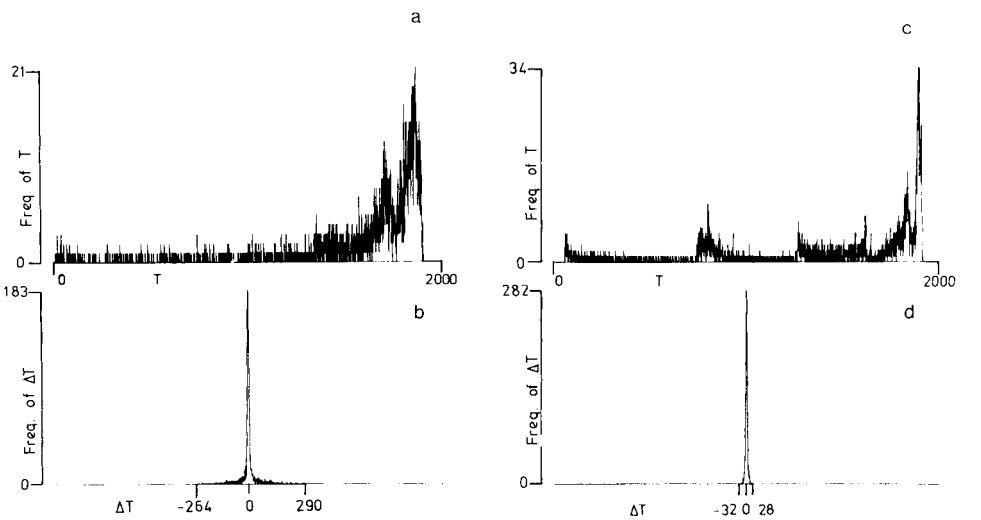

Fig. 3. Population distribution for the original spectral data of the 8-quinolinolate (a) and iron phosphate (c) and for the first-derivative data, (b) and (d).

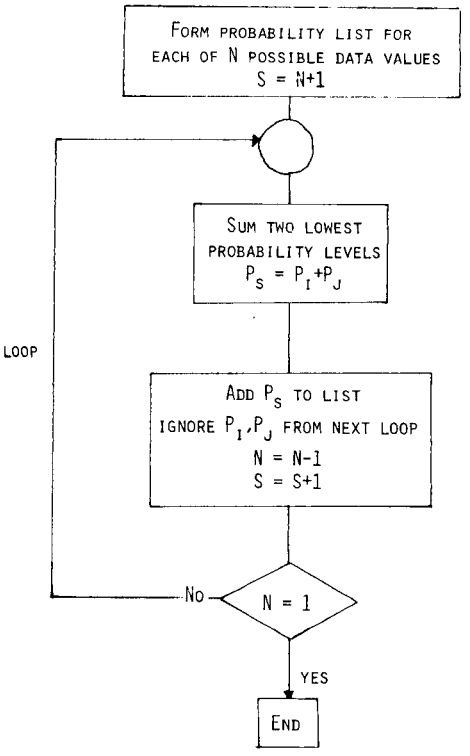

Fig. 4. An algorithm for the production of the binary tree from probability data.

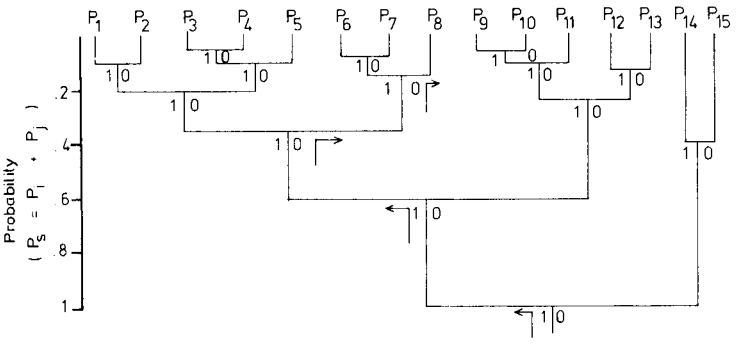

Fig. 5. A binary tree derived from the spectral data for the 9-quinolinolate derivative using thirteen values and two shift codes.

data considerably simplifies the binary tree diagram and in most cases has only a small adverse effect on the degree of compression achieved. The generation and use of the shift codes may be appreciated with reference to Fig. 6. The population distribution data from Fig. 3(b,d) containing $N = 4096$ possible levels, was divided into a number of intervals with each interval containing, in this case, 13 source symbols or codes. Outside the central interval, all remaining probabilities are summed to form two new levels, designated as the shift-up and the shift-down values. By using the algorithm from Fig. 4, the Huffman codes for the, now, fifteen levels can be computed, with the first symbol serving as the shift-down word and the fifteenth as shift-up word. This much simplified tree is illustrated in Fig. 5 for the 8-quinolinolate spectrum, with the Huffman codes in Table 1.

Rosenfeld and Kak [8] gave a detailed description of the functions and use of the shift-codes. For a data value contained within the central interval, a Huffman code is assigned, or decoded, in the normal way and the presence of the shift codes is ignored. Outside the main interval, however, e.g., for the ith symbol in the jth interval to the right of the central interval, this is coded by j repetitions of the shift-up code word followed by the code word for the ith symbol. For values to the left of the main interval, the shift-down

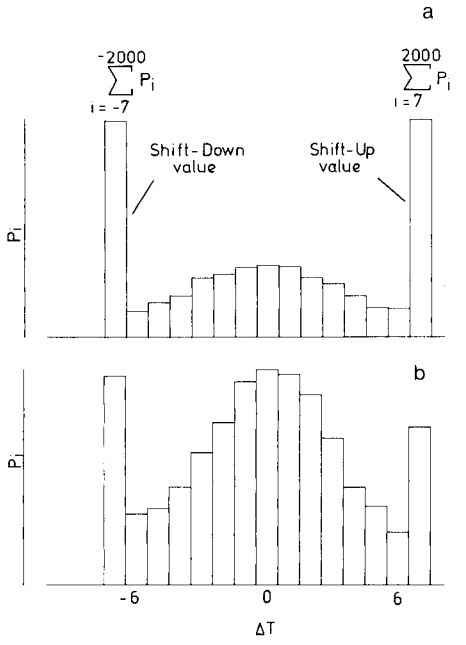

Fig. 6. The probability, P_i, histogram of the derivative data is divided into intervals, here containing thirteen values. All values outside the main interval are summed to form two new levels, the shift-up and shift-down values. The data illustrated are for (a) the 8-quinolinolate and (b) the iron phosphate.

TABLE 1

The formation and reading of Huffman codes for a 15-level population distribution of difference data[a]

Level No.	Diff. data (ΔT)		Probability	Huffman
1	2		0.05	11111
2	−3		0.05	11110
3	5		0.03	111011
4	−6		0.02	111010
5	3		0.05	11100
6	4		0.04	11011
7	−4		0.04	11010
8	1		0.07	1100
9	−5		0.03	10111
10	6		0.03	10110
11	−2		0.05	1010
12	0		0.07	1001
13	−1		0.06	1000
14	<−6	{UP} Shift	0.20	01
15	>+6	{DOWN} Levels	0.20	00

[a]To assign a Huffman code to a ΔT value, the appropriate bit pattern is derived by traversing the binary probability tree; e.g., see Fig. 5, for $\Delta T = 1$, the code is 1100.

To read a pattern code, the binary tree is traversed in reverse until a root value is reached. Thus, 10111101011011011011 gives ΔT values of −5, −2, 4, UP(13), −2, i.e. −5, −2, 4, 11.

code word is used. The number of intervals into which the spectral data is divided and, hence, the number of source symbols or codes within an interval is chosen by the user and is a compromise between ease of operation and relative compression efficiency. Few intervals with a large number of code words produce a large binary code tree but minimise the use of shift words and can approach the true minimum average length of code word. More intervals with fewer code words considerably simplify the binary tree but excessive use of shift codes can reduce data-compression efficiency. This effect can be illustrated by compressing spectral data using the shift code scheme with several values for the number of code words and evaluating the average length of code word used, R_1. From the population data for the derivative-signal levels used to construct Fig. 3(b,d), signal-level probability tables can be constructed and, with the aid of Eqn. 1, the minimum average length of code word, H, for the spectrum can be computed. The relative compression efficiency $[(R_0 - R_1)/(R_0 - H), R_0 = 11]$ of the shift coding technique as a function of number of source symbols within an interval is shown in Fig. 7. For a series of test spectra the values for H and R_1 using 15 source symbols are presented in Table 2.

The use of shift codes considerably simplifies the construction and use of

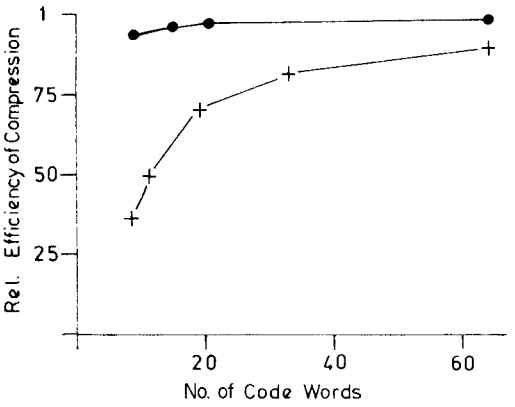

Fig. 7. The relative compression efficiency using shift coding as a function of the number of source values within an interval: (+) the 8-quinolinolate; (●) the iron phosphate.

TABLE 2

The average minimum number (H) of bits per point for a variety of derivative test spectra. The results using 15 symbol Huffman shift coding, $R1$, and fixed-length, 4-bit, coding with shift values, $R1^1$, are also presented. Samples 1 and 2 refer to the iron 8-quinolinolate and iron phosphate, respectively. The other samples were selected to provide a wide range of spectral types

No.	H	$R1(15)$	$R1^1(15)$	No.	H	$R1(15)$	$R1^1(15)$
1	6.0	7.7	9.9	6	3.8	4.0	4.4
2	4.4	4.6	4.7	7	4.0	4.2	4.5
3	4.9	5.1	5.4	8	3.9	4.1	4.3
4	3.5	3.5	4.1	9	4.3	4.7	4.9
5	4.1	4.7	5.1				

the binary tree for code-word assignment and data decoding. However, in the present scheme, each binary tree can be considered unique in belonging to a single spectrum, being derived from the frequency distribution of the derivative data. Thus, each compressed spectrum should be stored with its binary tree for decoding. It is of interest, therefore, to consider coding all spectral data by using a single binary tree. Several idealised binary-tree structures could be proposed and used for coding data, including, e.g., a Gaussian population distribution of the derivative data. One of the simplest schemes of code assignment, however, need not involve the computer storage of any binary tree but is based on a fixed code length with shift codes to describe less commonly occurring data values. This is equivalent to using a box-car, or square-wave, population distribution diagram. From the results for R_1 given in Table 2, it is evident that for most of the test spectra the original 11-bit data can be compressed to 4 or 5 bits. As a 4-bit, fixed-length code assignment is particularly easy to implement with 8-bit logic systems

and will provide for up to 16 different code words, the efficiency of using this scheme was examined. The results, $R1^1$, for fifteen 4-bit code words are given in Table 2 and can be compared with the predicted minimum code-word lengths and those using conventional Huffman shift codes. Although inferior to the Huffman code results, for most of the test spectra, a compression factor of more than two is achieved compared with the original 11-bit data.

CONCLUSION

A spectrometric data bank consists of a computer-readable collection of data and of a set of programs for management and retrieval of the data. For a good data bank, the full original spectra must be available to the user. With a typical recording system requiring more than 30000 bits per infrared spectrum, it is obvious that data-storage space and storage and retrieval times can rapidly outgrow all but the largest of laboratory computers. In such cases, it becomes necessary to consider the use of more efficient storage techniques than the conventional fixed bit-length storage associated with analog-to-digital conversion schemes. One method examined here is the use of Huffman shift coding. With this technique, a data point is stored not as its digital value but as a code word, the length of which is determined by the probability of occurrence of the data point (or its derivative). With a series of infrared test spectra, all recorded under identical instrumental conditions, the Huffman coding scheme provided some dramatic savings in computer storage. These savings can be attributed to a reduction in the effects of over-sampling regions of spectra between intense peaks.

The experimental system described above is based on an Apple micro-computer system and an Eclipse computer for data storage. With BASIC programs, only about nine spectra can be stored as text files per floppy disk. The use of Huffman shift coding can increase this to sixty or seventy per disk of typical inorganic mineral spectra. This increased efficiency of data storage not only reduces the need for back-up storage facilities for the Eclipse computer but also greatly increases the rate of access to the library of recorded spectra in the data bank.

REFERENCES

1 K. Maeda, Y. Koyama, K. Sato and S. Sasaki, Anal. Chim. Acta, 133 (1981) 561.
2 F. H. Heite, P. F. Dupuis, H. A. Van T'Klooster and A. Dijkstra, Anal. Chim. Acta, 103 (1978) 313.
3 J. Kwiatkowski and W. Riepe, Anal. Chim. Acta, 135 (1982) 285, 293.
4 P. D. Willson and T. H. Edwards, Appl. Spectrosc. Rev., 12 (1976) 1.
5 M. J. Adams and I. Black, J. Auto. Chem., 5 (1983) 9.
6 D. A. Huffman, Proc. IRE, 40 (1952) 1098.
7 R. Bracewell, The Fourier Transform and its Applications, McGraw-Hill, New York, 1965.
8 A. Rosenfeld and A. C. Kak, Digital Picture Processing, Academic Press, New York, 2nd edn. Vol. 1, 1982.

Analytica Chimica Acta, 189 (1986) 365—369
Elsevier Science Publishers B.V., Amsterdam – Printed in The Netherlands

Short Communication

REFLECTOMETRIC STUDY OF THE ACID—BASE EQUILIBRIA OF INDICATORS IMMOBILISED ON A STYRENE/DIVINYLBENZENE COPOLYMER

RAMAIER NARAYANASWAMY* and FORTUNATO SEVILLA III

Department of Instrumentation and Analytical Science, UMIST, P.O. Box 88, Manchester M60 1QD (Great Britain)

(Received 10th June 1986)

Summary. Reflectance was measured through optical fibres at different pH values for three acid—base indicators immobilised on Amberlite XAD-2 resin. The variation of reflectance with pH suggested the existence of simultaneous equilibria involving dissociation and adsorption. Acidity constants were determined through Kubelka-Munk functions. The results indicate that adsorption of the indicator on a nonpolar surface represses the dissociation of the solute.

Indicators immobilised on hydrophobic polymer supports have been utilised in the development of optical-fibre pH-sensing devices and have been noted to exhibit acid—base properties that are different from those in aqueous solutions [1]. In this communication, the acid—base equilibria of some indicators immobilised on XAD-2, a styrene/divinylbenzene copolymer, are further examined through a reflectance technique involving optical fibres. The effect of immobilisation on the behaviour of the indicators is also discussed. The effect of the ionisation of the solute on its retention on a nonpolar surface has already been demonstrated [2—4], but the effect of adsorption on the ionisation has not been considered previously.

Experimental

Indicators were chosen such that they could be immobilised on Amberlite XAD-2 resin and that their visible spectra exhibited distinct absorption peaks for the neutral and the ionised form. The indicators studied were bromophenol blue (BPB), bromothymol blue (BTB) and 2,6-dichlorophenolindophenol (DIP). These indicators were immobilised by procedures described earlier [1, 5].

Buffer solutions were prepared from a solution which was 0.1 M in potassium dihydrogenphosphate, 0.025 M in sodium tetraborate and 1.0 M in sodium chloride. The pH of the solution was adjusted to the appropriate value with 1 M hydrochloric acid or sodium hydroxide.

Reflectance spectra were obtained by using a system which featured a bifurcated optical fibre and a flow-cell arrangement [5]. The immobilised

0003-2670/86/$03.50

indicator was contained in a flow cell through which the buffer solution was continuously circulated. Spectra were measured at different pH values.

Discussion

Reflectance spectra. A well-defined isosbestic point was observed in the reflectance spectra of the indicators investigated (illustrated in Fig. 1 for DIP). The occurrence of this point suggests that the equilibrium involves only two absorbing species, i.e., the undissociated indicator, HIn, and its anion, In^-. For the spectra shown in Fig. 1, the isosbestic point appears at 530 nm, and the changes in reflectance at 460 nm and 660 nm can be attri-

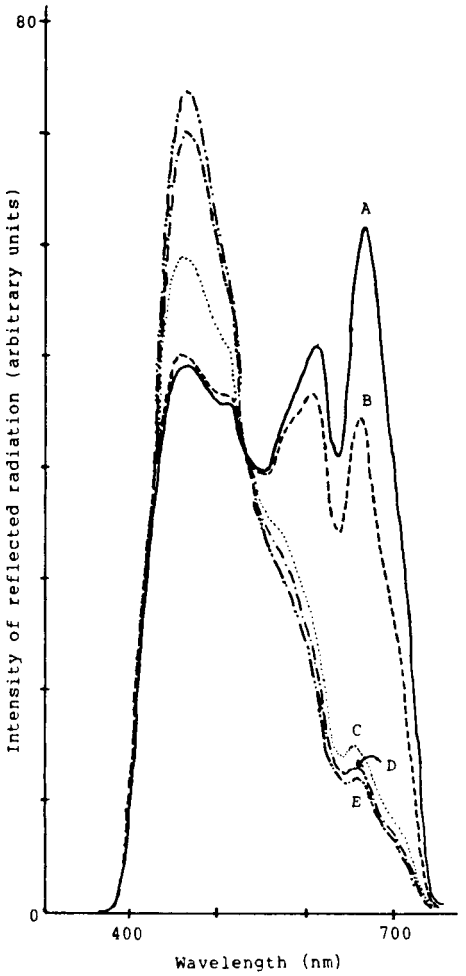

Fig. 1. Reflectance spectra of immobilised DIP at different pH values: (A) pH 4; (B) pH 6; (C) pH 8; (D) pH 10; (E) pH 11. Uncorrected for background absorption of the instrumentation system.

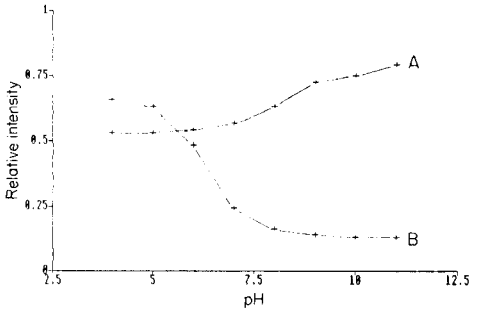

Fig. 2. Variation of relative reflectance of immobilized DIP with pH. (A) at 460 nm; (B) at 660 nm. The reference was XAD-2 without dye.

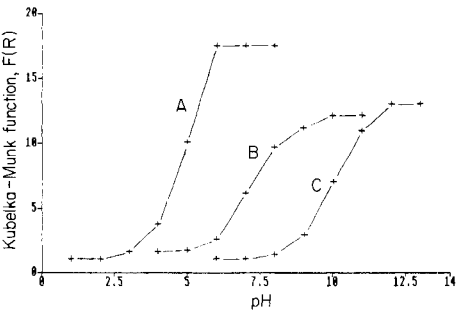

Fig. 3. Variation of the Kubelka-Munk functions of immobilised indicators with pH: (A) BPB at 590 nm; (B) DIP at 660 nm; (C) BTB at 590 nm.

buted to changes in the concentration of HIn and In^-, respectively. It should be noted that reflectance, unlike absorbance, decreases as the concentration of the absorbing species is increased.

Variation with pH. Figure 2 shows the effect of pH on the reflectance at 460 nm and 660 nm of DIP immobilised on XAD-2. At high pH values the reflectance at 460 nm, unlike that at 660 nm, does not level off as expected. The observed changes can be explained by the existence of the following equilibria:

$$\begin{array}{ccc} HIn\,(ads) & \overset{K_1}{\rightleftharpoons} & H^+(ads) + In^-\,(ads) \\ K_2 \Big\uparrow\downarrow & & \Big\uparrow\downarrow K_3 \\ HIn(sol) & \overset{K_4}{\rightleftharpoons} & H^+(sol) + In^-\,(sol) \end{array}$$

where $K_1 = [H^+]_{ads}[In^-]_{ads}/[HIn]_{ads}$, $K_2 = [HIn]_{sol}/[HIn]_{ads}$, $K_3 = [In^-]_{sol}/[In^-]_{ads}$ and $K_4 = [H^+]_{sol}[In^-]_{sol}/[HIn]_{sol}$. The subscripts ads and sol refer to the adsorbed and solution phases, respectively. As the pH is increased, the concentrations of HIn and In^- on the surface of the polymer change, as in an acid–base titration, and these are reflected in the sigmoidal curve in Fig. 2. However, after the equivalence point, the anionic species dominates and an adsorption/desorption equilibrium becomes significant. The charged anionic species is weakly adsorbed by the nonpolar polymer surface and tends to pass into the solution phase. The depletion of the anion on the surface of the adsorbent causes some of the adsorbed acid to dissociate so that the concentration of In^- is almost unchanged and that of HIn decreases.

Evaluation of pK values. A graphical method for the evaluation of pK similar to that used for absorbance data cannot be applied to reflectance data, because the measured reflectance is not directly proportional to concentration. For this case, the Kubelka-Munk function, $F(R)$, has to be used:

$$F(R) = (1 - R)^2/2R = kC \quad (1)$$

where R is the absolute reflectance, k is a constant involving the absorption and scattering coefficients, and C is concentration. Figure 3 shows the plot of $F(R)$ against pH for the indicators studied.

At any wavelength, the Kubelka-Munk function obtained from the reflectance data is the sum of the Kubelka-Munk functions of the two absorbing species, i.e., $F(R) = k_{HIn}\,[HIn]_{ads} + k_{In}\,[In^-]_{ads}$. At all times, the total concconcentration, C_{tot}, of the indicator is constant, i.e., $C_{tot} = [HIn]_{ads} + [In^-]_{ads} + [HIn]_{sol} + [In^-]_{sol}$. Here, $[HIn]_{sol}$ can be neglected, because the neutral undissociated form is strongly adsorbed by XAD-2. Combining these equations with the definitions of K_1 and K_3 yields

$$F(R) = \{k_{HIn}\,C_{tot}/[1 + (K_1/[H^+])\,(1 + K_3)]\} + \{k_{In}\,C_{tot}/[([H^+]/K_1) + (1 + K_3)]\} \quad (2)$$

Equation 2 can be shown to be consistent with the behaviour of $F(R)$, as depicted in Fig. 3. Under highly acidic conditions, $[H^+] > K_1$ and Eqn. 2 simplifies to $F(R)_{acid} = k_{HIn}\,C_{tot}$, which predicts a constant value for $F(R)$. Under strongly alkaline conditions, $[H^+] < K_1$ and Eqn. 2 becomes

$$F(R)_{alk} = \{k_{HIn}\,C_{tot}\,[H^+]/K_1\,(1 + K_3)\} + \{k_{In}\,C_{tot}/(1 + K_3)\} \quad (3)$$

At 660 nm, $k_{In} > k_{HIn}$, so that the first term can be ignored. Furthermore, based on the observation that at high pH values the colour of the adsorbed phase was much darker than that of the solution, it can be assumed that $K_3 \ll 1$. Consequently, Eqn. 2 reduces to $F(R)_{alk} = k_{In}\,C_{tot}$, which predicts a constant value for $F(R)$. This simplification is not valid at 460 nm, for which Eqn. 3 shows that $F(R)$ should decrease as the pH is increased.

At the equivalence point, $[HIn]_{ads} = [In^-]_{ads}$ and $[H^+] = K_1$. Equation 2 then becomes

$$F(R)_{eq} = (k_{HIn}\,C_{tot}/2) + (k_{In}\,C_{tot}/2)$$

At 660 nm, this expression can be rewritten as

$$F(R)_{eq} = 1/2\,[F(R)_{acid} + F(R)_{alk}] \quad (4)$$

This equation resembles that obtained by Patrick and Svehla [6] for the evaluation of pK values of indicators from absorbance/pH data. The pK value corresponds to the pH at the inflection point of the sigmoidal pH curve. A similar method could not be applied for the data obtained at 460 nm.

Comparison of p*K values.* The pK values obtained by using the procedure derived above are presented in Table 1. The pK values for BPB and BTB are different from those reported earlier [1], where the pK values were evaluated directly from pH vs. reflectance curves. Comparing these values with those obtained in solution, it can be inferred that immobilisation represses the ionisation of the indicator. If adsorption on XAD-2 is thought to occur

TABLE 1

Acidity constants (pK_{a1}) of indicators

Indicators	BPB	DIP	BTB
pK_{a1} (immobilised form)	4.65	7.01	9.95
pK_{a1} (aqueous solution)[a]	4.10	5.70	7.30

[a]At zero ionic strength [8], described in the scheme as K_4.

through the "solvent" action of the polymer matrix on the organic solute [7], this change in the extent of dissociation can be interpreted as a medium effect. The nonpolar environment on the surface of XAD-2 stabilises the neutral undissociated form of the indicator more than the anionic form.

A comparison of the expressions for the acidity constants in the immobilised state, K_1, and in the aqueous phase, K_4, leads to a conclusion which agrees with the results of this study:

$$K_1/K_4 = ([HIn]_{sol}/[HIn]_{ads})/([In]_{sol}/[In]_{ads}) = K_2/K_3 \quad (5)$$

where $K_2 < K_3$, because the neutral form is more strongly adsorbed by XAD-2 than the charged anionic form.

Conclusions

The acidity constants for immobilised indicators can be evaluated from reflectance measurements at different pH values. Previous papers have assumed that the acidity constant of an immobilised solute is equal to that in an aqueous solution [2–4]. The results obtained here show that adsorption on a nonpolar surface causes a decrease in the extent of dissociation of the solute. Immobilisation could therefore alter the dynamic range of analytical reagents, such as those used in optical-fibre sensors.

The authors acknowledge the financial support of Elf (U.K.) Ltd.

REFERENCES

1 G. F. Kirkbright, R. Narayanaswamy and N. A. Welti, Analyst, 109 (1984) 15.
2 M. D. Grieser and D. J. Pietrzyk, Anal. Chem., 45 (1973) 1348.
3 D. J. Pietrzyk, E. P. Kroeff and T. D. Rotsch, Anal. Chem., 50 (1978) 497.
4 C. Horvath, W. Melander and I. Molnar, Anal. Chem., 49 (1977) 142.
5 R. Narayanaswamy and F. Sevilla, Analyst, 111 (1986) 1085.
6 R. A. Patrick and G. Svehla, Anal. Chim. Acta, 88 (1977) 363.
7 P. Larson, E. Murgia, T. J. Hsu and H. F. Walton, Anal. Chem., 45 (1973) 2306.
8 E. Bishop, Indicators, Pergamon Press, Oxford, 1972.

Analytica Chimica Acta, 189 (1986) 371—377
Elsevier Science Publishers B.V., Amsterdam — Printed in The Netherlands

Short Communication

INTERFERENCES IN THE DETERMINATION OF COPPER IN NATURAL WATERS BY ANODIC STRIPPING VOLTAMMETRY

G. E. BATLEY

Analytical Chemistry Section, C.S.I.R.O. Division of Energy Chemistry, Private Mail Bag 7, Sutherland NSW 2232 (Australia)

(Received 14th April 1986)

Summary. Copper(I)-binding anions such as cyanide and thiocyanate, and polysaccharides, when present in non-saline waters are shown to produce an additional, more anodic wave during the determination of copper by stripping voltammetry. The origins of this wave and potential interferences in determinations of copper and copper-complexing capacities are discussed. The effect of inadequate oxygen removal is reported.

Of the heavy metals most commonly determined in natural waters by anodic stripping voltammetry (a.s.v.), copper causes the most difficulties. There are five main contributory factors: (i) the ability of copper to bind strongly with many organic and inorganic ligands; (ii) its existence in more than one oxidation state; (iii) the occurrence of the copper stripping peak at a potential where many organic species are adsorbed on the mercury electrode; (iv) the low solubility of copper in mercury; and (v) the irreversibility of the copper(II) reduction.

Several studies [2—6] have revealed the complexity of the processes associated with electrodeposition in estuarine waters. In chloride media, the copper stripping process is controlled primarily by the one-electron oxidation:

$$Cu(Hg) + 2Cl^- \rightarrow CuCl_2^- + e^- \quad (1)$$

Humic and fulvic acids and other organic substances capable of adsorbing on the hanging mercury drop electrode can enhance the adsorption of the Cu(I) intermediate [2]. Surfactants will also stabilize adsorbed $CuCl_2^-$ [2]. These effects, combined with Cu(II)/ligand interactions, can lead to spurious results when a.s.v. is used to measure both labile copper and copper-complexing capacities of saline waters.

Little has been written about the influence of such effects on the stripping voltammetry of copper in non-saline waters. Some unusual observations on lake-water samples indicated the need for further investigation of the nature of electrode processes interfering with the usual oxidation reaction in freshwaters:

$$Cu(Hg) \rightarrow Cu^{2+} + 2e^- \quad (2)$$

0003-2670/86/$03.50

Experimental

Stripping voltammetry was done with a Princeton Applied Research model 384 voltammeter connected to a model 303 static mercury drop electrode. Unless otherwise stated, the pulse amplitude was 25 mV and the scan rate 5 mV s^{-1}. The base electrolyte used in all studies was 0.05 M acetate buffer, pH 5.0. Unless otherwise stated, all potentials are given versus the Ag/AgCl electrode. All chemicals were of analytical-reagent grade. Fibrillar colloids, as a concentrated extract from Great Lakes waters, were supplied by Dr. G. G. Leppard, Canada Centre for Inland Waters.

Results and discussion

A typical differential-pulse stripping voltammogram for copper(II) in 0.05 M acetate buffer pH 4.7 at a hanging mercury drop electrode (25-mV pulse amplitude and 5-mV s^{-1} scan rate) has a peak potential near 0 V and a peak half-width of 67 mV. The latter compares with 44 mV for a totally reversible oxidation (e.g., Cd^{2+}). Copper(II)-binding ligands, e.g., humic and fulvic acids or nitrilotriacetic acid which are often encountered in fresh waters, produce a shift in the stripping peak to more cathodic potentials, the magnitude of the shift being related to the metal/ligand stability constant [4].

The binding abilities of natural ligands in water are best described by their copper-complexing capacities which can be determined by measuring the change in a.s.v. response to added Cu^{2+}. Although this procedure is adequate for most ligands, in some instances abnormal behaviour is displayed with additional anodic processes distorting the usual stripping peak for copper. Such behaviour was observed (Fig. 1) with organic fibrils isolated from the Great Lakes waters [5]. The fibrils are extracellular polymeric substances, often comprising cyanobacteria, and chemically consisting principally of

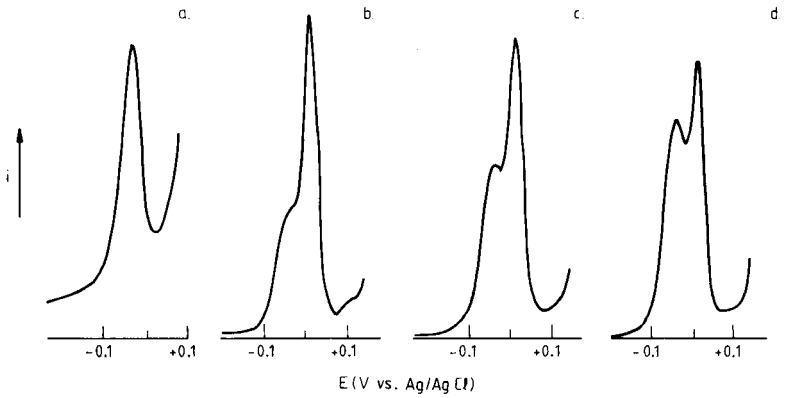

Fig. 1. Stripping voltammograms for a water sample containing fibrils (pH 5.0, 0.06 M acetate buffer) with successive additions of Cu^{2+}: (a) 0; (b) 1.0×10^{-7} M; (c) 1.5×10^{-7} M; (d) 2.0×10^{-7} M. Conditions: $E_{dep} = -0.4$ V, deposition time 180 s, pulse amplitude 25 mV, drop time 0.5 s.

polysaccharides [6]. They are believed to play an important role in trace-element binding in natural waters. The first stripping peak was the characteristic copper oxidation peak, but the second, more anodic peak, displayed the characteristics of an adsorption post-wave.

Increasing additions of copper(II) ion to a lake-water solution containing fibrils resulted in increases in the heights of both peaks. The more anodic adsorption peak increased rapidly with added copper to a limiting value, whereas the first peak exhibited a behaviour characteristic of a normal complexing-capacity titration. The breaks in the two curves almost coincided (Fig. 2).

A possible explanation for the additional wave was that it resulted from the oxidation of an adsorbed copper(I)/fibril complex. To test this theory, the behaviour of other ligands known to bind copper(I) was examined in the presence of copper(II) ion. Cyanide and thiocyanate were found to behave similarly to the fibrils. In each case, with increasing deposition time, a limiting peak current was reached, representing surface saturation. Increasing surface coverage made oxidation more difficult, with an anodic shift in the peak potential of the adsorption wave. The shift reached a maximum of 130 mV for thiocyanate, 120 mV for cyanide, and 68 mV for the fibrils.

The dependence of the height of the adsorption wave on ligand concentration over a limited range, has utility in the determination of traces of cyanide and thiocyanate. The former was reported by Berge and Jeroschewski [7] using linear sweep voltammetry at a hanging drop electrode. Similar behaviour for thiocyanate was observed here, but the range over which the anion concentration dependence was linear was very narrow ($1-10\times 10^{-7}$ M), significantly restricting the analytical utility of the procedure.

Several authors have examined the polarography of copper in the presence

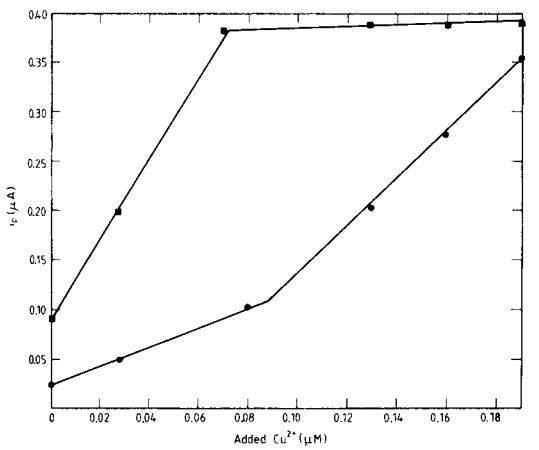

Fig. 2. Complexing-capacity titration of a fibril-containing sample pH 5.0, with Cu^{2+}: (▪) adsorption peak; (•) Cu^{2+} peak. Conditions: $E_{dep} = -0.4$ V, deposition time 90 s, pulse amplitude 25 mV, drop time 0.5 s.

of particular natural polysaccharides. Brezonik et al. [8] observed that mg l^{-1} concentrations of alkaline phosphatase, alginic acid and polygalacturonic acid broadened the copper stripping peak and shifted it anodically, although in certain instances two peaks were observed. The differential pulse polarography of copper(II) in the presence of selected polyuronates showed, in most cases, the appearance of a sharp anodic peak together with a second peak cathodic of the Cu(II) reduction [9]; both additional waves were attributed to post and pre-waves.

A closer examination of the effect of alginic acid showed a behaviour similar to that observed in the case of both fibrils and copper(I)-binding ligands. A second sharp peak was evident at a potential some 25 mV anodic of the parent copper peak. Resolution of this peak could only be achieved if a small pulse amplitude (10 mV) was used (Fig. 3). Although there is evidence that copper(II) binds to natural polysaccharides, albeit weakly [9], copper(I) can apparently form stable associations with adsorbed polyelectrolytes, as it does with cyanide and thiocyanate. The nature of the former associations may parallel that observed in saline media when adsorption of $CuCl_2^-$ is enhanced by adsorbed species [2].

In all cases, the formation of the adsorption peak was critically dependent on deposition potential; Table 1 shows the data obtained when cyanide was added. Deposition at increasingly negative potentials brought about a significant decrease in the adsorption peak height, whereas the height of the copper peak increased. At these potentials, the net charge on the mercury electrode with respect to the electrocapillary zero is negative, whereas near −0.4 V the electrode has a net positive charge which is favourable to the accumulation of adsorbed ligand. Increasing deposition time at −0.4 V resulted in an anodic shift of the adsorption wave with a constant peak current being achieved for saturation surface coverage (Table 2). Alternatively, it could be that the more cathodic deposition potentials are simply sufficient to cause the reduction directly to the metal, so that copper(I) cannot exist on the electrode. The former explanation is plausible if the electrode process involves the reaction of adsorbed ligand preventing reduction beyond copper(I). The latter could involve the reduction at the electrode surface of a diffusing copper(II)/-polysaccharide complex forming an insoluble film of the copper(I) complex on the electrode. In both instances, however, it is thought that the formation of an adsorbed copper(I) complex could explain the potential and characteristics of the second wave. It is worth noting that, even in the absence of added ligands, two peaks can sometimes be observed for copper during stripping voltammetry. The first, a broad peak cathodic of the copper wave, will be present if the solution is improperly degassed and is the first reduction wave for dissolved oxygen. This is best avoided by using a chromatographic oxygen trap or helium instead of nitrogen for degassing. The problem is less frequent in saline waters because of the reduced solubility of oxygen.

The problem of oxygen is illustrated in Fig. 4. With inefficient deoxygena-

tion, a broad wave characteristic of oxygen appears at −0.150 V in 0.008 M nitric acid/0.002 M sodium nitrate (curve a). After the conventional 5-min degassing with nitrogen, a residual disturbance of the copper wave is still evident (curve b). Calculations showed that the amount of oxygen giving rise

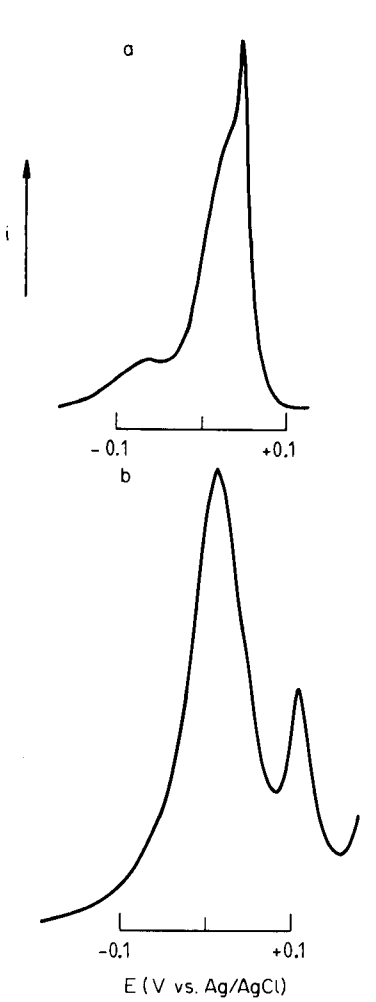

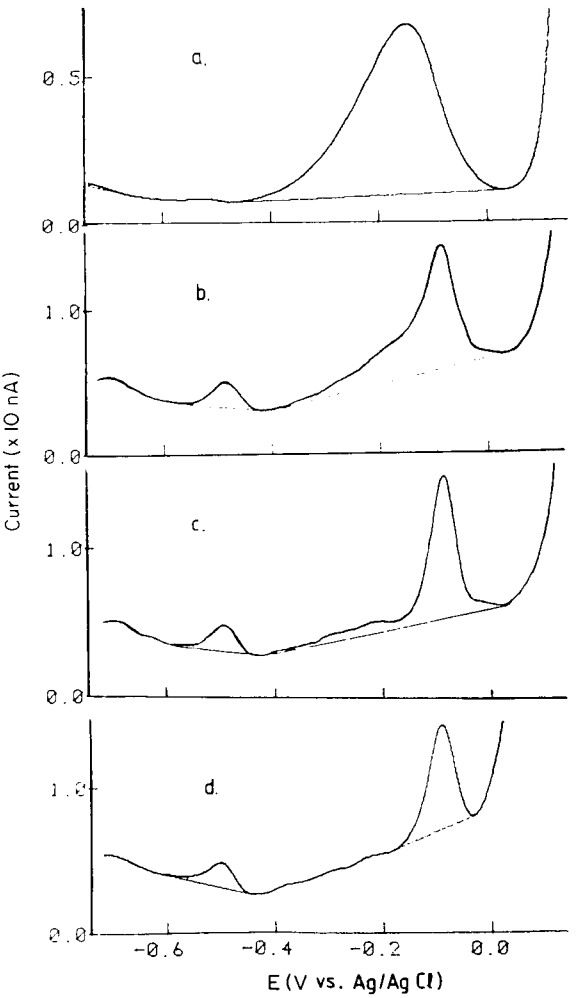

Fig. 3. (left) Stripping voltammograms for 1.25×10^{-7} M Cu^{2+} in the presence of (a) 0.5 mg l^{-1} alginic acid, (b) 1.5×10^{-6} M iodide. Conditions: E_{dep} = −0.4 V, deposition time 180 s, pulse amplitude 10 mV for (a), 25 mV for (b).

Fig. 4. (right) Stripping voltammograms for residual copper(II) in 0.008 M HNO_3/0.002 M $NaNO_3$: (a) 2-min degassing with nitrogen; (b) 5-min degassing with nitrogen; (c) 5-min degassing with helium plus vigorous helium stream over solution surface; (d) 5-min degassing with helium, after 1×10^{-4} M chloride addition. Conditions: E_{dep} = −1.25 V, deposition time 300 s, otherwise as for Fig. 2.

TABLE 1

Effect of deposition potential on Cu^{2+} in presence of cyanide[a]

E_{dep} (V)	E_{p_1} (V)	E_{p_2} (V)	i_{p_1} (μA)	i_{p_2} (μA)
−0.40	−0.032	0.062	0.13	0.11
−0.60	−0.036	0.060	0.15	0.07
−0.80	−0.036	0.060	0.16	0.05
−1.20	−0.036	0.060	0.18	0.02

[a]1.67 μM cyanide, 1.1×10^{-7} M Cu^{2+}, 0.1 M acetate buffer pH 5, deposition time 50 s.

TABLE 2

Effect of deposition time on Cu^{2+} in presence of cyanide[a]

Deposition time (s)	E_{p_1} (V vs. Ag/AgCl)	E_{p_2}	i_{p_1} (μA)	i_{p_2} (μA)
0	−0.028	0.042	0.02	0.04
25	−0.032	0.056	0.06	0.08
50	−0.032	0.062	0.13	0.11
90	−0.034	0.070	0.21	0.15
200	−0.036	0.076	0.41	0.15

[a]Conditions as for Table 1, except that the deposition potential was −0.4 V.

to this residual signal could have resulted from the 2×10^{-8} M oxygen produced at the auxiliary electrode. Its height increases with deposition time but, in the absence of deposition, a cathodic scan still revealed a residual oxygen wave. When the solution was degassed with helium for 5 min and the gas stream was then directed onto the solution surface in the vicinity of the mercury capillary, the oxygen peak could be substantially removed (curve c). With the addition of 1×10^{-4} M chloride, the oxygen wave virtually disappeared (curve d), as would be expected if the reaction at the auxiliary electrode becomes the oxidation of chloride to chlorine rather than water to oxygen. A closer examination, however, shows that encroachment of the anodic reaction of chloride at the working electrode on the copper wave can simply improve resolution of the copper wave, where previously there was some distortion observed on both the cathodic and anodic sides. Attempts to separate the auxiliary electrode proved inconclusive because ingress of oxygen could not be fully eliminated. The interfering peak was observed at other pH values in dilute electrolytes. This appears to be of particular concern with the PAR model 303 electrode cell assembly because the cell cannot be satisfactorily sealed to prevent entry of oxygen. Ingress of oxygen from outside the cell is therefore a likely source of interference in the determination of ultratrace levels of copper in fresh waters.

The copper wave can also be split when the solubility of copper in the mercury electrode is exceeded. This is more likely at a mercury film electrode (MFE) where the concentration of copper in mercury is significantly greater. Copper is soluble in mercury up to 4 mM but this solubility can be altered by the presence of other constituents in the film. At a typical MFE, the above solubility will be exceeded when the copper concentration exceeds 0.5 $\mu g\ l^{-1}$ for a 10-min deposition in situ with 4×10^{-5} M mercury(II) ion [10].

The experimental assistance of Bruce Saunders is gratefully acknowledged.

REFERENCES

1 E. A. Schonberger and W. F. Pickering, Talanta, 27 (1980) 11.
2 A. Nelson, Anal. Chim. Acta, 167 (1985) 273.
3 A. Nelson and R. F. C. Mantoura, J. Electroanal. Chem., 169 (1984) 233; 184 (1984) 253.
4 P. Valenta, in G. G. Leppard (Ed.), Trace Element Speciation in Surface Waters, Plenum, New York, 1981, p. 49.
5 G. G. Leppard, A. Massulski and D. R. S. Lean, Protoplasma, 92 (1977) 289.
6 G. G. Geesey, ASM News, 48 (1982) 9.
7 H. Berge and J. Jeroschewski, Z. Anal. Chem., 214 (1967) 9.
8 P. L. Brezonik, P. A. Brauner and W. Stumm, Water Res., 10 (1976) 605.
9 E. Reishofer, A. Cesaro, F. Delbin, G. Manzini and S. Paoletti, Bioelectrochem. Bioenergy., 12 (1984) 455.
10 G. E. Batley and T. M. Florence, J. Electroanal. Chem., 55 (1974) 23.

Analytica Chimica Acta, 189 (1986) 379—382
Elsevier Science Publishers B.V., Amsterdam — Printed in The Netherlands

Short Communication

A REVISED METHOD FOR THE SPECTROPHOTOMETRIC DETERMINATION OF GLYOXYLIC ACID

V. CAPRIO*

Dipartimento di Ingegneria Chimica, Università di Napoli, Piazzale V. Tecchio, 80125 Naples (Italy)

A. INSOLA

Istituto di Ricerche sulla Combustione, C.N.R., Piazzale V. Tecchio, 80125 Naples (Italy)

(Received 7th May 1986)

Summary. The spectrophotometric determination of glyoxylic acid at 520 nm based on formation of the 1,5-diphenyl formazan derivative is revised. The colour can be developed at room temperature if the acid or its sodium salt is pure. The molar absorptivity is improved to 32 250 l mol^{-1} cm^{-1}. The differences from the earlier procedures are discussed.

The ozonolysis of traces of organic substances in aqueous solution is actively investigated because of its connection with waste-water treatments [1]. Related studies obviously require the adoption of very sensitive methods for the determination of the organic compounds. Glyoxylic acid is one of the most frequent intermediates in the ozonolysis of aromatic pollutants, thus procedures for its determination are of general interest.

The method first proposed by Kramer et al. [2] for the determination of glyoxylic acid appeared to have satisfactory sensitivity. However, when the recommended procedure was checked before its adoption for a study of kinetics of glyoxylic acid ozonolysis in aqueous solution [3], some discrepancies in the experimental results were observed. Details of this checking and attempts to explain the observed discrepancies are given in this communication.

Experimental

Glyoxylic acid monohydrate (99% pure, EGA Chemie) was used as the starting material to prepare the aqueous test solutions. Solutions of about 0.1 M glyoxylic acid were standardized by titration with 0.1 M sodium hydroxide (phenolphthalein indicator). Potassium dichromate was used to evaluate the total oxygen demand of test solutions by a spectrophotometric procedure for COD [4]. Both titrimetric procedures gave similar results in terms of glyoxylic acid concentration and the values thus found were in good agreement with those expected on the basis of the degree of purity given for the starting glyoxylic acid. Sodium glyoxylate samples were prepared by addition of accurately measured sodium hydroxide to stirred and

0003-2670/86/$03.50

unstirred solutions of glyoxylic acid and multiple crystallizations from water/ethanol (9:1) solutions.

Both glyoxylic acid and glyoxylate solutions were used for calibration by the following procedure. A portion (2.5 ml) of known glyoxylic or glyoxylate solution ($0.2-2 \times 10^{-4}$ M) was mixed in a 15-ml test tube with 2.5 ml of a 1% (w/v) phenylhydrazine hydrochloride (Carlo Erba) solution. The solutions thus obtained were either incubated in a 110°C oven for 5 min, as recommended by Kramer et al. [2], or simply left for 2–3 min at room temperature. Then 2.5 ml each of concentrated hydrochloric acid and 1% (w/v) potassium hexacyanoferrate(III) (Merck, p.a.) were added. Bright red 1,5-diphenylformazan glyoxylic acid [5] was formed rapidly as the glyoxylic acid phenylhydrazone was oxidized by hexacyanoferrate(III). After about 2 min, the absorbance was measured at 520 nm in 1-cm quartz cells in a Perkin–Elmer 402 u.v.-visible spectrophotometer.

Results and discussion

The calibration graphs are plotted in Fig. 1. Molar concentrations are those calculated by assuming a 100% purity degree of each tested material. For standard glyoxylic acid solutions and for glyoxylate solutions obtained by rigorously controlled addition of sodium hydroxide, absorbances at 520 nm and concentrations (mol l^{-1}) follow the linear regression equation, $A = 32\,250\,C$, with a correlation coefficient (r) of 0.999, provided that no heating is used and the solutions are simply left at room temperature for 2–3 min

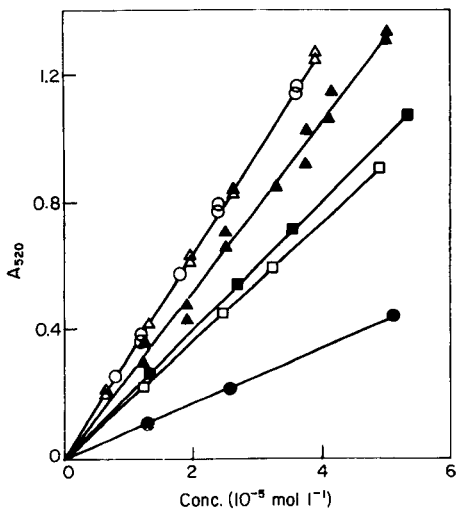

Fig. 1. Calibration plots: (△) glyoxylic acid, (○) sodium glyoxylate, both by the procedure without heating; (▲) glyoxylic acid by the heating procedure; (□) first crystallization sample from addition of sodium hydroxide (1.5 M) to an unstirred solution (1.5 M) of glyoxylic acid; (■) previous sample after double recrystallization; (●) sample from addition of glyoxylic acid solution to sodium hydroxide solution.

before addition of hydrochloric acid and hexacyanoferrate(III). When the solutions are heated at 110°C for about 5 min, as suggested by Kramer et al. [2], the linear calibration equation is $A = 26\,550\ C$ ($r = 0.995$). The heating procedure thus causes a systematic decrease in the sensitivity at 520 nm, and worse reproducibility.

These results are in striking discordance with those reported by Kramer et al. The molar absorptivity found is far larger than that (17 870 l mol^{-1} cm^{-1}) previously reported and the measurements are adversely affected by the heating procedure. The measurements made by Kramer et al. were based on the adoption of a starting material referred to as 99% pure sodium glyoxylate. No details of how this substance was prepared were given, and purity was assumed on the basis of carbon and hydrogen data.

The present results indicate that sodium glyoxylate, when accurately prepared, gives the same analytical response as glyoxylic acid. Deviations are observed only when the procedure for preparation does not include prevention of alkaline solutions. Depending on the stirring efficiency, even addition of the sodium hydroxide solution to the glyoxylic acid solution can produce temporary local alkaline conditions. In these circumstances, some rapid glyoxylate reaction occurs, as indicated by the remarkable decrease in the absorbance at 520 nm of crystallized products compared to pure glyoxylate (Fig. 1). Figure 1 also indicates that multiple crystallizations only slightly improve the optical properties of materials derived from imperfectly controlled neutralization of glyoxylic acid. The results thus indicate that the preparation of glyoxylate, despite its apparent simplicity, is not free from complications arising from the occurrence of reactions other than simple neutralization and that glyoxylate purification can be difficult.

If the above observations are used to explain the earlier results of Kramer et al., consideration must be given to the fact that the carbon and hydrogen data obtained for their starting material agree with values expected for pure glyoxylate. Therefore, the glyoxylate reactions must be such that some glyoxylate disappears without affecting the elemental composition of the resulting material. Polymerization reactions would meet this requirement; and a polymeric structure of the sample could explain the influence of heating on the analytical response as reported by Kramer et al. It is known that aldehydes can undergo base-catalyzed reactions leading to polymers containing the acetal repeating structure [6]. It is also known that the inductive properties of electron-withdrawing substituents of carbon linked to carbonyl have a marked promoting effect on polymerization [7]. Thus, some polymerization reaction of glyoxylate under alkaline conditions is not unlikely unless it is thermodynamically prevented by too low ceiling temperatures.

In conclusion, whatever the true explanation of discrepancies between the results obtained here and those of Kramer et al., the following points must be considered: glyoxylate production by means of acid neutralization can be affected by reactions leading to glyoxylate derivatives, purification of

glyoxylate from derivatives can be difficult, and a polymeric structure of the glyoxylate derivatives seems very likely.

REFERENCES

1 R. G. Rice, A. Netzer, Handbook of Ozone Technology and Applications, Vol. 1, Ann Arbor Science Publ., Ann Arbor, MI, 1982.
2 D. N. Kramer, N. Klein and R. A. Baselice, Anal. Chem., 31 (1959) 250.
3 V. Caprio and A. Insola, Oxid. Commun., 8 (1986) 263.
4 M. Scrinia and B. Amadio, Inquinamento, 2 (1977) 58.
5 A. W. Nineham, Chem. Rev., 55 (1955) 355.
6 J. Furukawa and T. Saegusa, Polymerization of Aldehydes and Oxides, Interscience-Wiley, New York, 1963.
7 I. Rosen, J. Macromol. Sci. Chem. A1, 2 (1967) 243.

Analytica Chimica Acta, 189 (1986) 383—387
Elsevier Science Publishers B.V., Amsterdam — Printed in The Netherlands

Short Communication

SPECTROPHOTOMETRIC DETERMINATION OF COBALT AFTER EXTRACTION OF TETRATHIOCYANATOCOBALTATE(II) WITH BRILLIANT GREEN INTO MICROCRYSTALLINE NAPHTHALENE

D. THORBURN BURNS* and N. TUNGKANANURUK

Department of Analytical Chemistry, The Queen's University, Belfast BT9 5AG (Northern Ireland)

(Received 2nd April 1986)

Summary. Cobalt (0—20 μg) is determined spectrophotometrically at 635 nm after its adsorptive extraction as tetrathiocyanatocobaltate(II) with Brilliant Green on microcrystalline naphthalene at pH 6.5 and dissolution of the solid phase in toluene. The effects of pH, diverse ions and masking studies are reported. The system is applied to the determination of cobalt (0.2—10%) in high-speed tool steels without prior separation of iron.

Brilliant Green (C.I. 42040) has been used for the liquid—liquid extraction spectrophotometric determination of various complex anions of transition metals [1—4] including tetrathiocyanatocobaltate(II) at pH 2 in the presence of gum arabic [5]. Other applications of the dye include the extraction of boron as its complex with 2,4-dinitronaphthalene-1,8-diol [6]. The acid—base equilibria, purification [7], and adsorptive [8] and dimerization effects [9] of Brilliant Green have been reported. So far no applications of liquid—solid separation of ion-pairs with basic dyes such as Brilliant Green have been described [10].

The present communication reports on the novel adsorptive extraction of Brilliant Green tetrathiocyanatocobaltate(II) by microcrystalline naphthalene. The solid naphthalene can subsequently be dissolved in toluene and determinations completed spectrophotometrically at 635 nm. The system is applied to the determination of cobalt in tool steels.

Experimental

Apparatus. Pye-Unicam SP8-400 and SP6-550 u.v.-visible spectrophotometers were used for recording absorption spectra and for routine absorbance measurements, respectively, with matched quartz 1-cm cells.

Reagents and solutions. Brilliant Green (Aldrich Chemical Company, dye content 95%) was used as supplied. Elemental analysis gave 66.9% C, 7.0% H, 5.6% N (theor. for $C_{27}H_{34}N_2O_4S$, 67.2% C, 7.1% H, 5.8% N). A 0.1% (w/v) solution was prepared in 75% ethanol, and stored in a dark brown glass bottle. A stock 1000 μg ml^{-1} cobalt(II) solution was prepared by dissolving

0003-2670/86/$03.50

2.630 g of anhydrous cobalt(II) sulphate (analytical grade dried to constant weight at 400°C) in exactly 1 l of distilled water. More dilute standard solutions were prepared as required. A pH 6.5 buffer was prepared by dissolving 10.89 g of potassium dihydrogenphosphate and 5.65 g of disodium hydrogenphosphate in 1 l of distilled water. The naphthalene solution was 20% (w/v) in acetone. All other reagents were of analytical grade. Twice-distilled water was used throughout.

General procedure. Place 1—4 ml of sample solution containing 5—20 μg of cobalt(II) in a stoppered Erlenmeyer flask. Add 3.0 ml of 5 M ammonium thiocyanate, 2.5 ml of pH 6.5 buffer and 0.5 ml of the Brilliant Green solution. Swirl to mix and allow to stand for 4 min. Add 2.0 ml of the naphthalene solution and shake vigorously for 30 s. Filter the blue solid formed through a sintered glass filter (no. 2 porosity). Wash with water, drain or suck dry, dissolve the solid in toluene and make up to volume in a 20 ml volumetric flask. Dry the solution by addition of 1—2 g of anhydrous sodium sulphate. Measure the absorbance at 635 nm against a reagent blank prepared in the same way. The toluene solution should be kept out of direct sunlight, and the absorbance should be measured within 5 min after transference to the cell.

Procedure for steel samples. For steel samples containing 2—10% or 0.2—1% cobalt, dissolve accurately weighed 0.01 or 0.1-g samples, respectively, in a mixture of 3 or 30 ml of concentrated hydrochloric acid and 1 or 10 ml of concentrated nitric acid, respectively, in 250-ml conical flasks. Heat to aid dissolution. Boil to near dryness, cool, add 1 or 10 ml of concentrated hydrochloric acid, and evaporate again to near dryness. Cool, add 50 ml of distilled water and heat to dissolve the solids. Cool, and filter through a Whatman No. 1 paper into a 100-ml volumetric flask. Wash the residual solids (silica, tungstic acid) with a small volume of hot 2% (v/v) hydrochloric acid followed by distilled water and make up to volume with distilled water. Dilute with twice the volume of distilled water. Transfer 2—10 ml aliquots containing 8—12 μg of cobalt into stoppered Erlenmeyer flasks. Add 3 ml of 10% (w/v) ammonium fluoride solution and 1.5 ml of saturated ammonium-D(+)-tartrate solution. The pH should be in the range 6.50—6.80 without adding buffer solution, so if necessary adjust the pH by adding a little 2 M ammonia. Proceed as in the general procedure but omit the addition of buffer which is not necessary in the analysis of steel when the masking agents have been added.

Prepare a calibration graph for the range 0—20 μg of cobalt after adding 2 ml of iron(III) nitrate solution containing 1.6 or 16.0 mg of iron to the cobalt solutions, followed by the other reagents as for the steel samples.

Examination of the main experimental variables

Naphthalene, diphenyl, 1,4-dichlorobenzene and benzophenone were each examined for their adsorptive/extraction properties using the microcrystalline solid formation from acetone solution. Benzophenone showed the highest

sensitivity (apparent molar absorptivity of 8.0×10^4 l mol^{-1} cm^{-1}) but also the highest reagent blank absorbance (0.635); naphthalene gave an acceptable sensitivity ($\epsilon_{app} = 2.52 \times 10^4$ l mol^{-1} cm^{-1}) and blank absorbance (0.135).

Solvents with a range of functional group types, including alcohols, ketones, esters, ethers and chlorinated and aromatic hydrocarbons, were examined for dissolution of the ion-pair and the naphthalene. The ion-pair was soluble in toluene, benzene, carbon tetrachloride, amyl alcohol, acetylacetone, acetonitrile, chlorobenzene, chloroform, dimethyl sulphoxide, diethyl ketone, 1,4-dioxane, isopropanol, methyl ethyl ketone, propylene carbonate, pentan-1-ol, pentan-2-ol, isopropyl ether, dimethylformamide, isoamyl acetate and xylene. The solutions in dimethylformamide, isoamyl acetate, isopropyl ether and xylene were unstable. Toluene was the most satisfactory solvent for dissolution of the complex based on the apparent molar absorptivity (at 635 nm) and reagent blank.

The effect of pH was examined for 20 μg of cobalt(II) by addition of 1 M hydrochloric acid or 1 M ammonia prior to extraction. The absorbances were measured as before and were almost independent of pH in the range 6.0—7.0, decreasing rapidly outside these limits. In subsequent work, the aqueous phase was buffered at pH 6.5. The extraction was constant with 2.0—4.0 ml of buffer; 2.5 ml of buffer was used in subsequent work.

The effects of varying the amounts of ammonium thiocyanate and Brilliant Green were examined for 20 μg cobalt(II). For ammonium thiocyanate, the absorbance increased to a constant value with increase in volume of reagent. For Brilliant Green the absorbance increased with increasing volume of reagent up to 0.5 ml, remained constant up to 0.7 ml and decreased slowly thereafter; the reagent blank increased slowly with increase in volume of reagent added. Convenient volumes in the plateau regions are specified in the general procedure. The extent of extraction was unaffected by ionic strength, phase volume ratios up to 10:1 water/naphthalene in acetone, sequence of addition of reagents prior to the addition of the extractant phase or by time of shaking. Dissolved extracts were stable for up to 7 days in diffuse daylight but faded slowly in direct sunlight.

The composition of the complex was established by Job's method [11] and by the mole ratio method [12, 13] to be $[C_{27}H_{33}N_2][Co(NCS)_4]$. Elemental analysis of the precipitate formed from aqueous solution was consistent with the same composition (required 65.6% C, 6.2% H, 10.55% N; found 65.8% C, 6.4% H, 10.3% N).

Results and discussion

A linear calibration graph was obtained for 0—20 μg of cobalt in 20 ml of final solution in toluene ($\epsilon_{app} = 2.55 \times 10^4$ l mol^{-1} cm^{-1}). For the determination of 10 μg of cobalt, the relative standard deviation was 0.75% (10 results).

The possible interferences of a number of cations and anions were checked for 10 μg of cobalt. Increased extraction occurred at high ratios of iron(III) to cobalt (2.0% for 1.6 mg of iron, 6.1% for 16 mg of iron) when 3.0 ml of

10% ammonium fluoride and 1.5 ml of saturated ammonium-D(+)-tartrate solutions were used to mask the iron(III). This mixed masking agent normally controls the pH in the range 6.2—6.3, but it may be necessary to add 1—2 drops of 2 M ammonia. Under these conditions, the addition of phosphate buffer is not needed. The slightly increased extractions can be compensated by the addition of an equivalent amount of iron to the standards and blanks. Linear calibration graphs were still obtained. The results of the interference and masking study are summarized in Table 1. The only ions which interfered significantly and are of interest in the analysis of steels were iron(III) (500:1), niobium and tin (200:1) and copper (50:1). Iron(III), niobium and tin can be masked by addition of ammonium fluoride and ammonium-D(+)-tartrate. The low tolerance limit for copper does not matter in the analysis of steels because the amount of copper is low compared to cobalt. Under the conditions

TABLE 1

Effect of various ions on the determination of cobalt

Ion[a]	Ratio to Co(II) (w/w)	Absorbance change (%)[b]	Ion[a]	Ratio to Co(II) (w/w)	Absorbance change (%)[b]
Cd^{2+}	200	+19	Sn^{4+}	200	+9
	120	—		150	—
Al^{3+}	200	+63		200	—[c]
	16	—	Hg^{2+}	200	+22
Mn^{2+}	200	+38		20	—
	20	—		200	—[d]
Pb^{2+}	200	+33	Fe^{2+}	200	—54
	20	—		200	—[d]
Cr^{3+}	200	+8	Cu^{2+}	50	—83
	80	—		4	—
	200	—[c]		60	—29[e]
Zn^{2+}	200	+88		60	+60[e]
	4	+45		60	—22[f]
Pd^{2+}	10	+41	Fe^{3+}	500	—77
	1	—		500	—[g]
U(VI)	200	+40	$C_2O_4^{2-}$	50	—
	20	—	Citrate	50	—
	200	—[c]	VO_3^-	50	—12
Bi^{3+}	200	+94		25	—
	15	—	WO_4^{2-}	500	+19
	200	—[c]		250	—
Nb^{5+}	200	—66	CN^-	25	—100
	200	—[c]	EDTA	25	—100

[a]Cations added as chloride, sulphate or nitrate; anions added as sodium salts. [b]— indicates <3% change in absorbance. [c]1.0—1.5 ml of 30% ammonium fluoride added. [d]1 drop of hydrazine hydrate added. [e]2 ml of 0.03 M sodium thiosulphate added. [f]1 ml of 0.3 M ammonium-D(+)-tartrate added. [g]3.0 ml of 10% ammonium fluoride, 1.5 ml of saturated ammonium-D(+)-tartrate and, if needed, 1 drop of 2 M ammonia added.

TABLE 2

Analysis of high-speed tool steels

B.C.S. steel	Cobalt in steel (% w/w)		
	Certified value	Certified range	Found[a]
220/2	0.32	0.31—0.33	0.33 ± 0.2
241/2	5.70	5.66—5.73	5.68 ± 0.07
482	0.24	0.21—0.27	0.268 ± 0.014
483	1.94	1.90—1.99	1.91 ± 0.02
484	10.20	10.10—10.39	10.34 ± 0.03
485	5.06	5.00—5.11	5.09 ± 0.05

[a]Mean ± 95% confidence limits for 5 replicates.

of the general procedure, the following cations at a weight ratio 200:1 were without appreciable effect: Na^+, K^+, NH_4^+, Mg^{2+}, Ni^{2+} and Zr(IV). Among the cations interfering at 200:1 ratios (Table 1), the effects of iron(II) and mercury(II) were avoided by the addition of hydrazine hydrate (which complexes Fe^{2+}) and those of Bi(III) and Cr^{3+} by ammonium fluoride. Among anions which did not interfere were fluoride, chloride, bromide, iodide, nitrate, carbonate, acetate, sulphate, hydrogenphosphate, molybdate, thiosulphate and tartrate. Cyanide and EDTA must be absent.

The results for the determination of cobalt in six British Chemical Standard steel samples (Table 2) are in good agreement with the certified values.

The method is rapid and more sensitive than the previously described liquid—solid extraction of cobalt [14], but it is slightly less precise, owing to the higher r.s.d. of the blank (0.39%, 10 results).

REFERENCES

1 A. G. Fogg, C. Burgess and D. Thorburn Burns, Talanta, 18 (1971) 1175.
2 A. G. Fogg, C. Burgess and D. Thorburn Burns, Analyst, 98 (1973) 347.
3 E. M. Donaldson, Talanta, 30 (1983) 497.
4 Y. K. Agrawal and K. T. John, Analyst, 110 (1985) 1041.
5 H. Yinglu and H. Degui, Fenxi Huaxue, 12 (1984) 389.
6 K. Toei, S. Motomizu, M. Oshima and H. Watari, Analyst, 106 (1981) 776.
7 A. G. Fogg, C. Burgess and D. Thorburn Burns, Analyst, 95 (1970) 1012.
8 D. Thorburn Burns, A. G. Fogg and A. Willcox, UV Group Bull., 2 (1974) 23.
9 A. G. Fogg, A. Willcox and D. Thorburn Burns, Analyst, 101 (1976) 67.
10 D. Thorburn Burns, J. M. Jones and N. Tungkananuruk, TRAC, 4(2) (1985) VI.
11 P. Job, Ann. Chim. (Paris), 9 (1928) 113.
12 J. H. Yoe and A. L. Jones, Ind. Eng. Chem. Anal., Ed., 16 (1944) 11.
13 K. Momoki, J. Sekino, H. Sato and N. Yamaguchi, Anal. Chem., 41 (1969) 1286.
14 T. Nagahiro, M. Satake, J. Lin and B. K. Puri, Analyst, 109 (1984) 163.

Analytica Chimica Acta, 189 (1986) 389—395
Elsevier Science Publishers B.V., Amsterdam — Printed in The Netherlands

Book Reviews

P. Mohr and K. Pommerening, *Affinity Chromatography, Practical and Theoretical Aspects.* M. Dekker, New York, 1985 (ISBN 0-8247-7468-X), pp. vii + 301. Price $69.75 (U.S. and Canada); $83.50 (all other countries).

This publication is Volume 33 in the Chromatographic Science Series and is a comprehensive account of affinity chromatography, a technique that is widely used for the purification of biologically active substances on a preparative scale, and is also developing into an important and powerful analytical tool. There are four major sections in the book, each consisting of several self-contained chapters.

The first section is entitled "General Problems" and is of interest to anyone working with immobilized biochemical reagents of any kind. Various types of solid support are considered, e.g., biopolymers, synthetic copolymers and inorganic materials, as are support modification and immobilization techniques, e.g., cyanogen bromide activation of sepharose and glutaraldehyde activation of controlled pore glass. The choice of affine ligands and adsorption and elution processes are also discussed.

Affinity chromatography is based on specific, reversible interactions between an immobilized reagent and certain components of the mobile phase. The second section covers applications based on bioadsorption, particularly immunosubstances, nucleic acids, lectins, glycoproteins, virus cells, and membrane-bound proteins. The third major section covers applications other than bioadsorption, e.g., dye—ligand, metal chelate and hydrophobic interactions and charge-transfer processes. There is also a section on related techniques, i.e., affinity partition, affinity electrophoresis and high-performance ligand affinity.

There are some defects. The index is less than extensive and in some chapters the references (which are listed alphabetically) are predominantly from the 1970s. Nevertheless, the content is very readable and the figures are exceptionally clear, and I would recommend this book as a good introductory text covering many aspects of affinity chromatography.

P. J. Worsfold

R. J. Hamilton and J. B. Rossell (Eds.), *Analysis of Oils and Fats.* Elsevier Applied Science Publishers, London, 1986 (ISBN 0-85334-385-3), pp. x + 441. Price £52.00.

All the methods described in this text are of relevance, in one way or another, to the determination of quality specifications or as aids in determining whether or not an oil or fat is of "good merchantable quality". The multinational authors represent industrial, academic and public sector

interests in this complex analytical field and thus give the book an authority that would not be possible from a single author or from a group of authors from a narrow sector.

The first chapter "Classical Analysis of Oils and Fats" (J. B. Rossell) is an excellent introduction to specific applications and difficulties encountered with certain oils. This is followed by "National and International Standardisation of Analytical Methods" (E. W. Hammond) which is an excellent survey of AOCS, FOSFA, IASC, ISO, IUPAC, AOAC, CODEX, EEC, IDF and OICC/AIFC standards, methods etc. A variety of relevant chromatographic techniques is surveyed, each in appropriate detail; these are "packed-column gas chromatography" (E. W. Hammond), "WCOT (Capillary) GLC" (R. G. Ackman), "GC/MS of triglycerides and related compounds" (the late A. Bhati) and "TLC and HPLC" (R. J. Hamilton). The importance and measurement of "Positional Distribution of Fatty Acids in Triglycerides" (W. W. Christie) includes results for various oils and fats and concludes with a discussion of several molecular distribution theories. The last two chapters deal with "Wide line" (D. Waddington) and "High Resolution NMR Spectroscopy" (M. Pollard) from the basic theoretical concepts to applications as subtle as the study of polymorphic forms of triacylglycerols.

This is an excellent, well referenced volume and will be of value to scientists and also to those in the international trade of oils and fats for many years to come.

D. T. Burns

D. M. Wieland, M. C. Tobes and T. J. Mangner, (Eds.), *Analytical and Chromatographic Techniques in Radiopharmaceutical Chemistry.* Springer-Verlag, Berlin, 1986 (ISBN 3-540-96185-2), pp. xviii + 300. Price DM 148.

Radiochromatography is one of several valuable hybrid techniques available to the analytical chemist. Its principal applications are in the pharmaceutical field and this book is therefore to be welcomed. However, because the book is a compilation of presentations made at a symposium, its coverage is a little uneven, despite a high standard of editing. The text is lavishly supplemented with Figures and Tables.

The first chapter is somewhat irrelevant, being dedicated mainly to optical scanning or high performance thin layer chromatograms. Radiochromatography is introduced only in the final paragraphs of the chapter, which include the one and only mention of autoradiography in the whole book. The publication has unfortunately coincided with the marketing, by Amersham, of high-performance autoradiography film. This may well lead to the reinstatement of autoradiography as a viable alternative to scintillation counting for radio-TLC, the technique with which the first section of the book is mainly concerned. Other chapters in this section cover "instant" thin-layer chromatography, and the imaging of thin-layer chromatograms using positron-sensitive wire chambers (PSWC). There are two chapters on

PSWC: the first is a short and readable review; the second gives details of the theory, construction and use.

The second and third sections are devoted to radio-HPLC. In the second section, components for radio-HPLC are described with the salutary warning, "Most people can use HPLC. However, only a small percentage of people have an innate ability with HPLC"! Complexities of some modern radio-HPLC systems are revealed and the value of these systems for handling the short-lived radionuclides ^{13}N and ^{11}C is demonstrated, with reference to gradient systems, pre-loops, guard and stripper columns, and detectors (radioactivity and mass). No mention is made of cost, but the impression is given that the sky is the limit. Flow-through detectors are preferred to fraction collectors and the cases for and against "do it yourself" detectors are stated. Applications of radio-HPLC are covered in the last section, where there are copious references to radiopharmaceuticals labelled with ^{99m}Tc, ^{11}C, ^{13}N, ^{15}O, or ^{18}F, and the advantages of HPLC as a rapid separative method for short-lived radionuclides are made evident. There is useful information on the pitfalls of labelling at high specific activity and on systems for delivering short-lived nuclides from cyclotron to patient. Concluding chapters cover the measurement of radiochemical purity, the detection of artefacts and the separation of labelled antibodies by size-exclusion chromatography.

The book is unique, and should be of value, both as a basic text and a sourcebook, to all analytical chemists, biochemists and pharmacists who specialise in nuclear medicine.

C. G. Taylor

G. Mahuzier et M. Hamon, *Abrégé de Chimie Analytique. II. Méthodes de Séparation, 2^de édn.*, Masson, Paris, (ISBN 2-225-80880-2), pp. x + 262. Price 116 FF.

L'ouvrage comprend neuf chapitres d'inégale longueur, qui présentent l'aspect fondamental des méthodes de séparation en insistant sur l'explication des principes physico-chimiques mis en oeuvre et en définissant bien le vocabulaire correspondant. L'ensemble est simple et clair.

Les séparations solides—liquides sont vues sous l'angle de la filtration et de la centrifugation, mais la cristallisation ni la précipitation ne sont traitées ici. Un chapitre important est consacré en majeure partie à l'extraction liquide—liquide. Il est complété par un autre intitulé "Séparation à contre courant" qui traite de l'aspect théorique de la séparation de deux composés d'une phase fixe extraits par une phase mobile. "L'extraction par un solide" aborde l'adsorption liquide—solide et l'échange d'ions. Quant à la "séparation par changement d'état", elle évoque principalement les aspects physico-chimiques de la distillation sans considérer les méthodes du génie chimique correspondantes.

Le lecteur est surpris de trouver un chapitre consacré aux "méthodes

chromatographiques" qui, à lui seul, représente environ la moitié du livre et qui revient sur certaines des séparations déjà abordées précédemment. De ce fait, il en résulte en partie une impression de redite. Enfin, l'ouvrage se termine par un chapitre sur les méthodes électrophorétiques.

Ce livre est le second tome d'un Abrégé de Chimie Analytique en trois volumes, de taille raisonnable. Ses auteurs, professeurs à la Faculté des Sciences Pharmaceutiques et Biologiques de l'Université Paris-Sud, le destinent essentiellement aux étudiants en pharmacie et biochimie et résument là la matière de leur cours. S'ils soulignent fréquemment l'importance de telle méthode dans la vie professionnelle du pharmacien ou du biologiste, ils ne détaillent cependant aucune application à des cas pratiques de séparation. De même, l'instrumentation n'est évoquée que sous l'aspect du principe de son fonctionnement. Ceci est peut être regrettable et risque de laisser insatisfait le Technicien ou l'Ingénieur qui cherche à résoudre son problème et souhaite être conseillé dans le détail du choix des méthodes.

J. Robin

J. C. Van Loon, *Selected Methods of Trace Metal Analysis, Biological and Environmental Samples.* Wiley, New York, 1985 (ISBN 0-471896349), pp. xix + 357. Price £56.25.

The author obviously considers an analytical method to consist of chemical pretreatment of material arriving in the laboratory followed by presentation to an instrument and the generation of a number. The omission of sampling, preservation and physical sample preparation and of a discussion of the reliability of the numerical result, due no doubt to the constraints of space, detracts from the overall usefulness of this book. The rather superficial early chapter on "techniques and instrumentation" in which atomic absorption and plasma emission spectrometries are described could well have been omitted in favour of some of the topics mentioned above. The book contains many instances of the author, an acknowledged expert in this field of applied analytical chemistry, passing on his experiences to the reader. It would be much more interesting to have learned of his procedure for the dilution of 1000 mg l^{-1} stock solutions to produce a range of calibration standards in the ng l^{-1} range than to suffer unsubstantiated claims for the supremacy of "Zeeman" over other types of background-correction methods. To conclude the negative aspects, the book contains rather too many printing errors and it was disappointing not to find "flow-injection" in the index.

More positively, the book provides an excellent treatment of the basic laboratory requirements for getting accurate answers and a detailed discussion of sample decomposition procedures. These chapters are followed by 6 chapters, all in essentially the same format, covering the different sample types referred to in the title. Each of these chapters contains summaries of selected key methods from the literature together with other references.

These represent useful sources of information. The book concludes with a substantial chapter on metal speciation in the various sample types and a short chapter on likely future developments, such as the direct analysis of solids and the plasma/mass spectrometer combination.

The positive features of the book far outweigh the shortcomings. The book should be compulsory reading for anyone embarking on this type of analysis and is strongly recommended as a bench-top reference source for those who already think they know what they are doing.

J. F. Tyson

William F. Erman, *Chemistry of the Monoterpenes. An Encyclopedic Handbook, Parts A + B.* M. Dekker, New York, 1985 (ISBN 0-8247-1573-X, Pt. A, ISBN 0-8247-7312-8, Pt. B), pp. 1709. Price $290.00.

The very thought of two large volumes solely on the monoterpenes fills the mind with horror: memories of the dull, albeit excellent, work on classical terpene chemistry come flooding back. And of all the many terpenes, were not the C_{10}-monoterpenes the dullest? As these books show so vividly, 'things ain't what they used to be'. The full army of modern analytical separation techniques is being mustered to isolate a new range of exciting natural products. Modern spectroscopic and crystallographic techniques quickly unravel fascinating structures, complete with stereochemical detail. Tracer studies unfold the mysteries of complex biogenetic pathways. Then there are exciting challenges in stereochemically controlled synthesis. Monoterpenes also undergo an incredible range of bizarre rearrangement reactions, and they provide superb examples of carbocation, carbanion, carbene, free radical and concerted processes. If all this is not enough, monoterpenes have important applications in modern society: for example, as flavours, perfumes, pesticides and pharmaceutical agents. These two books encompass all of the aforementioned aspects, and thus provide, within a fairly narrow field, a splendid overview of modern organic chemistry.

Part A contains a general introduction to the subject; then follow six chapters covering biogenesis, absolute configurations, acyclic monoterpenes, monocyclic dimethylcyclohexanes and cyclobutanes, the *p*-menthanes, and the cyclopentanes. The six chapters in Part B are devoted to the thujanes, the cavane-eucarvones, the pinanes, the bornanes, isocamphanes and fenchanes, the monoterpene phenols, and the pyrethrins.

This is a momumental, scholarly work, and it seems almost impertinent to draw attention to the few trivial errors that can be spotted here and there. Often the appearance of a book produced directly from a 'camera-ready' typescript leaves a lot to be desired. These volumes, however, are superbly produced, and the 1500 or so structures are clearly drawn. There are in excess of 2300 citations to the original literature.

Clearly these books are indispensable for any worker in the terpene field. In addition, they contain something for all who call themselves organic

chemists. This is the sort of work which becomes more fascinating every time you dip into it. The distinguished natural products chemist, Prof. Ralph Raphael, has recently declared that 'Monoterpenes are not Monotonous'. Could he too have been reading Erman's encyclopedia?

R. M. Scrowston

Bernhard Weiz, *Atomic Absorption Spectrometry, 2nd English edn.* Verlag Chemie, Weinheim, 1985 (ISBN 3-527-26193-1), pp. xiii + 506. Price DM 160.00.

The third German edition of this popular text was reviewed in this journal recently (183 (1986) 324). The review suggested that an English translation would be most worthwhile; this has indeed turned out to be so. The quality of the translation is high; the contents (as summarized in the review of the German edition) make it the best available text on the subject, and therefore compulsive and compulsory reading for all analytical chemists who use atomic absorption spectrometry or related techniques.

F. W. Karasek, O. Hutzinger and S. Safe (Eds.), *Mass Spectrometry in Environmental Sciences.* Plenum Press, New York, 1985 (ISBN 0-306-41552-6), pp. xix + 578. Price $75.00.

This book is a compendium of contributions from recognised experts working on highly specialized environmental applications of mass spectrometry. There are nine chapters dealing with a variety of mass spectrometric techniques in general terms, followed by seventeen chapters concerned with the analysis of specific chemical groups using mass spectrometric detection. The major aim of the book is therefore to provide in-depth information on each of the application areas considered.

The material is well presented and the typical approach to each application area contains an introduction, instrumental details, discussion of fragmentation patterns and several mass spectra. There is a strong emphasis on agrochemicals, e.g., DDT, organophosphorus compounds and chlorinated polynuclear hydrocarbons, and on suspected carcinogens, e.g., polycyclic aromatic hydrocarbons and *N*-nitrosamines.

This is a good reference book for anyone wishing to find the mass spectrum of a particular environmentally important molecule, but it also provides useful information for the elucidation of mass spectral data from environmental samples.

J. F. T. Todd (Ed.), *Advances in Mass Spectrometry 1985*. Wiley, New York, 1986 (ISBN 0-471-90831 2), Part A, pp. xxxix + 565; Part B, pp. xxxix + 1096. Price £195.00.

There can be no doubt that the Tenth International Mass Spectrometry Conference, held in Swansea in September 1985, was a great success, both scientifically and from the point of view of attendance (more than 1100 delegates). Its scientific content is recorded in these two extensive volumes, produced in camera-ready copy. Part A contains the various introductory speeches, the five plenary lectures (Horning, Schwartz, Todd, Lorquet et al. and Derrick) and 26 keynote lectures on subjects as diverse as MS in geo- and cosmo-chemistry (including Halley's comet), plasma source MS, LC/MS, applications in the biomedical sciences, laser mircoprobe mass analysis and tandem MS. Part B presents short ($\leqslant$2 pp.) summaries of the contributed papers, arranged in 15 sections: LC/MS, GC/MS, ion structures and mechanisms, instrumentation and novel techniques, laser-induced ionization and excitation, high temperature studies and inorganic analysis, isotopic measurements, cluster ions, physical and theoretical, data processing, biomedical applications, pyrolysis MS, new spectra, tandem MS and desorption ionization. The volume is completed by author and subject indexes.

The books will be valued differently by different groups of scientists. To those who attended the conference, they provide a record of a memorable experience. To those involved in MS research, Part A provides useful reviews of important, developing areas, whereas Part B gives a brief indication of who is working in which areas of MS. To the non-specialist or student, Part A will serve as a valuable account of recent developments in MS, but Part B will probably be of much less use. Intending purchasers will have to establish to which group they belong, before deciding whether purchase is worthwhile at the recommended price.

ANALYTICA CHIMICA ACTA, VOL. 189 (1986)

AUTHOR INDEX

0003-2670/86/$03.50

'inted in The Netherlands

VOL. 189 No. 2 ANALYTICA CHIMICA ACTA NOVEMBER 28, 1986

CONTENTS

(Abstracted, Indexed in: Anal. Abstr.; Biol. Abstr.; Chem. Abstr.; Curr. Contents Phys. Chem. Earth Sci.; Life Sci.; Index Med.; Mass Spectrom. Bull.; Sci. Citation Index; Excerpta Med.)